

**SYNTHESIS, CHARACTERIZATION AND APPLICATION OF  
FUNCTIONALIZED GRAPHENE QUANTUM DOTS  
INCORPORATED MICRO/NANO POLY (N, N – DIETHYL  
ACRYLAMIDE) HYDROGEL AS DRUG DELIVERY SYSTEM**

**THESIS**

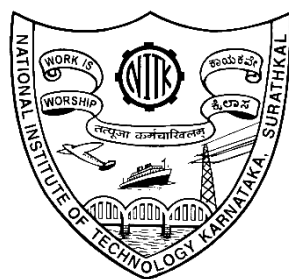
Submitted in partial fulfillment of the requirements for the degree of

**DOCTOR OF PHILOSOPHY**

by

**SUSHMA ISHWAR HAVANUR**

Register Number: 138016CH13F08



**DEPARTMENT OF CHEMICAL ENGINEERING  
NATIONAL INSTITUTE OF TECHNOLOGY KARNATAKA,  
SURATHKAL, MANGALORE - 575 025  
APRIL - 2019**



## DECLARATION

I hereby *declare* that the Research Thesis entitled “**SYNTHESIS, CHARACTERIZATION AND APPLICATION OF FUNCTIONALIZED GRAPHENE QUANTUM DOTS INCORPORATED MICRO/NANO POLY (N, N – DIETHYL ACRYLAMIDE) HYDROGEL AS DRUG DELIVERY SYSTEM**” which is being submitted to the **National Institute of Technology Karnataka, Surathkal** in partial fulfillment of the requirements for the award of the Degree of **Doctor of Philosophy** in Chemical Engineering is a *bonafide report of the research work carried out by me*. The material contained in this Research Thesis has not been submitted to any University or Institution for the award of any degree.

Name: Sushma Ishwar Havanur

Register number: 138016CH13F08

Department of Chemical Engineering

Place: NITK-Surathkal

Date: 27/04/2019





## C E R T I F I C A T E

This is to *certify* that the Research Thesis entitled “**SYNTHESIS, CHARACTERIZATION AND APPLICATION OF FUNCTIONALIZED GRAPHENE QUANTUM DOTS INCORPORATED MICRO/NANO POLY (N, N-DIETHYL ACRYLAMIDE) HYDROGEL AS DRUG DELIVERY SYSTEM**” submitted by **SUSHMA ISHWAR HAVANUR** (**Register Number: 138016CH13F08**) as the record of the research work carried out by her, *is accepted as the Research Thesis submission* in partial fulfillment of the requirements for the award of degree of **Doctor of Philosophy**.

**Chairman - DRPC**

**Research Guide**

Dr. P. E. JagadeeshBabu

Associate Professor

Department of Chemical Engineering

NITK, Surathkal



## ACKNOWLEDGMENT

This thesis arose in years of research that has been undertaken since I came to this prestigious institute, NITK. By that time, I had an opportunity to work with number of people whose contribution in assorted ways to the research and the making of the thesis deserves a special mention. It is pleasure to convey my gratitude to all of them in my humble acknowledgment.

First and foremost, I wish to express my sincere gratitude to my Research Guide, **Dr. P. E. Jagadeesh Babu**, Associate professor, Department of Chemical Engineering, NITK-Surathkal. Without his valuable guidance, support, enthusiasm and encouragement, I could never finish my Doctoral work. His wide knowledge of chemical engineering, drug delivery and logical way of thinking has been great value for me. I really thank him for graciously taking the time to read and offer the required improvements to the manuscripts and thesis. It is not sufficient to express my gratitude with only a few words.

I am extremely thankful to the RPAC committee members, **Dr. Uday Kumar Dalimba**, Department of Chemistry and **Dr. Keyur Raval**, Department of Chemical Engineering, for their valuable advice and suggestions which enabled me to notice the flaws in my research work and make necessary improvements according to their reviews and comments.

I humbly express my sincere gratitude to **The Director**, NITK-Surathkal. I wish to thank the former H. O. Ds of Chemical Engineering, **Dr. K. Vidya Shetty**, Professor, Department of Chemical Engineering, NITK-Surathkal, **Dr. B. Raj Mohan**, Professor, Department of Chemical Engineering, NITK-Surathkal and our present H. O. D **Dr. Hari Mahalingam**, Associate Professor, Department of Chemical Engineering, NITK-Surathkal for providing me necessary facilities, funding, and support during the phase of this research work. I would also like to thank all the faculty members of the Department of Chemical Engineering, NITK-Surathkal for their valuable support and encouragement. I would as well like to express my sincere thanks to **Mrs. Shashikala Mohan**, **Mr. Sadashiva**, **Mrs. Thrithila**, **Mrs. Bhavyashree**, and **Ms. Vijetha** and all

other non-teaching staffs for their helpful suggestions and timely maintenance of the laboratory equipment.

I greatly acknowledge **Dr. Nitesh Kumar**, Assistant Professor, Department of Pharmacology, MCOPS, Manipal, the research scholars **Ms. Sri Pragya Cheruku**, and **Mr. Karthik Gourishetti** for providing facilities and assisting to conduct animal studies and immunological analysis. I am extremely grateful to the authorities of **SAIF (Kochi University)**, **Innovation Center (Manipal University)**, **Department of Chemistry, NITK-Surathkal** and **Department of Polymer science, SJCE, Mysore** for various characterizations.

I am also grateful to all my former and current student colleagues **Dr. Maheswari. B., Dr. Pooja Nanda, Dr. Abhinav Nair, Ms. Shankamma. T. K., Mrs. Deepika Bhat, Ms. Thara Rathna, Mrs. Archana Naik, Mrs. Amruta shet, Mrs. Vrushali Kadam, Mr. Kishor Kumar. M. J, Mr. Lister Falleiro, Mr. Mukundan. E., Mr. Anand, Mr. Vishnu Nair**, the M. Tech students **Ms. Varesha Fahren** and **Ms. Inayat Batish** and all those who have helped me during my research work directly or indirectly.

I gratefully acknowledge to my friend **Santhosh. G.** for his constant support, help and encouragement for my Ph.D. tenure. Also, I thank my other friends **Dr. Ansari Rasheeda, Ms. Swapnali Pawar, Ms. Kezia Burga, Mr. Suman Das, Mr. Rohit Kalnake, Mr. Akash Anand, Mrs. Rashmi. B. S., Ms. Diksha Sharma, Ms. Priyanka Bhat**, for their care, support and encouragement.

Lastly, I would like to pay my heartfelt gratitude to my parent's **Sri. Ishwar Havanur** and **Smt. Ganga Havanur**, my sisters **Mrs. Laxmi** and **Mrs. Tanuja** for their constant encouragement in all ways and many years of support in all my endeavors and lifting me uphill during my career and life.

Above all, I would like to thank to the almighty **God** for giving me the strength, wisdom and health to carry out and accomplish this research work.

**SUSHAMA ISHWAR HAVANUR**

**DEDICATED  
TO MY BELOVED  
PARENTS**



## ABSTRACT

Cancer has emanated as a daunting menace to human-kind even though medicine, science, and technology has reached its zenith. Subsequent scarcity in the revelation of new drugs, the exigency of salvaging formerly discovered toxic drugs such as doxorubicin has emerged. The invention of the drug carrier has made drug delivery imminent which is ascribable to its characteristic traits of specific targeting, effective response to stimuli and biocompatibility. Temperature responsive polymers hold great promise in biological applications as they respond to change in environmental temperature to produce the desired effect like controlled drug delivery. The objective of this work is to develop macro and nano forms of temperature responsive hydrogels intended for drug delivery applications. This work deals with the synthesis and optimization of macroporous temperature responsive hydrogel poly (N, N-diethyl acrylamide) (PDEA) was via free-radical-polymerization. The optimized hydrogel was achieved by evaluating the swelling characteristics, physical stability, and mechanical strength; through altering the components namely concentration of N, N-diethyl acrylamide (monomer), ammonium peroxydisulfate (initiator), N, N'-methyl bisacrylamide (cross-linker) and N, N, N', N'-tetramethyl ethylenediamine (accelerator). LCST of the polymeric carrier has been modified by the addition of graphene quantum dots (GQDs). Inverse emulsion polymerization method was used to synthesize PDEA and GQDs incorporated PDEA nanohydrogels. Operating parameters like stirrer speed, water/oil ratio, and surfactant concentration were varied to optimize the conditions for the production of nanohydrogels.

From the temperature responsive studies, it has been observed that the equilibrium swelling ratio (ESR) and reswelling kinetics of the hydrogel significantly increased as the GQDs content was varied. The cancer drug Doxorubicin (DOX) (a hydroxyl derivative of anthracycline) release behavior was studied at above and below the LCST temperature. The particle size of pure PDEA nanohydrogel was in the range of 47 to 59.5 nm, and graphene quantum dots incorporated nanohydrogels was in the range of 68.1 to 87.5 nm. It was found that the DOX release from the DOX-loaded macro/nanohydrogels was significantly improved when the surrounding temperature of the release media was increased near to physiological temperature. The LCST of the

synthesized hydrogels has been found to be in the range of 28-42 °C. The hydrogels cumulative release profile at different surrounding temperature was fitted in different kinetic model equations and delineated a non-Fickian diffusion release mechanism for macrogels and Fickian diffusion release mechanism for nanohydrogels. The hydrogel was assessed for its cytotoxicity in B16F10 cells by MTT assay. *In-vivo* studies were done to study the lung metastasis using melanoma cancer, and the results showed a rational favorable prognosis which was confirmed by evaluating hematological parameters and the non-immunogenic nature of nanohydrogel through cytokine assay. Comprehensively, the results suggested that GQDs incorporated poly (N, N-diethyl acrylamide) hydrogels have potential application as a intelligent drug carrier for melanoma cancer.

**Keywords:** Doxorubicin, drug release, free-radical-polymerization, graphene quantum dots, inverse emulsion polymerization, melanoma, nanohydrogels, poly(N, N-diethyl acrylamide), temperature responsive.



## TABLE OF CONTENTS

CHAPTER NO.	CONTENTS	PAGE NO.
	<b>ABSTRACT</b>	i
	<b>TABLE OF CONTENT</b>	iii
	<b>LIST OF SCHEMES</b>	x
	<b>LIST OF FIGURES</b>	xi
	<b>LIST OF TABLES</b>	xvii
	<b>LIST OF ABBREVIATIONS</b>	xix
	<b>NOMENCLATURE</b>	xxv
<b>1</b>	<b>INTRODUCTION</b>	<b>1-10</b>
	1.1 Background of the research and motivation	1
<b>2</b>	<b>LITERATURE REVIEW</b>	<b>11-69</b>
	2.1 Hydrogels	11
	2.2 Application of hydrogels	15
	2.3 Classification of hydrogels	17
	2.4 Stimuli-responsive hydrogels	19
	2.4.1 Temperature responsive hydrogels	25
	2.5 Applications of temperature responsive hydrogels	27
	2.6 PDEA based temperature responsive hydrogels for drug delivery	32
	2.7 Tuning LCST of PDEA hydrogels for drug delivery	34
	2.8 Nanotechnology	38

<b>CHAPTER NO.</b>	<b>CONTENTS</b>	<b>PAGE NO.</b>
	2.9 Graphene quantum dots (GQDs)	42
	2.9.1 Application of GQDs in anticancer therapy	48
	2.10 Exploitation of tumor microenvironment for drug delivery	49
	2.10.1 Angiogenesis	50
	2.10.2 Enhanced permeability and retention (EPR) effect	50
	2.10.3 pH	52
	2.10.4 Temperature	53
	2.11 Mainstream drugs and their drawbacks	53
	2.11.1 Doxorubicin as an anticancer drug	53
	2.11.2 Mechanism of action for Doxorubicin	55
	2.11.2.1 Topoisomerase II poisoning	55
	2.11.2.2 DNA adduct formation	55
	2.11.2.3 Oxidative stress	56
	2.11.3 Limitations of Doxorubicin	56
	2.11.3.1 Doxorubicin resistance	56
	2.11.3.2 Doxorubicin toxicity	56
	2.12 Temperature responsive nanohydrogels	57
	2.13 Synthesis of hydrogels	58
	2.13.1 Synthesis of macrogels	58

<b>CHAPTER NO.</b>	<b>CONTENTS</b>	<b>PAGE NO.</b>
	2.13.2 Synthesis of nanohydrogels by inverse emulsion polymerization	58
	2.14 Drug delivery mechanism	61
	2.14.1 Reservoir systems	62
	2.14.2 Matrix systems	62
	2.14.3 Erodible systems	63
	2.14.4 Pendent chain systems (prodrugs)	64
	2.14.5 Osmotic-controlled systems	64
	2.14.6 Swelling-controlled systems	64
	2.14.7 Modulated release systems	64
	<b>2.15 Scope and objective of the work</b>	<b>66</b>
	<b>2.16 Outline of the thesis</b>	<b>68</b>
<b>3</b>	<b>MATERIALS AND METHODS</b>	<b>71-84</b>
	3.1 Materials	71
	3.2 Preparation of Graphene quantum dots (GQDs)	71
	3.3 Synthesis of poly(n,n-diethylacrylamide) (PDEA) hydrogels	72
	3.3.1 Optimization of process variables	73
	3.4 Characterization of GQDs and PDEA hydrogel	73
	3.5 Temperature-dependent equilibrium swelling ratio	74
	3.6 Time-dependent swelling of hydrogels	74

<b>CHAPTER NO.</b>	<b>CONTENTS</b>	<b>PAGE NO.</b>
	3.7 Deswelling kinetics measurement	75
	3.8 Drug loading and in-vitro release studies	75
	3.9 <i>In-vitro</i> drug encapsulation and drug loading	76
	3.9.1 Analysis of drug release pattern	76
	3.10 Cytocompatibility of hydrogels	77
	3.11 Synthesis of PDEA nanohydrogel by inverse emulsion polymerization	78
	3.12 Synthesis of GQDs grafted PDEA nanohydrogel	78
	3.13 Characterization of synthesized GQDs and nanohydrogels	79
	3.14 <i>In-vitro</i> drug encapsulation and drug loading	80
	3.15 <i>In-vitro</i> drug release of PDEA nanohydrogel	80
	3.16 Degradation of nanohydrogels	81
	3.17 Cells lines and media used for culturing	81
	3.17.1 Cytotoxicity studies of nanohydrogels	82
	3.18 Animals, murine melanoma model and in-vivo studies	83
	3.19 Haemtological parameters and tumor count evaluation	84
	3.20 Analysis of TNF- $\alpha$ and IL-6	84
	3.21 Statistical analysis	84
<b>4</b>	<b>RESULTS AND DISCUSSION</b>	<b>85-164</b>
	<b>PART I</b>	<b>85</b>



CHAPTER NO.	CONTENTS	PAGE NO.
	<b>PART III</b>	<b>128</b>
4.10	Synthesis and optimization of PDEA nanohydrogels	128
4.11	Effect of parameters on synthesis of PDEA nanohydrogels	129
4.11.1	Effect of stirrer speed	129
4.11.2	Effect of W/O ratio	131
4.11.3	Effect of surfactant concentration	132
4.12	Characterization of PDEA nanohydrogels	133
4.12.1	Size and morphological analysis of PDEA nanohydrogels	134
4.12.2	FT-IR and elemental analysis of nanohydrogels	135
4.12.3	Thermal gravimetric analysis of nanohydrogels	139
4.13	Studies on nanohydrogels degradation	140
4.14	Doxorubicin loading and <i>in-vitro</i> release behavior from nanohydrogels	142
4.15	Mathematical modelling of PDEA nanohydrogels	146
4.16	Biocompatibility studies of nanohydrogels	148
	<b>PART IV</b>	<b>151</b>
4.17	<i>In-vivo</i> studies on melanoma tumor model and its treatment	151
4.18	Therapeutic effect on change in body weight, organ weight and tumor count	152

<b>CHAPTER NO.</b>	<b>CONTENTS</b>	<b>PAGE NO.</b>
	4.19 Evaluation of hematological parameters	154
	4.20 Evaluation of cytokines level: TNF- $\alpha$ and IL-6	160
	4.21 Histopathological analysis	162
<b>5</b>	<b>SUMMARY AND CONCLUSIONS</b>	<b>165</b>
	5.1 Summary	165
	5.2 Conclusions	165
	5.3 Future scope	166
	<b>REFERENCES</b>	<b>167</b>
	<b>APPENDICES</b>	<b>213</b>
	<b>RESEARCH PUBLICATIONS</b>	<b>247</b>
	<b>BIO-DATA</b>	<b>248</b>

## LIST OF SCHEMES

SCHEME NO.	TITLE	PAGE NO.
4.1	Reaction scheme for synthesis of GQDs (GQDs- Bare GQDs; Leu-GQDs: Leucine functionalized GQDs; Met-GQDs: Methionine functionalized GQDs)	87
4.2	Schematic representation of free-radical-polymerization of PDEA synthesis (a) PDEA hydrogel preparation; (b) Chemical structure of monomer and cross-linked PDEA hydrogel	92
4.3	Schematic representation of polymerization of DEA in presence of GQDs	98
4.4	Schematic representation of PDEA nanohydrogel synthesis by inverse emulsion polymerization	128



## LIST OF FIGURES

<b>FIGURE NO.</b>	<b>TITLE</b>	<b>PAGE NO.</b>
1.1	Hydrogel swell in response to external stimuli	4
1.2	LCST and UCST behavior of temperature responsive polymer	5
1.3	Classification of emulsion	9
2.1	Histogram showing increase in a publication related to keyword 'hydrogel' from the past 58 years	12
2.2	General structure of hydrogel	13
2.3	The internal structure of hydrogel	14
2.4	General classification of hydrogels	18
2.5	Stimuli responsive swelling of hydrogels	20
2.6	Phase separation mechanism of temperature responsive polymer above and below LCST temperature	26
2.7	Architecture of poly(N-isopropylacrylamide) oligomer hydrogel	28
2.8	Temperature responsive hydrogel carrier for targeted drug delivery	29
2.9	Structure of Poly (N, N - diethyl acrylamide)	33
2.10	Schematic representation of top-down and bottom-up approaches for the synthesis of GQDs	44
2.11	Aberrations in normal and tumor tissues promoting EPR effect and utilization of nanocarriers	51

<b>FIGURE NO.</b>	<b>TITLE</b>	<b>PAGE NO.</b>
2.12	Structure of doxorubicin, its covalent bonding with DNA strands and intercalation in DNA structure	54
2.13	DNA adduct formation mechanism of doxorubicin by intercalation	55
2.14	Schematic representation of an inverse emulsion polymerization system	60
2.15	A schematic drawing illustrating the three mechanisms for controlled drug release from a polymer matrix	63
4.1	UV-vis absorption spectra of bare GQDs, leucine functionalized GQDs (GL) and methionine functionalized GQDs (GM)	86
4.2	PL spectra of GQDs excited at 365nm (a) bare GQDs prepared at varying time interval; (b) PL spectra of GQDs prepared by varying the Leucine content and (c) PL spectra of GQDs prepared by varying the Methionine content	87-89
4.3	TEM images of GQDs with a scale bar of 20 nm: (a) Bare GQDs; (b) Leu-GQDs; (c) Met-GQDs	91
4.4	Optimization of PDEA by varying monomer concentration with respect to weight of water absorbed by hydrogel	94
4.5	Optimization of PDEA by varying cross-linker concentration with respect to weight of water absorbed by hydrogel	95

<b>FIGURE NO.</b>	<b>TITLE</b>	<b>PAGE NO.</b>
4.6	Optimization of PDEA by varying initiator concentration with respect to weight of water absorbed by hydrogel	96
4.7	Optimization of PDEA by varying accelerator concentration with respect to weight of water absorbed by hydrogel	97
4.8	ESR measured from 20-60 °C (a) PDEA hydrogels prepared at different temperatures (25-40 °C); (b) Varying bare GQDs incorporated PDEA; (c) Varying Leucine functionalized GQDs added PDEA and (d) Varying Methionine functionalized GQDs content in PDEA hydrogels	100-101
4.9	SR measured at ambient temperature at different time intervals (a) PDEA hydrogels prepared at different temperatures (25-40 °C); (b) Varying bare GQDs incorporated PDEA; (c) Varying Leucine functionalized GQDs added PDEA and (d) Varying Methionine functionalized GQDs content in PDEA hydrogels	103-105
4.10	WR measured at 50 °C at different time intervals (a) PDEA hydrogels prepared at different temperatures (25-40 °C); (b) Varying bare GQDs incorporated PDEA; (c) Varying Leucine functionalized GQDs added PDEA and (d) Varying Methionine functionalized GQDs content in PDEA hydrogels	106-108
4.11	FTIR spectra (a) Bare GQDs; (b) Leu-GQDs; (C) Met-GQDs and (d) PDEA hydrogels	109-111
4.12	TGA and DSC thermogram of PDEA and GQDs incorporated PDEA hydrogels: (a) PDEA without GQDs	113-115

<b>FIGURE NO.</b>	<b>TITLE</b>	<b>PAGE NO.</b>
	(T36); (b) PDEA incorporated with bare GQDs (HG-4); (c) Leu-GQDs incorporated in PDEA (HL-7) and (d) Met- GQDs incorporated PDEA hydrogel (HM-5)	
4.13	SEM images of PDEA: (a) PDEA prepared at varying temperature; (b) PDEA with GQDs; (c) Leu-GQDs incorporated in PDEA and (d) PDEA incorporated with Met-GQDs	117-119
4.14	Cumulative % release of Hydrogels above and below LCST (a) at 30 °C; (b) at 37 °C and (c) at 40 °C	120-122
4.15	Percentage of Cell viability of B16F10 cells after treatment with (a) GQDs; (b) hydrogels extracts and (c) GQDs and hydrogels extracts	125-127
4.16	Particle size distribution of PDEA nanohydrogels prepared at stirring speed 600 with 1:4 w/o ratio and 2.25% of surfactant	130
4.17	Particle size distribution of PDEA nanohydrogels prepared at stirring speed 600 with 1:5 w/o ratio and 2.25% of surfactant	132
4.18	Particle size distribution of PDEA nanohydrogels prepared at stirring speed 600 with 1:5 w/o ratio and 3% of surfactant	133
4.19	TEM images of GQDs, functionalized GQDs and nanohydrogels with a scale bar of 20 nm: (a) GQDs; (b) GL; (c) GM; (d) N; (e) NG; (f) NL and (g) NM	135
4.20	FTIR spectra (a) GQDs, (b) GM, (c) GL and (d) PDEA nanohydrogels	136-138

<b>FIGURE NO.</b>	<b>TITLE</b>	<b>PAGE NO.</b>
4.21	TGA thermogram of PDEA nanohydrogels	140
4.22	Degradation of nanohydrogels in PBS buffer	141
4.23	Cumulative release (%) of PDEA nanohydrogels with varying temperature from 22 °C – 50 °C	143
4.24	Cumulative release (%) of PDEA nanohydrogels with varying time interval (a) at 30 °C; (b) at 37 °C and (c) at 40 °C	144-146
4.25	Percentage of cell viability of B16F10 cells after treatment: (a) with graphene quantum dots; (b) with nanohydrogels and (c) with DOX-loaded nanohydrogels	149-150
4.26	Fabrication of melanoma model via intravenous injection (tail vein) using B16F10 cell lines in C57BL6 mice. (a-c) demonstrating intravenous injection of B16F10 cell lines; (d-f) showing the appearance of tumor on the 7 <sup>th</sup> day after injection	151
4.27	Measured body weight of mice wrt time before inducing therapeutics	152
4.28	Organ weight index of mice after euthanization	153
4.29	Metastatic count of lungs of mice after euthanization	154
4.30	Estimation of hematological parameters after blood collection: (a) Lymphocyte count; (b) Red blood cell count; (c) Hemoglobin count; (d) Hemocratic count; (e) Platelet count; (f) White blood cell count; (g) Granulocyte count and (h) Monocyte count	156-159

<b>FIGURE NO.</b>	<b>TITLE</b>	<b>PAGE NO.</b>
4.31	Analysis of cytokine TNF- $\alpha$ levels from the collected blood plasma of mice	160
4.32	Analysis of cytokine IL-6 levels from the collected blood plasma of mice	161
4.33	Excised lung of mice from group I – VII. Histopathology of lung tissues (a-n) from groups I-VII at 100X resolution. (a-b) Normal control, absence of tumor cells can be distinctly seen; (c-d) Disease control, presence of melanin-producing colonies is evident; (e-f) DOX-treated group, no tumor formation can be seen; (g-h) N-DOX treated group [(g) displays presence of melanoma, (h) displays normal lung parenchyma]; (i-j) NG-DOX treated group [(i) reveals melanoma affected bronchus of lung, (j) reveals standard lung parenchyma]; (k-l) NGL-DOX-treated group [(k) exhibits appearance of melanoma tumor, (l) exhibits typical lung parenchyma]; (m-n) NGM-DOX-treated group [(m) demonstrate melanoma tumor cells, (n) demonstrate conventional lung parenchyma]	162-164

## LIST OF TABLES

<b>TABLE NO.</b>	<b>TITLE</b>	<b>PAGE NO.</b>
2.1	List of hydrogels with their corresponding applications	16
2.2	Examples of different types of stimuli responsive hydrogels along with their mechanisms in brief	21
2.3	Polymers with LCST/UCST behavior in aqueous solution	26
2.4	List of temperature responsive hydrogels and their applications	31
2.5	Tuning the LCST of PDEA hydrogel	35
2.6	Advantages and disadvantages of different nano-carriers used as DDS	42
2.7	Summary of top-down and bottom-up synthesis of GQDs	45
2.8	Profiles of the EPR effect	52
2.9	Physical and chemical properties of DOX	54
2.10	PDEA nanohydrogels synthesized by polymerization method	61
2.11	Ritger-Peppas diffusion exponent and mechanism of diffusional release from various swell-able controlled release systems	65
3.1	Feed composition of GQDs synthesis	72
3.2	Feed composition and sample designation of hydrogel	73
3.3	Optimization of nanohydrogels feed composition	79
4.1	Optimization of synthesized GQDs with respect to time and feed content, and their particle size and quantum yield	90
4.2	Feed composition of PDEA hydrogel preparation along with GQDs	99

<b>TABLE NO.</b>	<b>TITLE</b>	<b>PAGE NO.</b>
4.3	Elemental analysis of C, H, N and O from prepared hydrogels and their respective GQDs	112
4.4	Enthalpy of change from DSC analysis	116
4.5	Percentage of DOX encapsulation and loading into hydrogels	122
4.6	DOX release kinetics of T36, HG-4, HL-7 and HM-5 hydrogel at different temperatures	124
4.7	Release exponent (n), correlation coefficient ( $R^2$ ) and mechanism of drug release (Korsmeyer-Peppas model) T36, HG-4, HL-7 and HM-5 hydrogels at 30 °C, 37 °C and 40 °C	125
4.8	Effect of stirrer speed on the size of PDEA nanohydrogels	130
4.9	Effect of water:oil ratio on the size of PDEA nanohydrogels	131
4.10	Effect of surfactant concentration on the size of PDEA nanohydrogels	133
4.11	Particle size and molecular weight of nanohydrogels	134
4.12	Elemental analysis of GQDs and PDEA nanohydrogels	140
4.13	Percentage of DOX encapsulation and loading into nanohydrogels	142
4.14	DOX release kinetics of PDEA nanohydrogel (zero order kinetic, first-order kinetic, Higuchi model, Korsmeyer-Peppas model and Hixon-Crowell model) at a different temperature	147
4.15	Release exponent (n), correlation coefficient ( $R^2$ ) and mechanism of drug release (Korsmeyer-Peppas model) of PDEA nanohydrogels at 30 °C, 37 °C and 40 °C	148



## LIST OF ABBRIVATIONS

0D	Zero dimensional
1D	One dimensional
2D	Two dimensional
3D	Three dimensional
Angs	Angiopoietins
APS	Ammoniumperoxodisulfate
B(C <sub>6</sub> F <sub>5</sub> ) <sub>3</sub>	Tris(pentafluorophenyl)borane
B16F10	Murine melanoma cell line from a C57BL/6J mouse
BBB	Blood-brain barrier
C57BL/6	C57 black 6 is common inbred strain of laboratory mouse
CA	Citric acid
CMC	Critical micellar concentration
CNT	Carbon nanotube
CO <sub>2</sub>	Carbon dioxide
Conc	Concentration
CST	Critical solution temperature
CY	Cyclohexane
DDR	DNA damage response
DDS	Drug delivery system
DEA	N, N-diethylacrylamide

DLS	Dynamic light scattering
DMEM	Dulbecco's modified eagle media
DMSO	Dimethyl sulfoxide
DNA	Deoxyribonucleic acid
DOX	Doxorubicin
DSC	Differential scanning calorimetry
ECM	Extra cellular matrix
EDTA	Ethylenediaminetetra acetic acid
EE	Encapsulation efficiency
ELISA	Enzyme-linked immunosorbent assay
EPR	Enhanced permeability and retention
ESR	Equilibrium swelling ratio
FA	Folic acid
FDA	Food and Drug Administration
Fe <sub>3</sub> O <sub>4</sub>	Magnetite
FTIR	Fourier-transform infrared spectroscopy
GL	Leucine functionalized graphene quantum dots
GM	Methionine functionalized graphene quantum dots
GPC	Gel permeation chromatography
GQDs	Graphene quantum dots
H	Bare PDEA hydrogel
H <sub>2</sub> O	Water

H <sub>2</sub> O <sub>2</sub>	Hydrogen peroxide
H <sub>2</sub> SO <sub>4</sub>	Sulfuric acid
HA	Hyaluronic acid
HG	GQDs incorporated hydrogel
HGF	Hepatocyte growth factor
HL	Leucine functionalized GQDs incorporated hydrogel
HLB	Hydrophilic-lipophilic balance
HM	Methionine functionalized GQDs incorporated hydrogel
HMGB1	High mobility group box 1
IC <sub>50</sub>	Half maximal inhibitory concentration
IE	Inverse emulsion
IEP	Inverse emulsion polymerization
IL-6	Interleukin 6
IL-8	Interleukin 8
IPN	Interpenetrating network
LaB <sub>6</sub>	Lanthanum hexaboride
LC	Loading capacity
LCST	Lower critical solution temperature
Leu	L-Leucine
Leu-GQDs	Leucine functionalized graphene quantum dots
MBA	N,N'-methylenebisacrylamide
MEM-PR	Minimum essential medium without phenol red

mPa	Mega pascal
Met	L-Methionine
Met-GQDs	Methionine functionalized graphene quantum dots
MMSN	Magnetic mesoporous silica nanoparticles
MRI	Magnetic resonance imaging
MTT	3-(4,5-Dimethylthiazol-2-yl)-2,5-Diphenyltetrazolium Bromide
MW	Molecular weight
MWI	Microwave irradiation
N	Bare PDEA nanohydrogels
N	Nitrogen
NaOH	Sodium hydroxide
NBCS	Newborn calf serum
NCCS	National center for cell science
NG	GQDs grafted PDEA nanohydrogels
NIPAM	N-isopropylacrylamide
NL	Leucine functionalized GQDs grafted PDEA nanohydrogels
NM	Methionine functionalized GQDs grafted nanohydrogels
NVP	N-vinyl polyrolidine
O <sub>2</sub>	Oxygen
OD	Optical density
OVAT	One variable at a time
PBS	Phosphate buffered saline

PDEA	Poly(N, N-diethylacrylamide)
PDGF	Platelet derived growth factor
PEG	Poly(ethylene glycol)
PHEM	Poly(2-hydroxymethyl methacrylate
PHEMA	Polyhydroxyethylmethacrylate
PL	Photoluminescence
PLGA-PEG-PLGA	Poly(DL-lactic acid-co-glycolic acid)-polyethylene glycol- poly(DL-lactic acid-co-glycolic acid)
PIGF	Placental growth factor
pMMA	Poly(methyl methacrylate)
PNIPAM	Poly(N-isopropylacrylamide)
PPG	Poly(propylene glycol)
pSt	Polystyrene
PTX	Paclitaxel
QD	Quantum dots
RAFT	Reversible addition fragmentation chain transfer
RES	Reticuloendothelial system
ROS	Reactive oxygen species
RPM	Revolutions per minute
SEM	Scanning electron microscopy
SIPN	Semi-interpenetrating network
SP	Span 80

SR	Swelling ratio
ss	Single stranded
TEM	Transmission electron microscopy
TEMED	N,N,N',N'-tetramethylethylenediamine
T <sub>g</sub>	Glass transition temperature
TGA	Thermogravimetric analysis
TGF-beta	Transforming growth factor beta
THF	Tetrahydrofuran
TiO <sub>2</sub>	Titanium dioxide
TNF- $\alpha$	Tumor necrosis factor
UCST	Upper critical solution temperature
UV	Ultra violet
VEGF-A	Vascular endothelial growth factor A
w.r.t	With respect to
w/o	Water-in-oil
WGQDs	White light emitting graphene quantum dots
WR	Water retention

## NOMNCLATURE

%	Percentage
±	Plus or minus
≤	Less than or equal to
≥	Greater than or equal to
°C	Degree Celsius
μg/mL	Micro gram per milli-liter
μL	Micro liter
μmol	micro moles
cm	Centimeter
C <sub>0</sub>	Initial concentration of drug at t=0
C <sub>t</sub>	amount of drug released at t
g	Gram
gg <sup>-1</sup>	Gram per gram
h	Hour
k <sub>1</sub>	First order rate constant
k <sub>2</sub>	Higuchi constant
k <sub>3</sub>	Release rate constant
k <sub>4</sub>	Hixon-Crowel constant
k <sub>0</sub>	Zero order rate constant
M	Estimated amount of DOX loaded in the gels

$M_{DI}$	Initial mass of drug present in solution
$M_{DN}$	Mass of drug encapsulated within the gels
$M_{DSP}$	Mass of final drug present in supernatant after drug loading
mg/kg	Milli gram per kilogram
min	Minute
mL	Milli liter
mmol	Milli moles
$M_N$	Initial mass of lyophilized gels
$M_t$	Amount of DOX released from gels at time t
$M_t/M_\infty$	Fraction of drug release at time t
$M_w/M_n$	Polydispersity index
n	Release exponent
nm	Nanometer
ppm	Parts per million
Q	Cumulative release of drug in time t
R	Regression coefficient
t	time
Vol%	Volume percentage
$W_d$	Dried gel weight
$W_e$	Equilibrated swollen hydrogel weight at room temperature
$W_o$	Initial amount of drug in gel
$W_o$	Initial mass of dry nanohydrogels



$W_s$	Weight of equilibrated hydrogel at the particular temperature
$W_t$	Mass of undegraded dry nanohydrogels
$W_t$	Remaining amount of drug in gel at time t
wt:wt	Weight:weight ratio



# **CHAPTER 1**

# **INTRODUCTION**



# INTRODUCTION

## CHAPTER 1

### 1 INTRODUCTION

#### 1.1 Background of the research and motivation

Even in the 21<sup>st</sup> century cancer remains to be big threat to humans and about ~14 million cancer cases are recorded every year, and ~8.2 million cancer deaths are reported worldwide (Frédéric and Margaret. 2013; Yuekui *et al.* 2017; Max and Hannah. 2018). The term cancer is a group of diseases which involves uncontrollable and abnormal growth of cells/tissues and this abnormal growth probably invades or spreads to other healthy parts of the body (Thakur *et al.* 2017). Despite of significant improvement in cancer therapies, cancer patients' survival statistics have remained dreadful due to many factors like changing lifestyles of people, exposures to carcinogens or mutagens (radiation and chemicals), and carcinogenic infections (human papillomavirus, hepatitis B virus, hepatitis C virus, helicobacter pylori, Epstein-Barrvirus) (Frédéric and Margaret. 2013; Al-Badriyeh *et al.* 2017). The most recurrent and prime cause of cancer death all across the globe are breast cancer, lung cancer, prostate cancer, colorectal cancer and melanoma ( Ana *et al.* 2015; Torre *et al.* 2015). Although melanoma is in fourth place among the above mentioned cancers, it stands in sixth place as most common malignancy in men and women, and also melanoma ranks second to adult leukemia in terms of loss of years of potential life per death (Arrangoiz *et al.* 2016). In India, melanoma incidence is less than 0.5-2% of all diagnosed cancers (Deo *et al.* 2005).

Currently, tumor cells are treated by surgery, chemotherapy, radiotherapy, and immunotherapy which are proven to be effective to certain extent, but still, these therapies have some limitations. For example, in chemotherapy the cancer drugs used are highly toxic and are distributed non-specifically in the human body and thus these drugs affect both cancerous and healthy cells, tissues, and organs (Kytai. 2011). The adverse side effects of existing cancer treatment are hair-loss, fatigue, vomiting, dermatitis, and organ dysfunction (Vilar *et al.* 2012). Commonly used chemotherapeutic drugs are Carboplatin, Carmustine (also known as BCNU), Cisplatin, Dacarbazine (also called DTIC), Doxorubicin, Paclitaxel, Temozolomide, Vinblastine,

# INTRODUCTION

etc. These drugs are used either alone or along with other supporting drugs, and these drugs has a poor solubility, low bioavailability, and low half-life (Ramya and Chidvila. 2013; Cuiyun *et al.* 2014; Ana *et al.* 2015). Also, with time the cancer cells become resistant to these drugs due to drug efflux from cells, amplification of drug targets or changes in drug kinetics leading to a low quality of life for cancer patients (Tawona *et al.* 2014; Roberta *et al.* 2015; Sowmya *et al.* 2017; Sudipta *et al.* 2018). These concomitant problems and undesired side effects of the current cancer treatments often demand for the drug delivery method or process to transport the drug to the right area, at the right time and the right concentration (Ward and Georgiou. 2011). A flawless drug should be able to actively target cancer cells with less side effect, enhanced drug efficacy and with improved pharmacokinetics and pharmacodynamics profiles (Danhier *et al.* 2010). All these features of drug carrier are achieved through innovative engineered technologies called drug delivery system (DDS). In general, DDS allows the delivery of a drug/active compound in a controlled way (time and release rate), that can transport drug selectively to the diseased site and release the drug in affected area by maintaining the drug concentration in the body within a more acceptable therapeutic window (Li *et al.* 2009; Ana *et al.* 2015). There are different types of DDS and among them, the primary DDS include nanoparticles, liposomes, niosomes, implants, oral system, microencapsulation/microcapsules, transdermal materials, and polymeric materials (Mpho *et al.* 2013).

There are many obstacles to achieve successful drug delivery system like: low solubility of drug, environmental or enzymatic degradation of carrier, fast clearance rates from the body, non-specific toxicity of the carrier and inability to cross the biological barriers (Juillerat-Jeanneret. 2008). The drawbacks of DDS can be overcome by using controlled drug delivery systems. The controlled drug delivery systems have been devised to enable superior control of drug exposure over time, assist drug in crossing physiological barriers, shield drug from premature elimination and shepherd drug to the desired site of action while minimizing drug exposure in the body (Siegel and Rathbone. 2012). Controlled drug delivery can be achieved if the DDS are made out of smart material like polymer and loaded with a drug or biologically active agent and can

## INTRODUCTION

be released from the polymeric material in a pre-designed manner (Mahammad *et al.* 2012).

In recent years, polymeric materials received enormous attention and evolved to become more suitable material for biomedical application. Polymeric materials have porous and hydrated molecular structure, and these materials mimic the biological and physicochemical properties of tissue microenvironment (Saimak and Hassan. 2018). These polymeric carriers are capable of carrying the encapsulated or immobilized drugs, capable of releasing the drug in the inaccessible cancer site or targeted site without any damage, capable of carrying the drug over a long period of time, capable of releasing the drug in a cyclic dosage manner and capable of carrying both hydrophilic and hydrophobic drugs (Ijeoma and Andreas. 2006; William *et al.* 2010; Jung. 2017).

Among different polymeric DDS, polymeric hydrogels have gained extensive interest, though it has been more than 50 years since the first synthetic hydrogel i.e., cross-linked poly(2-hydroxyethyl methacrylate) (PHEM) was synthesized by Wichterle and Lim (1960). It is interesting to note that hydrogels were the first biomaterials designed for human system. Hydrogels are a type of polymeric material which has 3D polymeric cross-linked networks comprising of hydrophilic segments that are capable of acquiring a large amount of water, biological fluid or drug within them under physiological conditions without dissolution (Maheshwari *et al.* 2014; Chai *et al.* 2017). The 3D cross-linked network of the hydrogel are formed via chemical or physical cross-linking. The absorption capacity of the hydrogel depends on the presence of hydrophilic pendant moieties such as  $-\text{SO}_3\text{H}$ ,  $-\text{OH}$ ,  $-\text{CONH}_2$ ,  $-\text{COOH}$ ,  $-\text{CONH}-$  in the polymeric backbone (Bajpai *et al.* 2008; Pinar *et al.* 2017). Further, these hydrogels are categorized into several types on the basis of origin, composition, physical structure, morphology, response to environmental stimuli (chemical, physical or biological), ionic charges, nature of cross-linking, etc. (Qiu and Park 2001; Bindu *et al.* 2012; Susana *et al.* 2012). Over the last decade, stimuli-responsive hydrogel has received substantial attention among researchers due to its vast applications in many areas like: tissue engineering, drug delivery, self-healing materials, biosensors, and hemostasis bandages (Liu *et al.* 1993; Kim and Park. 1998; Chen and Chang. 2014; Chai *et al.* 2017). Hydrogel change their structure/chemical properties in response to external environmental such as

## INTRODUCTION

temperature, pH, solvent composition, electric field, and ionic strength and hence they are also called as stimuli-responsive hydrogel or smart polymers (**Figure 1.1**) (Kaith *et al.* 2010; Mah and Ghosh. 2013).

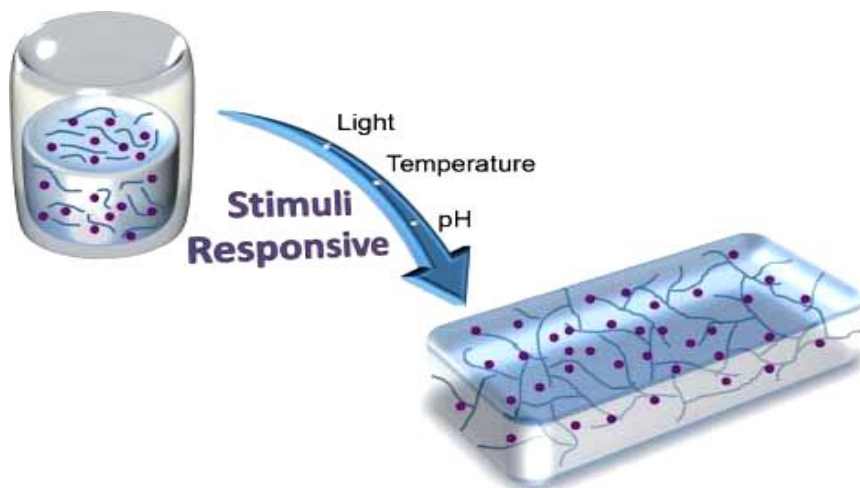


**Figure 1.1: Hydrogel swell in response to external stimuli**

The stimuli-responsive polymers can swell and de-swell according to the external environmental conditions and this behaviour makes them suitable for the synthesis of intelligent biomaterials and biomimetic materials (Yoshida and Okano. 2010). Particularly, intelligent/smart material like temperature-sensitive hydrogel are of specific interest in the drug delivery on the grounds of their solubility behavior that transforms sol to gel in response to the surrounding temperature (Xiao. 2007; Karimi *et al.* 2016; Kim and Matsunaga. 2017). The temperature has a stupendous corollary on the hydrophobic and hydrophilic interactions between the water molecules and polymeric chains (Bajpai *et al.* 2008). Thus, hydrogels undergo a volume phase transition at a critical temperature; namely a lower critical solution temperature (LCST) and upper critical solution temperature (UCST) (**Figure 1.2**). The hydrogels which have LCST exhibit a hydrophilic-to-hydrophobic transition with increasing temperature, whereas the hydrogels with UCST undergo hydrophobic-to-hydrophilic transition (Xu *et al.* 2006). In contrast to the UCST systems, the LCST systems have received more attention in drug delivery, because in UCST hydrogels the drug loading has to be done at a higher temperature, which might lead to denaturation of the drug or the biomolecules that in turn becomes lethal during formulation and release. Some common LCST/UCST temperature-sensitive polymers are poly(N-isopropylacrylamide),



## INTRODUCTION

poly(N-dimethylacrylamide), poly(N-4-vinylpyridone), poly(N,N-diethylacrylamide), poly(N-vinyl-n-butyramide), etc. (Schmaljohann. 2006; Matthew and Rachel. 2013; Arijit *et al.* 2015).

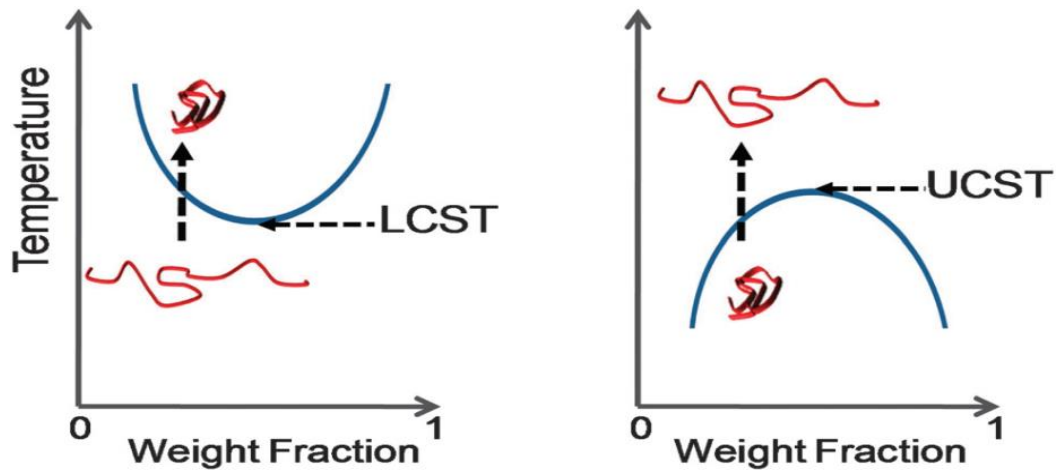


**Figure 1.2: LCST and UCST behavior of temperature responsive polymer**

(Matthew and Rachel. 2013)

The most widely used temperature-sensitive hydrogel is poly(N, N-diethyl acrylamide) (PDEA), which exhibits phase separation at lower critical solution temperature (LCST) of approximately 31 °C in aqueous solution (Marcelo *et al.* 2010; Sood *et al.* 2014). The tertiary amide group of N, N-diethyl acrylamide (DEA) makes it as hydrogen bond acceptor that can form a hydrogen bond with hydrogen bond donor (Wei *et al.* 2016). The PDEA exhibits LCST in water by balancing the hydrogen bonds and hydrophilic interactions along with a change in surrounding temperature. However, this temperature-sensitive hydrogel shows some disadvantages like poor mechanical strength and low swelling/deswelling properties (Qiu and Park. 2001).

Hydrogel properties can be modified in many ways like changing the constituents of monomers, controlling polymerization conditions, introducing functional groups to the synthetic polymers and by incorporation of nanomaterials within hydrogel (i.e., hydrated networks of cross-linked polymers) and all these techniques have emerged as useful methods for generating biomaterials with tailored functionality (Adnan *et al.* 2016). Recent trends indicate the growing interest in developing hydrogels with nanomaterials for various biomedical applications specially in drug delivery, biosensors, and regenerative medicine (Gaharwar *et al.* 2015). Nanomaterials are being

## INTRODUCTION

recognized as useful materials in oncology, with sensitive cancer detection capabilities and effective treatment outcomes due to their small size (Quader and Kataoka. 2017). The physical or covalent interaction between the nanomaterials and the polymeric chains of hydrogel has opened some new possibilities for tailoring the hydrogel properties (Peppas *et al.* 2007; Goenka *et al.* 2014). The hydrogel can be manipulated to achieve tailored properties with hydrophilic/hydrophobic moieties of nanomaterials like clay nano-sheets, carbon nanotubes, graphene oxide, gold nano-rods, silver nanowires, graphene quantum dots (Kuo *et al.* 2016; Zhang *et al.* 2016; Wang *et al.* 2017). The integration of temperature-sensitive polymer with fluorescent materials like graphene quantum dots (GQDs) can produce optically active smart material (Paek *et al.* 2014). Graphene sheets with lateral dimensions less than 100 nm in few layers (<10 layers) form a novel group of molecules called graphene quantum dots (GQDs), which has shown a substantial application in various fields (Song *et al.* 2015; Elvati *et al.* 2017). It has laid the foundation for an exceptional drug carrier due to the presence of various functional groups like carboxyl, hydroxyl, carbonyl, and epoxy groups and presence of significant delocalized  $\pi$  electrons (Dong *et al.* 2018). Presence of more active groups on the surface of GQDs and its unique structural properties have shown to influence many factors like chemotherapeutic efficiency of anticancer drugs, drug release and thus, proved their worth as excellent drug carriers (Iannazzo *et al.* 2017)

Generally, hydrogels are synthesized by using synthetic/natural polymers; by various polymerization methods such as: solution, bulk, and suspension polymerization by chemical and physical cross-linking routes (Maitra and Shukla. 2014; Ahmed. 2015). Chemically cross-linked hydrogels are extensively considered as drug carrier due to their excellent mechanical strength. The hydrogels synthesized in this study were synthesized by using a chemical method, i.e., free radical polymerization. Hydrogels are prepared using mono-functional or multi-functional monomers without any by-product as it happens in step polymerization. The steps involved in free-radical-polymerization are initiation of the active monomer, propagation or growth of the active (free-radical) chain by sequential addition of monomers and termination of the active chain to give the final polymer product. The first step of the initiation starts with the decomposition of the initiator by exposing it to heat or light, to produce free radicals.

## INTRODUCTION

When the radicals are generated, the free radicals attack one of carbon double bond (vinyl group) of the monomer and cross-linker molecule to form a new chemical bond between the monomer and cross-linker fragment. This process is repetitive, and the growing polymer chains become chemically cross-linked until exhaustion of the monomer to form 3D-network.

A few notable properties of the hydrogel are biocompatibility, hydrophilicity, flexibility, tunable biodegradability and porous structure that make it ideal for drug delivery matrix (Chai *et al.* 2017; Chintan and Gayathri. 2015). Hydrogel show good compatibility with blood and other body fluids. Thus, they are used in contact lenses (Aji *et al.* 2005), as barrier materials to maintain the biological adhesions (Bennett *et al.* 2003), wound dressings materials (Aji *et al.* 2005), encapsulation of cells (Cohen *et al.* 1997), cellular immobilization (Jen *et al.* 1996), and in the field of tissue engineering as matrices for repairing and regenerating a wide variety of tissues and organs (Lee and Shin, 2007). Despite of their widespread potential, hydrogels have some limitations in medical and biological applications. In tissue engineering, due to the fragile nature and low mechanical strength, cell necrosis happens due to diffusion limitations, even though these artificial scaffolds closely mimic the mechanical and chemical properties of the natural extracellular matrix (ECM). Macroscopic dimensions and its quick elution of drugs from the swollen hydrogel matrix makes it difficult to replicate the complexity of real tissues like cell-cell interactions. These challenges can be addressed through the use of nanohydrogel; hydrogel particles with nanoscale dimensions (Chintan and Gayathri. 2015; Chai *et al.* 2017).

Nanohydrogels are 3D polymeric network composed of hydrophilic macro-molecular cross-linked chains having a diameter of 1-100 nm (Chintan and Gayathri. 2015). These nanohydrogel have characteristics features of hydrogel and nanoparticles. Hence, they benefit from the hydrophilicity, flexibility, versatility, high water absorptivity and biocompatibility of hydrogel along with all the merits of nanoparticles (Schexnailder *et al.* 2009; Qian *et al.* 2013). These drug carriers has drawn huge interest and are currently under development stage due to their advantages like biocompatible, large surface area which can be modified to reach the targeted site, interact with specific cells, capable to carry the therapeutics to the targeted site with improved efficacy/reduced toxicity,

## INTRODUCTION

prolonged circulation in bloodstream, increased solubility of drugs, targeted delivery of drugs to specific cell/tissue/organ in a specific manner, stimulus controlled release of drugs with appropriate drug ratio, visualization of sites of drug delivery by combining therapeutic agents with imaging modalities, and/or real-time feedback on the in vivo efficacy of a therapeutic agent (Yu *et al.* 2016; Jinju *et al.* 2017; Janel *et al.* 2017). In cancer therapy, nanohydrogels may act as an intratumoral chemotherapy depot by promoting accumulation or maintenance of high intracellular levels of the chemotherapeutic agent (Roberta *et al.* 2015).

Although various strategies are available for the preparation of chemically cross-linked polymeric micro/nanohydrogels, which include top-down nanotechnologies, such as template-assisted nanofabrication (imprint photolithographic techniques), or bottom-up approaches such as micro-molding and micro-fluidic methods (Nicolas and Jutta. 2010). These methods need sophisticated facilities and are expensive. So, inverse emulsion polymerization (IEP) is a promising process to synthesize polymeric particles. The term emulsion referred as a dispersion of one phase into another continuous phase (immiscible to the dispersed) with the aid of an emulsifier (amphipathic molecule). Emulsions are categorized (**Figure 1.3**) based on the nature of dispersed and continuous phase as oil-in-water or direct or conventional, water-in-oil or inverse, water-in-oil-in-water or double (Tadros *et al.* 2004), mini-emulsions (Landfester, 2003), micro-emulsions (Klier *et al.* 2000).

Nano-emulsions are emulsions with droplet size in the nanometers range between 20 and 500 nm. Due to their small droplet size, nano-emulsions appear transparent or translucent to the naked eye. Nano-emulsions possess stability against sedimentation or creaming (Maria *et al.* 2018). Nano-emulsions are prepared by the dispersion or high-energy emulsification methods like high shear stirring, high-pressure homogenizers, and ultra sound generators. Energy supplied in the shortest time and with homogeneous flow rate produces the smaller sized emulsion droplets (Solans *et al.* 2005). High-pressure homogenizers meet these requirements and is most widely used to prepare nano-emulsions (Solans *et al.* 2005). Nano-emulsions are used as the template for synthesis of nanohydrogels. Water-in-oil (inverse) emulsion technique is the most

## INTRODUCTION

widely used method, and it does not require any complicated equipment and the size of the resultant nanohydrogels can be easily controlled (Enikő *et al.* 2017).

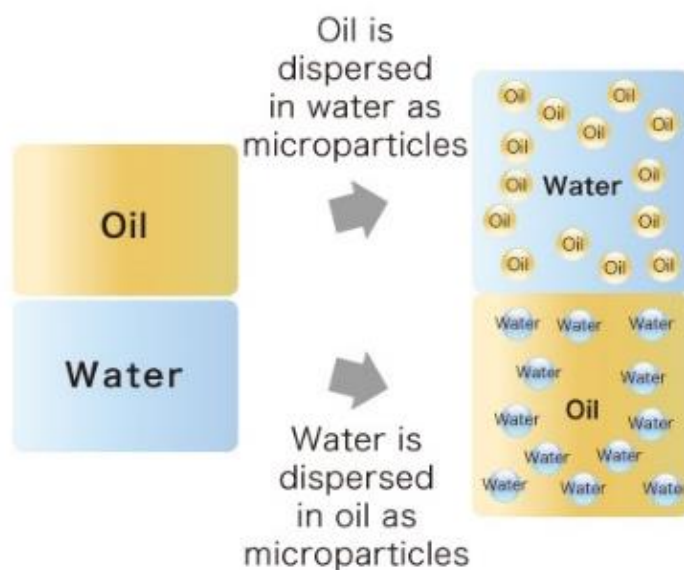


**Figure 1.3: Classification of emulsion**

Inverse emulsion polymerization (IEP) methodologies generate mono-dispersed solutions of kinetically stable aqueous w/o droplets through the use of an aqueous phase, surfactants and mechanical stirring in an organic medium (Kishore *et al.* 2017). The mechanism of polymerization strongly depends on the type of initiator used (oil soluble or water soluble) and as well as the oil-solubility of monomer. For hydrophilic initiators and monomers (homogeneous reaction mixture) the loci of initiation and propagation are the dispersed aqueous droplets, rather than the continuous phase or micellar structures (Thickett and Gilbert. 2007). The obtained particle size distribution is therefore mainly determined by the nano-droplet size distribution of the inverse emulsion, provided that reaction kinetics is faster than emulsion break-up. Thus, radical-polymerization is usually selected as the reaction scheme (Tauer *et al.* 2008). Inverse emulsion polymerization is a multi-parameter system, and its potential and versatility in fabricating aqueous-based nanomaterials are already established, and optimization of IEP may provide better-defined colloids for drug delivery applications.

In the present work, graphene quantum dots (GQDs), a fluorescent nanomaterial was fabricated by a simple, effective, facile and low-cost bottom-up approach using microwave irradiation method and citric acid. Further, PDEA hydrogel were prepared

## INTRODUCTION

by free-radical-polymerization using N, N-diethyl acrylamide (DEA) as a monomer, and N, N'-methylene bisacrylamide (MBA) as cross-linker, ammonium peroxydisulfate (APS) as an initiator. The process was optimized by varying DEA, MBA, APS and synthesis temperature. The optimized PDEA hydrogel are incorporated with GQDs to adjust the LCST of the polymer. The synthesized hydrogel and nanohydrogel were characterized by FTIR, SEM/TEM, TGA/DSC, and GPC. A model drug DOX was used to analyze the loading and release characteristics of the hydrogel and nanohydrogel. The release characteristics were studied at different temperatures with varying time intervals. Cytotoxic studies of the synthesized gels were performed on B16F10 melanoma cancer cell lines. Murine melanoma model was fabricated by intravenous injection (via tail vein) of B16F10 cell lines in C57BL/6 mice. Parameters like body weight, organ weight index, and metastatic tumor counts were assessed for a possible association with effectiveness along with injuriousness that might be instigated by nanohydrogel systems. Hematology and cytokine assays were conducted to evaluate potential toxicity, immunogenicity, and plausible prognosis. Histopathology was performed to confirm the presence of tumor that might not be evident by visual confirmation.

**CHAPTER 2**  
**LITERATURE**  
**REVIEW**





# LITERATURE REVIEW

## CHAPTER 2

### 2 LITERATURE REVIEW

Hydrogels are cross-linked polymeric networks with the ability to swell in an aqueous medium. Cross-linking in hydrogels occurs by chemical or physical means depending on the properties of various polymers, monomers, cross-linking agents and experimental conditions adopted for their synthesis. Due to different types of chemical structure and variety of cross-linking methods, extensive range of hydrogels are prepared for various applications in pharmaceutical and biomedical fields. This chapter describes about hydrogel, their classification, their methods of preparation, hydrogel as drug delivery system, different nanomaterials and their applications in drug delivery.

#### 2.1 Hydrogels

The terms ‘gels’ and ‘hydrogels’ are used interchangeably to describe polymeric cross-linked network structures by biomaterial, biomedical and food scientists. ‘Gels’ are defined as a substantially dilute cross-linked system. These gels are classified depending on their flow behavior as weak or strong gels (Ferry. 1980; Gulrez *et al.* 2011). In 1894, the word ‘hydrogel’ was first came into the light in literature. The term ‘hydrogel’ was used to describe a colloidal gel of inorganic salts (Bemmelen. 1894). Later, between 1950-1955, Wichterle postulated the fundamental properties required for a synthetic material (i.e., hydrogel) which will be in direct contact with living tissues (Wichterle, 1971). The postulates framed by Wichterle fail to cover the following properties: extractable impurities; mechanical properties similar to those of the surrounding tissue; sufficient permeability for water-soluble substances such as salts, proteins and oxygen; and resistance to degradation by enzymatic systems (Buwalda *et al.* 2014). In 1960, Wichterle and Lim prepared the first hydrogel polyhydroxyethylmethacrylate (PHEMA) a cross-linked network material prepared by free-radical-polymerization with high water affinity with above mentioned properties and then he used it as base material for contact lens. The PHEMA hydrogel was the first soft polymeric material synthesized to be utilized inside humans (Nierzwicki and Prins. 1975; Wichterle and Lim. 1960). Generally, the historical backdrop of hydrogels can be classified (Buwalda *et al.* 2014) as below:

## LITERATURE REVIEW

- The first generation of hydrogel were interested in random cross-linking trial and error experimental methods. The primary objective of this generation was to synthesize polymeric hydrogel materials with high swelling capacity and sensible mechanical properties (Buwalda *et al.* 2014).
- The second era of hydrogel included response to specific environmental stimuli like temperature, pH, concentration of solvent molecules and pressure. These stimuli were utilized in drug delivery systems. (Buwalda *et al.* 2014).
- Lastly, the third era of hydrogels concentrated on the advancement of cross-linked polymeric hydrogels with other physical interaction, e.g., cyclodextrins (Chung *et al.* 2008; Kirakci *et al.* 2014), and stereo-complexed materials, e.g., PEG-PLA interaction (Abebe and Fujiwara 2012; Yom-Tov *et al.* 2014).

Till today, hydrogels have fascinated many scientists and researchers, and many efforts have been made to synthesis and apply hydrogel in many fields. **Figure 2.1** shows the histogram of publications in the area of hydrogels.

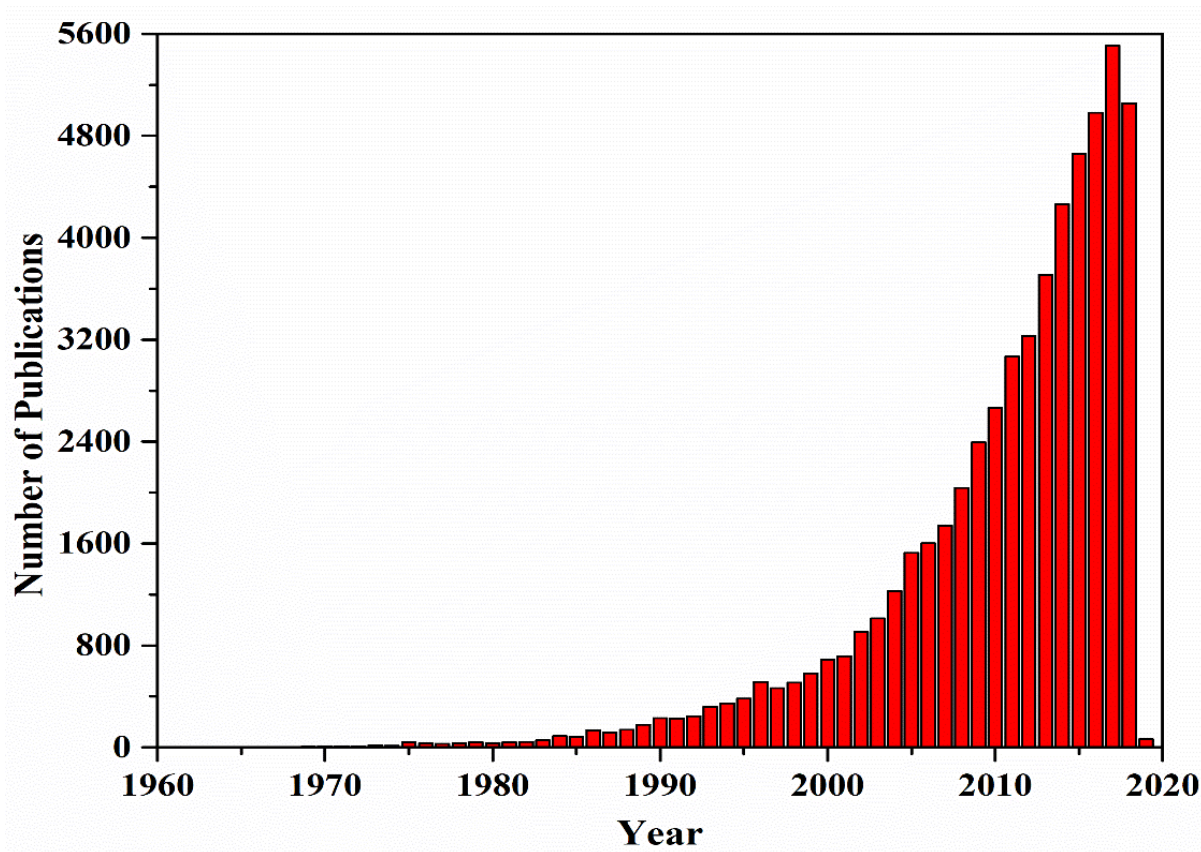


**Figure 2.4: Histogram showing increase in a publication related to keyword 'hydrogel' from the past 58 years (Source: Scoups.com/home.uri).**

## LITERATURE REVIEW

Hydrogels are 3-D cross-linked polymeric networks made-up of hydrophilic structures, that have ability to absorb large volumes of biological fluids or water with in them (Peppas *et al.* 1986). The 3D network is formed by the cross-linking of polymeric chains (**Figure 2.2**). The hydrogel polymeric networks composed of homopolymers or copolymers, and the presence of chemical cross-links (tie-points, junctions), or physical cross-links (entanglements or crystallites) and makes them insoluble in many solvents. (Kamath and Park 1993; Park and Shalaby 1993).

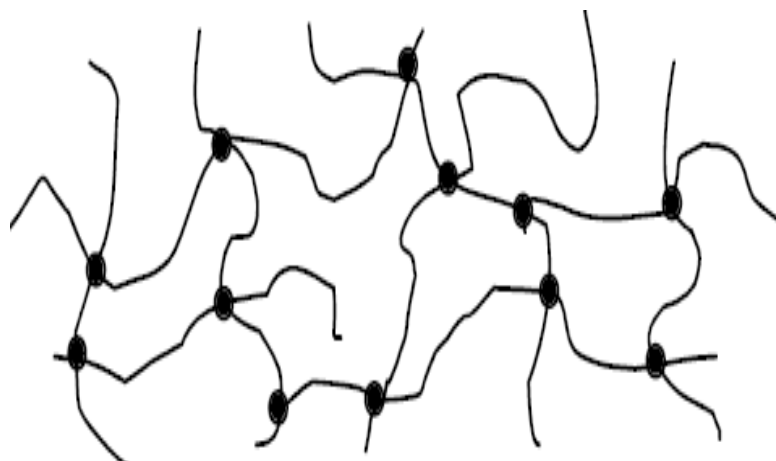


**Figure 2.2: General structure of hydrogel**

The chemical and physical cross-linking maintains the 3D structure of hydrogel even in its swollen state. Cross-linking also facilitates their insolubility in water for the specific interaction and hydrogen bonding. It also provides the essential mechanical strength as well as physical integrity to the polymeric hydrogels (Hoare and Kohane. 2008; Varaprasad *et al.* 2017). Hydrophilic polymer backbone of the hydrogel prevents it from dissolution process, although some of the hydrogels disintegrate and dissolve after absorbing a specific amount of water or chemical/biological fluids (Ahmed. 2015; Akhtar *et al.* 2016; Feksa *et al.* 2018). The interaction between polymeric networks and water or biological fluids occur through capillary, osmotic and hydration forces, which are balanced to attain equilibrium state, causing expansion of chain networks (Varaprasad *et al.* 2017). These interactions prevent the polymer from aggregation to form a compact mass while it prevents water flowing out. During swelling process hydrogels 3-D structure do not collapse, due to their cross-linked structure.

## LITERATURE REVIEW

Gibas and Janik (2010) and other researchers reported that the swelling of the hydrogel is a difficult process that includes numbers of steps. In the initial step, the hydrophilic groups of the polymeric hydrogel cross-linked networks are hydrated by water, this absorbed water is called as primary bound water (Ullah *et al.* 2015). In the second step, water molecules interacts with the outer hydrophobic groups present in the polymeric chain, this interacted water is called as secondary bound water. The total bound water is formed by combining the primary and the secondary bound water in the hydrogel network (Ullah *et al.* 2015). In the final step, the osmotic driving force of the hydrogel network towards infinite dilution is resisted by the chemical/physical cross-links, as a result additional water is absorbed by hydrogel network (Ullah *et al.* 2015). The water imbibed under equilibrium condition by the polymer network is called as free or bulk water, this water fills the empty spaces between the polymer chains or network and also in the center of the larger pores. The total volume of water taken up by a 3-D polymeric hydrogel network be influenced by the surrounding environment temperature and the specific interaction of the polymer chains with the water molecules, which is described by the Flory–Huggins theory (Ganji *et al.* 2010; Ullah *et al.* 2015). The hydrogel network is a cross-linked polymer chains (3D network), which is referred as a mesh (**Figure 2.3**). These mesh like structures hold the water/biological fluid, due to which an elastic force is developed by the contraction and expansion of the hydrogel network, hence, the solidity of the hydrogel is maintained (Ullah *et al.* 2015).

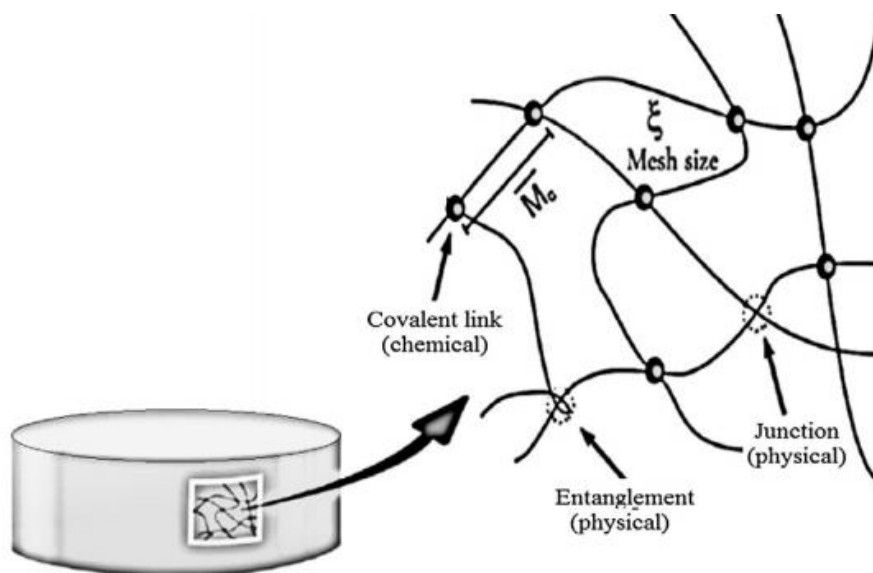


**Figure 5.3: The internal structure of hydrogel** (Ullah *et al.* 2015)

# LITERATURE REVIEW

The high-water-content of the hydrogel renders them biocompatible to living systems, and their soft nature can minimize damages to the surrounding tissues. Furthermore, the elastic and soft nature of gels minimizes irritability to the neighboring tissues (Akhtar *et al.* 2016). Due to these reasons, the hydrogel is used in drug delivery which has several advantages (Hamidi *et al.* 2008; Hoare and Kohane. 2008; Popat and Sonali. 2017) which are outlined as below:

- It is soft with high degree of flexibility and its hydrated nature of the hydrogel makes them very similar to the cell, tissue and other biological matters.
- Covalent bonds hold the polymer network together and offer control and integrity.
- It can be synthesized and modified over a wide range of particle sizes.
- It has easily tunable material properties and good transport properties which can be utilized to target a specific site.
- The decreased dose of administration by a physician also decreases side-effects of the drug.
- Improved drug utilization shows improved patient compliance.
- Drug loss is prevented by extensive metabolism/bio-transformation i.e., elimination of drug molecules from body.
- Sustained release of the entrapped molecules.

## 2.2 Application of hydrogels

Hydrogels received substantial attention by researchers due to its vast applications in major areas like medicine, biotechnology, and electronics (Liu *et al.* 1993; Kim *et al.* 1999; Chen *et al.* 2014). Different forms of hydrogels are used in broad range of applications like: (a) microparticles (e.g., as drug delivery vector in stomach, liver, colon, intestinal, brain, blood, nervous system, as bio-adhesive carriers to insulin, as wound dressing materials (Hoffman. 2012; Alejandro and Katia. 2017) and tumor-targeted delivery vectors); (b) pressed powder matrices (e.g., pills or capsules for oral, vaginal, nasal, rectal, ocular, subcutaneous and epidermal applications); (c) membranes or sheets (e.g., as wound dressing material, as a reservoir in a transdermal drug delivery of allergens in skin testing (Enrica and Vitaliy. 2015), as 2D electrophoresis gels);

## LITERATURE REVIEW

(d) encapsulated solids (e.g., in osmotic pumps); (e) coatings (e.g., as pills or capsules; as implants or catheters (Ullah *et al.* 2015); and as coatings on the inside capillary wall in capillary electrophoresis); (f) liquids (e.g., as cellular regenerator, as temperature maintaining medium, and in proliferation for growth of new extra cellular matrix (Pariksha *et al.* 2016)) and (g) solid molded forms (e.g., soft contact lenses) (Morteza *et al.* 2016). A list of hydrogels with their corresponding applications (Nikhil *et al.* 2014) is listed in **Table 2.1**.

**Table 2.1 List of hydrogels with their corresponding applications**

(Gulrez *et al.* 2011; Morteza *et al.* 2016; Sood *et al.* 2014)

Application	Polymers	Reference
Drug delivery pharmaceutical	Poly(vinylpyrrolidone), Starch, Carrageenan, Poly(vinylpyrrolidone), Poly(acrylic acid) Carboxymethylcellulose, Hydroxypropyl methylcellulose, Polyvinyl alcohol, Acrylic acid, Methacrylic acid, Chitosan, Glycerophosphate, Acrylic acid, 2-Acrylamido-2-methylpropane sulfonic acid, Acrylic acid, Carboxymethylcellulose, poly(2-oxazoline)-cholesteryl methyl carbonate	Bruguerolle. 1998; Ullah <i>et al.</i> 2015
Wound care	Polyurethane, Poly(propylene glycol), Xanthan, Poly (vinyl pyrrolidone), Polyethylene glycol, Agar, Methylcellulose, Carboxymethyl-cellulose, Alginate, Hyaluronan, collagen, and other hydrocolloids	Brownlee and Ceramic. 1979; Kamoun <i>et al.</i> 2017
Tissue engineering implants	Poly(lactic acid), Poly(ethylene glycol), poly(hydroxyethyl methacrylate), poly co-glycolic acid, polyhydroxybutyrate, polyvinyl alcohol, poly(N-isopropyl acrylamide-co-acrylic acid), or naturally occurring polymers	Calejo <i>et al.</i> 2012; Feksa <i>et al.</i> 2018

## LITERATURE REVIEW

Application	Polymers	Reference
	e.g., collagen, hyaluronan, heparin, chitosan, alginate, alginic acid, pectin, dextran, cellulose, chondrin sulfate, agarose, pullulan	
Dental material	Hydrocolloids (Ghatti, Karaya, Keren's gum), polylactic acid, polyglycolic acid, polylactide-co-glycolic acid, polycaprolactone, hydroxyapatite, beta-tricalcium phosphate, Hexafluoroisopropanol based silk	Cahalan <i>et al.</i> 1988; Saranya <i>et al.</i> 2014
Injectable polymeric system	Polyesters, Polyphosphazenes, Polypeptides, Chitosan, b-Hairpin peptide, Hyaluronic acid, chitosan, Oligolactide-(2-HEMA), P(L-glutamic acid), Fibroin, <i>etc.</i>	Chang. 1988; Kondiah <i>et al.</i> 2016
Technical products (cosmetic, pharmaceutical)	Starch, Gum Arabic, Xanthan, Pectin, Carrageenan, Gellan, Welan, Guar gum, locust bean gum, Alginate, Starch, Heparin, Chitin and Chitosan, methylcellulose-PEG based hydrogels	Chang. 1988
Others (agriculture, waste treatment, separation, food packaging, <i>etc.</i> )	Starch, Xanthan, Polyvinyl alcohol, Poly (vinyl methyl ether), Poly (N-isopropyl acrylamide), starch-g-poly (acrylamide), polyhydroxyalkanoates, polylactic acid	Cahalan <i>et al.</i> 1988; Ullah <i>et al.</i> 2015

### 2.3 Classification of hydrogels

The hydrogels are classified depending on their sources, nature of swelling, physical properties, origin, method of preparation, ionic charges, nature of cross-linking and rate of biodegradation which is shown in **Figure 2.4** (Qiu and Park 2001; Bindu *et al.* 2012; Susana *et al.* 2012; Ullah *et al.* 2015). In physically cross-linked hydrogel, the cross-linking process is achieved via physical processes such as hydrophobic association, chain aggregation, crystallization, polymer chain complexion, and hydrogen bonding

# LITERATURE REVIEW

(Varaprasad *et al.* 2017). Whereas, in chemically cross-linked hydrogel the chemical process like covalent cross-linking (pre/post or simultaneously in polymerization) is utilized to prepare a chemical hydrogel (Ullah *et al.* 2015; Varaprasad *et al.* 2017). The physical hydrogel is reversible because of the temporary changes, whereas chemical hydrogel is irreversible with permanent configurational changes (Ullah *et al.* 2015). Homo-polymer hydrogels are cross-linked networks of one type of hydrophilic monomer unit, whereas copolymer hydrogels are produced by cross-linking of two co-monomer units, at least one of which must be hydrophilic to render them swelling property. Multi-polymer hydrogels are made of three or more co-monomers reacting together (Peppas. 2012). On the basis of ionic charges hydrogels were classified as natural, cationic, anionic and amphoteric. Anionic hydrogels typically contain negative ions attached to the polymer network whereas cationic hydrogels include positive ions and neutral hydrogels must have equal numbers of positive and negative ions. Generally, it is assumed that a neutral hydrogel has uniform concentration of ions throughout the polymer matrix (Mahinroosta *et al.* 2018).

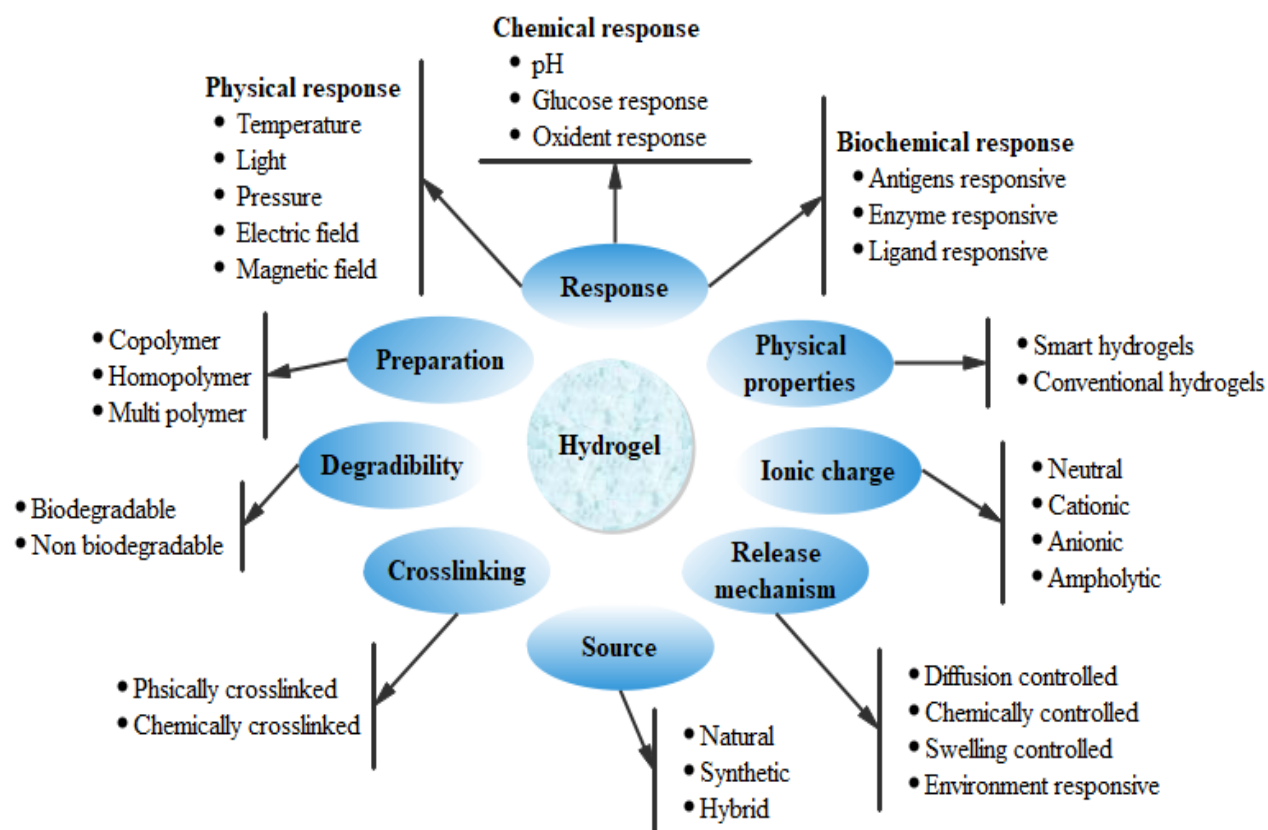


Figure 2.4: General classification of hydrogels



## LITERATURE REVIEW

Also, the hydrogels are categorized based on their dimension as macrogel, microgel and nanogel. Macrogel are frequently referred as 'bowl of jelly,' due to larger cross-linked structure, whose size range is in the millimeters (mm) (Thorne *et al.* 2011). Microgel or nanogel are smaller particles with cross-linked polymer network structures (Nolan *et al.* 2005; Thorne *et al.* 2011). This research work is concerned with the synthesis and characterization of temperature-sensitive hydrogels (macrogels) and nanohydrogels (nanogels) for drug delivery applications.

### 2.4 Stimuli-responsive hydrogels

Most of the conventional hydrogels undergo only the swelling-deswelling process depending on the availability of water in the environment. An additional property over the fundamental swelling-deswelling property makes a hydrogel as smart (Lee *et al.* 2013). Stimuli-responsive hydrogels are described as smart hydrogel (Galaev and Mattiasson. 2000), intelligent hydrogel (Kikuchi and Okano. 2002), environmental-sensitive hydrogel (Qiu and Park. 2001) when their sol-gel transition occurs at conditions that can be induced in a living body. Such hydrogels may be classified according to the nature of the stimulus used to induce their sol-gel transition, i.e., their ability to undergo rapid changes in their microstructure from a hydrophilic state to a hydrophobic state which is triggered by small changes in the surrounding environment. (Bawa *et al.* 2009; Jagur-Grodzinski. 2010; Sood *et al.* 2014). The environmental factors, also referred to as external stimuli (**Figure 2.5**), can be biological (antibody, enzyme, glucose) chemical (ionic strength, solvent, pH, and ion type) and physical (electricity, temperature, ultrasound, magnetic field, and pressure) (Cabane *et al.* 2012; Lee *et al.* 2013). Responses to these stimuli can be exhibited by changes in solubility, the formation of an intricate molecular assembly, surface characteristics, changes in shape, hydrophobic-hydrophilic balance or a sol-to-gel transition (Bawa *et al.* 2009). These responsive polymeric systems dictate in the delivery of drugs, because of their property to know when and at which time interval drug is being released from the system (Soppimath *et al.* 2002).

## LITERATURE REVIEW

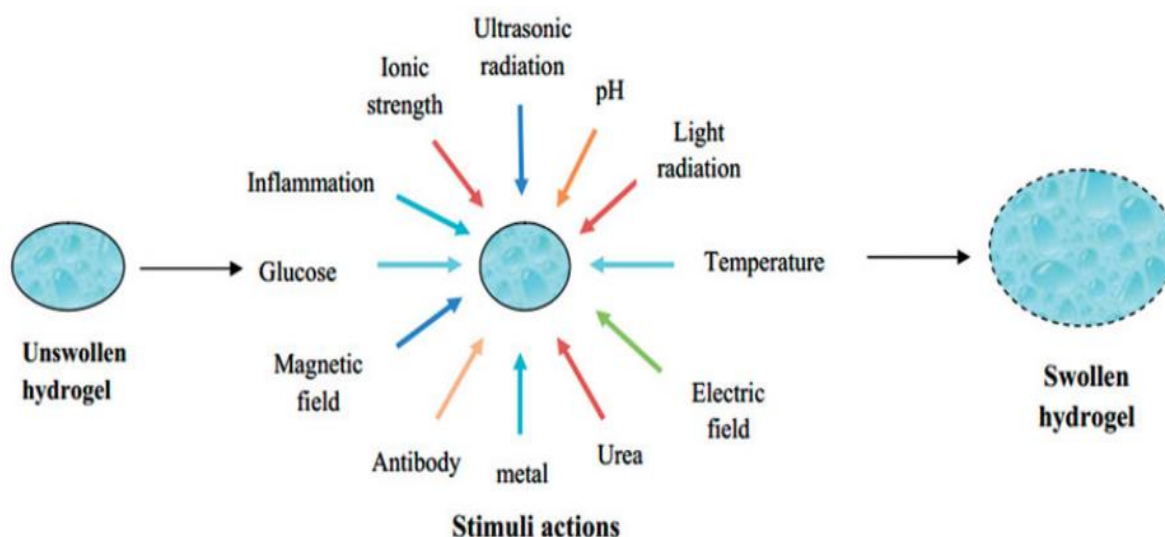


**Figure 2.5: Stimuli responsive swelling of hydrogels** (Sood *et al.* 2014).

The stimuli response characteristics of a polymer systems are very useful in bio-related applications such as drug delivery (Gupta *et al.* 2002; Jeong and Gutowska. 2002; Sershen and West. 2002), biotechnology (Galaev and Mattiasson. 2000; Sharma *et al.* 2003), and chromatography (Kobayashi *et al.* 2002; Anastase-Ravion *et al.* 2001). Some polymeric systems have been developed to combine two or more stimuli-responsive mechanisms into one polymeric system, for example, temperature-sensitive polymers may also respond to pH changes (Bignotti *et al.* 2000; Pinkrah *et al.* 2003; Peng and Cheng. 2001). On the other hand, some works have been reported that two or more signals could be simultaneously applied in order to induce a response in so-called dual responsive polymer systems (Kurisawa and Yui. 1998). Thus, stimuli-responsive hydrogels are interesting polymeric biomaterials for biotechnological, pharmaceutical, and biomedical applications (Kashyap *et al.* 2004). In **Table 2.2** we have listed out of different stimuli sensitive hydrogels, their mechanisms of response and examples of the polymers used in drug delivery.

## LITERATURE REVIEW

**Table 2.2: Examples of different types of stimuli responsive hydrogels along with their mechanisms in brief (Mura *et al.* 2013; Muhammad *et al.* 2017)**

Nature of Stimulus	Stimulus	Mechanism	Polymers	References
Biological stimuli	Antigen	Hydrogel respond to the free antigen and undergo swelling followed by drug release	<i>N</i> -succinimidyl acrylate based antigen-antibody entrapment hydrogel	Miyata <i>et al.</i> 1999; Miyata <i>et al.</i> 2002; Lu <i>et al.</i> 2003; Ullah <i>et al.</i> 2015
	DNA	Single stranded (ss) DNA grafted hydrogel probes show swelling in the presence of ssDNA	Single stranded DNA probe- <i>g</i> -poly(acrylamide) hydrogels	Murakami <i>et al.</i> 2006
	Enzyme	Enzymes cause hydrogel degradation and consequently the drug release. This is called a chemically controlled drug release mechanism.	Glycidylmethacrylate dextran- <i>g</i> -poly(acrylic acid)	Kim and Oh. 2005
Chemical stimuli	CO <sub>2</sub>	In CO <sub>2</sub> sensors, a pH sensitive hydrogel disc comes in contact with bicarbonate solution. On exposure to CO <sub>2</sub> , the pH of solution changes resulting in swelling or deswelling of the hydrogel which causes a change in pressure which is a	Poly(2-hydroxyethylmethacrylate)- <i>co</i> -(2-dimethylaminoethylmethacrylate)	Herber <i>et al.</i> 2003

## LITERATURE REVIEW

Nature of Stimulus	Stimulus	Mechanism	Polymers	References
		measure of the partial pressure of CO <sub>2</sub> .		
	Glucose	Hydrogels show swelling in response to increased glucose concentration. The complex formed between glucose and phenylboronic acid drives the swelling of the hydrogels and consequently insulin release	Poly(acrylamide)- <i>co</i> -(3-acrylamidophenylboronic acid)	Guenther <i>et al.</i> 2013
	Ionic strength	Change in ion concentration also causes swelling and drug release.	Kappa carrageenan- <i>g</i> -poly(acrylic acid) hydrogels	Rasool <i>et al.</i> 2013
	pH	Shift in pH causes change in the charge on the polymer chains leading to swelling and drug release.	Polyvinyl sulfonic acid, polymethacrylic acid, polydiethylamino ethyl methacrylate, polydimethylaminoethyl methacrylate, Poly(acrylic acid), Guar gum succinate, Kappa-	Eichenbaum <i>et al.</i> 1998; Kim <i>et al.</i> 2005; Sen and Sari, 2005; Bossard <i>et al.</i> 2006; Kozlovskaya <i>et al.</i> 2006 Vamvakaki <i>et al.</i> 2006

## LITERATURE REVIEW

Nature of Stimulus	Stimulus	Mechanism	Polymers	References
			carrageenan/poly(vinyl alcohol)	
	Redox	Disulfide linkages in reduction sensitive hydrogels cleave in the reductive environment (high level of glutathione concentration = 0.5–10 mM) in intracellular matrix and release bioactive molecules/drugs.	[poly(ethylene glycol) monomethyl ether]-graft-[disulfide linked poly(amido-amine)] and $\alpha$ -cyclodextrin	Yu <i>et al.</i> 2011
Physical stimuli	Electric	Changes in electrical charge distribution within the hydrogels matrix on the application of electric field cause swelling–deswelling and is consequently responsible for the on demand drug release.	Polythiophene and polypyrrole	Qiu and Park. 2001; Jeong and Gutowska. 2002
	Light	Exposure to light (UV and visible light) reversibly changes the hydrogel from its flowable form to non-flowable form and vice versa.	Poly(trimethylenium iminium trifluorosulfonimide) and 2,6-bis(benzoxal-2-yl)pyridine blend	Alvarez-Lorenzo <i>et al.</i> 2009; Kirschner, and Anseth. 2013
	Magnetic field	When a magnetic field is applied, it causes pores in	Magnetite nanoparticles and poly(acrylamide)	Namdeo <i>et al.</i> 2009

## LITERATURE REVIEW

Nature of Stimulus	Stimulus	Mechanism	Polymers	References
		the gel to swell leading to drug release.	composite hydrogels	
	Pressure	Swelling under increased pressure and vice versa. This fact is due to an increase in lower critical solution temperature (LCST) value of hydrogels with pressure. LCST is the temperature below which negative thermos-responsive hydrogels swell	Poly( <i>N</i> -isopropyl acrylamide), poly( <i>N,N</i> -diethylacrylamide )	Qiu and Park. 2001; Pan <i>et al.</i> 2014
	Temperature	Shift in temperature changes polymer-polymer and polymer-water interaction responsible for swelling and drug release.	Chitosan-Poly(acrylamide)	Khan <i>et al.</i> 2013
	Ultrasound	Exposure to ultrasound temporarily breaks the ionic cross-links in the hydrogels and the drug is released but cross-links are reformed on discontinuation of the ultrasound waves. This facilitates on-demand drug release	Calcium alginate Poly(lactic acid)	Huebsch <i>et al.</i> 2014; Zardad <i>et al.</i> 2016

# LITERATURE REVIEW

## 2.4.1 Temperature responsive hydrogels

Temperature responsive hydrogels are regarded as the essential materials in the biomaterial and biomedical applications, due to their ability to respond to temperature fluctuations like certain diseases manifest temperature changes in the body. (Cabane *et al.* 2012; Rasheed *et al.* 2018). Numerous researchers have studied about the applications of hydrogels in the area of water management, shape memory materials, smart drug delivery system, injectable scaffolds, smart fluids, biosensors and smart cell culture dishes (Peppas *et al.* 2000; Schmaljohann *et al.* 2003; He *et al.* 2008). Temperature responsive hydrogels have inherent ability to change its solution state to gel state (sol-gel phase transition) at a critical solution temperature (Peppas *et al.* 2000; Kashyap *et al.* 2004). These polymeric structures possess a unique feature called critical solution temperature (CST) wherein the polymer undergoes a phase transition. This transition causes changes in hydrophobic/hydrophilic balance, solubility and confirmation in the polymeric structure (Joglekar and Trewyn. 2013). Polymers that possess a lower critical solution temperature (LCST) typically undergo a sol-gel phase transition when heated above their LCST, whereas polymers that become soluble upon heating are expected to possess an upper critical solution temperature (UCST). (Fitzpatrick *et al.* 2012). Additionally, these polymeric units also contain hydrophobic groups such as ethyl, methyl, or propyl. CST can be finely tuned using a combination of hydrophobic and hydrophilic polymers. (Joglekar and Trewyn. 2013).

However, in the case of polymers with an LCST (**Figure 2.6**), the solubility decreases as temperature increases and therefore hydrogels made of these polymers shrink as the temperature increases above the LCST. This type of swelling behavior is known as inverse temperature dependence and occurs due to predominating hydrophobic interactions in the polymeric chain (Qiu and Park. 2001; Chaterji *et al.* 2007). These hydrogels are made of polymer chains that possess either moderately hydrophobic groups or a mixture of hydrophilic and hydrophobic segments. At lower temperatures, hydrogen bonding between the hydrophilic segments and water leads to enhanced dissolution; however, as the temperature increases, the hydrophobic segments are strengthened and thus resulting in shrinking of the hydrogels due to inter-polymer chain associations (Qiu and Park. 2001; Bawa *et al.* 2009)

## LITERATURE REVIEW

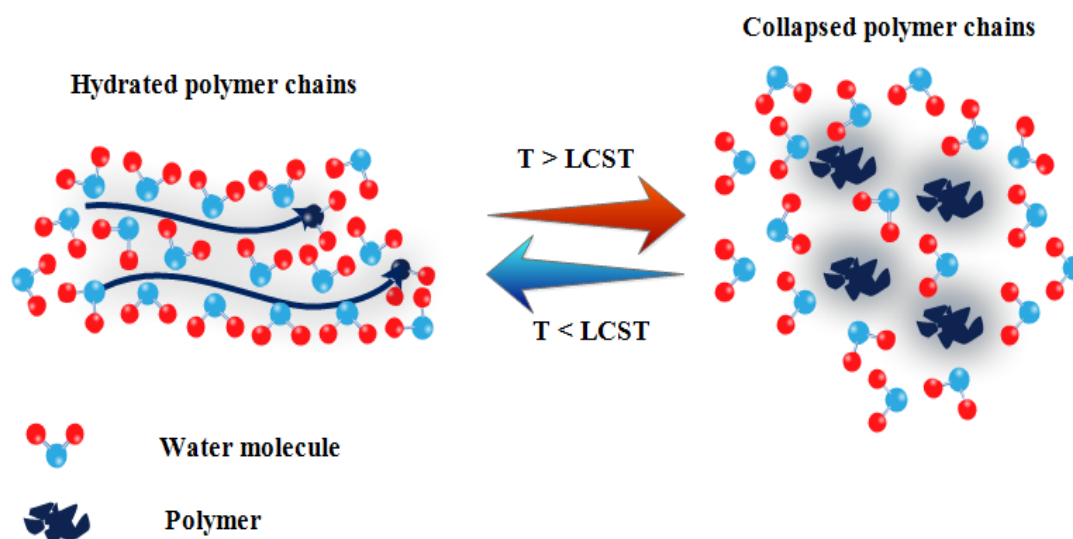


**Figure 2.6: Phase separation mechanism of temperature responsive polymer above and below LCST temperature.**

Consequently, the polymers collapse and aggregates and the phases separates because the hydrogen bonds between the hydrophobic parts of the polymer molecules are favored compared to the water molecules, which are re-organized around the non-polar polymer. The expansion or collapse that correlates with the critical shift in aqueous solubility has been utilized as a mechanism for drug delivery, membrane separation/cleaning, and recently, in situ gelling scaffolds for tissue regeneration (Koetting *et al.* 2015). The list of a few polymers used for the synthesis of thermosensitive hydrogels are shown in the below **Table 2.3** (Cao *et al.* 2015).

**Table 2.3: Polymers with LCST/UCST behavior in aqueous solution**

Polymer	Phase transition temperature in aqueous solution	Behavior in aqueous solution
Poly(N-isopropyl acrylamide)	30-34 °C	LCST behavior
Poly(N, N-diethyl acrylamide)	28-32 °C	
Poly(methyl vinyl ether)	37 °C	
Poly(N-vinylcaprolactam)	30-35 °C	



## LITERATURE REVIEW

Polymer	Phase transition temperature in aqueous solution	Behavior in aqueous solution
Poly(N-ethylmeth acrylamide)	58 °C	
Poly(2-ethoxyethyl vinyl ether)	20 °C	
Block copolymers of Poly(ethylene oxide) and Poly(propylene oxide)	20-85 °C	
Poly(pentapeptide) of elastin	28-30 °C	
Poly( <i>N</i> -vinyl- <i>n</i> -butyramide)	32 °C	
PAAm/PAAc IPN	25 °C	UCST behavior

### 2.5 Applications of temperature responsive hydrogels

Among all stimuli-sensitive hydrogels, temperature responsive hydrogels are widely studied because the change of temperature is not only relatively easy to control but also easy to apply in both *in vitro* and *in vivo* conditions. Thermo-sensitive hydrogels are widely used in surface coating industries and particularly in the automotive industry (Meléndez-Ortiz *et al.* 2015). It is also used in improving the rheological properties of paints. Thermo-sensitive hydrogels are being widely used in proteins (Kawaguchi *et al.* 1992; Fujimoto *et al.* 1993), cells (Achiha *et al.* 1995) and enzyme immobilization (Shiroya *et al.* 1995; Yasui *et al.* 1997). Currently, researchers are trying to use these hydrogels to recover oil from petroleum industries (Snowden *et al.* 1993), microgel-based photopolymers used as offset printing plates and photographic film (Sasa and Yamoka, 1994), as environmentally sensitive optoelectronic devices (Sawai *et al.* 1991; Weissman *et al.* 1996). Thermo-sensitive hydrogels are having either cationic or anionic surface charges which have potential applications for the removal of ionic contaminants from wastewater (Snowden *et al.* 1993). Among these applications, hydrogel-based drug delivery devices have become a major area of research. The sol-gel property of the temperature sensitive hydrogels above and below the critical

## LITERATURE REVIEW

temperature has been utilized in many ways in drug delivery, biomedical and biotechnology applications.

For drug delivery applications polymer response should be non-linear, i.e. with distinct ‘on’ and ‘off’ states and there is a drive to develop materials that display very sharp transitions for a small stimulus or change in environment. One way to accomplish this is by further elaboration of hydrogel structures at the micro- and nano-scale. In 1995, Yoshida and coworkers reported grafting of linear PNIPAM oligomers to existing cross-linked hydrogels has enhanced the rate of total gel collapse (20 min compared to 1 day) as a result of the rapid aggregation of the non-cross-linked oligomers, which then act as ‘hydrophobic nuclei’ to which the rest of the network can more quickly associate (Yoshida *et al.* 1995; Kikuchi and Okano. 2002), as shown in **Figure 2.7**.

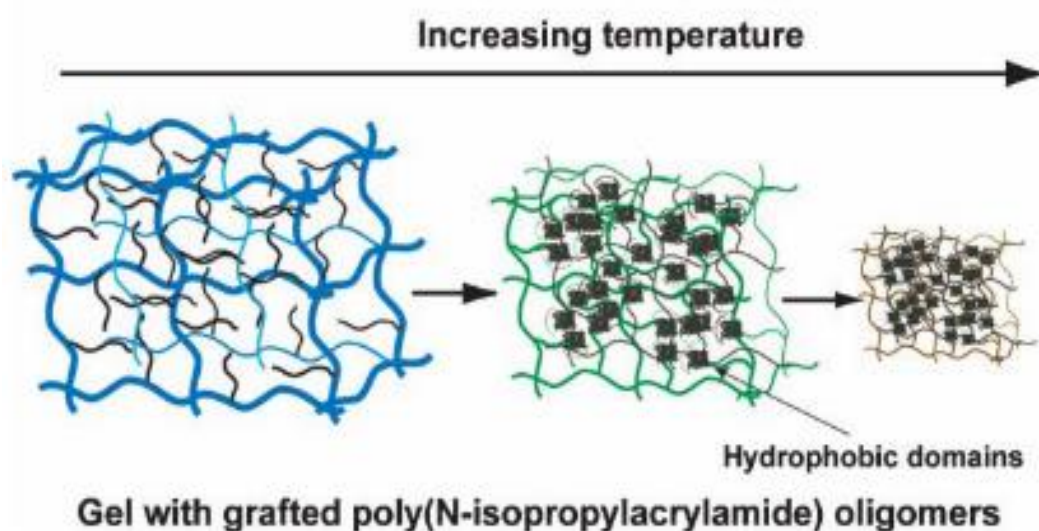


**Figure 2.7: Architecture of poly(N-isopropylacrylamide) oligomer hydrogel**  
(Yoshida *et al.* 1995; Kikuchi and Okano. 2002).

Li *et al.* (2008) used the PLGA-PEG-PLGA hydrogel to fabricate the novel thermosensitive hydrogel carriers. The sol-gel transition temperature of the hydrogel was below the body temperature, and the gel-sol transition temperature was greater than the physiological temperature but less than the temperature that the body can bear, about 40–44 °C. The drug release from these carriers at the physiological body temperature was too little, while at the high temperature (i.e., 42 °C), it had released large amount

## LITERATURE REVIEW

of drug. In this way, thermosensitive drug delivery system can undergo reversible structural transitions from a closed state to an open state with the help of external temperature stimuli, giving on-off switches for modulated drug delivery (**Figure 2.8**) (Li *et al.* 2008; Shoa *et al.* 2011).

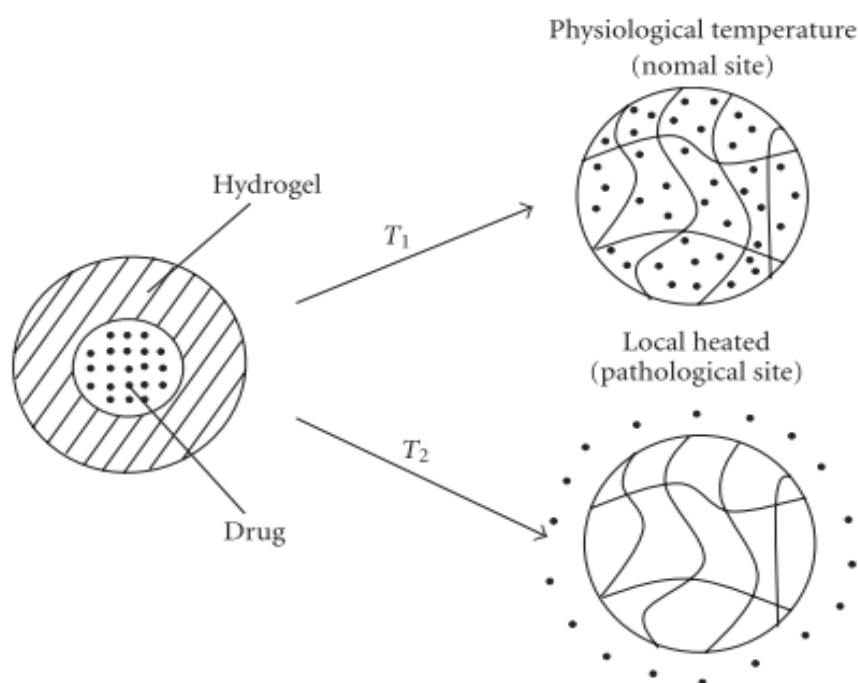


**Figure 2.8: Temperature responsive hydrogel carrier for targeted drug delivery**

(Li *et al.* 2008; Shoa *et al.* 2011).

Thermosensitive hydrogels for nasal drug delivery was developed using N-trimethyl chitosan chloride as polymer. Poly(ethylene glycol) and glycerophosphate showed promising role, particularly in rheological and mucoadhesive behavior, and a sol–gel transition was achieved at 32.5 °C within 7 min (Langer. 1998; Sood *et al.* 2014). Core-shell polymer particles and micelles consisting of temperature responsive polymers with an inner hydrophobic core and a hydrophilic shell have been utilized to control the drug release with temperature changes. The core has been loaded with hydrophobic drugs while the hydrophilic shell responds to the temperature and stabilizes the structure (Soga *et al.* 2005). As a result of the collapse of the shell, the structural deformation of the core controls the release of the drug. Selective removal or separation of substances from aqueous solutions can be obtained with temperature-sensitive

## LITERATURE REVIEW

polymers (Hoffman *et al.* 1986). Temperature sensitive hydrogels may be used to absorb toxins from the solutions upon relatively small temperature changes. In tissue repair, in-situ hydrogels offer an advantageous alternative to surgery, which can be injected in the body cavity that solidifies in the body temperature, shaping ideally (Jeong and Gutowska, 2002). Pharmaceutically best-known group of temperature sensitive polymers in situ-administration are block copolymers of ethylene oxide and propylene oxide, known as Poloxamers (Pluronics®). They can form a gel at 25 °C to 40 °C depending on the polymer chain composition. Increased solubility, metabolic stability and enhanced circulation time for the drugs have been achieved with Pluronics® (Kabanov *et al.* 2002).

Vuluga and co-workers reported the synthesis of a novel thermoresponsive cross-linked hydrogel based on different molecular weight of poly(propylene glycol)s (PPG) and diepoxy-terminated poly(ethylene glycol)s (PEG) to control the multi-block copolymer structure (Anghelache *et al.* 2014). In an ideal situation, the hydrogel structure is expected to contain one PPG block and two PEG chains linked to the same amine group, leading to a structure with each PPG block surrounded by four PEG blocks, while each PEG block has two PPG blocks and two PEG blocks as neighbors. Both thermoresponsive and swelling properties can be adjusted by controlling the molecular weight of the constituent blocks or the salt added in (Anghelache *et al.* 2014; Chai *et al.* 2017). Yan *et al.* (2018) developed different approach to treat cancer using the physical force for expanding stimuli-responsive hydrogel to rupture cancer cells attached on its surface. Specifically, they coated PNIPAM hydrogels with a layer of cell-adherent arginine-glycine-aspartate (RGD) peptides, by allowing cancer cells to attach onto the surface of the hydrogels and then applying a change in temperature. As the hydrogel underwent a chemical transformation and expanded due to the stimulus, the cancer cells attached to it ruptured. They reported breast and lung cancer cells died after the hydrogel expanded; that showed physical force for expanding hydrogel is strong enough to rupture the cancer cells (Yan *et al.* 2018). Various drugs delivered through temperature-responsive hydrogel are summarized in **Table 2.4.**

## LITERATURE REVIEW

**Table 2.4: List of temperature responsive hydrogels and their applications**

(Sood *et al.* 2014)

<b>Polymers</b>	<b>Application</b>	<b>Inference</b>	<b>Reference</b>
1-vinyl-2-pyrrolidinone and N-isopropyl acrylamide	Controlled analgesic drug delivery	The hydrogels were designed to achieve phase transition temperature near body temperature and further active component got released at a slower rate at temperature above LCST	Graham & Mc-Neil (1984)
Multiblock copolymers synthesized from pluronic and di-(ethylene glycol) divinyl ether	Used as delivery vehicle for controlled and sustained release of plasmid DNA	Acid-labile temperature-responsive sol–gel reversible polymer enhanced gene delivery to the myocardium and skeletal muscle cells	Hinrichs & Suhuermans (1999)
N-isopropyl acrylamide and N,N-dimethyl aminoethyl methacrylate	Delivery of DNA	Improved gene delivery and effective gene transfection	Harasaki <i>et al.</i> (2001)
Pluronic F127 and N-(3-aminopropyl) methacrylamide	Anabolic cell and tissue growth	Hydrogels exhibit swelling and collapse behavior in aqueous solution with the increase in temperature	Gong & Osada (2004)
Poly[(2-ethoxy) ethoxy ethyl vinyl ether]	Provide tumor-specific chemotherapy	Temperature-sensitive properties providing controlled drug release	Hejazi & Amiji (2003)
Polyethylenimine (PEI)-plasmid DNA complexes	Improved transfection efficacy	Acid-labile temperature-responsive sol–gel reversible polymer were prepared for	Hench & Jones (2005)

## LITERATURE REVIEW

		enhanced gene delivery to the myocardium and skeletal muscle cells	
Poly(N-isopropyl acrylamide) and Chitosan	Injectable opioid analgesic	The gelation temperature of hydrogel is well below body temperature which make it ideally suited to function as injectable drug depots.	Geisse (2009)
Chitosan, Polyethylene glycol and Polyacrylic acid	Nasal drug delivery	Hydrogel exhibit sol–gel transition at 32.5 C and hydrogel forms rheologically synergy	Gupta <i>et al.</i> (2010)
Pluronic	Controlled protein delivery	Multi-block hydrogels showed enhanced gel stability, linear mass erosion rates, mechanical strength and zero-order hGH release profile was observed.	Gorgieva & Kokol (2012)

### 2.6 PDEA based temperature responsive hydrogels for drug delivery

Recently, N-substituted polyacrylamide has received interest in the field of drug delivery. Poly(N, N-diethyl acrylamide) (PDEA) is the most used sensitive hydrogel among all the hydrogels. PDEA undergo phase separation at LCST of approximately 31 °C in aqueous solution (Marcelo *et al.* 2010; Sood *et al.* 2014). The tertiary amide group of N, N-diethyl acrylamide (DEA) make it as hydrogen bond acceptor that can form a hydrogen bond with hydrogen bond donor (Wei *et al.* 2016). The hydrophilic amide groups and hydrophobic diethyl side groups, the vinyl backbone in the main chain of the polymer structure is as shown in **Figure 2.9** (Li *et al.* 2009). With the fluctuations of the surrounding temperature, the PDEA demonstrates LCST in water by balancing the hydrogen bonds and hydrophilic interactions. However, temperature-sensitive hydrogel shows some disadvantages like poor mechanical strength and low swelling/deswelling properties (Qiu and Park. 2001).

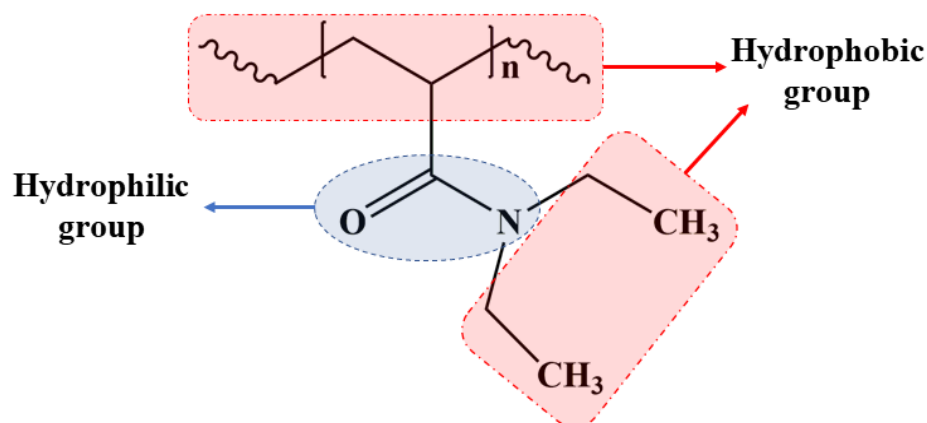


**Figure 2.9: Structure of Poly (N, N - diethyl acrylamide)**

Polymeric structure undergoes reversible hydration–dehydration changes in response to a temperature around their LCST temperature in aqueous media. PDEA hydrogel demonstrates LCST behavior near physiological temperature. The hydrophilic and hydrophobic group of PDEA repeated units holds a large amount of water (>90%, w/v). Presence of hydrophilic and hydrophobic groups in the PDEA can store and release the active agent exhibiting a rapid change in the swelling behavior and structure in response to temperature as an attractive candidate for controlled drug delivery (Ngadaonye *et al.* 2012). At low temperatures, a hydrogen bond is found between the amide groups and water molecules, outweighs the unfavorable free energy related to the exposure of hydrophobic groups to water molecules, leading to good solubility of the polymer in water. As the temperature increases, the hydrogen bond weakens, and hydrophobic interactions between the hydrophobic side groups strengthen. Above the LCST, the interactions between hydrophobic groups become dominant, leading to an entropy-driven polymer chain collapse and phase separation (Amélia *et al.* 2008; Strandmana *et al.* 2012). Otake *et al.* and others also suggested that this phase separation is attributable to the hydrophobic interactions (Taylor and Cerankowski. 1975; Otake *et al.* 1990; Feil *et al.* 1993). They proposed that the excellent solubility of the polymer at a lower temperature is due to the hydration and water molecules forming cage-like structures around the hydrophobic group. Increase in the temperature leads to the destruction of the structured water molecules around the hydrophobic groups and association of the hydrophobic groups of polymer chains start. The LCST phase separation occurs when

## LITERATURE REVIEW

the entropy contribution ( $T\Delta S$ ) to the Gibbs free energy ( $\Delta G$ ) exceeds the enthalpy ( $\Delta H$ ).

However, PDEA is considered to be more suited for drug delivery than poly(N-isopropylacrylamide) (PNIPAM) and it is most commonly used thermos-responsive polymer. As compared to NIPAM, DEA lacks amide hydrogen, can form a single intermolecular hydrogen bond as proton acceptor with water, but cannot form an intramolecular hydrogen bond as a proton donor. This structural difference makes the volume transition of PNIPAM gel release the drug abruptly, whereas PDEA gel release the drug continuously (Tirumala *et al.* 2006). Panayiotou *et al.* (2007) reported that the cytotoxicity of PNIPAM samples was more than that of PDEA when both were prepared similarly.

### 2.7 Tuning LCST of PDEA hydrogels for drug delivery

The LCST of PDEA is not always favorable for biomedical applications since the desired LCST for biomedical application should be or near the physiological temperature (37 °C) and in pathological states, this value can be higher than 41 °C (Siqueira *et al.* 2018). Therefore, modification of PDEA hydrogel by incorporating functional groups has become the focus of considerable research groups which may also increase drug release from thermos-sensitive polymers, thereby increasing the effectiveness of the treatment. It usually involves modifying DEA hydrogel by copolymerizing with hydrophilic or hydrophobic monomers, clay particles, nanoparticles, etc. (Kratz *et al.* 2000; Ma *et al.* 2004; Bradley and Vincent, 2005). Generally, the incorporation of hydrophobic monomers leads to decrease in LCST while the hydrophilic monomers lead to increase in LCST (Benrebouh *et al.* 2001; Liu *et al.* 2001). The goal of these modifications is to improve other properties of the hydrogel while retaining their sharp phase transition behavior.

In 1935, Heymann modified methylcelluloses (Heymann, 1935), and studied the water solubility (considered copolymers with a random distribution of hydrophobic and hydrophilic segments). Taylor and Cerankowski (1975) popularized the concept of copolymerizing hydrophilic and hydrophobic monomers to produce polymers with LCST phase behavior in water, and they recognized that it is possible to develop various



## LITERATURE REVIEW

temperature-responsive polymers by copolymerizing hydrophobic monomers with more water-soluble monomers. They also proposed building a monomer that would have a balance of hydrophobic and hydrophilic interactions that would allow one to homopolymerize it to form a temperature-responsive polymer. **Table 2.5** describes a few works related to shifting of LCST by copolymerizing with the suitable hydrophilic/hydrophobic monomer, and nanomaterials based on their application. The choice of co-monomer when designing biocompatible systems needs careful consideration. As a polymer, the co-monomer should be highly hydrophilic, stable, biocompatible polymer (Ma *et al.* 2009).

**Table 2.5: Tuning the LCST of PDEA hydrogel**

Polymer	Polymerization	LCST (°C)	Reference
Poly(N,N-diethylacrylamide-co-glycol methacrylate)	Transesterification of polyDEAAm-co-HEMA,	30-32 at pH 4	Bromberg, and Levin. 1996
Poly(N,N-diethylacrylamide)	Group transfer polymerization	29.8-30	Ecgert and Freitag. 1994
	Free radical polymerization	28.2-37	Lessard <i>et al.</i> 2003
	Free radical polymerization	30-32	Panayiotou and Freitag. 2005
	Surfactant-Free Emulsion Polymerisation	25-38	Panayiotou <i>et al.</i> 2007
	Reversible addition fragmentation chain transfer (RAFT) radical polymerization	23-34	Li <i>et al.</i> 2009
	Solution radical polymerization	26.95-35.76	Cai <i>et al.</i> 2001

## LITERATURE REVIEW

Polymer	Polymerization	LCST (°C)	Reference
Poly(N,N-diethylacrylamide-co-acrylic acid)	Free-radical-polymerization	Close to the physiological temperature	Liu <i>et al.</i> 2008
	Emulsion polymerization	29-46 at pH 5	Li <i>et al.</i> 2016
Poly(N,N-diethylacrylamide-co-methylacrylic acid)	Free-radical-co-polymerization	32-34	Liu and Liu. 2003
	Radical co-polymerization	25-38	Liu <i>et al.</i> 2008
poly(N,N-diethylacrylamide)-poly(acrylic acid)-poly(N,N-diethylacrylamide)	Anionic living polymerization	35	Angelopoulos and Tsitsilianis. 2006
Poly ( N , N - diethylacrylamide- co - 2-hydroxyethyl methacrylate )	Emulsion polymerization	20-28	Colonne <i>et al.</i> 2007
Kappa- carrageenan-g-poly(methacrylic acid)/poly(N,N-diethylacrylamide)	Free-radical-polymerization	28	Chen <i>et al.</i> 2009
Poly((2-dimethylamino)ethyl methacrylate)/poly(N,N-diethylacrylamide) semi-IPN	Free-radical-co-polymerization	31	Zhang <i>et al.</i> 2011
N, N-diethylacrylamide with 1-vinyl-2-pyrrolidinone and N,N-dimethylacrylamide	Free-radical-cross-linking co-polymerization	28.3-44.3	Luke <i>et al.</i> 2011

## LITERATURE REVIEW

Polymer	Polymerization	LCST (°C)	Reference
Poly(N,N-diethylacrylamide- co-(2-dimethylamino) ethyl methacrylate)	Free-radical-polymerization	31-39	Chen <i>et al.</i> 2011
Chitosan-poly(N,N-diethyl acrylamide) IPN films	Photopolymerisation	28.7-29.4	Jude <i>et al.</i> 2013; Jude <i>et al.</i> 2014
Laponite- crosslinked Poly(N,N-diethylacrylamide - (2-dimethylamino) ethyl methacrylate)	<i>In situ</i> free radical polymerization	26.66-29.98	Huili <i>et al.</i> 2015
Linear, cyclic, and star-shaped Poly(N, N-diethylacrylamide)	B(C <sub>6</sub> F <sub>5</sub> ) <sub>3</sub> -Catalyzed Group Transfer Polymerization	34.6-42.7	Kikuchi <i>et al.</i> 2016
Salecan/poly(N,N-diethylacrylamide)	Free-radical-polymerization	About 31	Wei <i>et al.</i> 2016
N, N-Dimethyl- $\alpha$ (hydroxymethyl) acrylamide with N, N-Diethylacrylamide	Radical polymerization	32-64	Yasuhiro and Yoshiaki. 2016
Interpenetrating (IPN) and semi interpenetrating (SIPN) network hydrogels of poly(N,N-diethylacrylamide)/ polyacrylamide	Free-radical-polymerization	29.75 (PDEA), 29.85-36.55 (IPN), 31.85-36.75 (SIPN)	Lenka <i>et al.</i> 2016

## LITERATURE REVIEW

Polymer	Polymerization	LCST (°C)	Reference
Poly(vinyl alcohol)-graft-poly(N,N-diethylacrylamide)	Microwave-assisted graft copolymerization	29–31	Nuran and Hacer. 2018
Poly(N,N-diethylacrylamide) grafted pectin copolymer	Microwave induced copolymerization	31	Nuran and Şeyma. 2018
poly (N,N-diethylacrylamide-b-N-vinylpyrrolidone)	Reversible addition fragmentation chain transfer polymerization	33.3-36	Xiayun <i>et al.</i> 2018
Poly (N,N-diethylacrylamide-co-N,N-dimethylacrylamide) side chains	Free radical copolymerization and grafting onto technique in aqueous solution	31.7-52.4	Xu <i>et al.</i> 2018

### 2.8 Nanotechnology

Over 130 years' nanomaterials have been successfully applied in medicine, like colloidal silver used for the prevention of infections. From 1960s, in modern medicine iron dextran is used in nanomedicines (McDonald *et al.* 2015). The first results related to the development of nanomedicine is reported in the late 1960's at ETH Zurich (Boisseau and Loubaton. 2011). Anticipated application of nanotechnology in medicine includes drug delivery, both in vitro and in vivo diagnostics, nutraceuticals and production of improved biocompatible materials (De Jong and Borm. 2008). Nanotechnology is the manipulation of matter on an atomic, molecular, and supramolecular scale involving the design, production, characterization, and application of different nanoscale materials in several vital areas providing innovative technological advances mainly in the field of medicine (so-called Nanomedicine) (Silva *et al.* 2014). By applying nanotechnology to medicine, nanoparticles have been created to mimic or alter biological processes (Singh and Lillard. 2009). Nanoparticles are

## LITERATURE REVIEW

stable, colloidal particles with a size range from 10 nm to <1000 nm; however, for nanomedical application, the preferred size is less than 200 nm (Biswas *et al.* 2014).

Development of novel nano-sized particulate drug delivery systems (DDS) has shown the profound impact on disease prevention, diagnosis, and treatment. Although, the drug delivery system (DDS) concept is not new, considerable progress has been made in the treatment of variety of diseases. Targeting delivery of drugs to the diseased lesions is one of the most critical aspects of DDS. To convey a sufficient dose of the drug to the lesion, suitable carriers of drugs are needed. These delivery systems offer numerous advantages compared to conventional dosage forms, which include improved efficacy, reduced toxicity, and improved patient compliance and convenience. Such systems often use macromolecules as carriers for the drugs. By doing so, treatments that would not otherwise be possible are now in conventional use. This field of pharmaceutical technology has grown and diversified rapidly in recent years. Understanding the derivation of the methods of controlled release and the range of new polymers can be a barrier to involvement from the non-specialist. Among different DDS, nano-sized particles are important, due to their tendency to accumulate in diseased areas of the body. Attractive properties of nano-sized particles occupy a unique position in drug delivery technology (Kumar. 2000).

Nanoscale drug delivery systems such as nanoparticles, liposomes, dendrimers, fullerenes, nanopores, nanotubes, nanoshells, quantum dots, nanocapsule, nanosphere, nanovaccines, nanocrystals, etc. are believed to have potentials to revolutionize drug delivery systems (Mukherjee *et al.* 2014). The nanomaterials used as DDS should be soluble, safe and biocompatible as well as bioavailable. Further nanomaterials on chips, nanorobotics, and magnetic nanoparticles attached to a specific antibody, nanosize empty virus capsids, and magnetic immunoassay are new dimensions of their use in drug delivery (Mukherjee *et al.* 2014).

**Liposomes** are a tiny bubble (vesicle) in which an aqueous volume is surrounded by a membrane composed of a phospholipid bilayer (Dhandapani *et al.* 2013). Liposomes, sphere-shaped vesicles consisting of one or more phospholipid bilayers, were first described in the mid-60's. Since then, liposomes have made their way to the market. Among several new drug delivery systems, liposomes characterize an advanced

## LITERATURE REVIEW

technology to deliver active molecules to the site of action, and at present, several formulations are in clinical trial. Research on liposome technology has progressed from conventional vesicles to ‘second-generation liposomes’, in which long-circulating liposomes are obtained by modulating the lipid composition, size, and charge of the vesicle. Liposomes with modified surfaces have also been developed using several molecules, such as glycolipids or sialic acid (Akbarzadeh *et al.* 2013).

**Micelles** are self-assemblies of amphiphiles that form supramolecular core-shell structures in the aqueous environment. Hydrophobic interactions are the predominant driving force in the assembly of the amphiphiles in the aqueous medium. Nanosized micellar delivery systems are made up of amphiphilic polymers that consist of a low molecular weight hydrophobic core-forming block. Due to low monomer concentration in equilibrium with the micelles, these micellar delivery systems have reduced toxicity and are more thermodynamically stable. The biodistribution and pharmacokinetics of drugs such as doxorubicin, cisplatin, and paclitaxel are altered favorably (Kumar. 2009).

**Dendrimer** chemistry was first introduced in 1978 by Fritz Vogtle and coworkers (Babu *et al.* 2010). They synthesized the first “cascade molecules”. In 1985, Donald A. Tomalia (Babu *et al.* 2010), synthesized the first family of dendrimers. At the same time, Newkome’s group independently reported the synthesis of similar macromolecules, they called them “arborols” (Babu *et al.* 2010). The term “cascade molecule” is also used, but ‘dendrimer’ is the best established one. Due to their multivalent and monodisperse character; dendrimers have stimulated broad interest in the field of chemistry and biology, especially in the field of drug delivery, gene therapy and chemotherapy (Bai *et al.* 2006). They are hyperbranched and monodisperse three-dimensional molecules with defined molecular weights, large numbers of functional groups on the surface and well-established host-guest entrapment properties. They are made up of layers of polymer surrounding a central core (Babu *et al.* 2010). The dendrimer surface contains many different sites to which drugs may be attached and also attachment sites for materials such as polyethylene glycol (PEG) which can be used to modify the way the dendrimer interacts with the body (Padilla *et al.* 2002).

## LITERATURE REVIEW

**Metal nanoparticles** are more flexible particles compared to other nanomaterials owed to the possibility of controlling the size, shape, structure, composition, assembly, encapsulation and tunable optical properties (Huang *et al.* 2007; Figueiredo *et al.* 2014). Applications of metal nanoparticles have been dominated by the use of nano-bioconjugates that started in 1971 after the discovery of immune gold labeling by Faulk and Taylor (Hayat. 1989). Metal nanoparticles have been used in various biomedical applications including probes for electron microscopy to visualize cellular components, drug delivery (vehicle for delivering drugs, proteins, peptides, plasmids, DNAs, etc.), detection, diagnosis and therapy (targeted and non-targeted) (Bhattacharya and Mukherjee. 2008; Goldman *et al.*, 2004; Alivisatos and Gu. 2005).

**Nanohydrogels** are composed of flexible hydrophilic polymers in the nanosize scale. Upon equilibrium or swelling in water, the drug can be loaded spontaneously into the nanohydrogels, resulting in the reduction of the solvent volume, leading to gel collapse and formation of dense nanoparticles. The swelling and collapse properties of the nanohydrogels are unique for the nanoscale pharmaceutical carriers and provide multiple benefits for engineering optimal drug loading and release of drugs. Furthermore, nanohydrogels can be chemically modified to incorporate various ligands for targeted drug delivery, triggered drug release or preparation of composite materials. Preclinical studies suggest that nanohydrogels can be used for efficient delivery of biopharmaceuticals in cells as well as for increasing drug delivery across cellular barriers (Kumar, 2009).

**Quantum dots** are tiny semiconductor nanocrystals type of particles generally no larger than 10 nanometers that can be made to fluoresce in different colors when stimulated by light. The biomolecule conjugation of the QD can be modulated to target various biomarkers (Gangrade. 2011). They can be tagged with biomolecules and used as highly sensitive probes. QD can also be used for imaging of sentinel node in cancer patients for tumor staging and planning of therapy. This technology also outlines some early success in the detection and treatment of breast cancer (Gao and Dave. 2007). QD may provide new insights into understanding the pathophysiology of cancer and real-time imaging and screening of tumors. The advantages and disadvantages of different nano-carriers are given in **Table 2.6** (Mpho *et al.* 2013).

## LITERATURE REVIEW

**Table 2.6: Advantages and disadvantages of different nano-carriers used as DDS**

(Mpho *et al.* 2013).

<b>Drug Delivery Systems</b>	<b>Applications</b>	<b>Advantages / Disadvantages</b>
Nanosystems	Metallic nanoparticles - gold, silica, copper, silver	Magnetic resonance imaging and photothermal ablation of cancer cells. Carriers can cross the BBB
	Polymeric nanoparticles - synthetic/natural polymers such as /lipid/proteins	Biodegradable, surface modification for targeted and responsive drug delivery and biocompatibility
	Carbon nanotubes	High propensity to cross cell membrane via endocytosis. Can deliver therapeutics in the form of peptides and nucleic acids.
Dendrimer	Scaffold - multiple and highly branched monomers emerge from the central core	Modifiable surface allowing easy conjugation for target specificity and multiple drug conjugation.
Micelles	Polymeric micelles - Amphiphilic copolymers	Suitable for the water-insoluble drug. Useful for targeted drug delivery.
Liposomes	Self-assembling spheres composed of lipid bilayers	Biocompatible and can deliver sensitive therapeutics (DNA). Engulfed by endoreticulum.



# LITERATURE REVIEW

## 2.9 Graphene quantum dots (GQDs)

Carbon is one of the most abundant elements on the earth, exists in many forms of allotropes. The football-shaped fullerenes first characterized in 1985 by Kroto (1985), and the needle-like carbon nanotubes (CNTs) was discovered in 1991 by Iijima, and has generated an enormous and growing interest in the field of carbon materials. In 2004, Geim and Novoselov discovered graphene and then won the Nobel Prize for physics in 2010. They used a special kind of tape to spin out a graphite flake into graphene with one layer of carbon atoms (Katsnelson and Novoselov. 2007). Compared with zero-dimensional (0D) fullerenes and one-dimensional (1D) CNTs, two-dimensional (2D) graphene has opened new ways to study some fundamental quantum relativistic phenomena which have always been considered as very exotic. 2D graphene has a large surface area, high intrinsic carrier mobility, excellent mechanical properties, and superior flexibility (Young *et al.* 2012; Zhao *et al.* 2015; Zhang *et al.* 2015). However, it has a few shortcomings like easy aggregation and poor dispersion in common solvents (Zhang *et al.* 2014; Yu *et al.* 2017). Moreover, it is hard to observe photoluminescence (PL) from pristine graphene (Li *et al.* 2013). All the above disadvantages of graphene limit its potential biomedical applications.

In recent years, there has been great enthusiasm to further convert graphene to 0D graphene quantum dots (GQDs), which are defined as graphene sheets with a plane size less than 100 nm and a thickness of fewer than 10 layers (Li *et al.* 2012; Nirala *et al.* 2015). GQDs emerge as superior and universal fluorophores because of their unique physical and chemical properties, including small size, chemical inertness, stable photoluminescence (PL), low cytotoxicity, and excellent biocompatibility (Shin *et al.* 2015; Liu *et al.* 2015). Due to their stable PL and low cytotoxicity, GQDs could be utilized as suitable alternatives in bio-imaging and optical sensing (Zheng *et al.* 2014). Their small size and biocompatibility, GQDs could also serve as active carriers for drug delivery while simultaneously monitoring the release of the drug (Shen *et al.* 2012). Furthermore, their unique merits promise various biomedical application.

Extensive efforts have been made to synthesize high quality, monodisperse GQDs. The approaches for the synthesis of GQDs is categorized into two; one is top-down and another is bottom-up approach as shown in **Figure. 2.10**. The top-down approach refers

## LITERATURE REVIEW

to cleavage and exfoliation of carbonaceous materials like graphite, graphene, graphene oxide or carbon nanotubes as well as biomass, coal, and carbon fibers, under harsh reaction conditions (Iannazzo *et al.* 2017) (including electron beam lithography, oxygen plasma treatment, acidic exfoliation and oxidation, electrochemical oxidation, hydrothermal or solvothermal synthesis.). Bottom-up methods involve solution chemistry methods or carbonizing some particular precursors like polycyclic-aromatic compounds, fullerene, etc. using multi-step cage-opening or oxidation-condensation reactions in organic solutions (Wang and Qiu. 2015; Iannazzo *et al.* 2017; Keheng *et al.* 2017; Valappil *et al.* 2017). Both methods have advantages and disadvantages and the choice of method is dependent on the application for which the material has been produced as shown in **Table. 2.7**.

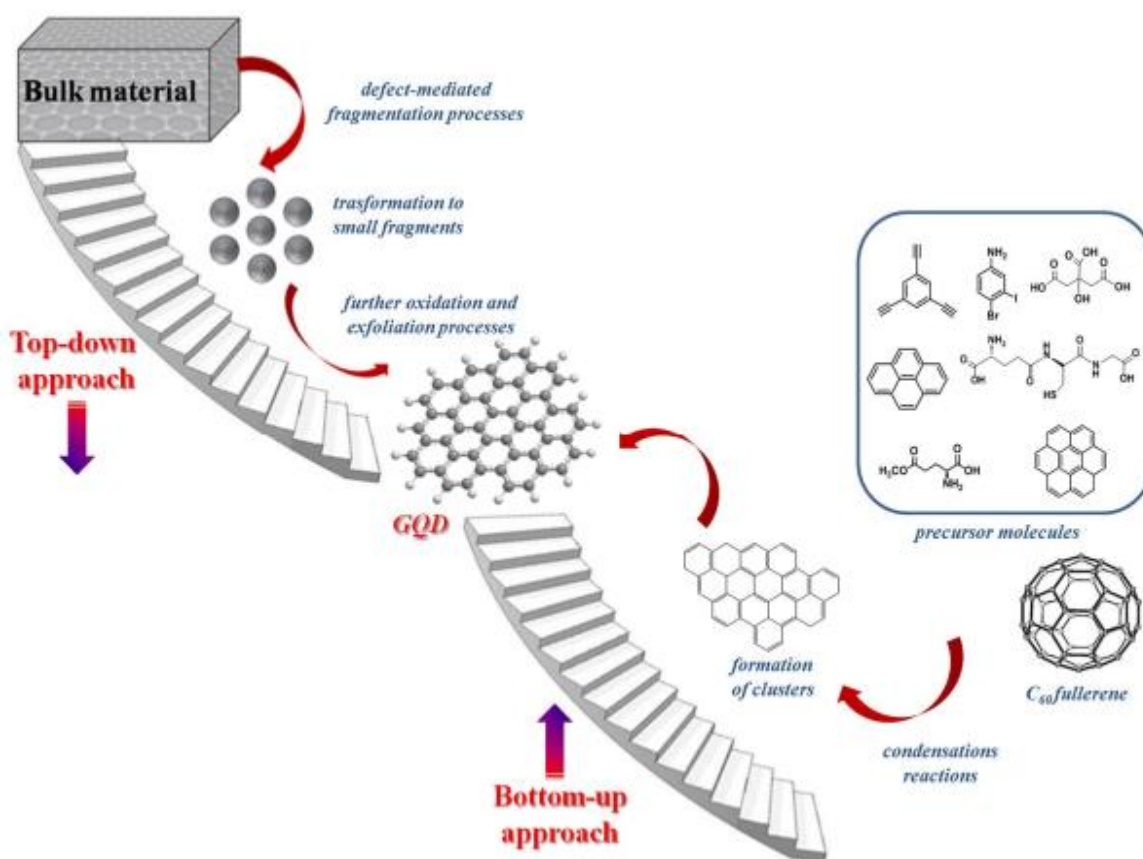


**Figure 2.10: Schematic representation of top-down and bottom-up approaches for the synthesis of GQDs (Iannazzo *et al.* 2017)**

## LITERATURE REVIEW

**Table 2.7: Summary of bottom-up and top-down synthesis of GQDs** (Dong *et al.* 2012; Li *et al.* 2013; Li *et al.* 2017; Iannazzo *et al.* 2017; Valappil *et al.* 2017)

Synthesis Method	Carbon Precursor	Size (nm)	Advantages and disadvantages	Application
Hydrothermal cutting	Carbon fibers	4.3±0.9	Narrow size distribution, but a lengthy acidic oxidation procedure to prepare starting material	Optoelectronics
	Graphene sheets	9.6		Optoelectronics
Solvothermal method	Graphite powder	3.8		-
Microwave-assisted solvothermal method	Graphene oxide	1.5 – 4	Shortened reaction time, improved GQDs yield, narrow size distribution, but sophisticated equipment	Electrocatalyst for oxygen reduction
Electro-chemical exfoliation method	Graphite rods	5 – 10	Facile methods, high yield of GQDs, multiple types of starting materials	Stem cell labeling
Nanolithography	Graphene crystals	10		Ferric ions detection, MRI imaging
	3D graphene	3		Molecular scale electronics, single electron transistors

## LITERATURE REVIEW

Synthesis Method	Carbon Precursor	Size (nm)	Advantages and disadvantages	Application
Microwave-assisted hydrothermal method	Glucose	3.2 – 11.9	Various starting materials, cost-effective, precise size the control allows the natural inheritance of heteroatoms	Photonic devices
Microwave-assisted pyrolysis	Citric acid	2.3± 7.9		Live cell imaging
Ultrasonication	Graphene	3.5		Bioscience and optoelectronics
Plasma-assisted	Graphene	3 – 7		Photoelectrochemical hydrogen evaluation
Fullerenes cage opening oxidative condensation	C60	2.7		Ultrafast high-density spintronic devices
	Polyphenylene dendritic precursors	13.5		Solar cell sensitizers

Top-down approaches are widely used in comparison to bottom-up strategies. In bottom-up methods GQDs is synthesized using small carbon precursors like aromatic molecules, citric acid, glucose, glutamic acid, etc. (Yan *et al.* 2010; Zhou *et al.* 2013; Tang *et al.* 2012; Wu *et al.* 2013; Wang *et al.* 2014). Yan *et al.* (2010) described the synthesis of large colloidal, uniform and tunable size GQDs by solution chemistry. The starting material used are 3-iodo-4-bromoaniline and benzene derivatives, the end

## LITERATURE REVIEW

product formed was comprised of 132, 168, and 170 conjugated carbon atoms. The spectral range of synthesized GQDs was from UV to near-infrared, hence they are used prominently in photovoltaics (Yan *et al.* 2010). Liu *et al.* (2011) synthesized the GQDs by pyrolysis using polycyclic aromatic hydrocarbon as carbon source i.e., hexa-peri-hexabenzocoronene. The size of the synthesized GQDs was uniform (~60 nm diameter and 2-3 nm of thickness) with ordered morphology, demonstrated the influence of the pyrolysis temperature on synthesis of GQDs (Liu *et al.* 2011). In 2013, Zhou *et al.* also synthesized photoluminescent GQDs through carbonization and reduction reaction under acidic condition by using polycyclic aromatic hydrocarbon as carbon precursor and hydrazine as reducing agent. The synthesized materials with size in the range of 5–10 nm, showed good optical stability, tunable photoluminescence properties, and high water solubility (Zhou *et al.* 2013). GQDs were prepared using glutathione and citric acid as starting materials as carbon source, with a fluorescence quantum yield of 33.6% (Liu *et al.* 2013). Wu and coworkers (2013) synthesize GQDs by a pyrolysis method using L-glutamic acid, showed a broad emission range and a quantum yield of 55% with a stable, strong excitation-dependent PL around 815 nm, suggesting their potential for *in-vitro* and *in-vivo* fluorescence imaging (Wu *et al.* 2013). Wang *et al.* (2014) described the synthesis of water-soluble, highly fluorescent pyrene functionalized GQDs by the controlled condensation of aromatic compound like 1,3,6-trinitropyrene as precursor molecule. The synthesized GQDs showed outstanding optical properties like long-term photo stability, large molar-extinction-coefficients and strong excitonic absorption bands (Wang *et al.* 2014). In 2015, Li *et al.* reported a bottom-up pyrolysis process for the synthesis of nitrogen-doped GQDs, using citric acid and tris(hydroxymethyl)aminomethane. GQDs showed a strong blue fluorescence under UV light excitation (365 nm) with a quantum yield of 59.2%. Furthermore, high ionic strength, high resistance to photo-bleaching, and an excitation-independent behavior was detected (Lin *et al.* 2015).

Recently, Luo and co-workers (2016) reported a facile two-step microwave-assisted hydrothermal method to prepare white-light-emitting GQDs (WGQDs). Interestingly, they firstly fabricated yellow-green fluorescent GQDs via exfoliation of oxidized graphite under ultra-sonication and microwave irradiation. After that, the pH of the prepared GQDs was tuned to 13 and reacted for 8 h at 200 °C under microwave

## LITERATURE REVIEW

irradiation. The WGQDs were obtained after further dialysis for 3 days. The size and thickness of the GQDs were changed under the microwave irradiation. The collected WGQDs showed a uniform size of 2–5 nm and a thickness of 1.25–2.75 nm. Therefore, it can be concluded that the microwave-assisted method could shorten the reaction time and improve the product yield, but it is limited by the need for sophisticated equipment.

### 2.9.1 Application of GQDs in anticancer therapy

Graphene quantum dots (GQDs) are promising new generation of graphene-based nanomaterial for biomedical applications. They are widely explored for cellular imaging and drug delivery due to their peculiar characteristics like large surface area, low toxicity, high intrinsic fluorescence, high photo-stability, rich in delocalized  $\pi^*$  electrons with a functional groups that include carbonyl, carboxyl, epoxy, hydroxyl groups. Due to their  $\pi$ - $\pi^*$  interactions and the functionalization of oxygen groups GQDs are enormously used as a potential drug delivery carrier (Chandra *et al.* 2014; Schroeder *et al.* 2016). A cancer drug doxorubicin (DOX) is used in conjunction with GQDs, which restricts the DNA replication, transcription, and damage repair by direct intercalation with DNA helices. Release of DOX from GQDs is pH-responsive, because DOX binds on the surface of GQDs by hydrophobic interactions and  $\pi$ - $\pi^*$  stacking. Acidic environment is observed in the tumor site compared to the normal cells hence release of DOX from GQDs tends to occur under acidic conditions (Schroeder *et al.* 2016). Miao *et al.* (2013) reported that DOX/GQDs conjugates increase the uptake of DOX by the cancer cells/drug resistant cells and enhance the DNA cleavage activity of DOX that may improve the chemotherapeutic efficacy. (Miao *et al.* 2013).

Abdullah *et al.* (2013) reported a way to achieve efficient and site-specific delivery of GQDs using hyaluronic acid (HA) as a targeting agent. The quenching behavior of DOX and quantitative analysis showed that surface of GQDs was loaded with 75% of DOX. The release of DOX quickly reached 42% within 6 h in mildly acidic conditions (pH 5.0), and complete DOX was released within 48 h from the GQDs-HA matrix. While the release of DOX at pH 7.4 was slower (only 20%) after 48 h. This pH-dependent behavior was advantageous because tumor has slightly acidic environment (Abdullah *et al.* 2013). Moreover, the target specificity on cancer cells and tumor tissue

## LITERATURE REVIEW

was confirmed from both in vivo distribution investigation and in vitro cellular imaging. Wang *et al.* (2014) utilized folic acid-conjugated GQDs to load DOX. The fabricated nano-assembly can unambiguously discriminate cancer cells from normal cells and efficiently deliver the drug to targeted cells. The fluorescence stability of GQDs enables real-time monitoring of the cellular uptake of the DOX–GQD–FA nano-assembly and the following release of drugs (Wang *et al.* 2014). Qiu *et al.* (2015) synthesized a multifunctional drug carrier by using GQDs, reduced graphene dots, and DOX, which is simultaneously assists in tracking the diseased site and targeted drug delivery for prostate cancer treatment (Qiu *et al.* 2015).

Meanwhile, GQDs could also be combined with other nanoparticles as fluorescent tracers for drug delivery. For instance, Yao *et al.* (2017) fabricated a multifunctional nanocomposite of GQDs as caps and local photo-thermal generators, and magnetic mesoporous silica nanoparticles (MMSN) as drug carriers and magnetic thermos-seeds. MMSN/GQDs nanoparticles with an average size of 100 nm could load DOX and trigger DOX release by low pH environments and could generate heat to the hyperthermia temperature under an alternating magnetic field or by near infrared irradiation. More importantly, a DOX-MMSN/GQDs nano-system exhibited a high efficacy to kill cancer cells because the increase in temperature could accelerate the drug release rate (Yao *et al.* 2017). Jing *et al.* reported the synthesis of GQDs based multifunctional core-shell capsules, comprised of olive oil, magnetite ( $\text{Fe}_3\text{O}_4$ ), a dual-layer porous  $\text{TiO}_2$  shell, and capsules were loaded with paclitaxel (PTX). These capsules were used for cellular imaging, magnetic targeting and initial burst release is controlled by loading hydrophobic drug (Jing *et al.* 2011).

### **2.10 Exploitation of tumor microenvironment for drug delivery**

The journey for successful acquisition for treatment of cancer started in 1930's with strategies like chemotherapy, surgery, and radiotherapy to modern day treatments like immunotherapy, gene therapy, nanoscale drug delivery systems, hyperthermia etc (Arruebo *et al.* 2011). Paradoxically, still in 21<sup>st</sup> century, cancer remains the major cause of death all over the world despite advancement in treatments, superior knowledge of cancer biology and genetics, investment of the exceptional amount of

## LITERATURE REVIEW

money and endeavors (Greaves and Maley. 2012). Delineation of an anticancer therapy requires comprehension of variable factors between normal and tumor cells. Some differences between normal and tumor affected tissues like differences in vascular morphology, pH, temperature etc. constitutes tumor microenvironment and opens windows to create a useful therapeutic blueprint for anti-cancer action (Danhier *et al.* 2010).

### 2.10.1 Angiogenesis

Vasculogenesis is a standard but an essential process in the human body that allows the formation of nascent vessels from pre-existing ones by tripping the net balance of pro and anti-angiogenic molecules resulting in 'angiogenic switch'. This is the most common pathway leading to malignancy and its fatal nature. Some of the pro-angiogenic molecules are: pro-angiogenic growth factors/receptors: VEGF-A, fibroblast growth factor-2, -3, hepatocyte growth factor (HGF), extracellular matrix proteins, proteases, interleukin-8 (IL-8), placental growth factor (PIGF), transforming growth factor-beta (TGF-beta), platelet-derived growth factor (PDGF), angiopoietins (Angs) and others. Characteristic events leading to the development of tumor angiogenesis are excess production of pro-angiogenic signals, lack of angiogenesis inhibitors, path-finding signals or maturation factors, thus leading to excessive tip-cell formation and migration of endothelial cells.

Now, pathological aspects of tumour angiogenesis that can be exploited for antagonistic effect pertaining to cancer are: endothelial cell migration/tip cell formation, structural abnormalities of tumour vessels, hypoxia, lymphangiogenesis, elevated interstitial fluid pressure, poor perfusion, disrupted circadian rhythms, tumor-promoting inflammation, tumor-promoting fibroblasts and tumor cell metabolism/acidosis (Prager and Poettler. 2012; Wang *et al.* 2015).

### 2.10.2 Enhanced permeability and retention (EPR) effect

As an organ is affected by cancer, the standard vasculature is distorted by high permeability that facilitates amassment of macromolecules in tumor interstitial spaces and jeopardized lymphatic filtration retains their presence. The phenomena explained



## LITERATURE REVIEW

above is summarized as enhanced permeability and retention effect and proved effectual for macromolecular drugs loaded on nanocarriers. Many abnormalities accompanying tumor vasculature are high proportion of proliferating endothelial cells, pericyte deficiency, and aberrant basement membrane formation leading to enhanced vascular permeability. Mostly the permeabilized vasculature allows a broad cut off size, i.e. 200-800 nm granting easy access nanocarriers of range 20-200 nm. Outline of abnormal vasculature accompanying tumor and allows selective macromolecular drug targeting is given as follows and in **Figure 2.11**.

- Extensive angiogenesis and hyper vasculature
- Lack of smooth-muscle layer, pericytes
- Defective vascular architecture
- No constant blood flow and direction
- Inefficient lymphatic drainage that leads to enhanced retention in interstitium of a tumor
- Slow venous return that leads to accumulation from then interstitium of a tumor

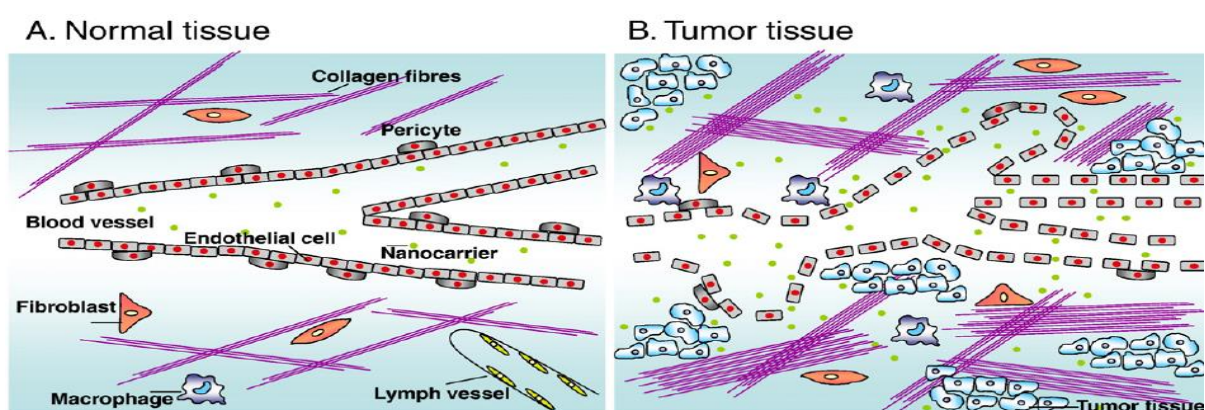


**Figure 2.11: Aberrations in normal and tumor tissues promoting EPR effect and utilization of nanocarriers (Danhier *et al.* 2010)**

EPR effect allows the profile of specific molecules to infiltrate and stay in tumor vasculature. Solid tumors exhibit EPR effect more prominently. Thus, drug effective for them can be exploited for delivery using nanocarriers. Profile of the EPR effect is explained in **Table 2.8** (Danhier *et al.* 2010; Maeda 2012; Torchilin 2011).

# LITERATURE REVIEW

**Table 2.8: Profiles of the EPR effect (Maeda 2012).**

<b>Characteristics</b>	<b>Comments</b>
Molecular size	Above 40 kDa; 800 kDa still shows an active EPR effect
Biocompatibility	No coagulation, no interaction with blood components and blood vessels, no cell lysis, no RES clearance (e.g., macrophages). Protease bound protease-inhibitor is cleared in a few mins even though biocompatible macromolecules.
The time required to achieve EPR effects	More than several hours in circulation in mice. The trend can be seen even first 30 min.
The drug retention time of macromolecular drugs in a tumor	Mostly days to weeks, in high contrast to passive targeting of low MW drugs which is only a few minutes.
pH (isoelectric point)/surface charge	Weakly acidic to weakly cationic. Polycationic particles will disappear rapidly from circulation.

### 2.10.3 pH

One of the indicative underrated behavior of invasive tumor cells is a disparity in pH from normal tissues, irrespective of the tissue behavior and genetic background. Average extracellular tumor pH varies from 6-7, whereas normal tissue exhibit pH of ~ 7.4. Increase in pH is the consequence of higher proliferative and glycolytic rates producing metabolic acids and Warburg effect linked to hypoxia in cancer cells. pH-dependent behaviors of cancer cells that can be applied for construction of anticancer therapies are intracellular acidification promoting cell survival and limiting apoptosis, metabolic adaptation to Warburg effect, facilitation metastasis and invasion (Danhier *et al.* 2010; Webb *et al.* 2011).

## LITERATURE REVIEW

### 2.10.4 Temperature

Tumor microenvironment constitutes of well-defined hyperthermia as a result of neoplastic fever that allows the body temperature to increase to 39-42 °C naturally. Above occurrence is resultant to immune response because malignancy indicates infection. This is included in paraneoplastic syndrome in some cancers like Castleman's disease, Hodgkin's and non-Hodgkin's lymphoma, renal cell carcinoma, hepatocellular carcinoma, acute myeloid leukemia, hairy cell leukemia, glioblastoma multiforme, blast crisis of chronic myelogenous leukemia, ovarian cancer, and atrial myxoma. The release of cytokines from macrophages induces prostaglandin E2 which acts on the hypothalamus, causing a change in the thermostatic set point thus increasing temperature naturally (Alsirafy *et al.* 2011).

### 2.11 Mainstream drugs and their drawbacks

Chemotherapy, surgery, and radiotherapy are one of the primary treatments for cancer till this date — currently a combination of chemotherapeutic drugs with other therapies like hormone therapy, immunotherapy, radiotherapy, etc. The USA Food and Drug Administration (FDA) has mandated many anticancer drugs in which anthracyclines predominate, e.g., Doxorubicin, Daunorubicin, idarubicin, valrubicin, etc. Out of all anthracyclines, doxorubicin is considered the most promising drug for effectual broad-spectrum treatment (Carvalho *et al.* 2009; Tacar *et al.* 2013)

#### 2.11.1 Doxorubicin as an anticancer drug

Doxorubicin was first extracted from *Streptomyces peucetius var. caesius* in the 1970s and due to its broad spectrum it was customarily used in the treatment of several cancers including breast, lung, gastric, ovarian, thyroid, non-Hodgkin's and Hodgkin's lymphoma, multiple myeloma, sarcoma, and pediatric cancers. Doxorubicin possesses alkyconic and sugar moieties. The sugar, termed daunosamine, is attached by a glycosidic bond to one of the rings and consists of a 3-amino-2,3,6-trideoxy-L-fucosyl moiety and its side chain terminates with primary alcohol. The aglycone consists of a tetracyclic ring with adjacent quinone-hydroquinone groups, a methoxy substituent and a short side chain with a carbonyl group. (Carvalho *et al.* 2009). As it is a planar

## LITERATURE REVIEW

structure, it intercalates between DNA base pairs forming supercoils thus resulting in torsional stress and destabilizing the nucleosome which is considered to be the most plausible mechanism for its operation. Structure and intercalation of doxorubicin with DNA is explained in **Figure 2.12** as follows: Some chemical and physical properties of doxorubicin is listed in **Table 2.9**.

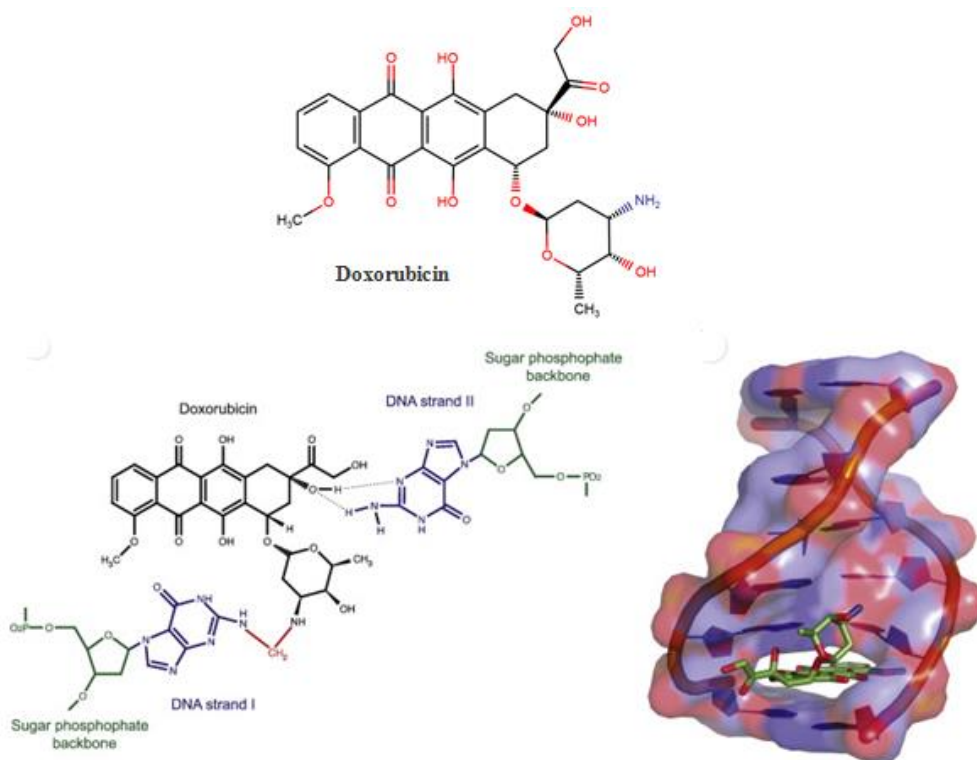


**Figure 2.12: Structure of doxorubicin, its covalent bonding with DNA strands and intercalation in DNA structure** (Carvalho *et al.* 2009; Yang *et al.* 2014)

**Table 2.9: Physical and chemical properties of DOX**

(<https://pubchem.ncbi.nlm.nih.gov>)

Property name	Property value
Molecular weight	543.525 g/mol
Physical description	Solid
Colour	Red, crystalline solid
Melting point	229-231 °C
Log P	1.27
Dissociation constant.	pKa <sub>1</sub> = 7.34(phenol); pKa <sub>2</sub> = 8.46 (amine); pKa <sub>3</sub> = 9.46 (ester)

## LITERATURE REVIEW

### 2.11.2 Mechanism of action for Doxorubicin

Following are the majorly followed mechanism of action proposed:

#### 2.11.2.1 Topoisomerase II poisoning

One of the main enzymes involved in DNA replication, transcription and other nuclear processes by regulating DNA's topology, is the most common and paramount mechanism proposed for doxorubicin action. It is an ATP-dependant enzyme that prevails in two isoforms and is responsible for the release of torsional stress on DNA during replication & decatenation of DNA. Doxorubicin ambushes topoisomerase at breaking points stabilizes the whole complex and hinder DNA resealing. Distinctly, it will affect dividing cells although the literature suggests that this might not be the only mechanism for doxorubicin (Yang *et al.* 2014).

#### 2.11.2.2 DNA adduct formation

Intercalation of doxorubicin in DNA structure permits formation DNA adduct formation (**Figure 2.13**). According to literature, it elicits DNA damage response (DDR) by activating DDR proteins succeeding DNA damage stimuli manifesting cell cycle arrest, DNA repair mechanisms & cell death processes. Thus the formation of DNA adduct is an essential process for the action of doxorubicin (Forrest *et al.* 2012).

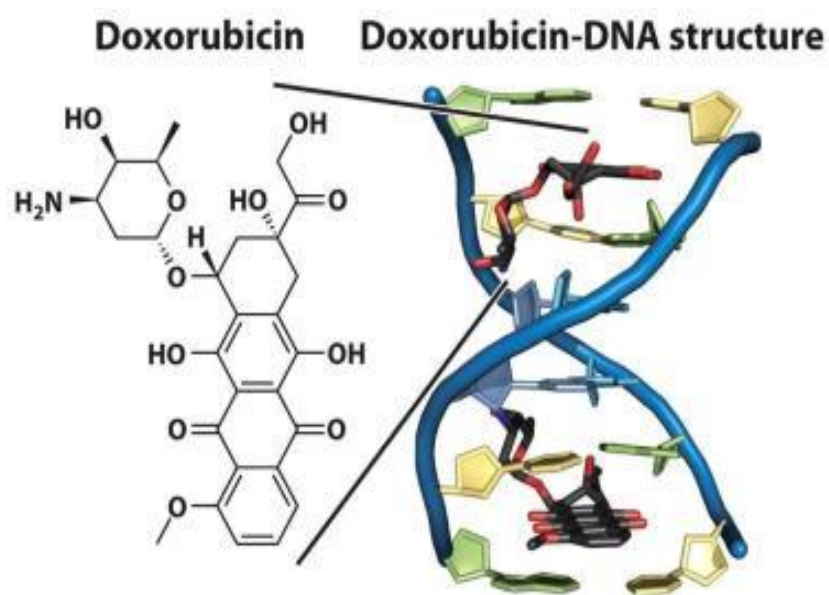


**Figure 2.13: DNA adduct formation mechanism of doxorubicin by intercalation**

## LITERATURE REVIEW

### 2.11.2.3 Oxidative stress

It has been proposed that production of ROS (reactive oxygen species) leads to an imbalance between ROS generation and degradation by cellular antioxidant mechanisms, this deregulation is called oxidative stress. High levels of ROS participate in genomic instability and lead to aggressiveness and progression of carcinogenesis. This process is accompanied by the activation of various gene and transcription factors in cancer cells. Superoxide radical is generated in many cellular processes mainly by the electron transport chain into mitochondria. Doxorubicin causes oxidative damage in tumour cells and it is based on Redox cycling accompanied by the release of iron from cells. The drug-iron complex catalyzes  $O_2$  and  $H_2O_2$  conversion into more potent radicals. Oxidative damage mechanism has been considered as an important antitumoral mechanism in cancer cells (Pilco-Ferreto and Calaf. 2016).

### 2.11.3 Limitations of doxorubicin

Major complication caused by doxorubicin is resistance to its action and toxicity caused by it to various parts of the body, due to which its utilization in cancer treatment becomes limited.

#### 2.11.3.1 Doxorubicin resistance

It is vital to study the mechanisms of anti-cancer drug resistance to know the action of DOX to determine apoptotic and autophagic biomarkers. The study of mechanism helps in development of improved doxorubicin formulation and efficacy. The high mobility group box 1 protein (HMGB1) has a significant role in regulating nuclear events such as DNA replication and repair. It is also a critical regulator of both selective and non-selective autophagy. Despite this, it has shown to contribute to drug resistance in osteosarcoma cells significantly. Results have shown that inhibiting both autophagy and HMGB1 increases osteosarcoma cell sensitivity to doxorubicin both *in vivo* and *in vitro*.

#### 2.11.3.2 Doxorubicin toxicity

The main side effects of anthracycline drugs are the multidirectional cytotoxic effects, with cardiotoxicity due to non-specific targeting of the tumor site as it can affect the

## LITERATURE REVIEW

growth of many other cell types in the body. This results in the immune system becoming depressed, and as the numbers of immune cells reduce, the patient becomes more susceptible to microbial infections, fatigue and healing time decreases. It is known to affect heart, liver, brain and kidneys with other adverse effects known are cutaneous injuries induced by the treatment. Doxorubicin is also known to cause fever, urticaria and anaphylaxis that are associated with hypersensitivity. Further incidences have shown doxorubicin affecting the gastrointestinal system causing patients to vomit and experience mucositis during the early stages of therapy (5–10 days). Most patients recover within the next 10 days of treatment, although those with severe reactions have shown signs of ulceration and necrosis, often causing severe infections in the colon and caecum which can be fatal (Tacar *et al.* 2013).

### 2.12 Temperature responsive nanohydrogels

Nanohydrogels are nano-sized structures, where the hydrogel is confined to a spherical shape with a diameter ranging from 10 to 1000 nm. Nanohydrogels can be designed as drug delivery vehicles, which may offer significant benefits over conventional delivery mechanisms. These benefits include better stability, the possibility of transporting hydrophilic and hydrophobic drugs, high loading capacity due to significantly increased surface area, higher bioavailability, invasion by the reticuloendothelial system is prevented, systems that allow controlled and sustained release rates or release upon an external stimulus, and the possibility to exploit a range of patient-friendly delivery routes, e.g. oral, cutaneous or inhalation. Nanohydrogels are nanometric scale networks of chemically or physically cross-linked polymer particles (Guterres *et al.* 2007; Oh *et al.* 2009). They have a porous 'sponge-like' structure which swells in a particular solvent under specific environmental stimuli such as temperature (Galaev and Mattiasson. 2007), pH (Vincent. 2006; Galaev and Mattiasson. 2007; Don *et al.* 2008), ionic strength (Don *et al.* 2008) and type of solvent (e.g. water, ethanol or buffer) (Lopez *et al.* 2004; Vincent. 2006; Das *et al.* 2006), then, undergoing rapid conformational changes and releasing the solvent again following the environment change. The temperature responsive nanohydrogels have become increasingly attractive as a carrier for the drug delivery applications since the size and shape of the delivery vehicle can be used to control the rate of release and to target delivery to specific locations in the

## LITERATURE REVIEW

body. PDEA, which has a sharp phase transition around 32 °C in water, has been most extensively investigated among a variety of LCST polymers (Schild 1992; Pelton. 2000). Since the LCST of PDEA in water is slightly below body temperature, it is desirable for pharmaceutical use and is widely used for the design of thermosensitive drug delivery systems. Also, various polymers having PDEA-related structures (N-substituted acrylamide and methacrylamide polymers) and different LCST's are also investigated as thermosensitive nanohydrogels (Chytry *et al.* 1997; Liu and Zhu, 1999). By emulsion polymerizing DEA with the 2-hydroxyethyl methacrylate (HEMA), the resulting poly(N, N-diethylacrylamide-co-2-hydroxyethyl methacrylate) size of 66.7-77.8 nm showed an LCST of 20-28 °C (Colonne *et al.* 2007). The release of paclitaxel from poly(N, N-diethylacrylamide-co-acrylamide)-block-poly(g-benzyl l-glutamate) was suitable for localized hyperthermia treatment also showed less cytotoxicity.

### 2.13 Synthesis of Hydrogels

#### 2.13.1 Synthesis of Macrogels

Size of bulk gels (macrogels) may vary from a millimeter to several centimeters. In the early 1960s, Wichterle synthesized the first polymeric hydrogel, poly(hydroxyethyl methacrylate) (PHEMA), for biomaterial applications. Bulk gels are often described as three-dimensional, hydrophilic, polymeric networks composed of a monomer, cross-linker, and initiator. Synthesis of macrogels is carried out by simultaneous cross-linking polymerizations and the employment of a cross-linking agent during polymerization to form a three-dimensional network. The free radical formed by the decomposition of initiator tends to react with monomer and cross-linked molecules to obtain polymeric chains along with some cross-linking points. Cross-linking may be intermolecular or intramolecular. Intermolecular cross-linking leads to the formation of branched and highly network structure that ultimately is responsible for macroscopic gel product whereas the intramolecular cross-linking process is responsible for the formation internally of cross-linked polymer chain networks.

#### 2.13.2 Synthesis of nanohydrogel by inverse emulsion polymerization

Currently, micro/nanohydrogels are being synthesized and are considered for research based upon their applicability in the biomedical field as drug delivery vehicles, in tissue



## LITERATURE REVIEW

engineering, and for chromatographic or separation technology. Elford (1930), first coined “microgel” for his membrane filtration study on Nitrocottons. Staudinger *et al.* (1935) were the first to synthesize microgels using styrene cross-linked by divinylbenzene. Microgel/nanohydrogels are traditionally obtained by conventional emulsion polymerization of loci of particle growth (oil in water emulsion polymerization) with micelles stabilized by emulsifiers. Through the mentioned process, hydrophobic micro/nanohydrogels are generally synthesized. Dunn and Chong, 1970, and Kotera *et al.* 1970 proposed that hydrophobic monomers, i.e., vinyl acetate and styrene, could polymerize in water to form polymeric lattices at elevated temperature in the absence of a surfactant, this synthesis process is termed as “surfactant-free emulsion polymerization.”

Majority of micro/nanohydrogels synthesized around the 1980`s were hydrophobic microgels, such as polystyrene (pSt) and poly(methyl methacrylate) (pMMA), were stabilized by their surface charge or hydrophilic coating present in the aqueous phase in which they are being synthesized. Pelton and Chibante (1986), synthesized hydrophilic thermoresponsive microgel composed of poly(*N*-isopropylacrylamide) (pNIPAm) via surfactant-free radical precipitation polymerization of NIPAm and cross-linker, *N,N'*-methylene bisacrylamide (MBA), in the aqueous phase. The hydrophilic (water soluble) monomers can be polymerized by the inverse (water-in-oil) emulsion polymerization where water-soluble monomers are first emulsified in an oil phase using an emulsifier (surfactant) and polymerized later by the radicals decomposed from the initiator. This method has advantages like a high degree of monomer conversion, monodispersed particle size, nano-size particles being formed without agglomeration. The literature available in this area is minimal.

A schematic representation of an inverse emulsion polymerization method is shown in **Figure 2.15**. Inverse (water-in-oil) emulsions (IE) were initially developed as an alternative to acrylamide polymerization in solution but soon found their way in the field of hydrophilic nanoparticle formation (Candau, 1997). In inverse (water-in-oil) emulsions polymerization method, emulsification of the aqueous phase in the oil (commonly consisting of hydrocarbons) is achieved by amphiphiles with low ‘hydrophilic-lipophilic balance’ (HLB) values; the lower the HLB, the more

## LITERATURE REVIEW

hydrophobic the emulsifier. Stabilization occurs exclusively through steric effects since the dielectric constant of oils is very low. Inverse emulsions are generally thermodynamically unstable and tend to phase separation with time. Thermodynamic stability is achievable (for low aqueous volume fractions) at the expense of high emulsifier concentrations. The mechanism of polymerization depends strongly on the type of initiator (oil soluble or water soluble) as well as the oil-solubility of monomer(s). For hydrophilic initiators and monomers (homogeneous reaction mixture) the loci of initiation and propagation are the dispersed aqueous droplets, rather than the continuous phase or micellar structures. The obtained particle size distribution is therefore mainly determined by the nano-droplet size distribution of the inverse emulsion, provided that reaction kinetics is faster than emulsion break-up.

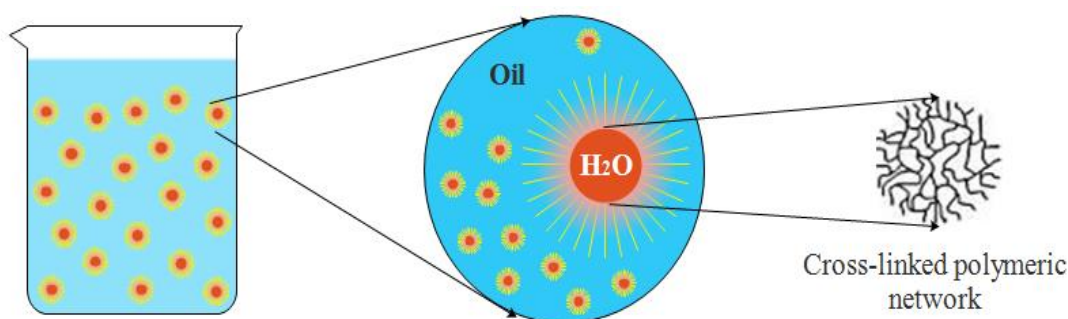


**Figure 2.14: Schematic representation of an inverse emulsion polymerization system**

For this reason, typically radical polymerization has been selected as the reaction scheme. Inverse emulsion polymerization is a multi-parameter system, whose potential and versatility in fabricating aqueous-based nanomaterials is already established, and whose optimization may provide better-defined colloids for drug delivery applications. **Table 2.10** describes some of the PDEA nanohydrogels synthesized along with polymerization method.

## LITERATURE REVIEW

**Table 2.10: PDEA nanohydrogels synthesized by polymerization method**

Polymer	Polymerization	Size (nm)	Reference
poly(2-methoxyethyl acrylate- co- poly(ethylene glycol methyl ether acrylate) and	Reversible addition-fragmentation chain transfer (RAFT) mediated dispersion polymerization	28-99	Liu <i>et al.</i> 2012
Poly(N,N-diethylacrylamide-co acrylamide)-block- poly(g- benzyl-l- glutamate)	Dialysis	129	Li <i>et al.</i> 2009
Poly(N,N-diethylacrylamide- N,N-dimethylacrylamide)	Surfactant-free emulsion precipitation polymerization	165-275	Lu <i>et al.</i> 2011
Poly(N,N-diethylacrylamide-co- acrylic acid)	Surfactant-free emulsion precipitation polymerization	200-800	Zhang <i>et al.</i> 2012

### 2.14 Drug delivery mechanism

Hydrogels are used as controlled drug delivery systems as they possess sustained constant concentration of therapeutically active compound in the blood with minimum fluctuations, release rates are predictable and reproducible over a long period, protection of bioactive compounds having very short half-lives, elimination of side effects, waste of drug and frequent dosing, optimized therapy and better patient compliance and overcome the drug stability problem.

A typical drug-delivery system consists of a polymer carrier in which the drug is uniformly distributed or dispersed — Langer and Peppas, 1983 classified Drug-delivery systems based upon the mechanism controlling the drug release.

## LITERATURE REVIEW

- Diffusion-controlled systems
  - Reservoir (membrane systems)
  - Matrix (monolithic systems)
- Chemically-controlled systems
  - Bioerodible and biodegradable systems
  - Pendant chain systems
- Solvent-activated systems
  - Osmotic-controlled systems
  - Swelling-controlled release systems
- Modulated-release systems

In all these systems, diffusion is always involved. For a non-biodegradable polymer matrix, drug release is due to the concentration gradient by either diffusion or matrix swelling (enhanced diffusion). For the biodegradable polymer matrix, the release is typically controlled by the hydrolytic cleavage of polymer chains that lead to matrix erosion, even though diffusion may be still dominant when the erosion is slow. **Figure 2.15** shows three mechanisms for controlled drug release from the polymeric matrix (Bajpai *et al.* 2008).

### 2.14.1 Reservoir systems

In these devices, the drug core is encapsulated in a polymeric membrane. Drug diffusion through the membrane is the rate-limiting step and controls the overall drug release rate. The saturated concentration of the drug inside a reservoir is essential to maintain a constant concentration gradient across the membrane. The drug transport mechanism through the membrane is usually a solution-diffusion mechanism. Drug transport occurs first by dissolving the drug in the membrane on one side followed by diffusion through the membrane and desorption for the other side of the membrane (Bajpai *et al.* 2008).

### 2.14.2 Matrix systems

In matrix systems, the drug is uniformly dissolved or dispersed. An inherent drawback of the matrix systems is their first-order release behavior with continuously decreasing release rate. This is a result of the increasing diffusional path length and the decreasing area at the penetrating diffusion front as matrix diffusion proceeds. Different

## LITERATURE REVIEW

geometries can be used to achieve a zero-order release rate. Zero-order release is obtained by using unique shapes to compensate for the increasing diffusional distance and decreasing area at the penetrating diffusion front generally encountered in matrix systems. For example, a hemispherical polymer matrix that is coated on all surfaces with an impermeable coating except for an aperture in the center face has been demonstrated to provide near-constant rate profiles (Bajpai *et al.* 2008).

### 2.14.3 Erodible systems

In these systems, the polymer matrix erodes due to the presence of hydrolytically or enzymatically labile bonds. As the polymer erodes, the drug is released in the surrounding medium. Erosion may be either surface or bulk erosion in origin (Bajpai *et al.* 2008).

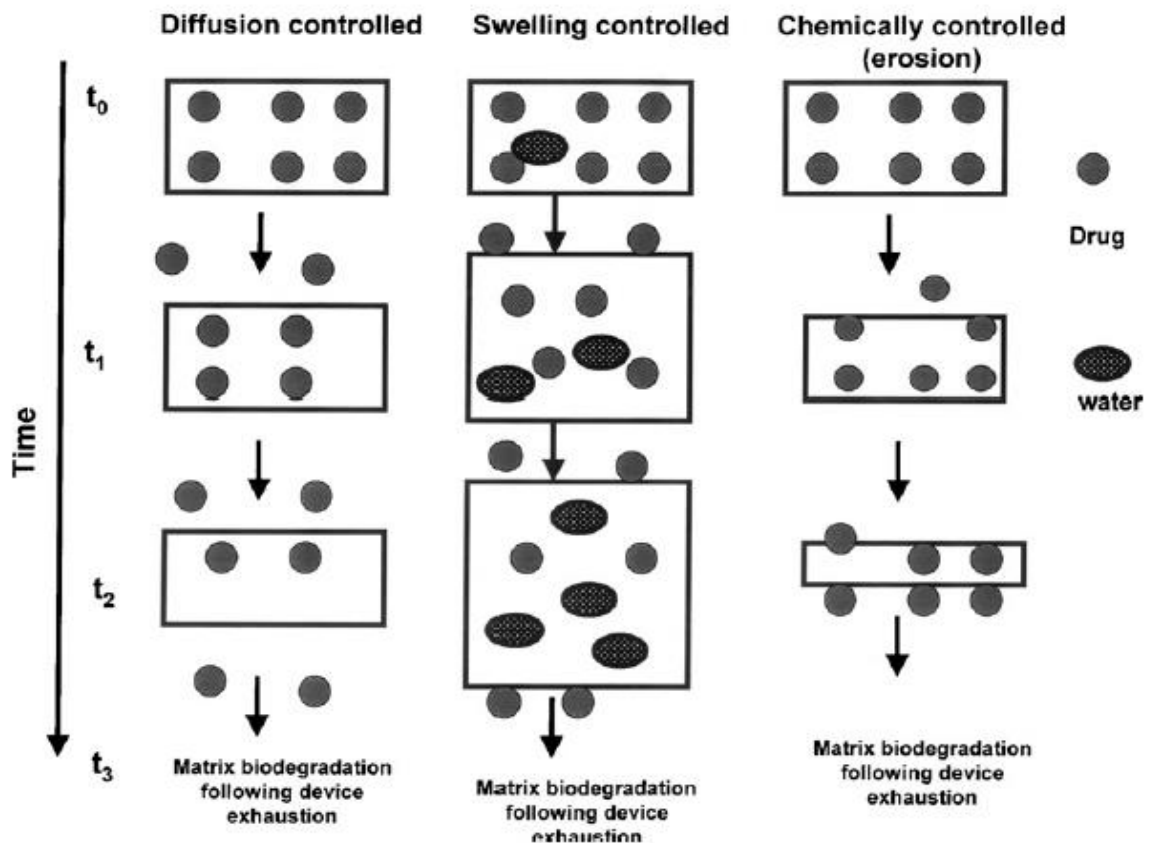


Figure 2.15: A schematic drawing illustrating the three mechanisms for controlled drug release from a polymer matrix (Bajpai *et al.* 2008)

# LITERATURE REVIEW

## 2.14.4 Pendant chain systems (prodrugs)

In these systems, the drug molecule is chemically bonded to a polymer backbone, and the drug is released by hydrolytic or enzymatic cleavage. The rate of drug release is controlled by the rate of hydrolysis. This approach provides an opportunity to target the drug to a particular cell type or tissue. Natural polymers, e.g., polysaccharides, as well as synthetic polymers, e.g., polylysine, copolymers of 2-hydroxypropylamide and others have been used as drug carriers in such systems. The structure of these polymers can be modified by the incorporation of sugar residues or sulfonyl units to obtain a specific tissue affinity (Bajpai *et al.* 2008).

## 2.14.5 Osmotic-controlled systems

In an osmotic system, a semi-permeable membrane is used to control the permeation of water. The rate of water influx controls the overall rate of drug release. The release rate remains constant as long as the drug concentration across the membrane is constant. Osmotic drug-delivery systems are capable of providing extended not only time-independent release but also delivery rates much higher than those achievable by the solution-diffusion mechanism (Bajpai *et al.* 2008).

## 2.14.6 Swelling-controlled systems

When the glassy polymer comes into contact with an aqueous solution, it begins to imbibe water. This water uptake can lead to considerable swelling of the polymer. Due to the swelling action, the drug which is dispersed in the polymer begins to diffuse out. Thus, drug release depends upon two simultaneous rate processes: water diffusion into the polymer and chain relaxation. The continued swelling of the matrix causes the drug to diffuse out at a faster rate. The overall drug release rate is controlled by the rate of swelling of the polymer network. Depending on the rate of water diffusion and macromolecular chain relaxation, the time dependence of the rate of drug release can be determined (Bajpai *et al.* 2008).

## 2.14.7 Modulated release systems

In these systems, the drug release is controlled by external stimuli such as pH, ionic strength, temperature, magnetism, ultrasound and electromagnetic radiation (Alfrey *et*

## LITERATURE REVIEW

*al.* 1966). Hydrogel which would respond to these external stimuli can be used as controlled-release devices. Ritger and Peppas (1987a; 1987b) and Korsmeyer and Peppas (1983) developed an empirical equation to analyze both Fickian and non-Fickian release of drug from swelling as well as non-swelling polymeric delivery systems.

$$M_t/M_\infty = kt^n \quad 2.1$$

$M_t$  and  $M_\infty$  are the amounts of drug released at time  $t$  and the equilibrium, respectively.  $k$  is a proportionality constant and  $n$  is the diffusional exponent.

Ritger and Peppas. 1987 introduced this exponential equation to describe the drug release behavior from polymeric matrixes and analysis of Fickian and Non-Fickian diffusional behavior relative to the value of the exponent  $n$  was performed. Diffusional exponent values for planer, cylindrical and spherical drug release systems were related to the mechanism of delivery. For Ritger-Peppas models, the release exponent  $n \leq 0.5$  for Fickian diffusion release from slab (non swellable matrix),  $0.5 < n < 1.0$  for non-Fickian release (anomalous), this means that drug release followed both diffusion and erosion-controlled mechanisms and  $n = 1$  for zero order release, where drug release is independent of time as shown in **Table 2.11** (Korsmeyer and Peppas. 1983; Ritger and Peppas. 1987).

**Table 2.11: Ritger-Peppas diffusion exponent and mechanism of diffusional release from various swellable controlled release systems**

Diffusion Exponent ( $n$ )			Mechanism
Film	Cylinder	Sphere	
0.5	0.45	0.43	Fickian diffusion
$0.5 < n < 1$	$0.45 < n < 0.89$	$0.43 < n < 0.85$	Anomalous (non-Fickian) transport
1	0.89	0.85	Case II transport

The equation 2.1 has however been shown to be valid only for the first 60% of the total amount of drug released regardless of the geometry of the polymer (Ritger and Peppas. 1987).

# LITERATURE REVIEW

## 2.15 Scope and objective of the work

Based on the literature survey, it is very clear that there is a huge requirement for the development of smart hydrogel, particularly in the field of drug delivery system. The increasing number of diseases is the concrete evidence for the urgent need of new smart drug carriers. Smart polymers can be potentially used as drug carriers, but the research in smart polymers are still in the early stage. To reach preclinical and clinical stage, many factors should be extensively studied under both *in-vitro* and *in-vivo* conditions. In the present scenario, extensive research is going on to use smart polymer as drug delivery system and these smart polymers can change their structure and properties in response to external stimuli such as temperature, pH, ionic strength, etc. These smart polymers are expected to contribute significantly to the development of next generation biomaterials for biomedical applications.

The smart temperature sensitive hydrogel that are intended as drug carrier should meet certain criteria's like stability, size, biocompatibility, non-toxicity and its lower critical solution temperature (LCST) close to physiological body temperature (37 °C) (Zhang and Jandt, 2008; Jun *et al.* 2006). Poly (N, N-diethylacrylamide) (PDEA), is a linear polymer with repeating units of hydrophilic amide group and a hydrophobic diethyl pendent group which can hold large amount of water (Ngadaonye *et al.* 2012). PDEA is non-toxic, biocompatible, and biodegradable (Patil *et al.* 2014). Though PDEA has many advantages compared to other polymers, it lacks in-terms of LCST and its absorbing capacity. To make PDEA as a suitable drug delivery system its LCST and absorbing capacity should be improved. The LCST of PDEA could be adjusted by altering the hydrophilic or hydrophobic property of the polymer by adding suitable nanomaterial during its polymerization reaction. Researchers have tried to change the LCST of PDEA using different monomers like DMAAm, NVP (Luke *et al.* 2011) and clay particles (Li *et al.* 2015), but they could not retain or improve mechanical strength, release characteristics, *in vitro*, and *in-vivo* biocompatibility of native PDEA. This gap in the literature will be addressed through this research work by using GQDs to alter the PDEA property as per the requirement. In this study, PDEA hydrogel is produced along with GQDs, to increase the LCST of PDEA, improve structural stability and biocompatibility. The aim of the present work is to synthesize GQDs incorporated



## LITERATURE REVIEW

micro/ nano PDEA hydrogel system with desired LCST and to characterize the properties of the hydrogel, and to evaluate the biocompatible efficacy of DOX loaded hydrogel by in vitro and in-vivo performance in murine melanoma model.

**The main objectives of the present research work are:**

Objective I: Synthesis and optimization of Graphene quantum dots (GQDs) and its functionalization using amino acids (Leucine and Methionine).

1. Effect of operating variables (synthesis time and amino acid concentration).
2. Characterization of GQDs using UV, DLS, FTIR, PL, TEM.

Objective II: Synthesis and characterization of the stable/biocompatible hydrogel using Poly (N, N-diethyl acrylamide) through free radical polymerization.

1. Effect of operating variables (monomer concentration, cross-linker concentration, initiator concentration, temperature, and GQDs) on a synthesis of PDEA hydrogel.
2. Characterization of hydrogel using FTIR, DSC, TGA, SEM.
3. Studies on thermo-responsive nature of hydrogel.
4. Studies on release kinetics and development of release model using drug release studies.

Objective III: Synthesis and characterization of Poly (N, N-diethyl acrylamide) micro/nanohydrogel by inverse emulsion polymerization.

1. Effect of operating variables (w/o ratio, surfactant concentration, RPM) on the synthesis of PDEA micro/nanohydrogel.
2. Characterization of the micro/nanohydrogel using DLS, TEM, FTIR, TGA.
3. Studies on release kinetics and development of release model using drug release studies.

Objective IV: *In-vitro* and *in-vivo* studies of micro/nanohydrogel using a model drug.

# LITERATURE REVIEW

## 2.16 Outline of the thesis

**The present research work is divided into following chapters:**

**Chapter 1** presents the **Introduction**. This chapter discusses the background of research, need for the study, and importance of the present study. It starts with a brief introduction about the hydrogel, temperature responsive hydrogel, graphene quantum dots and also about the nanohydrogels and its importance in the field of drug delivery to cancer cells. Based on the scope, the objectives were formulated and presented at the end of this chapter.

**Chapter 2** presents the detailed **Literature Review**. This chapter summarizes the relevant literature review carried out during the current study, highlighting the research gaps in existing literature reports and the critical research questions.

**Chapter 3** presents the **Materials and Methods**. This chapter lists the materials used and its purity, followed by the description of the experimental methodologies and the analytical procedures adopted to achieve the stated objectives.

**Chapter 4** deals on **Results and Discussion**. Experiments were performed as per the methodologies presented in Chapter 3 to achieve the objectives of the present research work. This chapter consists of four parts:

**Part I** deals with the results and discussion on the synthesis of graphene quantum dots and its functionalization and its characterization.

**Part II** deals with the synthesis of PDEA hydrogel and GQDs grafted PDEA hydrogel and its characterization, and the effect of GQDs contents on the LCST of the hydrogels, and also its temperature responsive study using DOX as a model drug; and the release data obtained were fitted to model equation to find out the release mechanism.

**Part III** deals with the results on the synthesis of PDA nanohydrogel using inverse emulsion polymerization method and effect of operating parameters on the particle mean size of PDEA nanohydrogel. The optimized condition was used to synthesize GQDs grafted PDEA nanohydrogel and characterization of nanohydrogel. The release profile of a model drug from nanohydrogel were presented and discussed and the release data obtained were fitted to the model equation to find out the release

## LITERATURE REVIEW

mechanism. The *in vitro* biocompatible evaluation of the PDEA nanohydrogel is essential for a drug carrier to be biocompatible and non-toxic so that it can be used in biomedical applications. The *in-vitro* evaluations of the hydrogel and nanohydrogel were carried out by cellular toxicity test, and degradation for long-term usage.

**Part IV** deals with the *in-vivo* analysis using DOX-loaded nanohydrogel in lung metastasis in mice. The evaluation of hematological parameters and cytokine assays were presented in this part. Results were presented in the form of tables and figures wherever necessary. Detailed discussion on the results with proper justification and literature support is also presented in this chapter.

**Chapter 5** presents the **Summary and Conclusion** of the present work along with the **future scope** for research.

# LITERATURE REVIEW

**CHAPTER 3**  
**MATERIALS AND**  
**METHODS**



# MATERIALS AND METHODS

## CHAPTER 3

### 3 MATERIALS AND METHODS

#### 3.1 Materials

N, N – diethyl acrylamide (DEA, 98%) was purchased from Tokyo Chemical Industry co., Ltd. (TCI), Tokyo, Japan. N, N'-methylbisacrylamide (MBA, 99%) was purchased from Loba Chemie, Mumbai, India. Ammonium peroxodisulfate (APS, 98%), was purchased Merck Specialities Pvt. Ltd., Mumbai, India. N, N, N', N'-tetramethyl ethylenediamine (TEMED, 99%) from HiMedia Laboratories Pvt. Ltd., Mumbai, India. Citric acid (CA, 99%) was purchased from Molychem, Thane, India. L-Leucine (Leu, 99%) was purchased from Sisco Research Laboratories Pvt. Ltd. (SRL), Mumbai, India. L-Methionin (Met, 99%) was purchased from Sisco Research Laboratories Pvt. Ltd. (SRL), Mumbai, India. Span 80 (SP, 95%), Cyclohexane (CY, 99.5%) and Doxorubicin Hydrochloride Pharmaceutical secondary standard (DOX) was purchased from Sigma-Aldrich. All the chemicals were used without further purification. Milli-Q water was used for all the experiments.

#### 3.2 Preparation of Graphene quantum dots (GQDs)

GQDs was fabricated by microwave-assisted pyrolysis of CA. In a typical procedure, 5 g of CA was weighed and powdered using mortar and piston. The obtained powder was placed in the preheated domestic microwave (Onida, Model: 20 Solo Dlx) at 700 W. During pyrolysis, CA was liquidated and the color of liquid changed from colorless to dark brown. Further, the dark brown product was dissolved in 1 molL<sup>-1</sup> of NaOH solution and preserved at 4 °C for further characterization and use. Further, the same procedure was followed to modify the GQDs by the addition of amino acids (Leu and Met) as shown in **Table 3.1**. The effect of process variables, such as time for synthesis of bare GQDs, concentration of Leu or Met for synthesis of functionalized GQDs was studied and optimized using OVAT (one variable at a time) method.

## MATERIALS AND METHODS

**Table 3.1: Feed composition of GQDs synthesis**

Conc. CA (mmol)	Time of MWI (min)	Conc. Leu (mmol)	Conc. Met (mmol)
26.024	2	0.763	0.670
26.024	3	1.906	1.675
26.024	4	3.812	3.351
26.024	5	5.718	5.026
26.024	6	7.624	6.702

### 3.3 Synthesis of poly (n, n-diethyl acrylamide) (PDEA) hydrogel

The Poly (N, N-diethyl acrylamide) (PDEA) hydrogel was synthesized by free-radical-polymerization (Maheswari *et al.* 2014). Briefly, the known amount of monomer DEA (2.179 – 15.2 mmol), cross-linker MBA (129.7  $\mu$ mol), initiator APS (87.67  $\mu$ mol), milli-Q water (5 mL) were stirred vigorously in a beaker, and then TEMED (50  $\mu$ L) was added dropwise to accelerate the reaction. The polymerization reaction was performed at ambient room temperature (28 °C) for 4 h. After polymerization reaction, the synthesized hydrogels were immersed in milli-Q water for 48 h to eliminate the residual unreacted molecules and the water was replaced with fresh water for every 4 h. The synthesized polymeric hydrogels were examined visually for their physical strength, rigidity and mechanical stability. Further, maximum swelling ability of the synthesized hydrogel was measured using water and the water content in the swollen hydrogel was calculated as follows.

$$\text{Water content in hydrogel} = W_W / W_D \quad (3.1)$$

Where,  $W_W$  is the weight of equilibrated hydrogel at room temperature and  $W_D$  is the dry weight of the hydrogel.

The hydrogel which imbibed large amount of water was considered for further optimization i.e., cross-linker MBA (38.91 – 324.3  $\mu$ mol), initiator APS (21.91 – 175.3



## MATERIALS AND METHODS

$\mu\text{mol}$ ), TEMED (20 - 100  $\mu\text{L}$ ) and temperature (25 – 40  $^{\circ}\text{C}$ ) by varying one variable at a time method **Table 3.2**.

### 3.3.1 Optimization of process variables

The effect of process variables, such as concentration of monomer, cross-linker, initiator, synthesis temperature of hydrogel and GQDs (bare GQDs and functionalized GQDs) content was studied. Further, reaction contents were optimized using OVAT (one variable at a time) method.

**Table 3.2: Feed composition and sample designation of hydrogel**

Sample ID	DEA (mmol)	MBA ( $\mu\text{mol}$ )	APS ( $\mu\text{mol}$ )	TEMED ( $\mu\text{L}$ )	Temperature ( $^{\circ}\text{C}$ )	Water (mL)
T25	8.717	129.7	175.3	100	25	5
T28	8.717	129.7	175.3	100	28	5
T30	8.717	129.7	175.3	100	30	5
T32	8.717	129.7	175.3	100	32	5
T34	8.717	129.7	175.3	100	34	5
T36	8.717	129.7	175.3	100	36	5
T38	8.717	129.7	175.3	100	38	5
T40	8.717	129.7	175.3	100	40	5

### 3.4 Characterization of GQDs and PDEA hydrogel

UV-vis absorption was carried out using UV/Vis/NIR spectrophotometer (HITACHI, U-2900 UV/vis Spectrophotometry). Fluorescence spectra was obtained by using Fluorescence spectrophotometer (Horiba, JY, Fluoromax-4). The particle size were measured using Horiba Scientific nano Partica, nano particle size analyzer, SZ-100. Elemental analysis was carried out using Elementar Vario EL III. FTIR analysis (Bruker) was carried out in the range between 4000 - 500  $\text{cm}^{-1}$  to confirm their chemical properties. The weight change in the lyophilized sample was measured using thermogravimetric differential thermal analyzer (Exstar, 6000 TG-DTA 6300) under nitrogen atmosphere at a flow rate of 50  $\text{mL min}^{-1}$ . The temperature was raised from

## MATERIALS AND METHODS

room temperature to 700 °C using a linear programmer at a heating rate of 10 °C min<sup>-1</sup>. Differential scanning calorimetric (DSC) analysis of the samples were carried out using TA instruments, Model Q150 at a heating rate of 10 °C min<sup>-1</sup>. Scanning electron microscope (SEM) was used to analyze the interior structure of the hydrogels. Prior to SEM, the samples were cut to required dimensions and sputtered with gold and then observed (JEOL, JSM-6360 LV analytical SEM).

### 3.5 Temperature-dependent equilibrium swelling ratio

The standard gravimetric method was followed to measure the equilibrium swelling ratio (ESR) of the hydrogels. The temperature dependence of equilibrated hydrogels in milli-Q water at a predetermined temperature range between 20 °C to 60 °C was studied. The hydrogels were immersed in milli-Q water for 30 mins to reach swollen equilibrium at each predetermined temperature. The hydrogel samples were then taken out, and excess water on the sample surface was wiped with wet filter papers and weighed until constant weight was attained. After the measurement, the hydrogels were re-equilibrated in milli-Q water using the same method as mentioned above. The weight of each dried sample was then noted after drying the sample under vacuum at room temperature. The equilibrium swelling ratio, ESR, was defined as follows:

$$\text{ESR} = (W_s - W_d)/W_d \quad (3.2)$$

where,  $W_d$  is the dry weight of the hydrogel and  $W_s$  is the weight of equilibrated hydrogel at the particular temperature.

### 3.6 Time-dependent swelling of hydrogels

The method mentioned in above section (ESR), was followed to record the swelling ratio (SR) of hydrogels. The dried gels were immersed in milli-Q water at ambient temperature (28 °C) and the SR measurement was done gravimetrically weighed at every 30 mins. The swelling ratio (SR) at time  $t$  was defined as follows:

$$\text{SR} = (W_t - W_d)/W_d \quad (3.3)$$

where,  $W_d$  is the dry weight of the hydrogel and  $W_t$  is the weight of equilibrated hydrogel at time  $t=30$  min.

## MATERIALS AND METHODS

### 3.7 Deswelling kinetics measurement

Formed hydrogels were placed in milli-Q water to swell. After reaching the equilibrium swollen state, hydrogels were immediately transferred from milli-Q water (28 °C) to 50 °C. Ensured that the surface water on the hydrogel was wiped with wet filter paper, the difference in weight was recorded. Water retention ( $W_R$ ) was calculated by,

$$W_R = 100 \times (W_t - W_d) / (W_e - W_d) \quad (3.4)$$

Where,  $W_e$  is the equilibrated swollen hydrogel weight at room temperature,  $W_t$  is the weight of hydrogel at regular time point ( $t=30$  min) and  $W_d$  is the dried gel weight.

### 3.8 Drug loading and *in-vitro* release studies

The model drug loading (DOX) in cross-linked polymer matrix was accomplished by equilibrium partitioning in presence of the drug. A calibration curve was developed for the known concentration of DOX at 480 nm using UV-Vis spectroscopy (HITACHI, U-2900 UV/vis Spectrophotometry). In the present study, the hydrogels (0.1 g each) were submerged in a 30 ppm of DOX solution, kept at 4 °C for 24 h for sufficient absorption by the hydrogel network. The total drug loading was estimated by measuring the change in the mass of hydrogels before and after loading. The samples were removed from drug solution after imbibition, the drug release experiment was performed at 30 °C, 37 °C and 40 °C. The accurately weighed DOX encapsulated hydrogels were suspended in 10 mL of freshly prepared PBS. At regular time interval, 1 mL of the solution was withdrawn and analyzed using UV-vis spectroscopy at 480 nm to determine the amount of DOX released. The withdrawn solution was replaced back to maintain original volume. The results were presented in terms of cumulative release as a function of time, which is calculated as follows,

$$\text{Cumulative amount release (\%)} = (M_t / M_\infty) \times 100 \quad (3.5)$$

where,  $M_\infty$  is the estimated amount of drug loaded in the hydrogel and  $M_t$  is the amount of drug released from hydrogel at time  $t$ .

Further, the continuous response of the hydrogel between the temperatures from 20 °C to 60 °C was studied using the above mentioned protocol.

# MATERIALS AND METHODS

## 3.9 *In-vitro* drug encapsulation and drug loading

The drug encapsulation efficiency (EE) and loading capacity (LC) of hydrogels was determined by knowing the initial drug concentration before suspending the dry hydrogel. The final drug concentration was measured after 24 h of incubation of hydrogels. EE and LC were calculated from the following equations:

$$\text{Encapsulation efficiency (\%)} = ((M_{DI} - M_{DSP}) / M_{DI}) \times 100 \quad (3.6)$$

$$\text{Loading Capacity (\%)} = (M_{DN} / M_N) \times 100 \quad (3.7)$$

where,  $M_{DI}$  is the initial mass of drug present in solution,  $M_{DSP}$  is the mass of the final drug present in supernatant after drug loading,  $M_{DN}$  is the mass of drug encapsulated within the hydrogels ( $M_{DN} = M_{DI} - M_{DSP}$ ) and  $M_N$  is the initial mass of the lyophilized hydrogels.

### 3.9.1 Analysis of drug release pattern

Release of the solute from the cross-linked structure is based on the swelling behaviour of the polymers and rate of diffusion. To determine the release mechanism, drug release from the cross-linked networks of PDEA hydrogels has been analysed using zero-order, first-order, Higuchi, and Korsmeyer-Peppas models. Following equations are the model equations used to analyse drug release mechanism (Suvakanta *et al.*, 2010; Ronald *et al.*, 2012).

Zero-order kinetic model:  $C_t = C_0 - k_0 t \quad (3.8)$

Where,  $C_0$  is the initial concentration of drug (at  $t=0$ ),  $C_t$  is the amount of drug released at time  $t$  and  $k_0$  is the zero-order rate constant.

First-order kinetic model:  $\log C_t = \log C_0 - k_1 t / 2.303 \quad (3.9)$

Where,  $C_0$  is the initial concentration of drug (at  $t=0$ ),  $C_t$  is the amount of drug released at time  $t$  and  $k_1$  is the first-order rate constant.

Higuchi model:  $Q = k_2 t^{1/2} \quad (3.10)$

Where,  $Q$  is the cumulative release of drug in time  $t$  and  $k_2$  is the Higuchi constant.

## MATERIALS AND METHODS

Korsmeyer-Peppas model: 
$$\frac{M_t}{M_\infty} = k_3 t^n \quad (3.11)$$

Where,  $\frac{M_t}{M_\infty}$  is the fraction of drug release at time t,  $k_3$  is the release rate constant and n is the release exponent.

Hixon-Crowel model: 
$$W_o^{1/3} - W_t^{1/3} = k_4 t \quad (3.12)$$

Where,  $k_4$  is the Hixon-Crowel constant,  $W_o$  is the initial amount of drug in gel and  $W_t$  is the remaining amount of drug in gel at time t.

### 3.10 Cytocompatibility of hydrogels

According to Francis and Rita (1986) the MTT assay was accomplished. The monolayer of B16F10 (murine melanoma) cell culture was trypsinized and cell count was altered to  $1.0 \times 10^5$  cells/mL using DMEM medium containing 10% NBCS. The diluted cell suspension of 0.1 mL (approximately 10,000 cells) was added to each well of the 96 well microtiter plate. After 24 h, the supernatant was discarded from partially formed monolayer, then washed with DMEM solution and 100  $\mu$ L of different hydrogel extract concentrations was added to the cells in the microtiter plates. The plates were then incubated under 5% CO<sub>2</sub> atmosphere for 3 days at 37 °C and for every 24 h the cells were examined under inverted microscope. After 72 h, the hydrogel extract solutions were discarded from the wells and 50  $\mu$ L of MTT in MEM – PR (Minimum essential medium without phenol red) was added to each well. The plates were gently shaken and incubated under 5% CO<sub>2</sub> atmosphere for 3 h at 37 °C. Further, the supernatant was removed and 50  $\mu$ L of propanol was added and the plates were gently shaken to solubilize the formed formazan. The absorbance was measured using a microplate reader at a wavelength of 540 nm. The percentage cell viability was calculated using the following formula:

$$\text{Viability (\%)} = \left[ \frac{\text{Mean OD of the individual test group}}{\text{Mean OD of the control group}} \times 100 \right] \quad (3.13)$$

## MATERIALS AND METHODS

### 3.11 Synthesis of PDEA nanohydrogel by inverse emulsion polymerization

PDEA nanohydrogels were synthesized by inverse emulsion polymerization (IEP) technique. The monomer, DEA (8.717 mmol), cross-linker, MBA (129.7  $\mu\text{mol}$ ), and initiator, APS (175.3  $\mu\text{mol}$ ) were dissolved in 5 mL of milli-Q water at room temperature and transferred to a cylindrical round-bottom flask containing cyclohexane with non-ionic surfactant Span 80. The mixture was homogenized at 10,000 rpm for 1 h to produce nanospheres at room temperature. Homogenization emulsifies the water phase in to the organic phase and produce nanospheres. Then the mixture was stirred continuously with magnetic stirrer and the polymerization reaction was initiated by adding 150  $\mu\text{L}$  of TEMED. The reaction was initially purged with nitrogen to remove dissolved oxygen and the reaction was continued for 6 h under nitrogen atmosphere. After the completion of reaction, the products were allowed to settle, and the surfactant was removed by rinsing the product with pure CY. The product was then re-dispersed in deionized water and subjected to repeat centrifugal washing. During centrifugal washing, the hydrogel particles were immersed in milli-Q water and centrifuged at 12,000 rpm for 30 min to remove SP and un-reacted chemicals like monomer, cross-linker and initiator. Then the particles were lyophilized to produce free flow powder and stored for further studies. Optimization of process parameters was done by studying the effects of process variables, such as water-oil ratio, surfactant concentration and stirring rate on the particle size of the nanohydrogels synthesized (**Table 3.3**). The particle size and size distribution of the nanohydrogels were characterized by dynamic light scattering (DLS) technique.

### 3.12 Synthesis of GQDs grafted PDEA nanohydrogel

GQDs grafted PDEA nanohydrogels were synthesized by IEP technique as discussed in section 3.11 using the optimized composition and process variables as in **Table 3.3**. Further, similar protocol was used to synthesize PDEA incorporated GQDs by addition of bare GQDs (0.075 g) and functionalized GQDs (GL-0.5 g and GM-0.1 g) separately with optimized process parameters water and cyclohexane ratio of 1:5 at stirrer speed of 600 rpm and surfactant concentration of 3%.

## MATERIALS AND METHODS

**Table 3.3: Optimization of nanohydrogels feed composition**

<b>Sample ID</b>	<b>Stirrer speed (RPM)</b>	<b>Water-oil ratio (wt:wt)</b>	<b>Surfactant (Vol% in cyclohexane)</b>
N-1	300	1:2	1.5
N-2	400	1:3	1.75
N-3	500	1:4	2
N-4	600	1:5	2.25
N-5	700	1:6	2.5
N-6	800	-	2.75
N-7	-	-	3

### 3.13 Characterization of synthesized GQDs and nanohydrogels

UV-vis absorption was carried out using UV/Vis/NIR spectrophotometer (HITACHI, U-2900 UV/vis Spectrophotometry). Fluorescence spectra was obtained by using Fluorescence spectrophotometer (Horiba, JY, Fluoromax-4). The particle size of GQDs and nanohydrogels were measured in water using Horiba Scientific nano Partica, nano particle size analyzer, SZ-100. FTIR analysis (Bruker) was carried out in the range between 4000 - 500  $\text{cm}^{-1}$  to confirm their chemical properties. Elemental analysis was carried out using Elementar Vario EL III. The weight change in the lyophilized hydrogel was measured using thermogravimetric differential thermal analyzer (Exstar, 6000 TG-DTA 6300) under nitrogen atmosphere at a flow rate of 50  $\text{mL min}^{-1}$ . The temperature was raised from room temperature to 700  $^{\circ}\text{C}$  using a linear programmer at a heating rate of 10  $^{\circ}\text{C min}^{-1}$ . Gel permeation chromatography (GPC) was performed using a Perkin Elmer (Model: Turbo matrix - 40) equipped with a PLgel Mixed-D column (dimension: 300 mm length, 7.5 mm internal diameter and 5  $\mu\text{m}$  particle size; molecular weight range 2590-275000) in THF. The number average molecular weight ( $M_n$ ) and polydispersity index ( $M_w/M_n$ ) of the synthesized polymers were determined on the basis of a polystyrene calibration. To prepare a sample for the TEM measurement, an aqueous solution of prepared GQDs and the polymer ( $0.01 \text{ mg mL}^{-1}$ ) was stirred

## MATERIALS AND METHODS

for 24 h at room temperature to reach thermodynamic equilibrium. A drop of the polymer solution was then deposited onto a 200-mesh carbon coated copper grid and dried overnight in a desiccator to achieve dryness. The TEM measurement was performed by the instrument JOEL (Model: JEM 2100) on the obtained polymer sample at an acceleration voltage of 200 kV using LaB<sub>6</sub> source.

### 3.14 *In-vitro* drug encapsulation and drug loading

The applicability of synthesized nanohydrogels in controlled release of drug were investigated by subjecting these gels to drug encapsulation and drug loading using DOX as model drug. A calibration curve was developed for the known concentration of DOX at 480 nm using UV-Vis spectroscopy (HITACHI, U-2900 UV/vis Spectrophotometry). In case of nanohydrogels, known weight of dried gels were placed in 10 mL of loading solution (30 ppm of DOX solution) and allowed to equilibrate for 48 h at room temperature. Then the gels were removed from the loading solution and rinsed with water. The DOX content in the nanohydrogels were determined by measuring the concentration of DOX in the loading solution before and after loading, using UV/Vis spectrophotometer at 480 nm. The entrapment efficiency and the loading capacity of the nanohydrogels were calculated using equation. 3.14 and 3.15 respectively.

$$\text{Encapsulation efficiency (\% W/W)} = ((M_{DI} - M_{DSP}) / M_{DI}) \times 100 \quad (3.14)$$

$$\text{Loading Capacity (\% } \mu\text{g/mL)} = (M_{DN} / M_N) \times 100 \quad (3.15)$$

where,  $M_{DI}$  is the initial mass of drug present in solution,  $M_{DSP}$  is the mass of the final drug present in supernatant after drug loading,  $M_{DN}$  is the mass of drug encapsulated within the nanohydrogels ( $M_{DN} = M_{DI} - M_{DSP}$ ) and  $M_N$  is the initial mass of the lyophilized nanohydrogels.

### 3.15 *In-vitro* drug release studies of PDEA nanohydrogel

It is practical and important to examine the release profile of the nanohydrogel at temperature below and above the LCST. The drug release experiments were performed at three different temperatures 30 °C (below LCST), 37 °C and 40 °C



## MATERIALS AND METHODS

(above LCST). Accurately weighed DOX encapsulated gels were suspended in 10 mL of PBS buffer. At regular time interval, 1 mL of solution was withdrawn and analyzed using UV/Vis spectrophotometer at 480 nm to determine the amount of DOX released. The withdrawn solution was replaced back to maintain original volume. The DOX content in the nanohydrogels were determined by measuring the concentration of DOX in the loading solution before and after loading, using UV/Vis spectrophotometer at 480 nm. The results were presented in terms of cumulative release as a function of time, which is calculated as per the equation (3.16):

$$\text{Cumulative amount released (\%)} = \frac{M_t}{M_\infty} \times 100 \quad (3.16)$$

Where,  $M_t$  is the amount of DOX released from the gels at time  $t$  and  $M_\infty$  is the estimated amount of DOX loaded in the gels.

Further, the response of the nanohydrogel at different temperatures from 20 to 60 °C was studied by same protocol as mentioned in section 3.15.

### 3.16 Degradation of nanohydrogels

Degradation is indirectly proportional to mass of the nanohydrogel. The synthesized nanohydrogels (0.1 g) were immersed in 10 ml of phosphate buffered saline (PBS: 1X, 7.4 pH) and incubated at temperature of 37 °C. At specific time interval, the mass of dry gel (dried using lyophilization) was measured until constant value was obtained. Degradation of nanohydrogel was estimated by measuring the residual weight as follows:

$$\text{Degradation (\%)} = \frac{(W_0 - W_t)}{W_t} \times 100 \quad (3.17)$$

Where,  $W_0$  is the initial mass of dry nanohydrogel and  $W_t$  is the mass of undegraded dry nanohydrogel

### 3.17 Cells lines and media used for culturing

The murine melanoma cell line (B16F10) were acquired from National Centre for

## MATERIALS AND METHODS

Cell Science (NCCS), Pune, Maharashtra, India. The cells were cultured in Dulbecco's modified eagle medium (DMEM; Sigma, Saint Louis, MO, USA) with 10% fetal bovine serum (Hyclone, Logan, UT, USA) and 1% of penicillin–streptomycin (Himedia, India). Quintessential growth of cells was attained using ambient conditions of 37 °C and 5% CO<sub>2</sub> for humidity.

### 3.17.1 Cytotoxicity studies of nanohydrogels

The cytotoxicity of the nanohydrogels (PDEA and GQDs grafted PDEA) was evaluated by performing 3-(4,5-dimethylthiazol-2-yl)-2,5-diphenyltetrazolium bromide (MTT) assay. The nanohydrogel samples were sterilized and exposed to the DMEM medium for 16 h. After sufficient exposure, the supernatant was taken and filtered through syringe filter to remove undissolved nanohydrogel debris. This filtrate was used as the test sample. For the cytotoxicity test, exponentially growing B16F10 cells were harvested and the cell count was adjusted to 50000 cells mL<sup>-1</sup> of medium. 100 µL of this suspension was seeded to each well of a 96 well plate. The plate was incubated at 37 °C in an atmosphere consisting of 5% CO<sub>2</sub> for 24 h for cell adhesion. After 24 h, the medium was replaced with different concentration of the test samples. Cells were incubated further for a period of 48 h in the same conditions. After the incubation, the medium in each well was replaced with 50 µL of MTT reagent (2 mg mL<sup>-1</sup> MTT reagent in PBS buffer). The cells were incubated for another 4 h at 37 °C in dark. On completion of incubation, the MTT reagent was removed and the formazan crystals formed were dissolved in 100 µL dimethyl sulfoxide (DMSO) solution. The optical density (OD) was measured at 540 nm with a micro plate reader. The cell viability rate was calculated as follows;

$$\text{Viability (\%)} = \frac{OD_{\text{treated}}}{OD_{\text{Control}}} \times 100 \quad (3.18)$$

Where, OD<sub>control</sub> is the optical density obtained in the absence of nanohydrogel and OD<sub>treated</sub> is the optical density obtained in the presence of nanohydrogel.

## MATERIALS AND METHODS

### 3.18 Animals, murine melanoma model and *in-vivo* studies

The mice (C57BL/6) aged 8-10 weeks with weight of 18-30 g were procured from central animal research facility of Manipal University, Manipal, Karnataka, India. All the animals were transferred to polypropylene cages, placed in ambient housing conditions  $23\pm 2$  °C temperature and  $50\pm 5\%$  atmospheric moisture. Aseptic food and water were provided *ad libitum*. Mandating process of experimental procedure was done by Institutional Animals Ethics Committee (94/PO/ReBi/S/1999/CPCSEA) and experimentation was done following the specification approved by committee for the purpose of control and supervision of experiments on animals.

The mice were separated into seven groups with n number of mice (n=5/group) in each group, to study the anti-tumour effect of nanohydrogels as cancer drug carrier. The melanoma model was established by injecting 0.1 mL of B16F10 cell having cell count of approximately  $10^6$  cells via intravenous route (tail vein) for six groups, one group was injected with PBS buffer as normal control. After the development of melanoma, anti-cancerous activity of drug loaded nanohydrogels (N-bare PDEA nanohydrogel; NG-GQDs grafted PDEA nanohydrogel; NL-GL grafted PDEA nanohydrogel and NM-GM grafted PDEA nanohydrogel) were tested. Nanohydrogel dose concentration to be injected was established according to their encapsulation efficiency that was determined earlier, homologous to 2.5 mg/kg of DOX (Mingqiang *et al.* 2015; Swapnil *et al.* 2015). Groups were entitled and classified as follows:

**Group I:** Mice injected with PBS buffer only

**Group II:** Mice injected with B16F10 cell lines only

**Group III:** Mice injected with cell lines and treated with standard DOX

**Group IV:** Mice injected with cell lines and treated with N loaded with DOX

**Group V:** Mice injected with cell lines and treated with NG loaded with DOX

**Group VI:** Mice injected with cell lines and treated with NL loaded with DOX

## **MATERIALS AND METHODS**

**Group VII:** Mice injected with cell lines and treated with NM loaded with DOX

After four weeks of treatment, mice were humanly euthanized and used for further studies. Mice weight were noted throughout the experiments, after euthanization all organs were excised and their respective weight was recorded.

### **3.19 Haematological parameters and tumor count evaluation**

The blood sample was collected from the retro-orbital plexus of animals in tubes with EDTA as an anticoagulant and further, analysed using a veterinary blood cell counter (KE-210 VET. ERMA Inc. Tokyo. Japan). Metastatic spots present on excised lung was counted manually.

### **3.20 Analysis of TNF- $\alpha$ and IL-6**

Plasma was collected from blood by centrifugation at 14000 rpm for 4 minutes in tubes with EDTA as anticoagulant. For TNF- $\alpha$  analysis, mouse ELISA kit (catalogue number - KMC3011) of thermo fisher scientific was used. Also, for IL-6 analysis, Quantikine<sup>®</sup> ELISA kit (catalogue number - M6000B) of R & D systems was utilized. Standard curve and sample analysis was conducted in accordance with manufactures instructions. Both assay for samples was done in duplicates for accuracy.

### **3.21 Statistical analysis**

The animal study experiments were statistically analyzed using ANOVA for significant differences. All the data were compared with normal and disease control. Indication of significance was done by \*P<0.05 (significant) w.r.t normal control, \*\*P<0.01 (highly significant), \*\*\*P<0.05 (significant), and \*\*\*\*P<0.05 (highly significant) w.r.t disease control also, <sup>a</sup>P<0.05 and <sup>b</sup>P<0.01 compared with doxorubicin.

**CHAPTER 4**  
**RESULTS AND**  
**DISCUSSION**



# RESULTS AND DISCUSSION

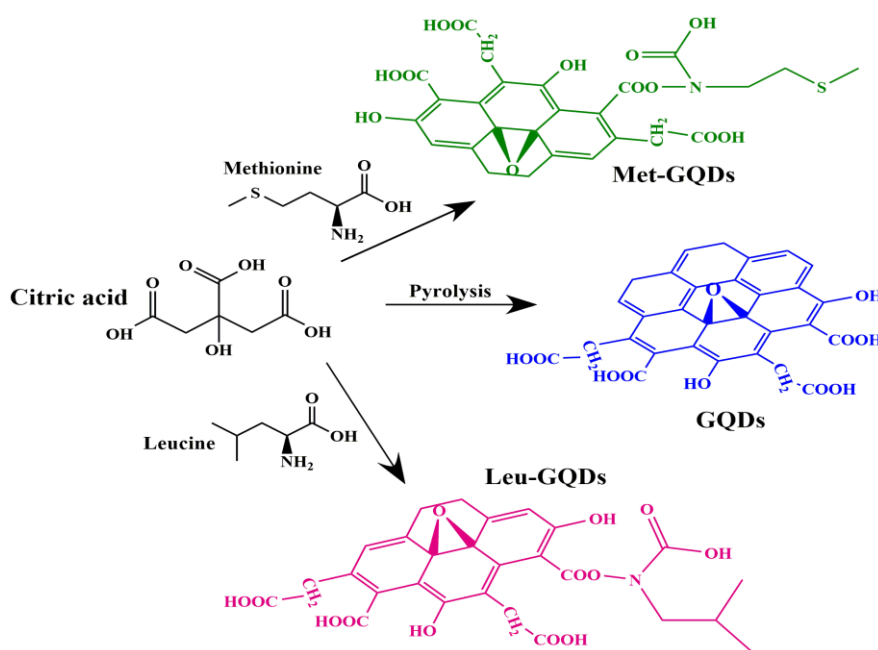
## CHAPTER 4

### 4 RESULTS AND DISCUSSION

#### PART I

##### 4.1 Synthesis and optimization of Graphene quantum dots (GQDs)

GQDs were prepared by pyrolysis of citric acid as a starting material as shown in **Scheme 4.1**. It is a simple, efficient and eco-friendly bottom-up approach to fabricate GQDs by microwave – assisted heating method. After reaction, a light-yellow solution with blue emission under UV light (365 nm) was obtained. Under basic reaction condition, the citric acid molecules self-assembled into sheet structure followed by condensation reactions through intermolecular dehydroxylation, forming nanocrystalline GQDs. The final GQDs have unreacted functional groups such as -OH, -CH<sub>2</sub>-, -COOH, -COOR groups on its surface (Qu *et al.* 2014; Zhao *et al.* 2015).



**Scheme 4.1:** Reaction scheme for synthesis of GQDs (GQDs- Bare GQDs; Leu-GQDs: Leucine functionalized GQDs; Met-GQDs: Methionine functionalized GQDs)

In this study, GQDs were synthesized along with amino-acids (Leucine and Methionine) to functionalize GQDs with amino acid to enhance hydrophilicity and

## RESULTS AND DISSCUSSION

photoluminescence properties. Citric acid was used as carbon source, leucine and methionine were used as  $-NH_2$  source. In functionalized GQDs,  $-NH_2$  molecules have strong electron donating ability where it can donate its lone pair of electron to carbon molecule due to which the photoluminescence of GQDs is enhanced. During the process, the  $-NH_2$  group of leucine and methionine reacts with carboxyl or hydroxyl groups of the GQDs to form leucine functionalized GQDs and methionine functionalized GQDs (Wu *et al.* 2014). Hao *et al.* (2015) reported, synthesis of nitrogen atom doped graphene in three different state, like pyridinic-N, graphitic-N and pyrrolic-N. He has reported an enhancement in the catalytic activity of GQDs doped with nitrogen atom. The enhanced catalytic activity of nitrogen doped graphene over undoped graphene is due to the increased active sites in nitrogen doped graphene in the form of pyridinic-N or pyrrolic-N, and graphitic-N which has improved the electro-catalytic activity because of its higher electronic conductivity. In 2014, Qu *et al.* reported that nitrogen addition on GQDs can improve its photoluminescence (PL) properties.

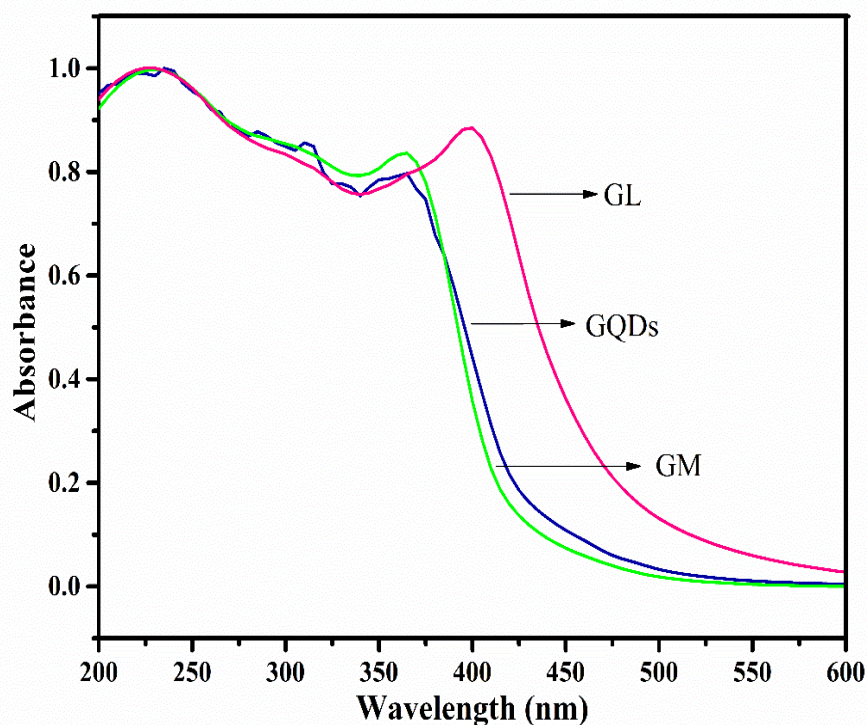


**Figure 4.1: UV-vis absorption spectra of bare GQDs, leucine functionalized GQDs (GL) and methionine functionalized GQDs (GM)**



## RESULTS AND DISCUSSION

In this study, experimental parameters such as reaction time and feed concentrations were systematically optimized as shown in **Table 4.1** to obtain bright photoluminescence (PL) of bare GQDs and amino-acid functionalized GQDs. The UV-vis absorption spectra of GQDs are shown in **Figure 4.1**. The synthesized GQDs showed a well-defined broad absorption band at 230 nm and between 365-400 nm and the peaks are ascribed to the  $\pi-\pi^*$  electron transition of the conjugated C=C bond and  $n-\pi^*$  electron transition of the C=O bond, which resulted in strong fluorescence (Wu *et al.* 2014; Lei *et al.* 2016; Xuan *et al.* 2017).

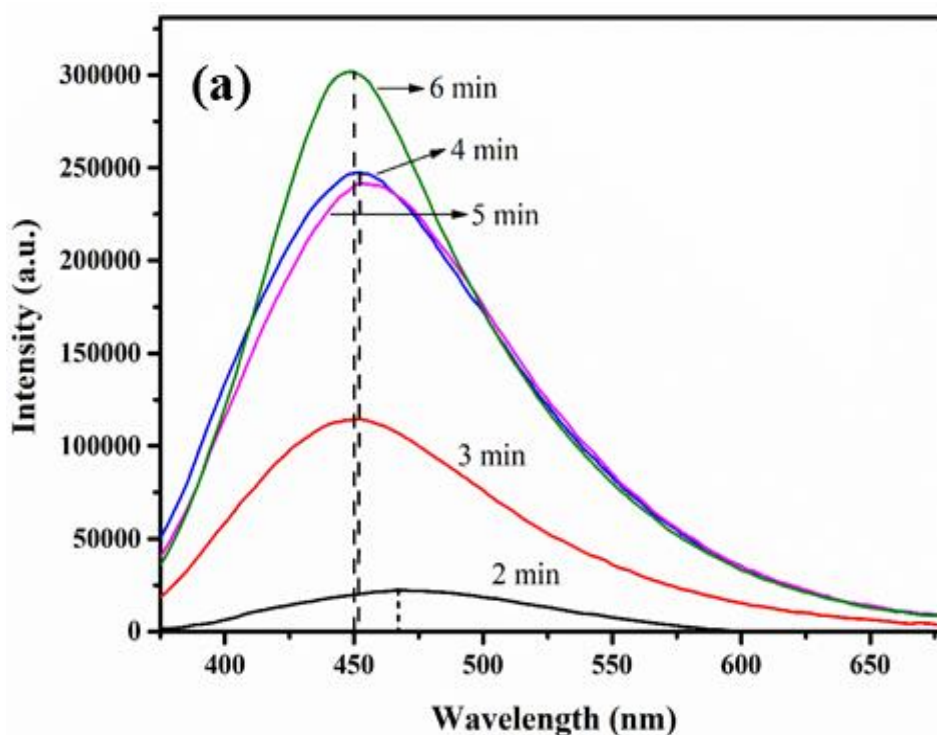


**Figure 4.2a: PL spectra of GQDs excited at 365nm - bare GQDs prepared at varying time interval**

The photoluminescence (PL) spectra were recorded upon excitation with a 365 nm beam as shown in **Figure 4.2**. The GQDs spectra in **Figure 4.2a** shows a strong peak at 450 nm. (Liang *et al.* 2013). A significance shift in the PL spectra was observed after functionalization of GQDs with leucine and methionine comparing with bare GQDs. The emission peak of leucine functionalized GQDs (**Figure 4.2b**) shifted from 430 nm to 457 nm at the excitation wavelength of 365 nm and further, red shift was observed as the leucine content was increased. Similarly, the Met-GQDs (**Figure 4.2c**) excited at

## RESULTS AND DISSCUSSION

365 nm showed the emission peak from 450 nm to 550 nm and a blue shift was observed with an increase in Met content. In all the three spectra, emission intensity increased with increase in reaction time and amino acid content, and it reached a maximum intensity at 5 min microwave irradiation for bare GQDs and for functionalized GQDs maximum intensity was observed at 1.9059 mmol of leucine and 3.3509 mmol of methionine, after which the peak intensity decreased (Hao *et al.* 2015).

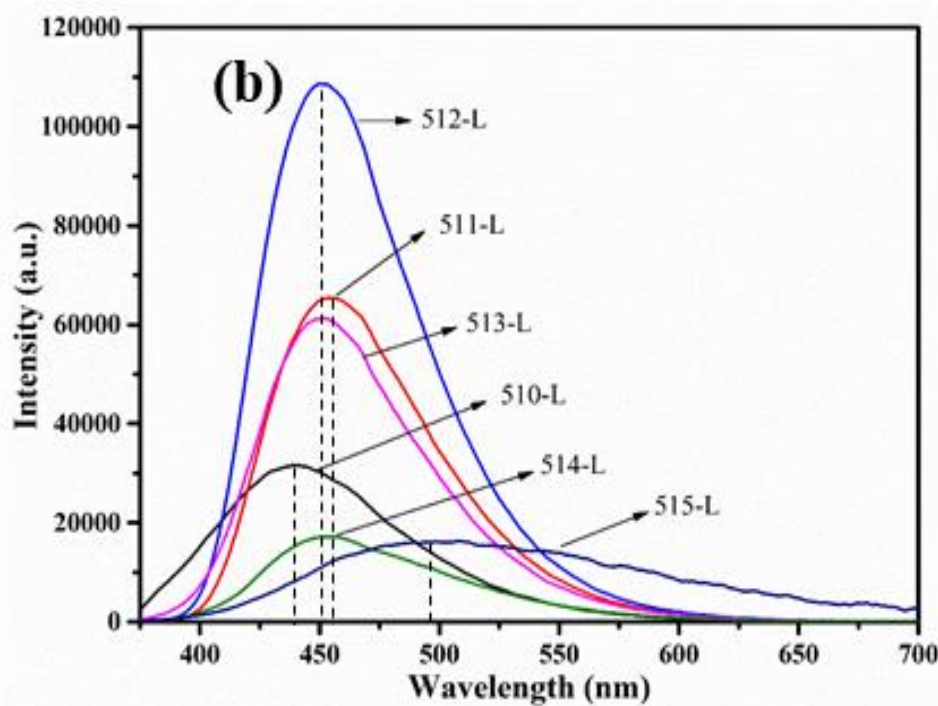


**Figure 4.2b: PL spectra of GQDs excited at 365nm - PL spectra of GQDs prepared by varying the Leucine content.**

These type of spectral shift and intensity phenomenon has been reported in the literature for carbon-based quantum dots (like carbon nanotubes (CNT), graphene oxide (GO)) (Luk *et al.* 2012; Ju *et al.* 2014). The shift is due to the difference in the particle size and difference in the emission sites of the formed GQDs (Luk *et al.* 2012; Ju *et al.* 2014). In this study, the enhanced photoluminescence (PL) properties were attributed to the formation of the pyrrolic-N in GQDs i.e., non-radiative oxygenated moieties were replaced by  $-NH_2$  group which act as a radiative centres of functionalized GQDs (Kumar *et al.* 2014; Hao *et al.* 2015).

## RESULTS AND DISCUSSION

The effect of synthesis time and amino acid concentration on particle size and quantum yield of the prepared GQDs is as shown in **Table 4.1**. The particle size was measured using DLS technique and the absolute quantum yield was measured by using quinine bisulfate method (0.1M in H<sub>2</sub>SO<sub>4</sub> as a standard sample) at 360 nm excitation at different time interval (2 – 6 min) and the quantum yield along with other variables are listed in **Table 4.1**.

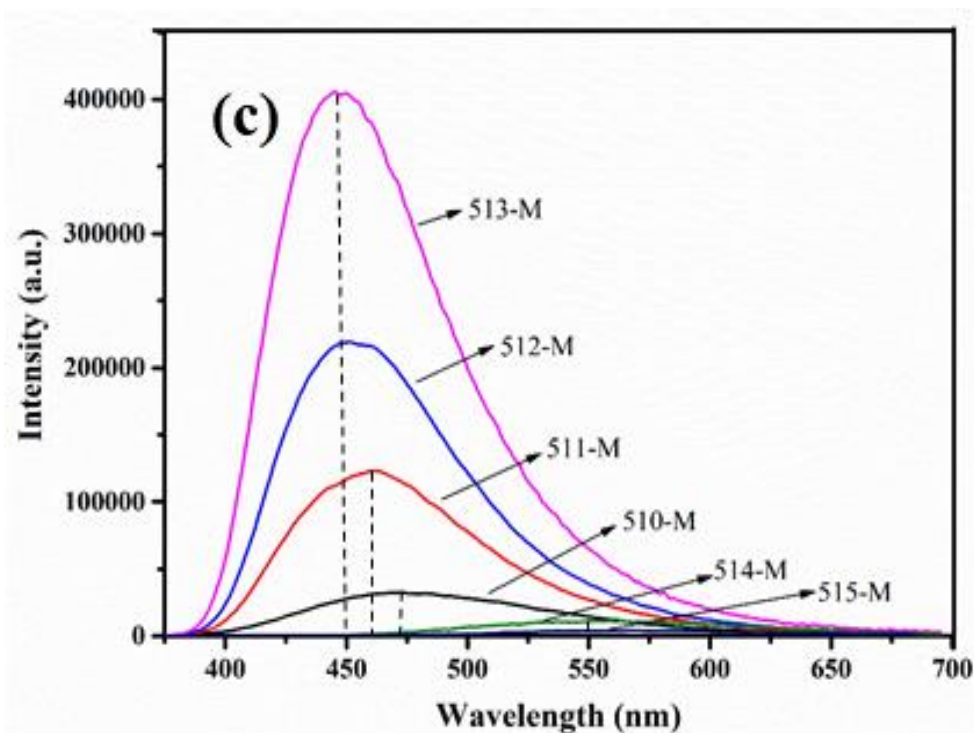


**Figure 4.2c: PL spectra of GQDs excited at 365nm - PL spectra of GQDs prepared by varying the Methionine content.**

From the table it can be observed that the quantum yield varied along with time of microwave irradiation and concentration of amino acid. The variation in the quantum yield of the prepared GQDs was due to the incomplete pyrolysis reaction of citric acid and also due to the formation of surface defects (Dong *et al.* 2012). The quantum yield of GQDs also varied with the synthesis methods and the associated surface chemistry. Since the GQDs contain epoxy and carboxylic groups on their surface which acts as non-radiative electron-hole recombination center, due to which the expected quantum yield for the prepared GQDs was 18.75%, whereas the amine functionalized GQDs

## RESULTS AND DISSCUSSION

gave a quantum yield of 20.26% for leucine functionalized GQDs and 16.82% for methionine functionalized GQDs (Valappil *et al.* 2017).

**Table 4.1: Optimization of synthesized GQDs with respect to time and feed content, and their particle size and quantum yield.**

Conc. CA (mmol)	Time of MWI (min)	Conc. Leu (mmol)	Conc. Met (mmol)	Particle size (nm)			Quantum yield (%)		
				Bare GQDs	Leu-GQDs	Met-GQDs	Bare GQDs	Leu-GQDs	Met-GQDs
26.024	2	0.763	0.670	7.6±2.3	25.2±3.1	56.1±2.7	2.696	7.092	0.654
26.024	3	1.906	1.675	2.5±1.9	12.1±2.5	45.1±4.7	3.752	20.26	4.026
26.024	4	3.812	3.351	1±3.2	54.1±2.8	27.8±2.8	5.104	7.282	16.826
26.024	5	5.718	5.026	0.7±1.5	60.7±1.3	56.1±3.8	18.756	1.294	5.382
26.024	6	7.624	6.702	1.8±1.7	70.6±1.6	98.9±1.9	9.725	0.915	0.390

Further, the prepared GQDs were characterized using TEM and the results are shown in **Figure 4.3**. The synthesized GQDs were nearly in spherical shape and their size was observed to be in the range of 14-16 nm in case of bare GQDs, 11-54 nm in case of leucine functionalized GQDs and 34-67 nm in case of methionine functionalized GQDs. Due to the functionalization of GQDs with leucine and methionine the average particle diameter has increased and also the functionalized GQDs showed mild agglomeration. It was confirmed that the prepared GQDs were well surface passivated (i.e., surface and edges of GQDs was coated by the oxygenated groups like –OH, –COOH, –NH<sub>2</sub> to avoid further reaction) by incompletely carbonized citric acid (Linbo *et al.* 2015).

## RESULTS AND DISCUSSION

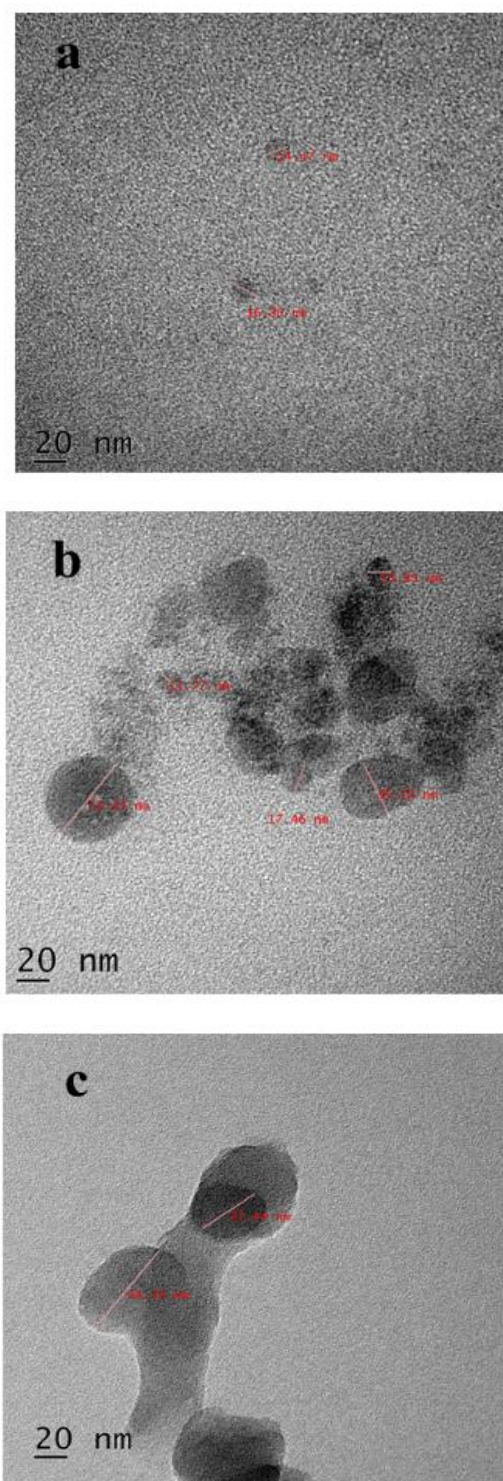


**Figure 4.3: TEM images of GQDs with a scale bar of 20 nm: (a) Bare GQDs; (b) Leu-GQDs; (c) Met-GQDs.**

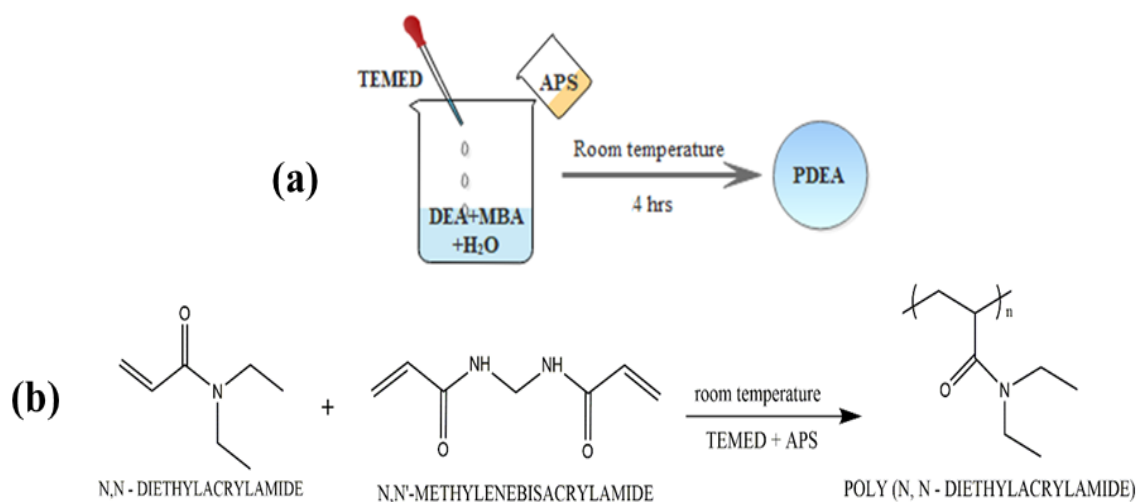
# RESULTS AND DISCUSSION

## PART II

### 4.2 Synthesis and optimization of PDEA hydrogels

#### 4.2.1 Synthesis of PDEA hydrogel

The PDEA hydrogel was synthesized by free-radical-polymerization reaction and the scheme of the polymerization reaction is illustrated in **Scheme 4.2(a-b)**. DEA in an aqueous solution was polymerized using MBA and APS/TEMED at ambient room temperature (28 °C). The polymerization reaction occurs in two stages. In the first stage, TEMED facilitates the decomposition of APS into free radicals and in the second stage, the free radical initiator attacks the monomer to initiate polymerization. The free radical attacks one of carbon double bonds (vinyl group) of the monomer molecule to form a new chemical bond between the monomer and initiator fragment. This process repeats and polymer chains become chemically cross-linked through the random incorporation of MBA until the exhaustion of monomer. **Scheme 4.2 (a)** is the schematic representation of the synthesis of PDEA hydrogel and **Scheme 4.2 (b)** is the reaction mechanism of the free-radical-polymerization reaction. The success of polymerization reaction depends on the



**Scheme 4.2: Schematic representation of free-radical-polymerization of PDEA synthesis (a) PDEA hydrogel preparation; (b) Chemical structure of monomer and cross-linked PDEA hydrogel**

## RESULTS AND DISCUSSION

operating variables like monomer concentration, cross-linker concentration, initiator concentration and accelerator concentration. In this part, the reaction parameters were optimized to achieve required properties like better swelling ratio and better physical stability.

### 4.2.2 Effect of process parameters

Process parameters like feed composition plays a major role in the desired properties of the hydrogel. The feed compositions were optimized at ambient room temperature (28 °C) to achieve better swelling ratio and better stability. The stability was quantified by visual observation and swelling ratio was analyzed using gravimetric method in the presence of water. The composition of monomer, cross-linker, initiator and accelerator was optimized by varying one variable at a time and the effects are discussed below.

#### 4.2.2.1 Effect of monomer concentration

To understand the effect of monomer (DEA) on the swelling capability of the PDEA hydrogels, experiment was conducted with different monomer concentration (2.179, 4.358, 6.538, 8.717, 10.8, 13 and 15.2 mmol) while keeping the other variables constant (MBA – 129.7  $\mu\text{mol}$ ; APS – 87.65  $\mu\text{mol}$  and TEMED – 50  $\mu\text{l}$ ). **Figure 4.4** shows the influence of monomer concentration on the water absorption capacity of the prepared hydrogel. It was evident from the figure, that water absorption improved with increase in monomer concentration upto 13 mmol, and beyond 13 mmol a slight decrease in water absorption was observed. It is clear that beyond 13 mmol the PDEA hydrogel achieved saturation. It was also visually observed that below 8.717 mmol of monomer concentration the gel had very poor structural stability. Above 8.717 mmol of monomer concentration, gels were mechanically stable under swollen state and had brittle nature due to increased intermolecular cross-linking. In order to form a stable gel, the monomer content was reduced to improve the intermolecular cross-linking (Sponarova and Horak, 2008). The optimal monomer concentration was found to be 8.717 mmol (i.e., in 5 mL of water 1.2 g of DEA) which was used for the further studies.



## RESULTS AND DISCUSSION

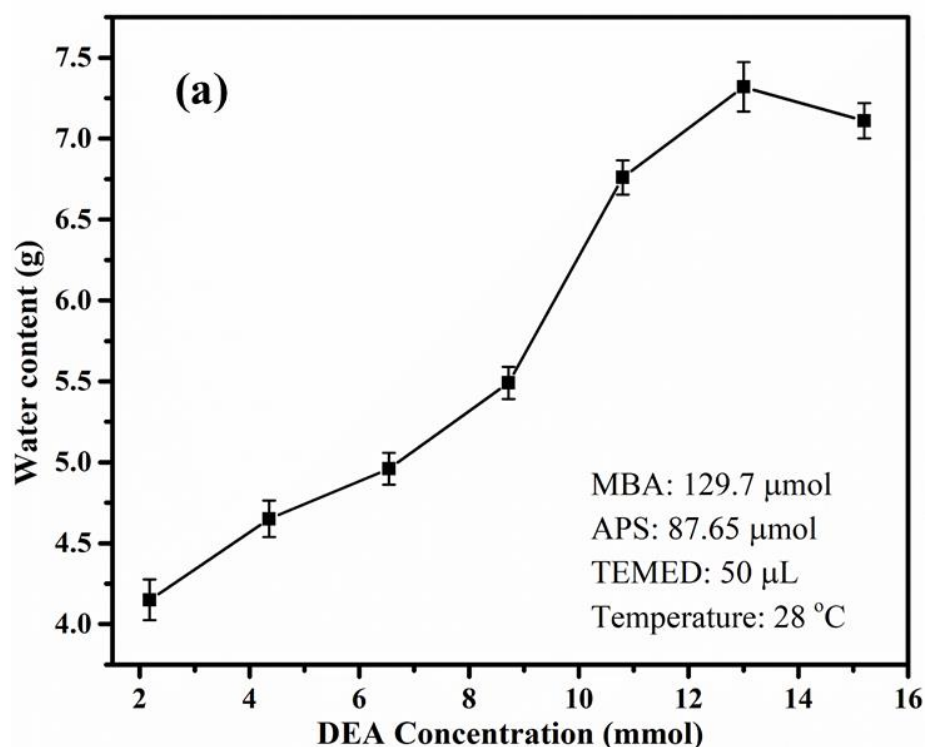


**Figure 4.4: Optimization of PDEA by varying monomer concentration with respect to weight of water absorbed by hydrogel**

### 4.2.2.2 Effect of cross-linker concentration

A stable hydrogel should have better crosslinking to prevent dissolution of the hydrophilic polymer chains in an aqueous environment. Capability to swell or uptake water is an essential trait of a temperature responsive hydrogel; therefore, the optimal cross-linker concentration was determined based on the amount of water absorbed by the hydrogel. PDEA hydrogel was prepared by varying the MBA concentration (38.91, 103.7, 129.7, 194.5 259.4 and 324.3 μmol) while keeping the other variables constant (DEA – 8.717 mmol; APS – 87.65 μmol and TEMED – 50 μl). Hydrogels prepared with less than 129.7 μmol cross-linker concentrations were sticky and had weaker network formation (**Inset Figure 4.5 (i)**). Hydrogels prepared with more than 129.7 μmol cross-linker concentration retained their structural stability and was easy to handle (**Inset Figure 4.5 (ii)**). Influence of cross-linker concentration in the PDEA hydrogel matrix with respect to H<sub>2</sub>O holding capacity is shown in **Figure 4.5**. The hydrogel prepared with 129.7 μmol cross-linker concentration could hold more water



## RESULTS AND DISCUSSION

after equilibrating it in water. As the concentration of cross-linker was increased, the degree

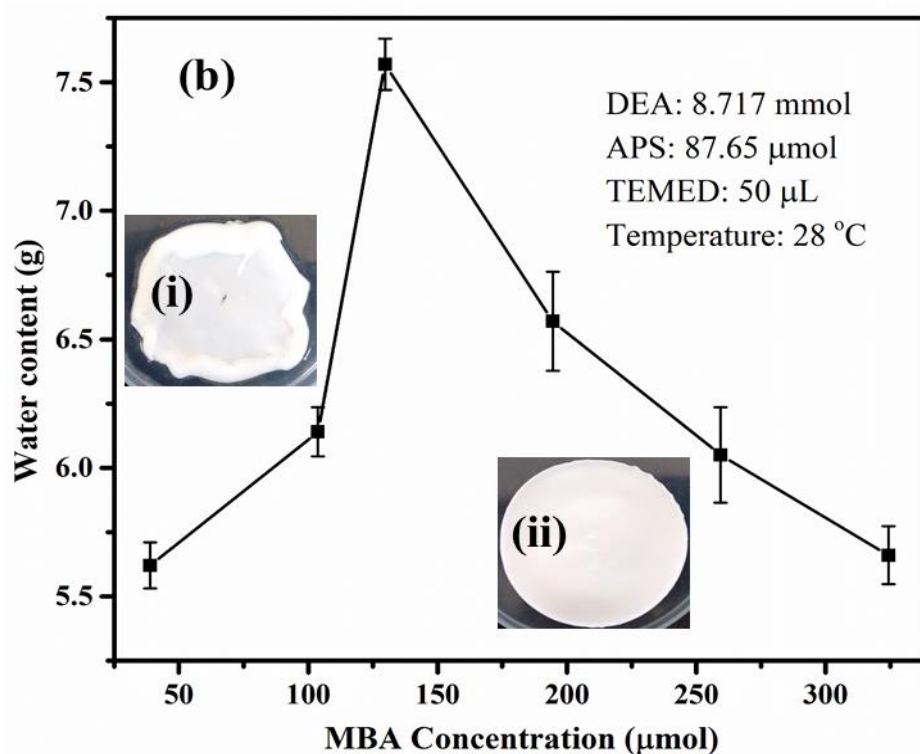


**Figure 4.5: Optimization of PDEA by varying cross-linker concentration with respect to weight of water absorbed by hydrogel (Inset image: Digital images of PDEA hydrogels with different cross-linker concentration (i) 38.91  $\mu\text{mol}$  and (ii) 324.3  $\mu\text{mol}$  cross-linker content).**

of swelling tends to decrease and exhibited the formation of hydrogel with a denser network which affected the water uptake. Water uptake capacity of a hydrogel depicts the migration of  $\text{H}_2\text{O}$  molecules into pores of the polymeric structure. Denser structure of hydrogel reduces the accessibility of  $\text{H}_2\text{O}$  molecules to hydrophilic segments of the polymer; therefore, limited amount of water penetrated into the hydrogel structure. According to Flory's theory, excessive concentration of cross-linker will impel the generation of immoderate crosslink points which have a tendency to augment the crosslinking density (Flory. 1953; Barron *et al.* 2016). As a result, the network voids for holding water reduces and the water absorption decreased. In 2010, Wang and Qin reported similar observations in the case of guar gum-g-poly(sodium acrylate) hydrogel (Wang and Qin. 2010).

## RESULTS AND DISCUSSION

### 4.2.2.3 Effect of initiator and accelerator concentration

The effect of initiator concentration was also studied as mentioned above. PDEA hydrogel was prepared by varying the concentration of APS (21.91, 43.82, 87.65, 131.5 and 175.3  $\mu\text{mol}$ ) while keeping the other variables constant (DEA – 8.717 mmol; MBA – 129.7  $\mu\text{mol}$  and TEMED – 50  $\mu\text{l}$ ). The initiator contributes a salient role in the polymerization, primarily in the nucleation stage. The mechanical stability of the hydrogel was improved with increase in the initiator concentration.

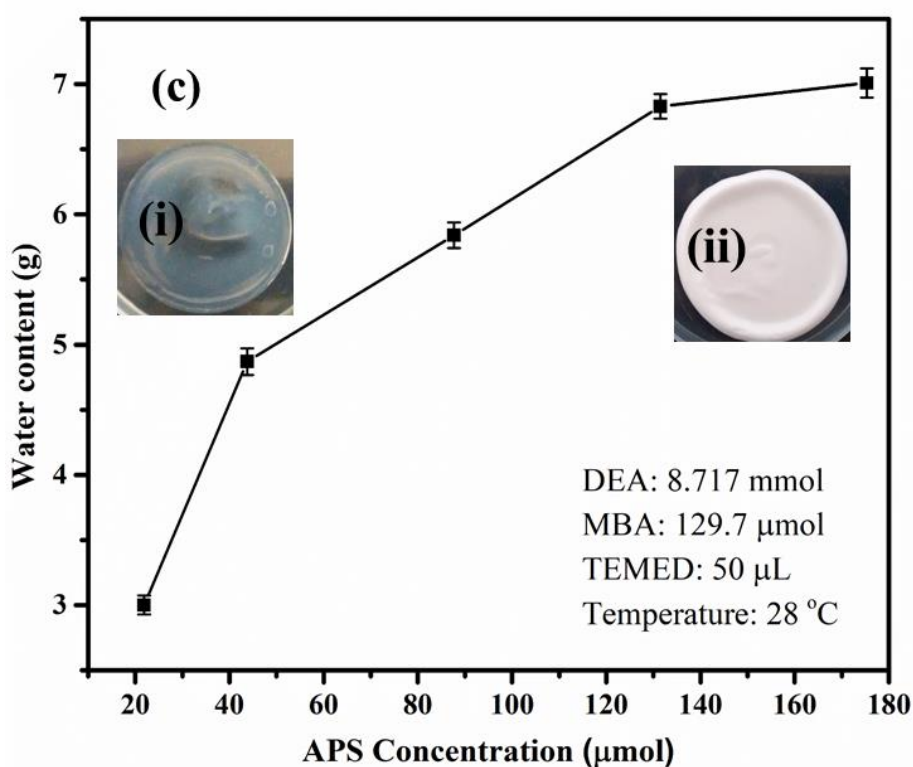


**Figure 4.6: Optimization of PDEA by varying initiator concentration with respect to weight of water absorbed by hydrogel (Inset image: Digital images of PDEA hydrogels with different initiator concentrations (i) 21.91  $\mu\text{mol}$  and (ii) 175.3  $\mu\text{mol}$  APS content).**

The inset **Figure 4.6 (i-ii)** shows the digital images of a hydrogel prepared using different initiator concentration. From the inset **Figure 4.6**, it was understood that hydrogel with 21.91  $\mu\text{mol}$  of initiator concentration resulted in a transparent hydrogel, which made it evident that the crosslinking structure was homogeneous, but as the concentration of initiator was increased (above 21.91  $\mu\text{mol}$ ) an opaque hydrogel was

## RESULTS AND DISCUSSION

formed, which signifies formation of heterogeneous hydrogel structure. It was also found that the absorption of water in hydrogel increased by increasing APS concentration, this perhaps attributed to the escalation of active free radicals. The maximum water content in the hydrogel was observed at 175.3  $\mu\text{mol}$  (0.04 g) of APS. Similarly, the accelerator concentration was also optimized by varying the TEMED (20, 40, 60, 80 and 100  $\mu\text{l}$ ) while keeping the other variables constant (DEA – 8.717 mmol; MBA – 129.7  $\mu\text{mol}$  and APS – 175.3  $\mu\text{mol}$ ). The time of polymerization reaction decreased with increase in accelerator concentration and also water holding capacity within the hydrogel was enhanced as shown in **Figure 4.7**. In this work, APS – TEMED are the redox initiators used to initiate the radical polymerization. To acquire fast polymerization and high initiation efficiency, the combination of APS and TEMED are vastly utilized (Zhang *et al.* 2011).

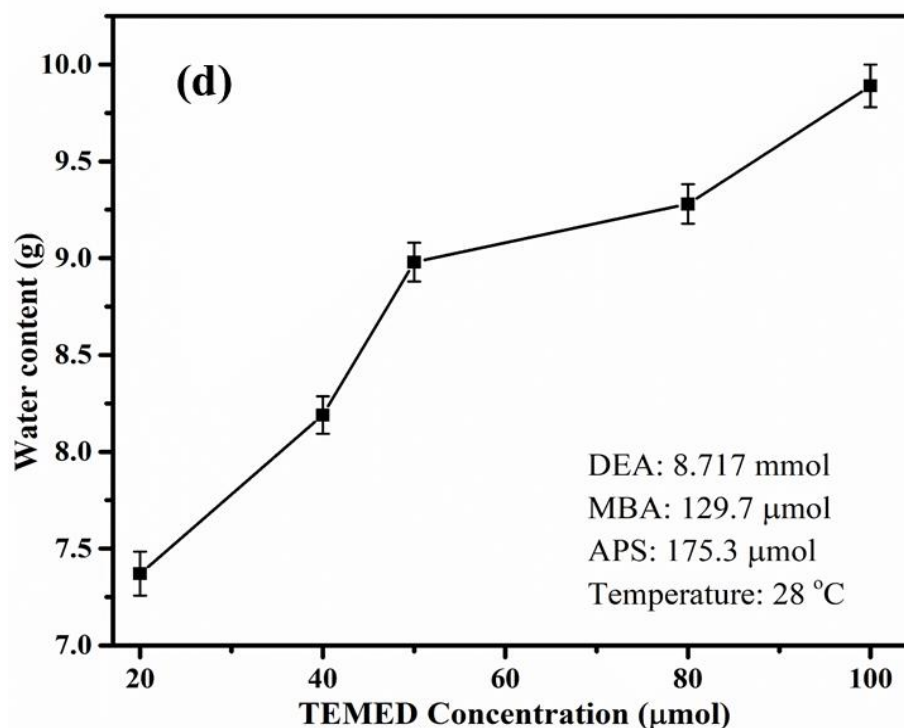


**Figure 4.7: Optimization of PDEA by varying accelerator concentration with respect to weight of water absorbed by hydrogel.**

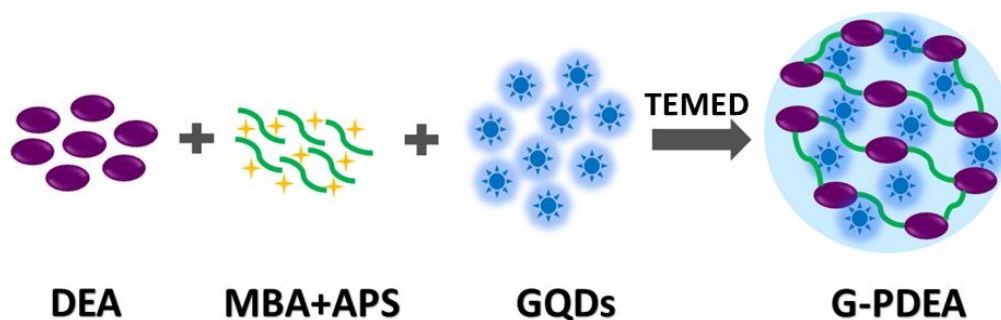
From the above discussion, we could conclude that the optimum composition to produce PDEA hydrogel with good mechanical stability and high-water absorption capacity are DEA – 8.717 mmol; Water – 5 mL; MBA – 129.7  $\mu\text{mol}$ ; APS – 175.3

## RESULTS AND DISSCUSSION

$\mu\text{mol}$  and TEMED 100  $\mu\text{L}$ . This optimized composition was further used to prepare hydrogels at various temperature (25–40  $^{\circ}\text{C}$ ) and its temperature dependencies were further studied as discussed in section 4.3-4.5.

### 4.2.3 Synthesis of GQDs incorporated PDEA hydrogels

The GQDs incorporated PDEA hydrogels were prepared by free-radical-polymerization using optimized composition as discussed in section 3.2.1 and 3.2.2. Hydrogels were prepared by varying GQDs content as shown in **Table 4.2**. The schematic representation of GQDs incorporated PDEA hydrogels is shown in **Scheme 4.3**.



**Scheme 4.3: Schematic representation of polymerization of DEA in presence of GQDs**

The presence of more -OH and -COOH group on the GQDs indicate the successful incorporation of GQDs in the PDEA hydrogel matrix. It was seen that formed hydrogels were opaque and soft, but with an increase in GQDs content the hydrogel mechanical strength decreased but an increase in its fluorescence under UV light at 365 nm. Further, the Leu and Met functionalized GQDs were used separately in the preparation of hydrogels and the feed composition is shown in **Table 4.2**. All the hydrogels were optimized by varying the bare GQDs, leucine functionalized GQDs and methionine functionalized GQDs content by studying their temperature responsive properties.

## RESULTS AND DISCUSSION

**Table 4.2: Feed composition of PDEA hydrogel preparation along with GQDs**

Sample ID	DEA (mmol)	Bare GQDs (g)	Leu-GQDs (g)	Met-GQDs (g)	MBA ( $\mu\text{mol}$ )	APS ( $\mu\text{mol}$ )	TEMED ( $\mu\text{L}$ )	Water (mL)
H	8.717	0	0	0	129.7	175.3	100	5
H-1	8.717	0.01	0.01	0.01	129.7	175.3	100	5
H-2	8.717	0.025	0.025	0.025	129.7	175.3	100	5
H-3	8.717	0.05	0.05	0.05	129.7	175.3	100	5
H-4	8.717	0.075	0.075	0.075	129.7	175.3	100	5
H-5	8.717	0.1	0.1	0.1	129.7	175.3	100	5
H-6	8.717	0.25	0.25	0.25	129.7	175.3	100	5
H-7	8.717	0.5	0.5	0.5	129.7	175.3	100	5
H-8	8.717	0.75	0.75	0.75	129.7	175.3	100	5

### 4.3 Effect of temperature on Equilibrium Swelling Ratio (ESR)

The ESR is one of the important parameter for evaluating the LCST behavior of the hydrogels. ESR of pure PDEA (prepared at varying temperatures from 25-40 °C) and PDEA with GQDs (**Table 4.2**) hydrogels in distilled water showed that the hydrogels were swollen at a lower temperature and shrank gradually with increase in the temperature. The hydrophilic (-CONR<sub>2</sub>) and hydrophobic (-CH<sub>2</sub>CH<sub>3</sub>) regions of polymeric network undergo many interactions (hydrogen bond, polymer-polymer hydrophobic interactions, etc), which result in a hydration-dehydration change in the hydrogel in response to the surrounding temperature. From the **Figure 4.8**, it has been observed that ESR of hydrogels decreases as the temperatures increases from 20 to 60 °C, but PDEA hydrogels synthesized at varying temperature showed different ESR with an increase in synthesis temperature (**Figure 4.8a**).

Similar results were observed for PDEA incorporated with different concentrations of GQDs. The ESR values of bare PDEA (prepared at varying temperatures from 25-40 °C) at 20 °C for T36 and T25 was 18.332 gg<sup>-1</sup> and 12.59 gg<sup>-1</sup> respectively. The ESR

## RESULTS AND DISSCUSSION

values for GQDs incorporated PDEA (prepared at varying GQDs content as in **Figure 4.8b** at 20 °C for H and HG-3 were 4.13 gg<sup>-1</sup> and 5.95 gg<sup>-1</sup> respectively.

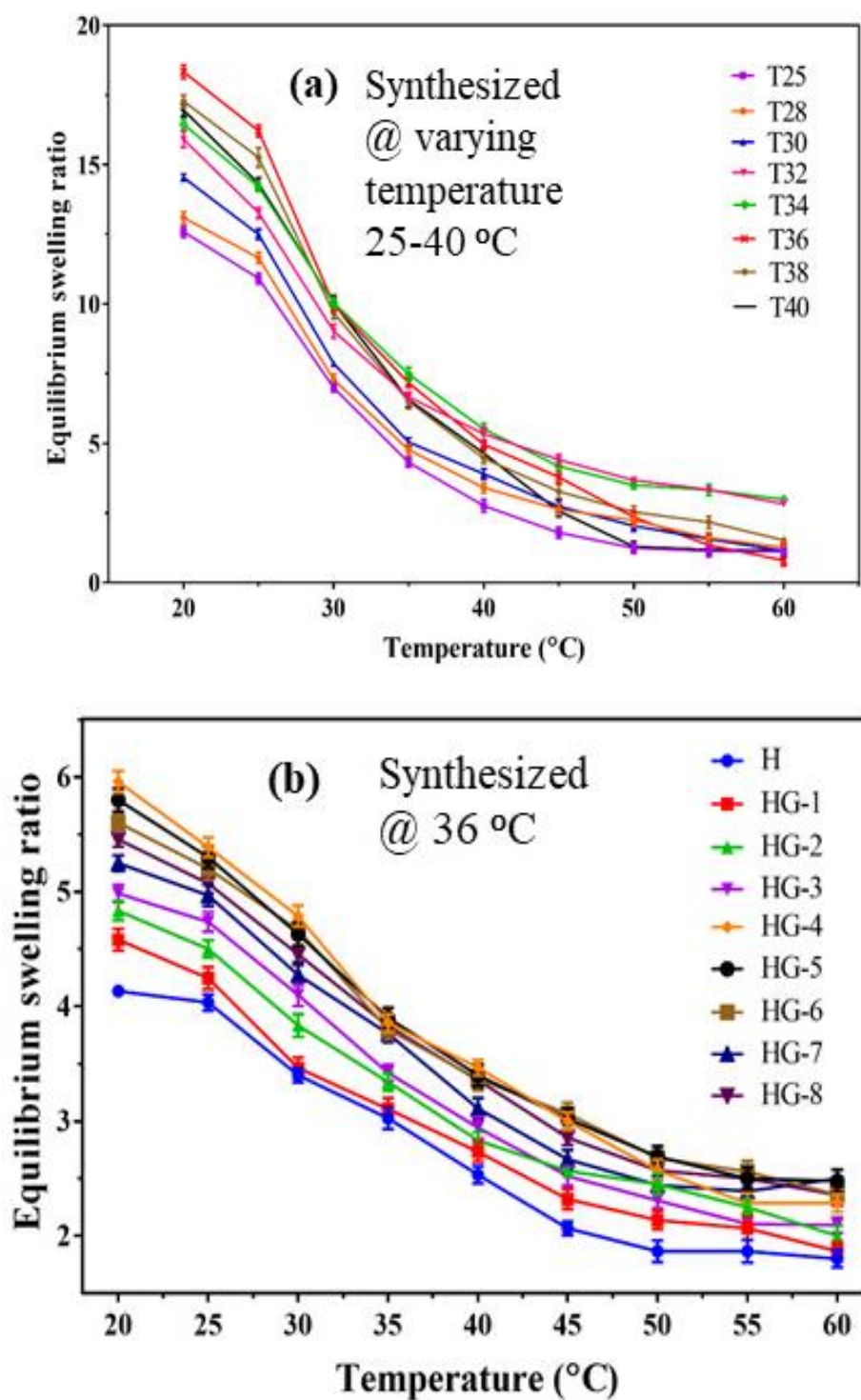


Figure 4.8: ESR measured from 20-60 °C (a) PDEA hydrogels prepared at different temperatures (25-40 °C); (b) Varying bare GQDs incorporated PDEA.



## RESULTS AND DISCUSSION

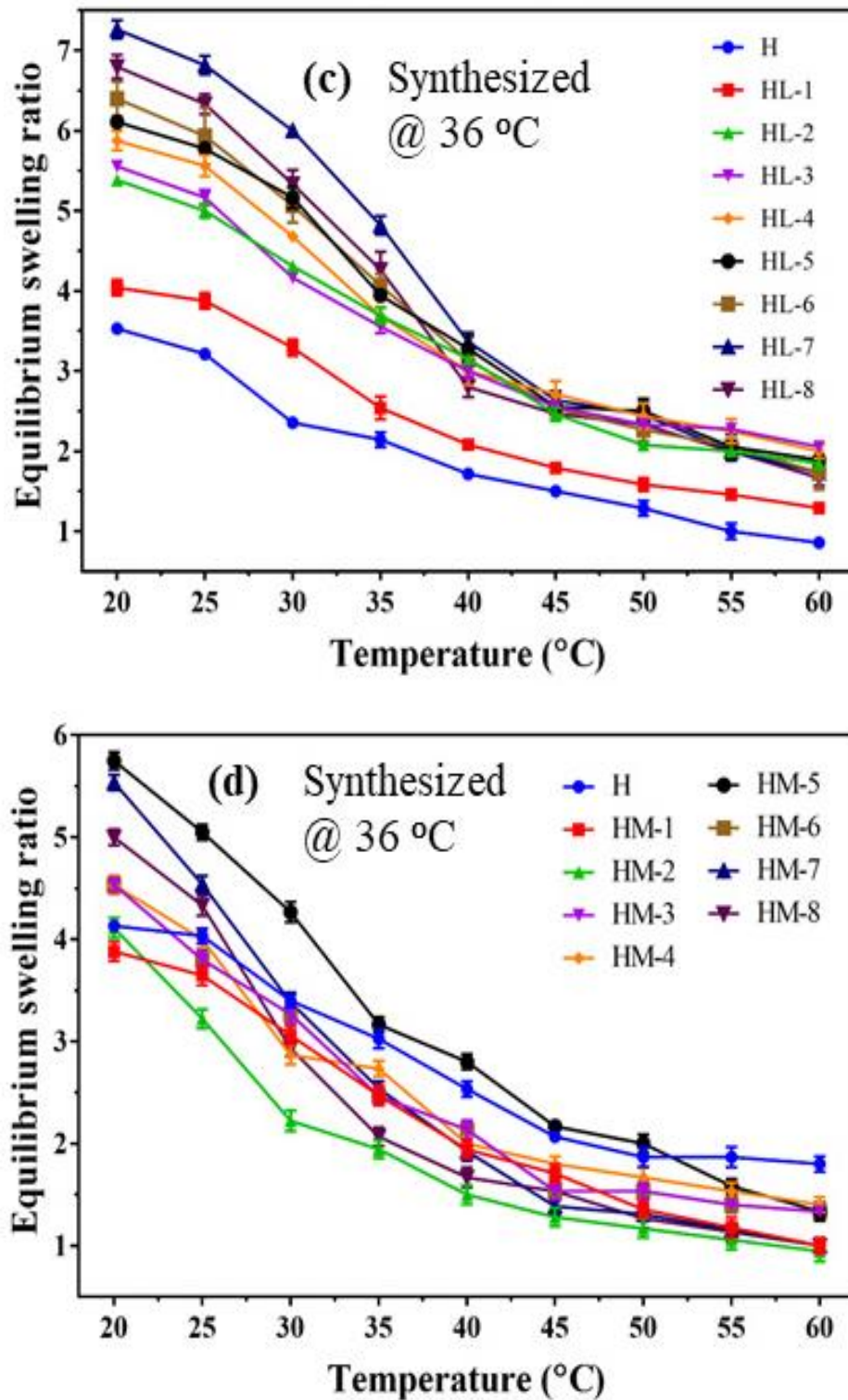


Figure 4.8: ESR measured from 20-60 °C (c) Varying Leucine functionalized GQDs added PDEA and (d) Varying Methionine functionalized GQDs content in PDEA hydrogels.

## RESULTS AND DISSCUSSION

PDEA prepared by varying the leucine functionalized GQDs (**Figure 4.8c**) at 20 °C for H and HL-7 were 3.52 gg<sup>-1</sup> and 7.26 gg<sup>-1</sup> respectively. Similarly, for methionine functionalized GQDs in PDEA (**Figure 4.8d**) at 20 °C for H and HM-5 were 3.89 gg<sup>-1</sup> and 5.75 gg<sup>-1</sup> respectively. In all the hydrogels, as the temperature increased from 20 to 60 °C, the ESR values decreased nearly to 1 gg<sup>-1</sup>. (Note: The dry weight of the samples was PDEA  $\approx 2.5 \pm 0.3$  gm, HG  $\approx 0.1 \pm 0.05$  gm, HL  $\approx 0.1 \pm 0.05$  gm and HM  $\approx 0.1 \pm 0.05$  gm). This illustrates, that the incorporation of different GQDs in PDEA increased the ESR due to the presence of functional group (-COOH, -OH) in GQDs.

At lower temperatures, the hydrophilic regions of the hydrogels bind with water molecules forming hydrogen bonds and form a stable coating around hydrophobic groups. Hence, exhibits greater water uptake by changing their appearance from transparent to translucent (in bare PDEA), but the appearance did not change in HG, HM and HL, despite difference in the swelling capacities. Change in transparency of the PDEA was the indication of change in LCST. As the temperature increases, the appearance of the hydrogel changes to opaque due to the collapse of hydrogen bonds and the hydrophobic interactions among them and the polymer network increases and consequently hydrogel shrink by releasing out the entrapped water molecules that exhibit the phase separation. ESR also decreases instantly with an increase in surrounding temperature of the hydrogel. The LCST of the PDEA increased by the incorporation of GQDs. The LCST of the PDEA hydrogels was observed to be around 29 °C, and for HG LCST was around to 36 °C; and for HL LCST around 40 °C and for HM LCST was around 35 °C. In all the hydrogels, the LCST increased with increase in GQDs content upto a certain concentration and then further increase in GQDs, LCST decreased and this could be due to effective crosslinking in hydrogel. Increase in the cross-linking density would lead to reduction in swelling capacity. Incorporation of GQDs in PDEA provide more interaction between water molecules and hydrogels network, which created hydrogen bonding between water molecules and polymeric network and thus hold more water than bare PDEA. HG hydrogels have a higher swelling ratio and delayed volumetric changes in response to temperature changes (Lo *et al.* 2011).



## RESULTS AND DISCUSSION

### 4.4 Time-dependent Swelling ratio of hydrogels

The water uptake of each hydrogel varies due to the difference in the inter-connected pore structures and that lead to swelling rate (Yin *et al.* 2007). Initially, dried hydrogels rapidly absorb water molecules by hydrating the hydrophilic regions that expand the polymeric hydrogels inter-connected network. As the hydrophilic regions attain saturation, the polymeric network then exchanges the free water molecules with the external water molecules (Hoffman. 2012). The swelling behavior of the lyophilized hydrogel sample in distilled water at ambient temperature was measured gravimetrically.

From **Figure 4.9**, it can be found that the GQDs incorporated PDEA exhibits faster swelling than PDEA. It can be observed that the swelling rate of PDEA **Figure 4.9a** T36 increased to  $6.37 \text{ gg}^{-1}$  in 30 min and reached to a maximum swelling with in 450 min, whereas swelling rate of T25 was increased to  $1.30 \text{ gg}^{-1}$  and then reached a constant swelling within 270 min.

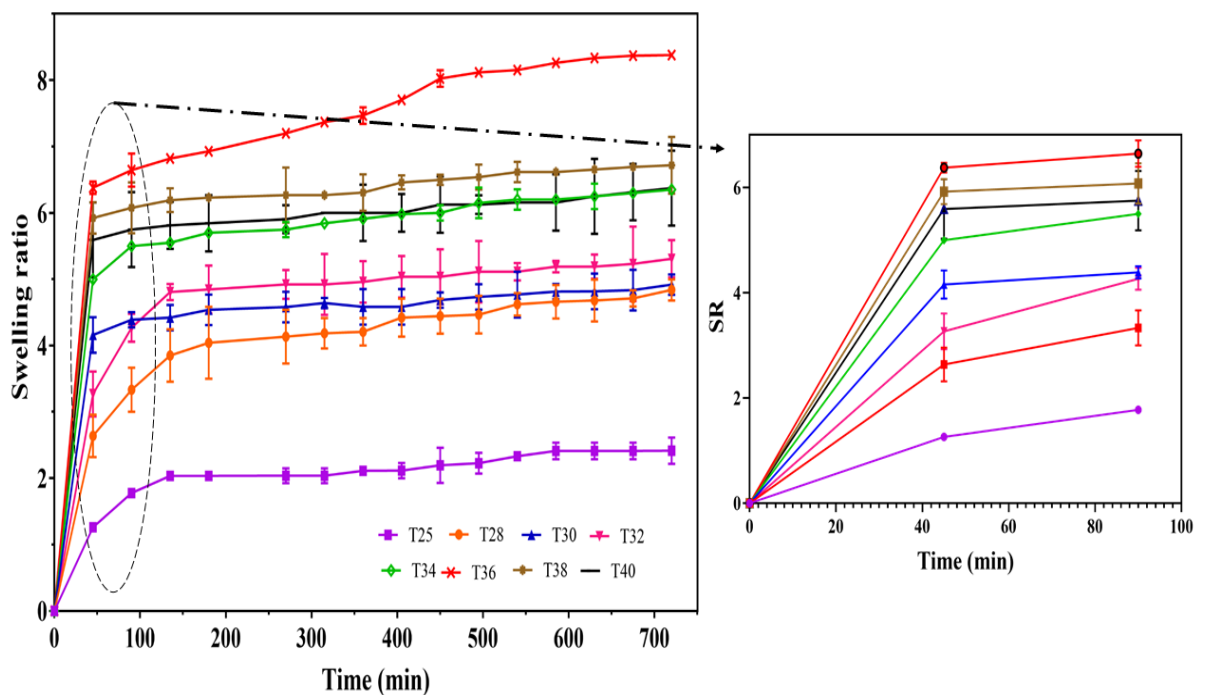


**Figure 4.9: SR measured at ambient temperature at different time intervals**  
**(a) PDEA hydrogels prepared at different temperatures (25-40 °C) (Inset image: Expanded graph from time interval of 0-100 min)**

## RESULTS AND DISCUSSION

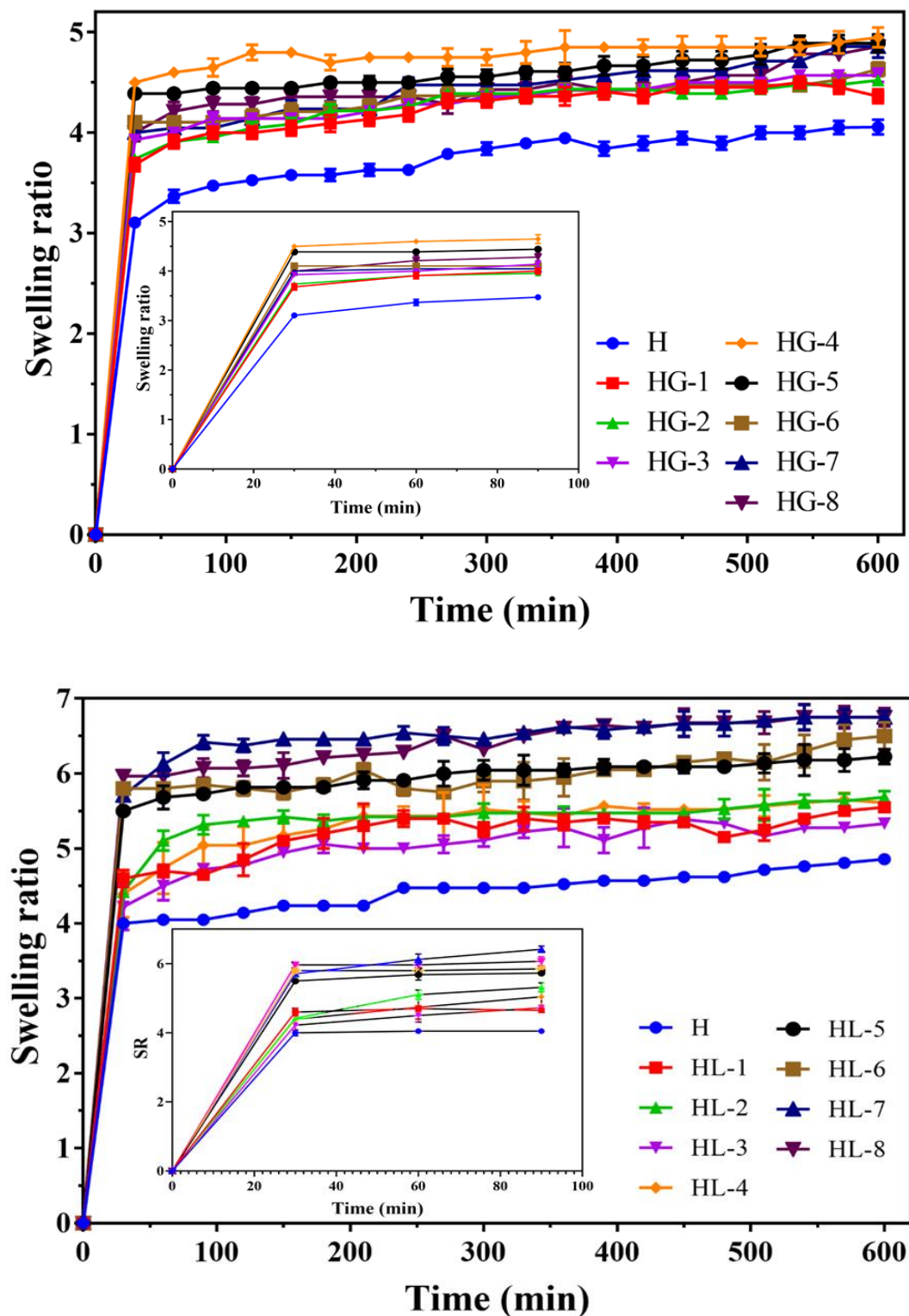
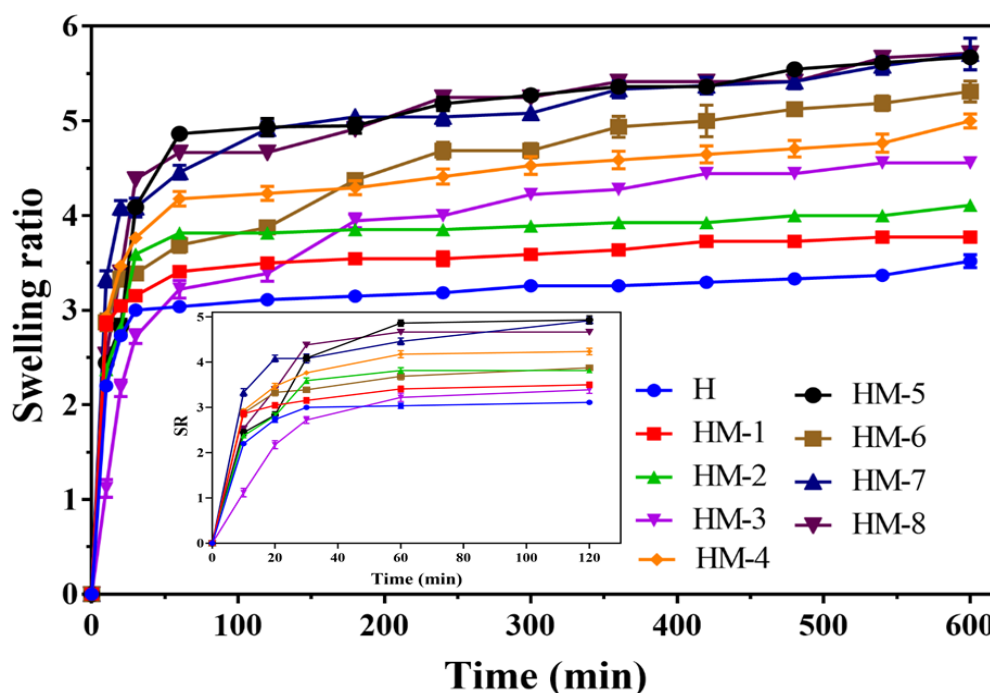


Figure 4.9: SR measured at ambient temperature at different time intervals (b) Varying bare GQDs incorporated PDEA; (c) Varying Leucine functionalized GQDs added PDEA (Inset image: Expanded graph from time interval of 0-100 min).

## RESULTS AND DISCUSSION

The SR of hydrogel synthesized with different GQDs as shown in **Figure 4.9b** can be observed that SR of HG-4 is about  $4.5 \text{ gg}^{-1}$  in 30 min and reached maximum of  $4.85 \text{ gg}^{-1}$  in 360 min. Hydrogels incorporated with leucine with functionalized GQDs (**Figure 4.9c**) showed the SR of  $5.708 \text{ gg}^{-1}$  (HL-7) in 30 min and then gradually increased to  $6.406 \text{ gg}^{-1}$  and became constant. **Figure 4.9d** shows the SR of hydrogels incorporated with methionine functionalized GQDs, the maximum SR was attained by HM-5 that is  $3.33 \text{ gg}^{-1}$  in the initial 30 min and the swelling reached to  $5.7 \text{ gg}^{-1}$  after 600 min (Note: The dry weight of hydrogels was bare PDEA is  $\approx 2.5 \pm 0.3 \text{ gm}$ ; HG is  $\approx 0.1 \pm 0.05 \text{ gm}$ ; HL is  $\approx 0.1 \pm 0.05 \text{ gm}$  and HM is  $\approx 0.1 \pm 0.05 \text{ gm}$ ). The diffusion of water molecules and porosity of the polymer matrix are responsible for swelling behaviour of the polymeric hydrogels. Less SR is because of less packed polymeric structure which favoured hydrophobic interaction in the PDEA. Increased SR attribute to the more polymer-water interactions due to the existence of GQDs, where water molecules could easily diffuse into the hydrogel network, and the expansion of polymer chains could easily occur.



**Figure 4.9:** SR measured at ambient temperature at different time intervals (d) Varying Methionine functionalized GQDs content in PDEA hydrogels (Inset image: Expanded graph from time interval of 0-120 min).

## RESULTS AND DISCUSSION

### 4.5 Deswelling kinetics or water retention (WR) at 50 °C

The response rate of the thermosensitive hydrogel is one of the most important factors and in particular, high rate is required in many applications. The deswelling kinetics of all the synthesized hydrogels were equilibrated at ambient room temperature to 50 °C as shown in **Figure 4.10**. The data illustrate that the deswelling rate of hydrogels (bare PDEA as in **Figure 4.10a**) prepared at higher temperature is faster and lose more water with respect to change in surrounding temperature than those hydrogels prepared at lower temperature at the same interval. Samples T36, T38 and T40 hydrogels lost nearly 80% of water with in 20 min, while T25, T28 lost about 50% water. The deswelling in GQDs incorporated hydrogels shows slow water retention as observed in **Figure 4.10 (b-d)**. (Note: The dry weight of hydrogels for bare PDEA was  $\approx 2.5 \pm 0.3$  gm; HG was  $\approx 0.1 \pm 0.05$  gm; HL was  $\approx 0.1 \pm 0.05$  gm and HM was  $\approx 0.1 \pm 0.05$  gm).

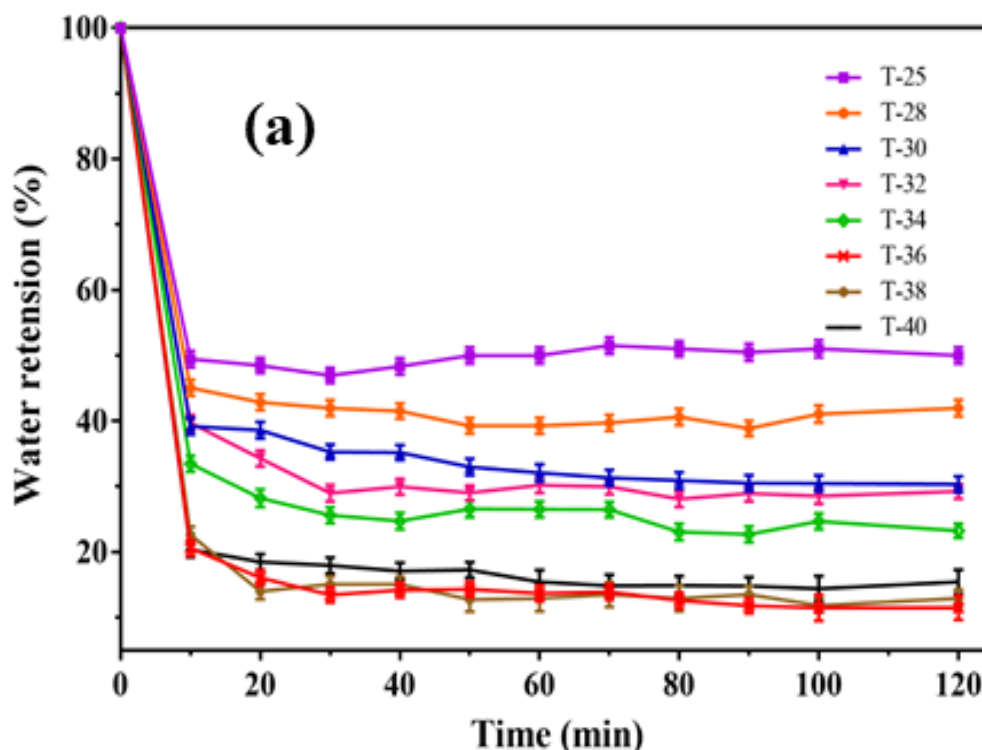


**Figure 4.10: WR measured at 50 °C at different time intervals (a) PDEA hydrogels prepared at different temperatures (25-40 °C).**

## RESULTS AND DISCUSSION

In **Figure 4.9b**, HG-4, HG-5 hydrogels lose nearly 45% of water with in 10 min then gradually reached to 1% in 110 min. Similar trend was observed for HL samples as shown in **Figure 4.9c** HL-7, HL-8 hydrogels lost nearly 40% of water with in 10 min and reached to  $\approx 1\%$  in 100min. In **Figure 4.9d** hydrogels with Met-GQDs showed the 40% water retention in the initial 10 min then reached to  $\approx 5\%$ . When hydrogels were immersed in 50 °C water, the outer most region of the hydrogel would be affected and the hydrophilic interactions among the hydrophobic groups become stronger, which leads to a rapid shrinkage of the outermost surface and then forms a dense skin layer. Once this skin is formed, the water molecules in the hydrogels are prevented from diffusing out, which results in the slow response rate (Wang *et al.* 2008). During deswelling process, the dense layer present on the surface of the hydrogel acted as resistance for the flow of liquid and hence the deswelling ratio was low (Maheshwari *et al.* 2014).

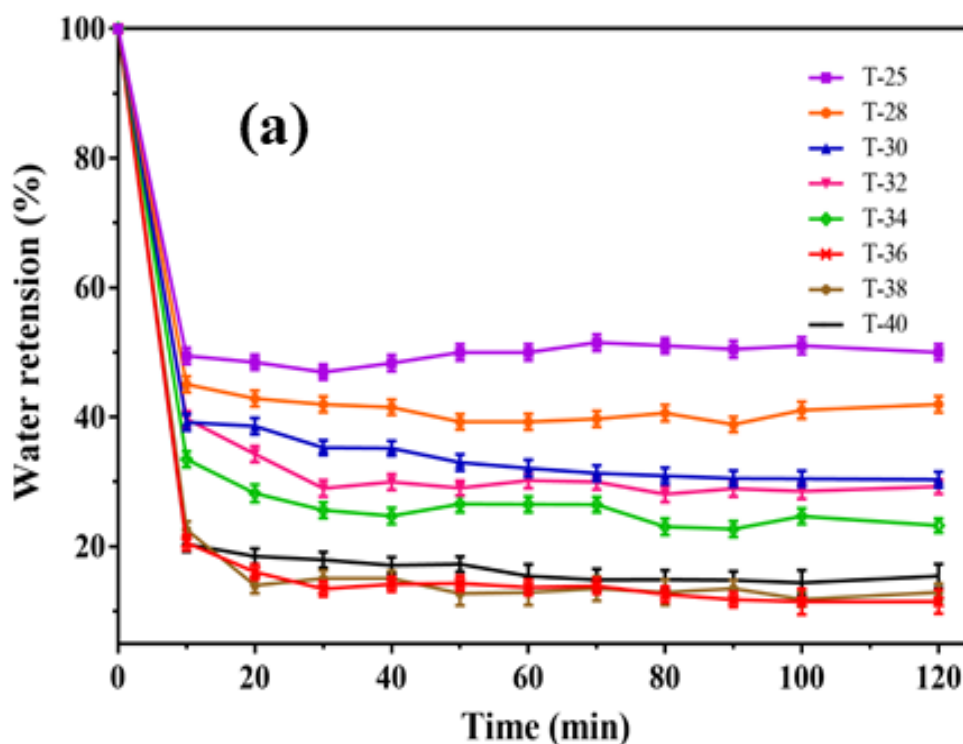


**Figure 4.10: WR measured at 50 °C at different time intervals (b) Varying bare GQDs incorporated PDEA.**

## RESULTS AND DISCUSSION

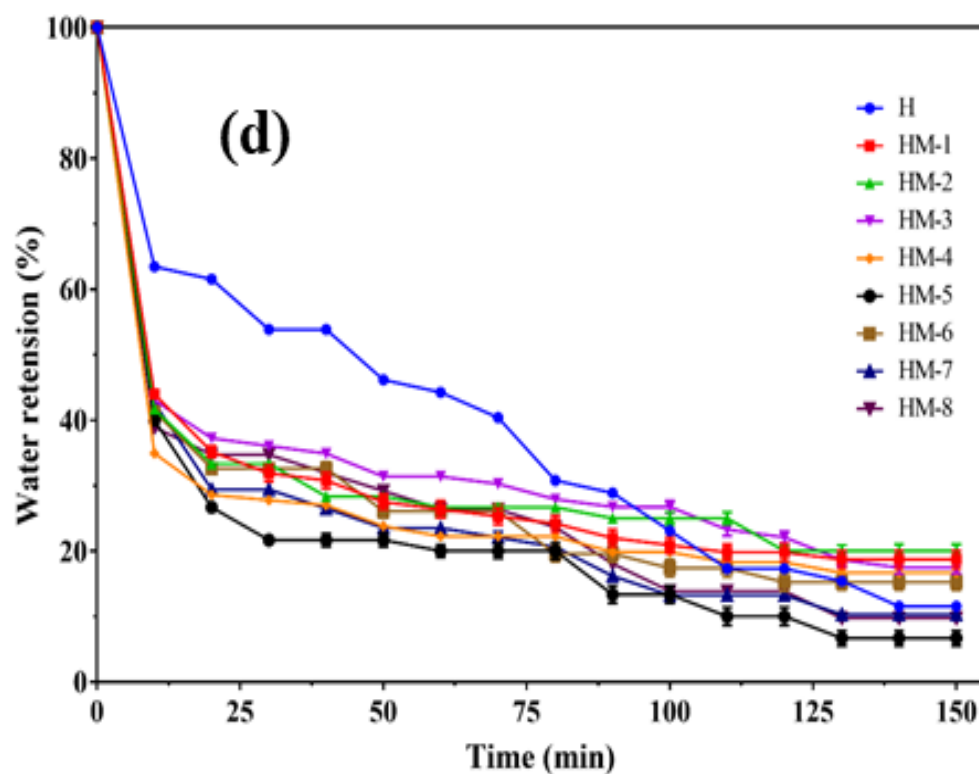
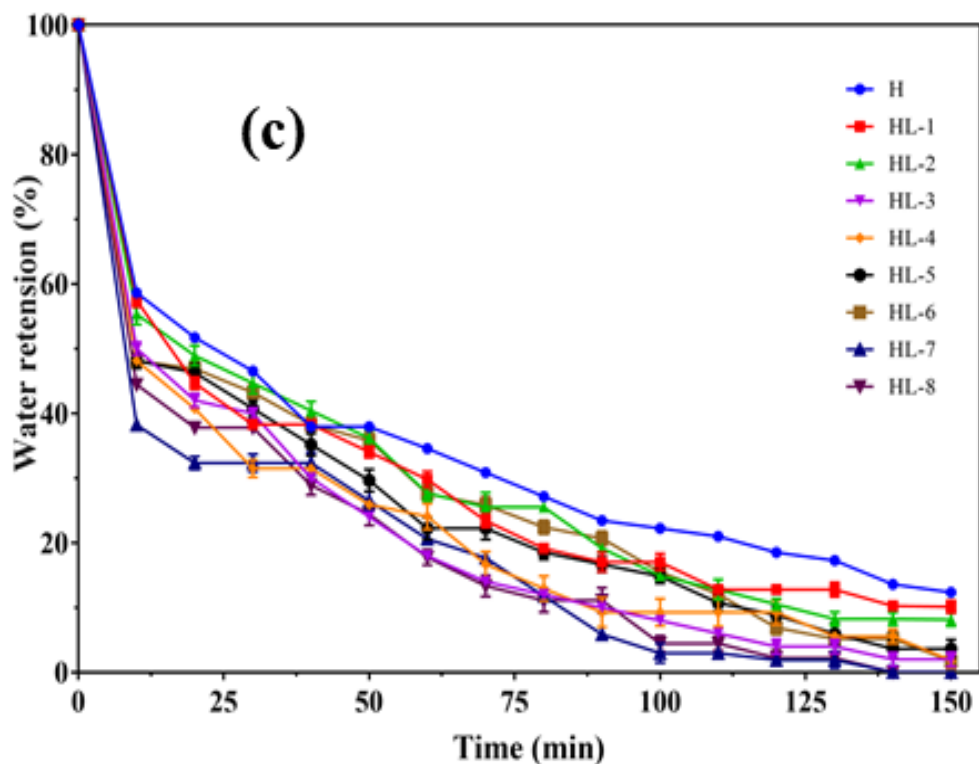


Figure 4.10: WR measured at 50 °C at different time intervals (c) Varying Leucine functionalized GQDs added PDEA and (d) Varying Methionine functionalized GQDs content in PDEA hydrogels.

## RESULTS AND DISCUSSION

From sections 4.3, 4.4 and 4.5 we found that the hydrogel synthesized at 36 °C has good temperature responsive behavior. Similarly, the hydrogels prepared with different GQDs also showed optimum temperature responsive behavior like HG-4, HL-7 and HM-5. Further these hydrogels were characterized and *in-vitro* release studies were performed.

### 4.6 Characterization of PDEA hydrogels

#### 4.6.1 Structure and composition analysis

The molecular structure of synthesized hydrogels like H, HG, HL, HM and GQDs (bare GQDs, leucine functionalized GQDs and methionine functionalized GQDs) was investigated using ATR – FTIR (Fourier transform infrared spectroscopy) which is shown in **Figure 4.11**. The absorption peaks at 2918  $\text{cm}^{-1}$  to 2957  $\text{cm}^{-1}$  (**Figure 4.11 (a-c)**) and peak at 2924  $\text{cm}^{-1}$  to 2984  $\text{cm}^{-1}$  (**Figure 4.11d**) are resulting from the C-H stretching vibrations of  $-\text{CH}_3$  and  $-\text{CH}_2-$  side groups in formed GQDs and PDEA hydrogels respectively (Chen *et al.* 2011; Wei *et al.* 2016).

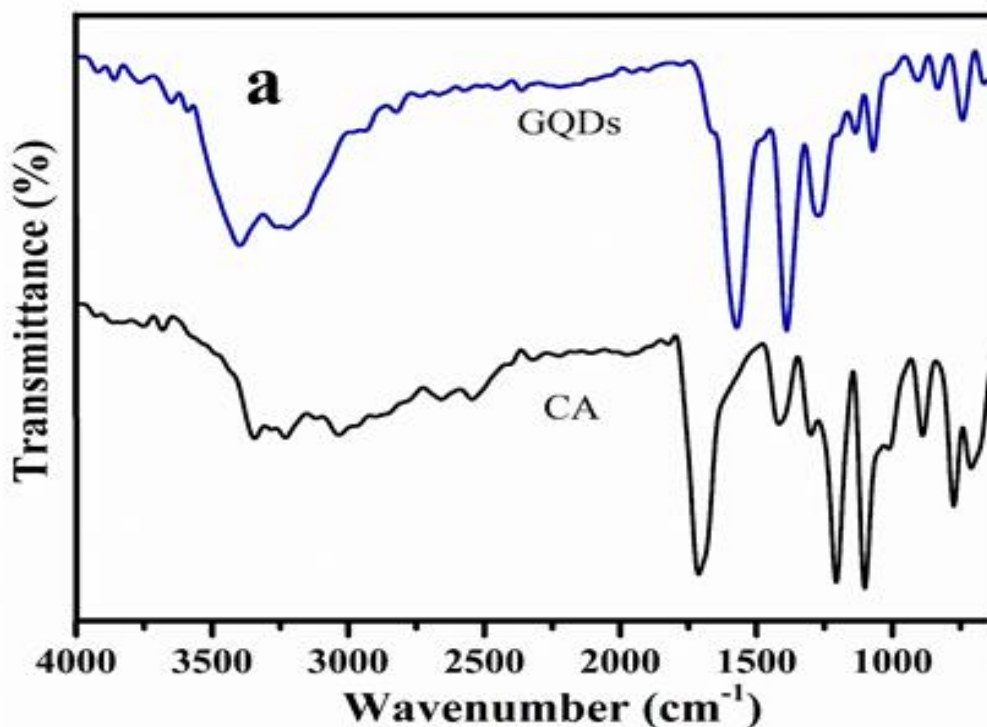


**Figure 4.11: FTIR spectra (a) Bare GQDs**



## RESULTS AND DISCUSSION

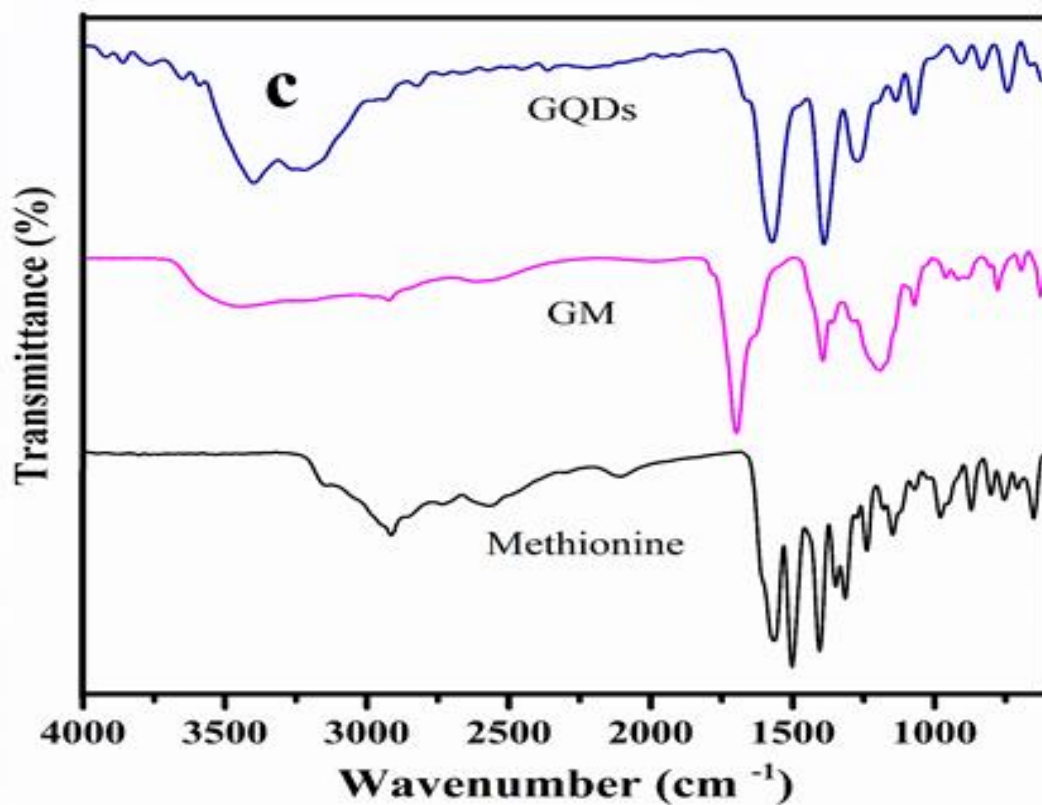
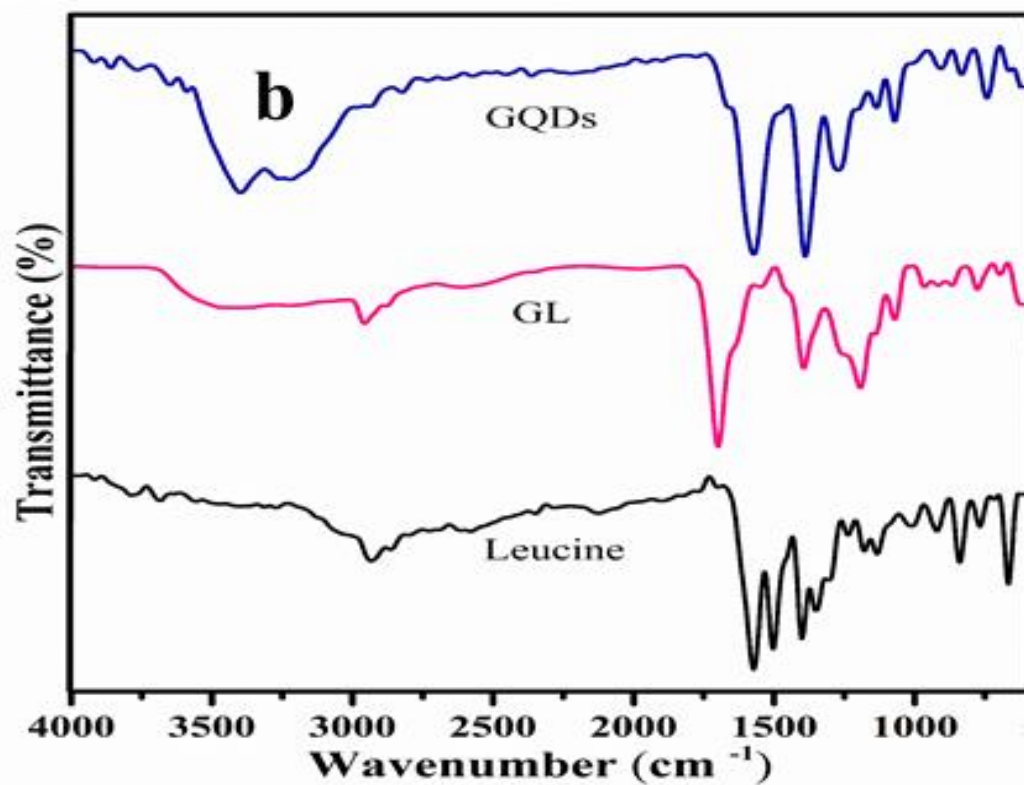
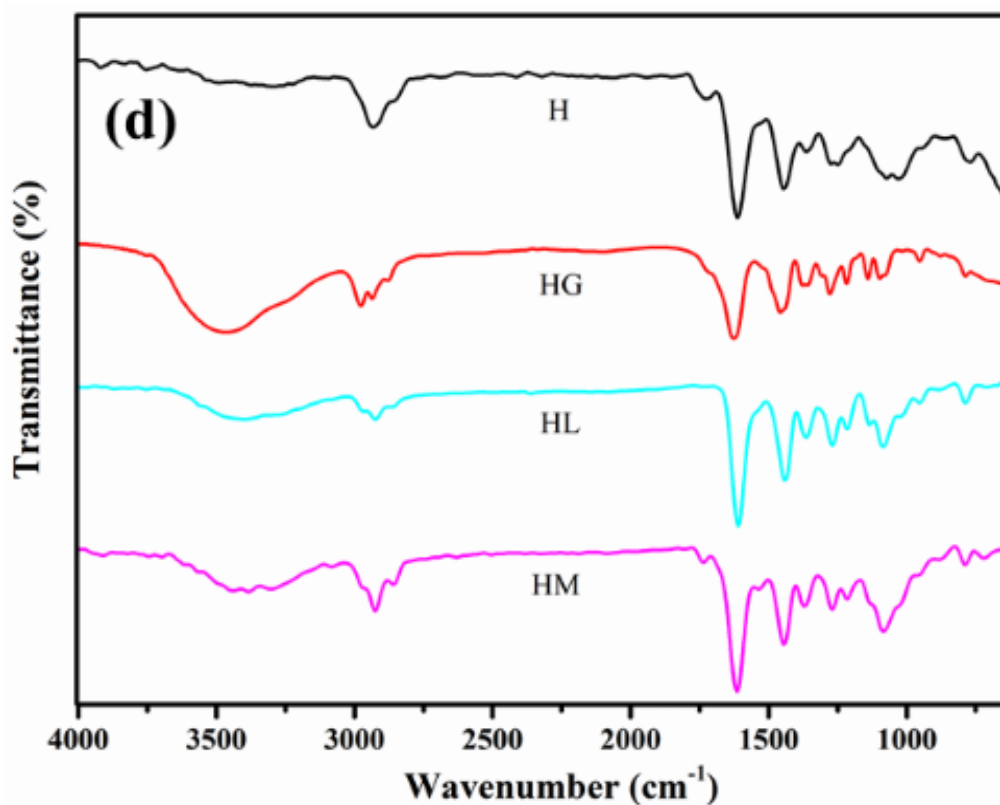


Figure 4.11: FTIR spectra (b) Leu-GQDs; (C) Met-GQDs



## RESULTS AND DISCUSSION



**Figure 4.11: FTIR spectra (d) PDEA hydrogels**

The significant peaks at  $1607\text{ cm}^{-1}$  to  $1621\text{ cm}^{-1}$  (**Figure 4.11d**) in the PDEA hydrogels can be attributed to the characteristic peak of the carbonyl group (amide I) C=O stretching vibration (Chen *et al.* 2010; Ngadaonye *et al.* 2013). The peak at  $1441\text{ cm}^{-1}$  to  $1450\text{ cm}^{-1}$  in hydrogels was due to symmetrical C-H bending. The bands ranging from  $1011\text{--}1289\text{ cm}^{-1}$  are attributed to the stretching of C-N (amide III) bond in the polymer (Chen *et al.* 2009). The characteristic band of -OH in both GQDs and GQDs incorporated PDEA are in the range of  $3220\text{--}3471\text{ cm}^{-1}$  (Naik *et al.* 2017). A characteristic stretching vibration band of aromatic C-C was observed at  $1509\text{--}1697\text{ cm}^{-1}$  for GQDs and  $1444\text{--}1454\text{ cm}^{-1}$  for PDEA polymers (Li *et al.* 2013). A strong peak in GQDs at  $1388\text{--}1401\text{ cm}^{-1}$  is due to the C-H stretching vibration (Zeng *et al.* 2016) and C-O stretch represents the alcohol, carboxylic acid, and ester weak bands which were observed in the range of  $1101\text{--}1206\text{ cm}^{-1}$  (Qiu *et al.* 2015). The disappearance of the characteristic peaks of C=O stretch at  $1735\text{ cm}^{-1}$  and C-H bending at  $1441\text{ cm}^{-1}$  in GQDs incorporated PDEA shows the successful binding of GQDs with PDEA. The

## RESULTS AND DISSCUSSION

appearance of broad –OH peak at 3466 cm<sup>-1</sup> and small C-C peak at 1452 cm<sup>-1</sup> in GQDs incorporated PDEA confirm the presence of GQDs in PDEA. Further the presence of bare GQDs and fuctionalized GQDs was confirmed by elemental analysis.

The elemental analysis of the bare PDEA, HG-4, HL-7 and HM-5 are shown in **Table 4.3**, where it represents the weight percentage of C, H, N and O. Increase of carbon and hydrogen percentage in different GQDs incorporated hydrogels confirmed the presence of GQDs. Also the presence of N confirms the fuctionalization of GQDs with lucine and methionine.

**Table 4.3: Elemental analysis of C, H, N and O from prepared hydrogels and their respective GQDs**

Sample	Carbon (%)	Hydrogen (%)	Oxygen (%)	Nitrogen (%)
Bare GQDs	66.65	2.61	30.74	-
Leu-GQDs	46.04	6.03	42.67	5.26
Met-GQDs	54.90	7.12	32	5.98
T36	50.62	10.08	29.14	10.16
HG-4	54.22	11.69	24.89	9.2
HL-7	50.52	10.50	29.74	9.24
HM-5	52.21	12.03	26.06	9.70

### 4.6.2 Thermal analysis

Thermal behaviour of the synthesized hydrogel was analysed by TGA and DSC analysis which is illustrated in **Figure 4.12**. Thermogravimetric analysis of the T36, HG-4, HL-7 and HM-5 hydrogel was performed as a function of weight loss (%) versus temperature. TGA curve reveal the thermal stability of the dry hydrogels. As can be seen from **Figure 4.12**, three regions of weight losses are observed at temperatures like 68.37, 459.17 and 727.89 °C for T36 hydrogel; 68.54, 156.30 and 308.01 °C for HG-4 hydrogel; 69.93, 232.61 and 417.24 °C for HL-7 hydrogel; similarly, for HM-5 76.78, 246.80 and 564.41 °C. The initial weight loss of 6.39%, 8.53%, 11.26% and 9.56% from T36, HG-4, HL-7 and HM-5 respectively can be related to the evaporation of entrapped water molecules causing the dehydration from the polymer (Yu *et al.* 2015; Alper and

## RESULTS AND DISCUSSION

Nuran. 2016). The second weight loss of 84.99% for T36, 85.2% for HG-4, 66.06% for HL-7 and 68.71% for HM-5 between 156.30 to 459.17 °C is due to the cleavage of the side-chain (-N(CH<sub>2</sub>CH<sub>3</sub>)) from PDEA, also the decomposition of oxygen-related functional groups and amides from polymer matrix (Jin *et al.* 2014; Nuran and Hacer, 2018).

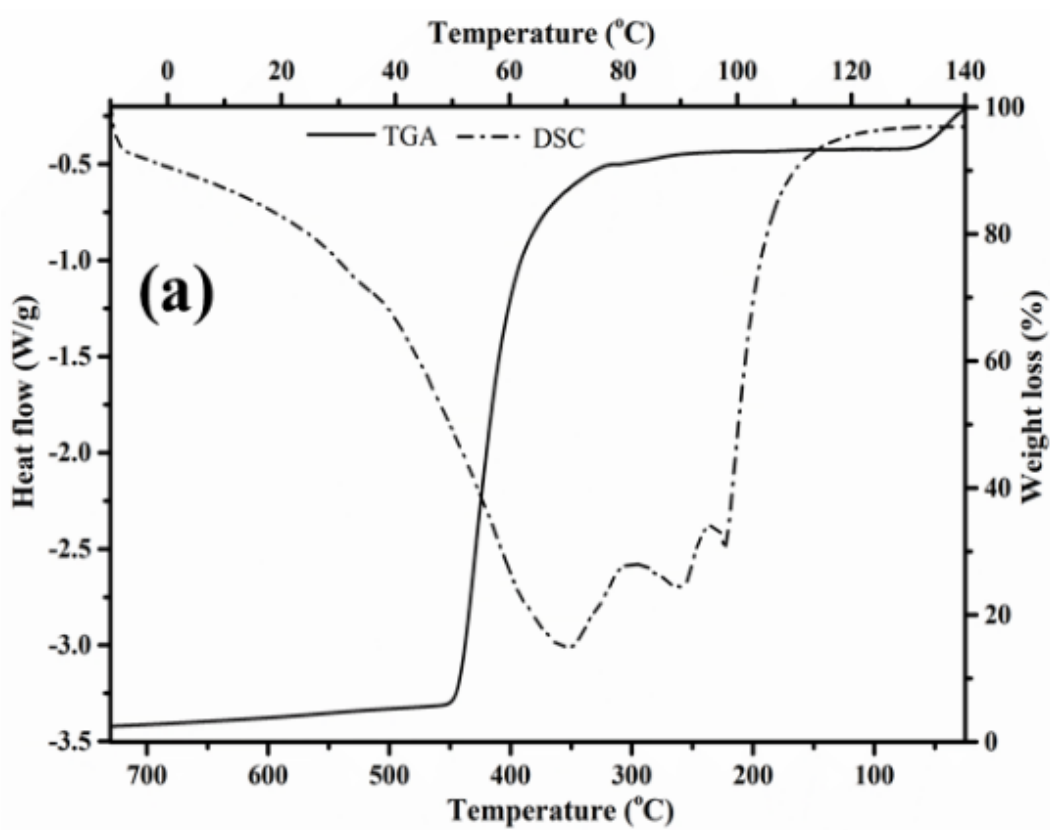


**Figure 4.12: TGA and DSC thermogram of PDEA and GQDs incorporated PDEA hydrogels: (a) PDEA without GQDs (T36).**

The weight loss from HG-4, HL-7 and HM-5 hydrogels at temperatures of 156.30 to 432.63 °C region is due to the decomposition of functional groups containing O<sub>2</sub> such as amide, carbonyl, carboxyl, epoxy and hydroxyl groups from the polymer matrix and GQDs (Huang *et al.* 2016). Final weight loss of 3.24% from T36, 3.49% from HG-4, 18.62% from HL-7 and 3.27% from HM-5 are ascribed to the decomposition of carbon material and polymer backbones in PDEA and GQDs incorporated PDEA.

## RESULTS AND DISCUSSION

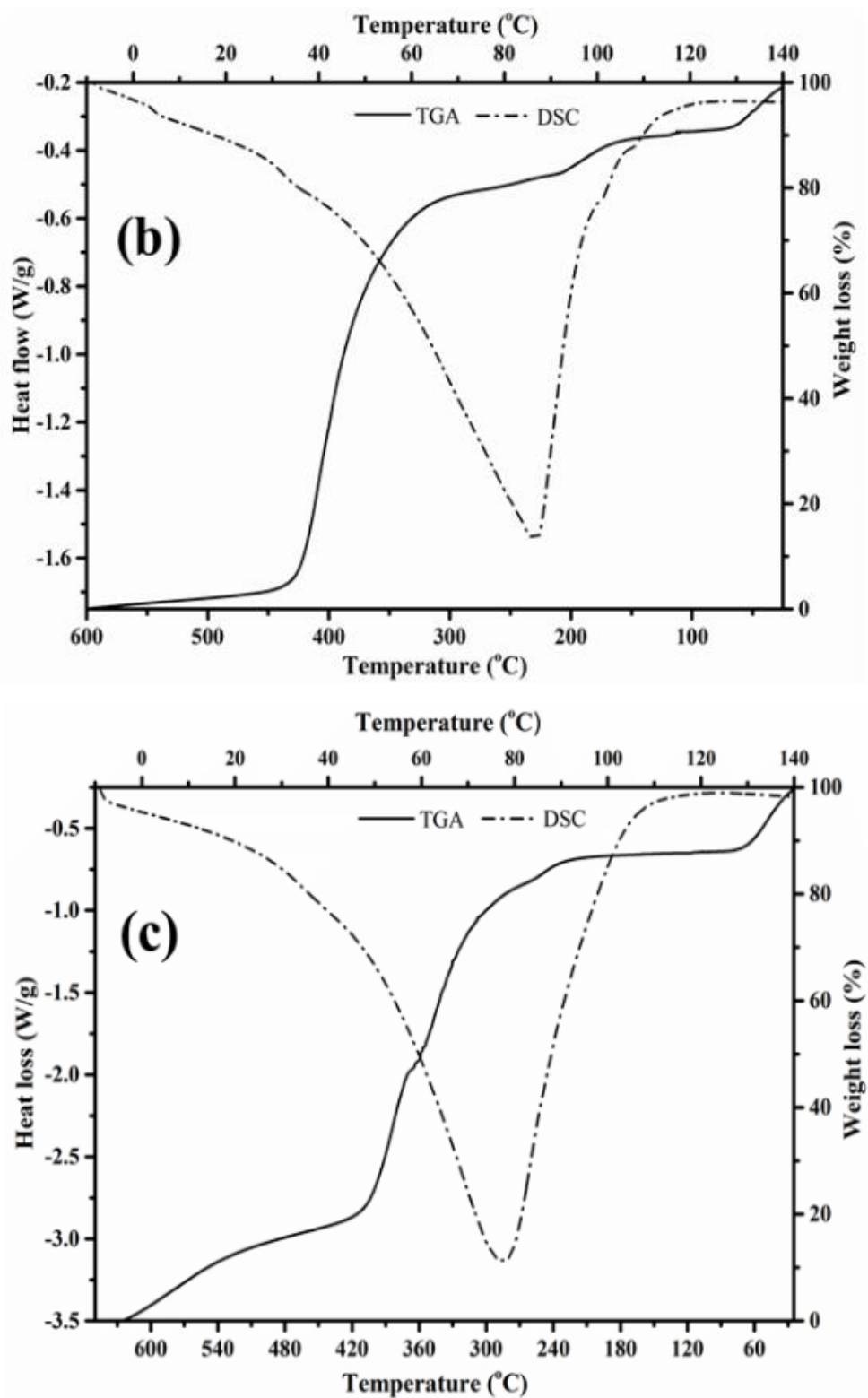
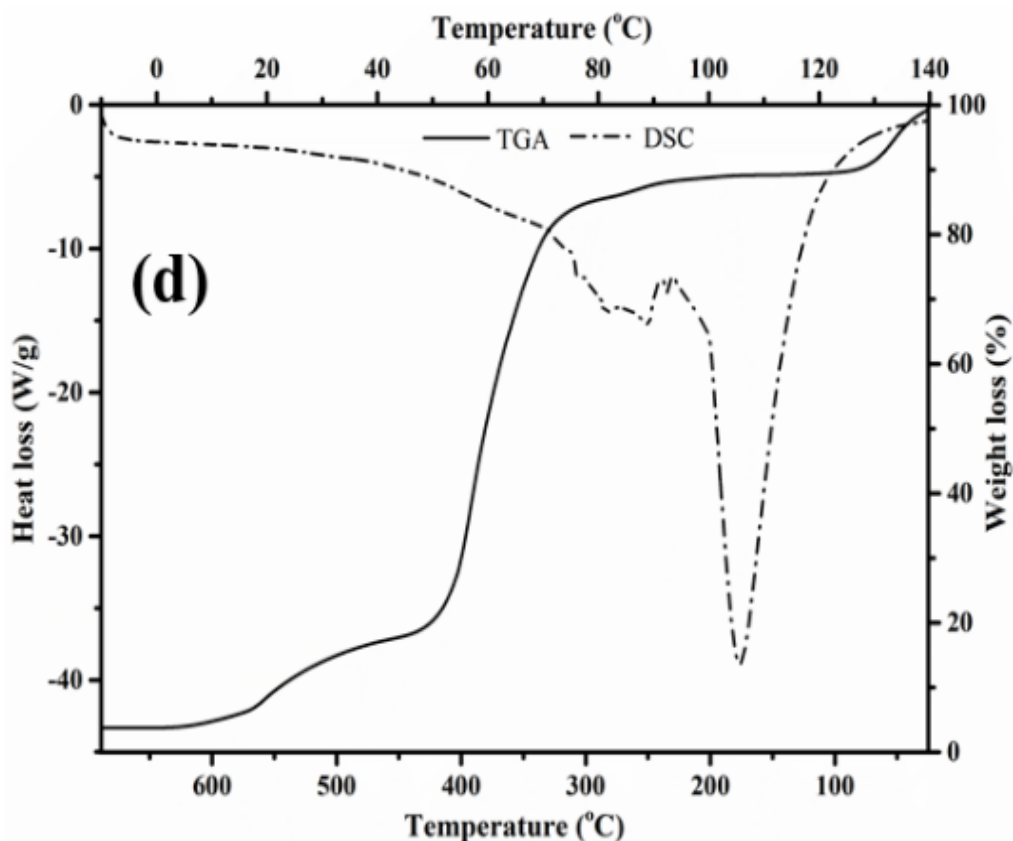


Figure 4.12: TGA and DSC thermogram of PDEA and GQDs incorporated PDEA hydrogels: (b) PDEA incorporated with bare GQDs (HG-4); (c) Leu-GQDs incorporated in PDEA (HL-7)

## RESULTS AND DISCUSSION



**Figure 4.12: TGA and DSC thermogram of PDEA and GQDs incorporated PDEA hydrogels: (d) Met-GQDs incorporated PDEA hydrogel (HM-5).**

Fifty percentage weight loss was observed at a temperature of 417.22 °C for T36, 385.80 °C for HG-4, 358.77 °C for HL-7 and 380.63 °C for HM-5, which reveals that polymer is more thermal stable. The improved thermal resistance is due to the combination of more covalent bonding through MBA as a cross-linker in PDEA (Alper and Nuran. 2016) and the presence of GQDs in PDEA showed slower weight loss with stepwise degradation indicating that the GQDs affect the stability of the PDEA.

The thermodynamic parameters of hydrogels are obtained by the DSC (digital scanning calorimetry) thermograms. From the thermograms of DSC (**Figure 4.12**), a shift was observed for all hydrogel samples which correspond to the glass transition temperature ( $T_g$ ). The  $T_g$  value of PDEA hydrogel was observed at three peaks i.e., at 69 °C, 90 °C and 97 °C. For HG, HL, HM the  $T_g$  was 86.75 °C, 77.45 °C, 105 °C respectively. The value of  $T_g$  increased on addition of the GQDs to the PDEA hydrogels. When GQDs were added to the PDEA hydrogels, the number of interconnected pores increases,

## RESULTS AND DISSCUSSION

which increase the activity of chain segment and thereby  $T_g$  of the hydrogels reduced (Zhang *et al.* 2011). Below the  $T_g$ , the polymer chains are frozen in their glassy structure. Above the  $T_g$ , polymer chain vibrates causing movement or rotation in the polymer molecules. Numerous factors like structural change in molecules, cooling rate and incorporation of additives alter the  $T_g$ . these observations were further confirmed using SEM.

Generally, the state of water in the polymer can be classified as either free, freezing bound, or nonfreezing bound water. The free water is water that does not take part in hydrogen bonding with the polymer molecules. It has a similar transition temperature, enthalpy, and DSC curve as pure water. The freezing bound water or intermediate water, is water that interacts weakly with the polymer molecules. The nonfreezing water or bound water, is water molecules that are bound to the polymer molecules via hydrogen bonding. The nonfreezing of water shows no peak in the temperature range -50 to 0°C. Figure 4.12 shows the DSC thermograms of a water swollen hydrogels sample. The peaks in the DSC curves for the hydrogels, indicate that free and freezing bound waters exist in the hydrogels (Bouwstra *et al.* 1995; Seon *et al.* 2004).

**Table 4.4: Enthalpy of change determined from DSC analysis**

Sample ID	Area under the curve (mJ)	Weigh of sample (mg)	Enthalpy of change (J/g)	Maximum ESR (g/g)
H	208.558	4	52.139	7.336
HG	93.625	4	23.406	5.957
HL	162.197	4	40.549	7.263
HM	596.948	4	149.237	5.750

From the **Table 4.4**, the low enthalpy values measured for the hydrogels are ascribed to the result of a compensation of the favorable intermolecular hydrogen-bond formation and the unfavorable enthalpy component of the hydrophobic effect (Vicent *et al.* 2012). During hydrophobic effect, the enthalpy increases due to the interaction between polymer and water will be eliminated and the water–water and polymer–

## RESULTS AND DISCUSSION

polymer interaction will be favored. The dramatic increase in the hydrophobic interactions between polymer chains, at the sol–gel transition temperature, the polymer chains quickly dehydrate and collapse to a more hydrophobic structure (Qinyuan *et al.* 2017).

### 4.6.3 Scanning electron microscopy analysis

The 3D morphology and 3D network structure of the synthesized hydrogels have been studied using SEM analysis. SEM images of freeze-dried swollen hydrogel samples are shown in **Figure 4.13**. In **figure 4.13a**, it was observed that as the synthesis temperature was increased the porosity of the hydrogels also increased. PDEA prepared at 36 °C has the uniform interconnected pores.

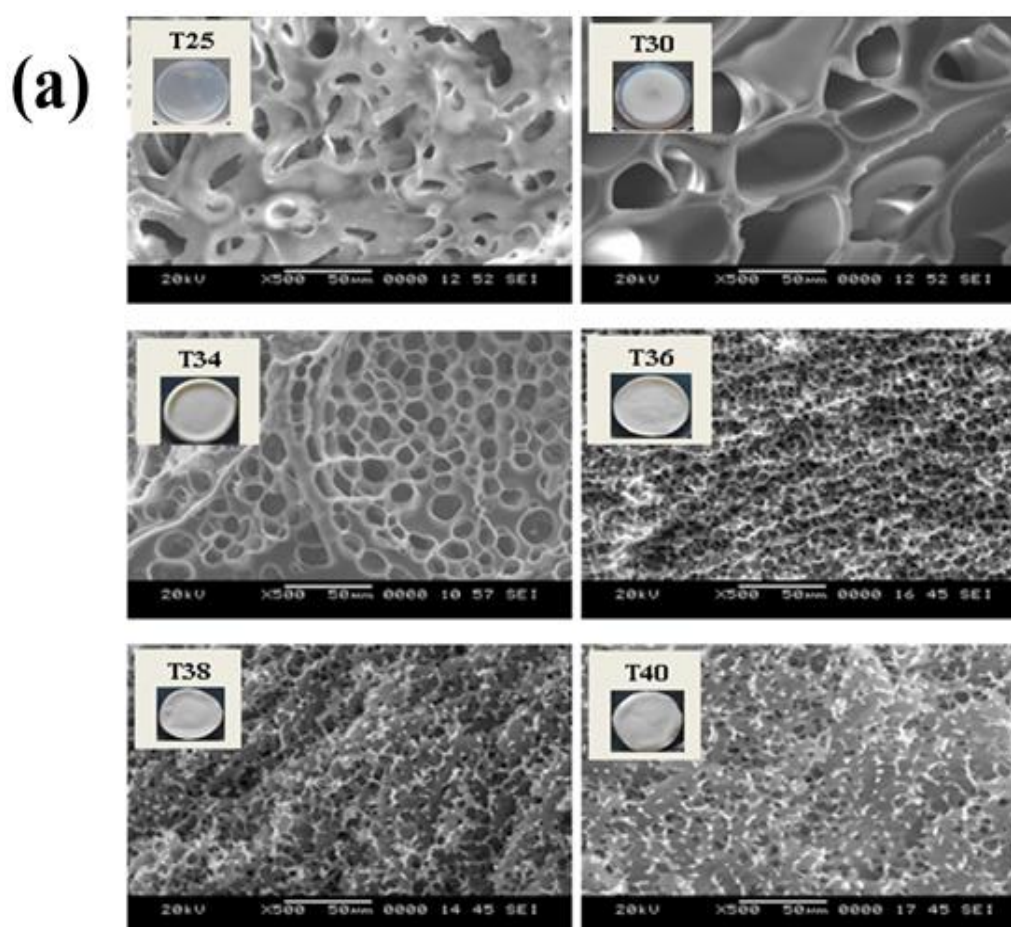


**Figure 4.13: SEM images of PDEA with the magnification of 500x: (a) PDEA prepared at varying temperature**

## RESULTS AND DISSCUSSION

**Figure 4.13(b-c)** shows the hydrogels prepared at varying GQDs content. It can be observed that the hydrogel network has more interconnected porous structure, and a change in interior morphology was observed on addition of GQDs. Water molecules can easily diffused into the hydrogel due to numerous interconnected pores in the hydrogel network. A Higher number of pores with decreased pore size were observed after the addition of GQDs, and this is due to the crystallization of water molecules in its swollen state, that acts as the pore-forming agent. The porosity of the hydrogels increased with increase in GQDs content. The GQDs in hydrogels act as a template for pore generation.

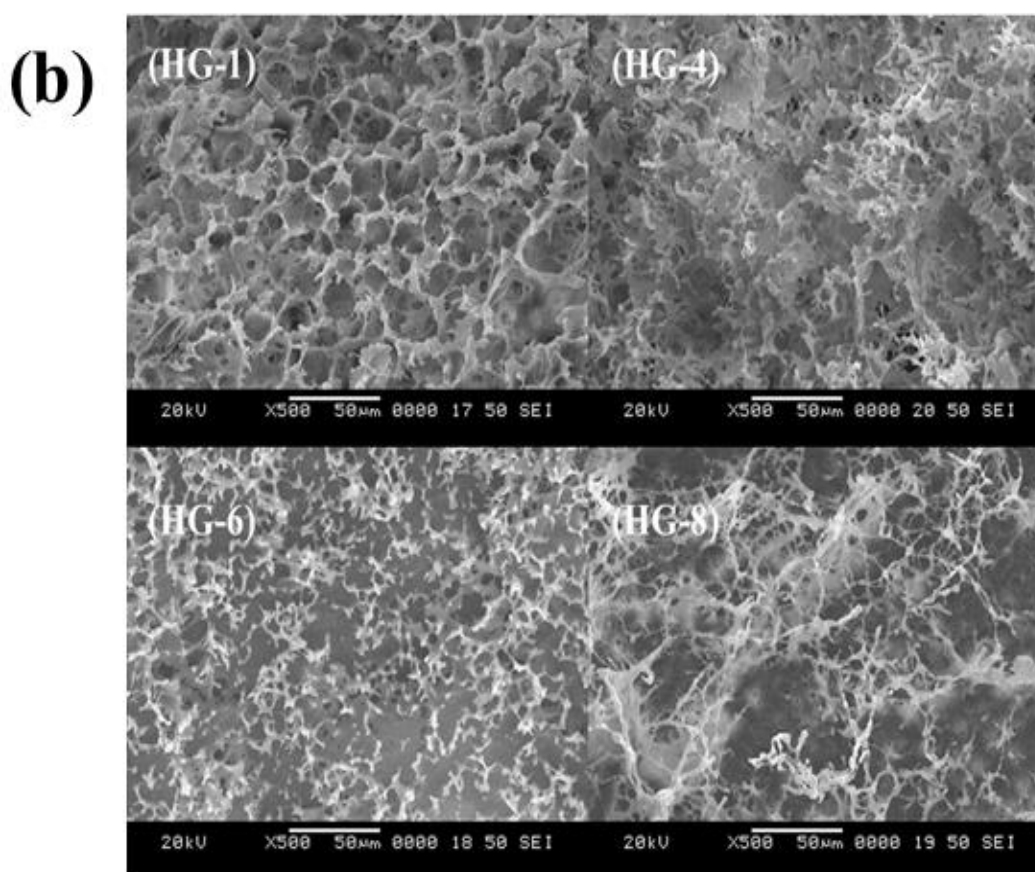


**Figure 4.13: SEM images of PDEA with the magnification of 500x: (b) PDEA with GQDs.**



## RESULTS AND DISCUSSION

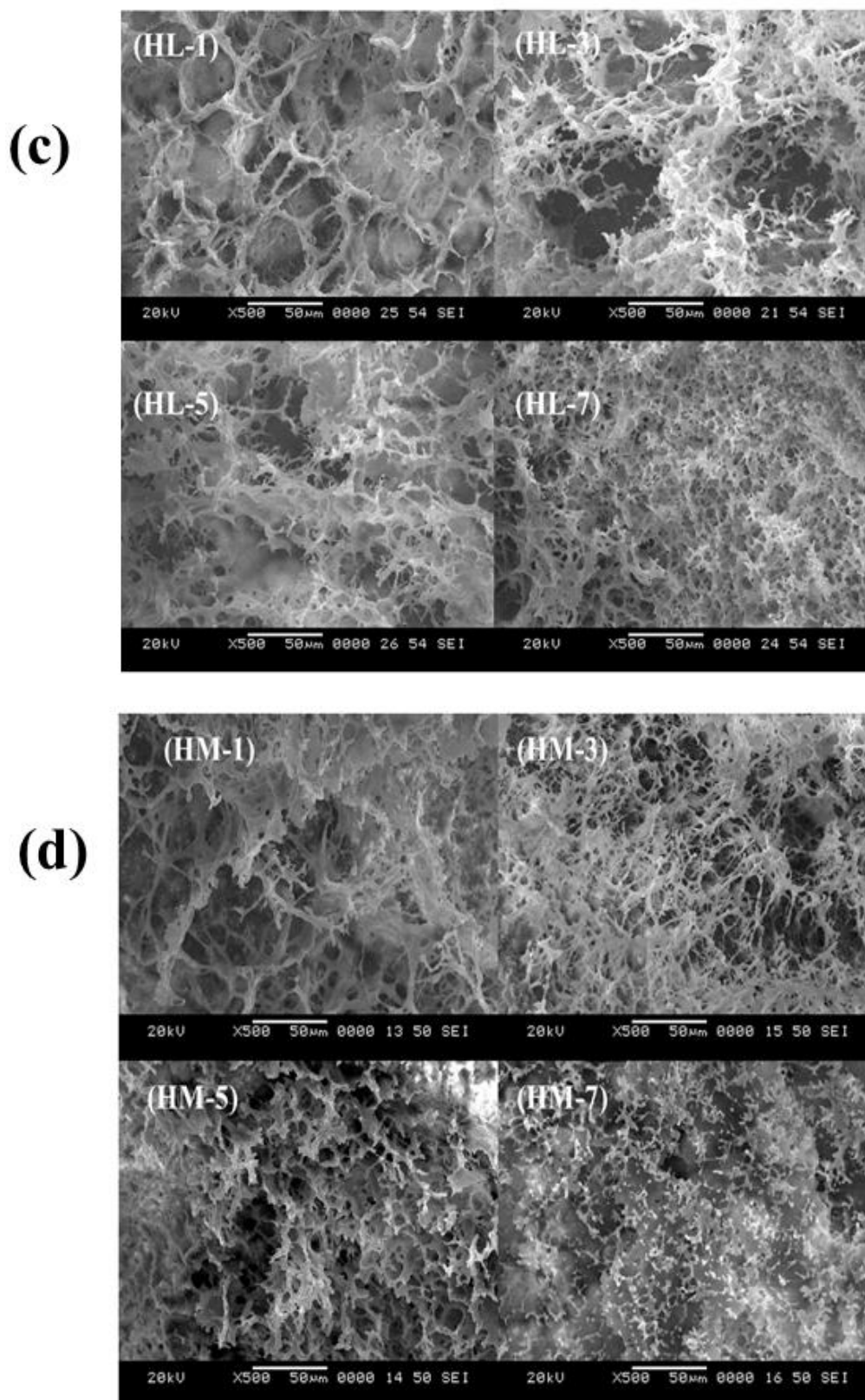
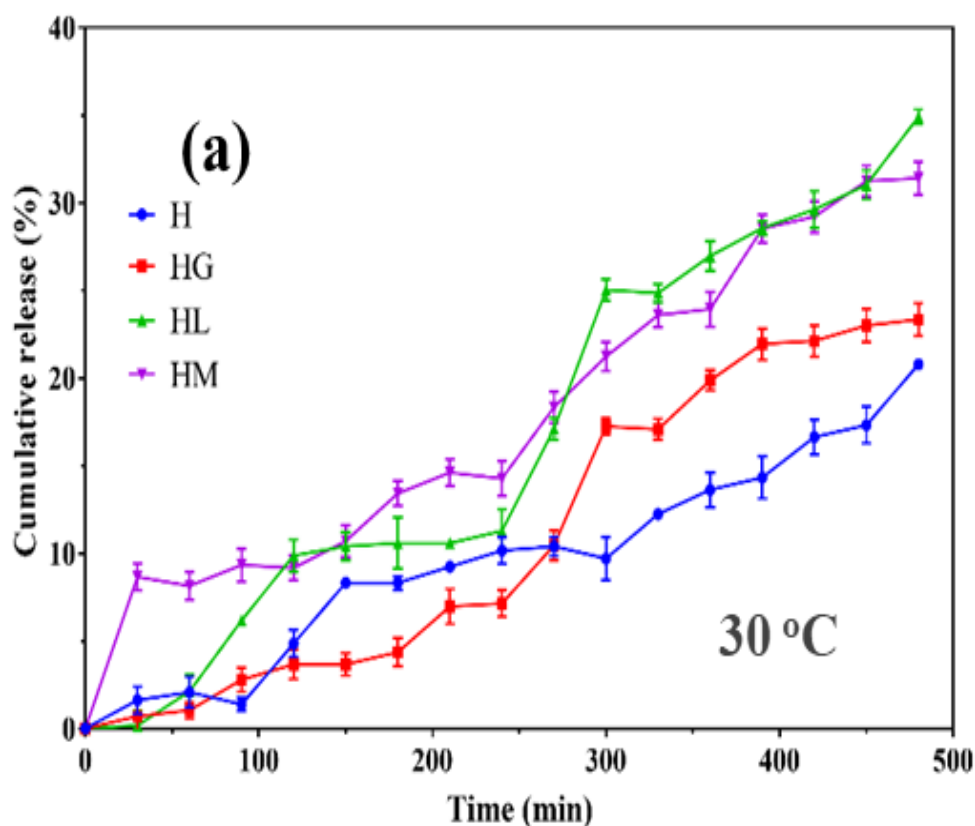


Figure 4.13: SEM images of PDEA with the magnification of 500x: (c) Leu-GQDs incorporated in PDEA and (d) PDEA incorporated with Met-GQDs.

## RESULTS AND DISSCUSSION

### 4.7 *In-vitro* drug release of the PDEA hydrogels

Drug release from the polymer matrix is closely related to many factors such as drug affinity to polymer chains, drug release, the solubility of the drug in water and swelling behavior of polymer matrix (Brazel and Peppas 1999; Hoffman, 2002). The effect of drug release from polymer matrix is observed at three different temperatures i.e., at 30 °C, 37 °C and 40 °C which is shown in **Figure 4.14**. In this study, DOX is used as model drug and it is water soluble anthracycline drug. The cumulative release of DOX (30 ppm) from T36, HG-4, HL-7 and HM-5 hydrogel samples were used. When the dry samples (0.1g) were immersed in 10 mL of 30 ppm drug solution, their final equilibrium weights were noted to be  $0.3\pm 0.05$  g (concentration of drug solution loaded in the hydrogel was 19.69, 16.33, 15.97 and 16.49 ppm respectively).



**Figure 4.14: Cumulative % release of Hydrogels above and below LCST (a) at 30 °C.**

## RESULTS AND DISCUSSION

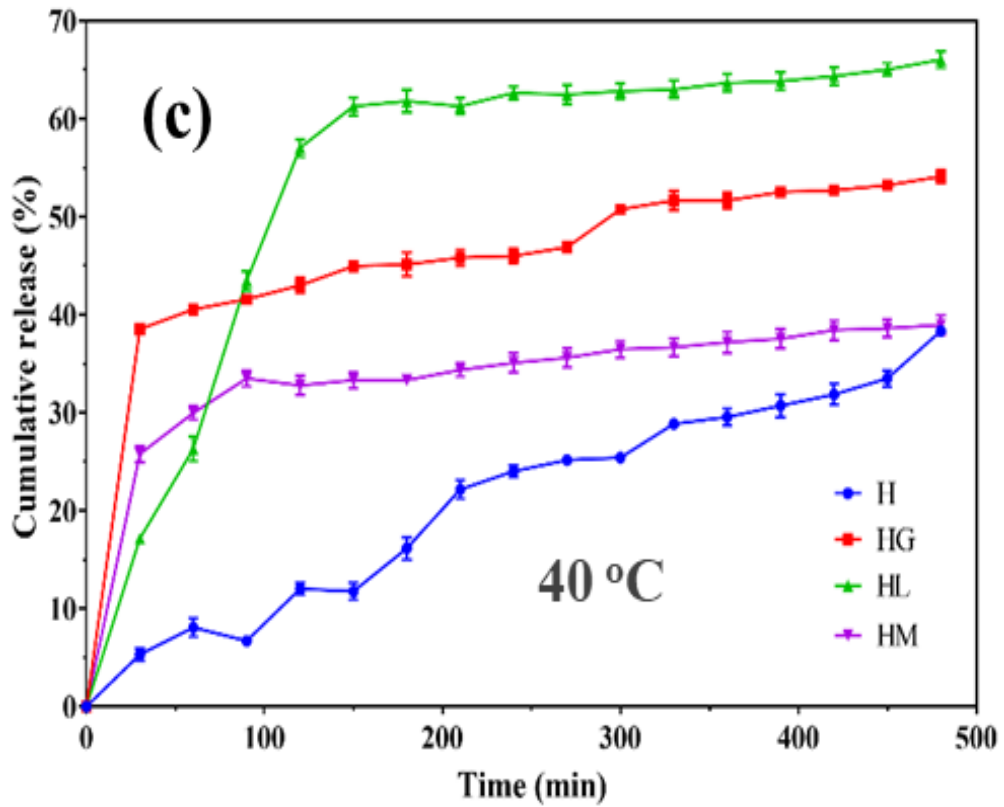
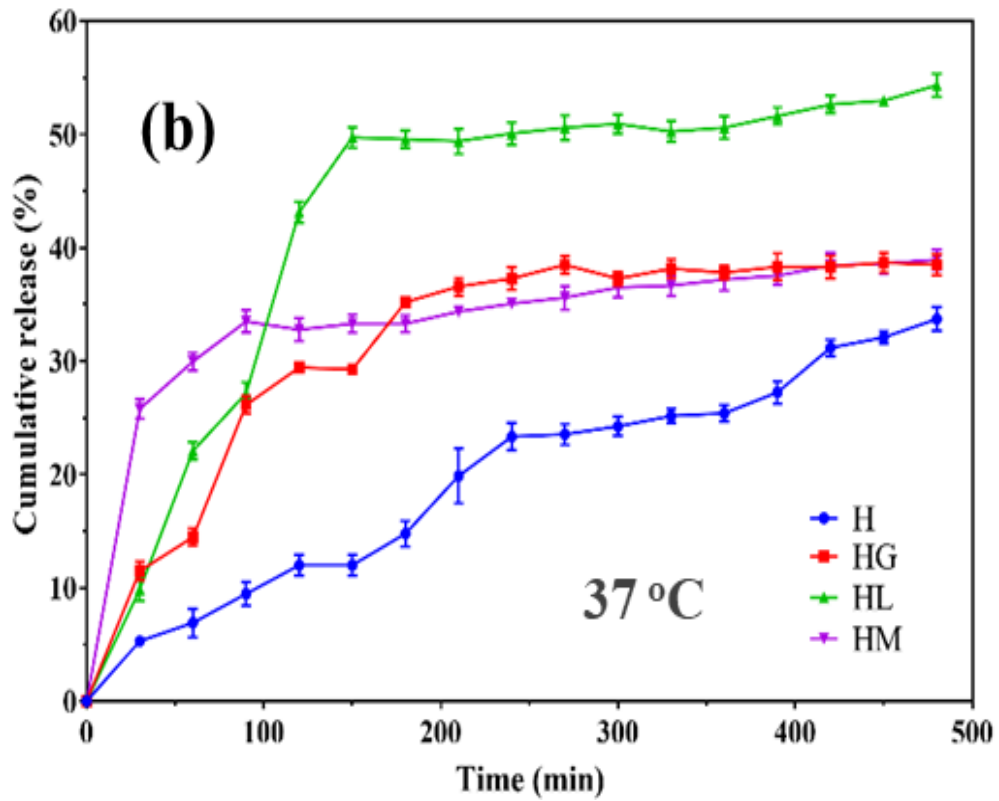


Figure 4.14: Cumulative % release of Hydrogels above and below LCST (b) at 37 °C and (c) at 40 °C.

## RESULTS AND DISSCUSSION

The difference in the initial and final concentration of drug solution showed an interesting behavior of the hydrogels, where the hydrogels have a capacity to accumulate drug molecules within it. The encapsulation efficiency and loading capacity of T36, HG-4, HL-7 and HM-5 hydrogels was shown in **Table 4.5**. The swelled hydrogels were then placed in 10 mL PBS solution at 30 °C, 37 °C and 40 °C to study its release characteristics.

**Table 4.5: Percentage of DOX encapsulation and loading into hydrogels**

Sample ID	Encapsulation efficiency (%)	Loading Capacity (%)
T36	34.365	10.309
HG-4	45.556	13.667
HL-7	46.746	14.024
HM-5	45.026	13.507

From the **Figure**, it can be noticed that the drug released by hydrogels at 30 °C (**Figure 4.14a**) was found to be between 20-39%, at 37 °C was in between 33-54% and at 40 °C the release was 38-66% of the total absorbed drug in the hydrogel. The drug release percentage increased with increase in temperature. Also, drug release in all the samples varied due to varying content of GQDs in them. Leucine functionalized GQDs incorporated hydrogel showed maximum release of DOX. When these gels are transferred to the temperature above the gel collapse point, we could observe the fast contraction of the polymer matrix. As a result, the gel collapsed, followed by slower release of drug molecules from shrunken and physically compact gels. It was also observed that the hydrogels took 8 h to release the absorbed DOX molecules with respect to time at three different temperatures (30, 38 and 40 °C) i.e., controlled and sustained release was due to the time required for drug molecules to move from the center of hydrogels to the surrounding PBS medium. The incorporation of GQDs in the PDEA can be used as drug carrier in drug delivery applications.

## RESULTS AND DISCUSSION

### 4.8 Mathematical modeling of DOX release

The drug (DOX) release at different temperature (30, 37 and 40 °C) was analysed in phosphate buffer solution having pH 7.4 as shown in figure 5.14. Further, the obtained data was fitted in zero-order, first-order, Higuchi and Korsmeyer-Peppas models to evaluate the DOX release pattern from T36, HG-4, HL-7 and HM-5 which are given in **Table 4.6** and **Table 4.7**. During the drug release process, the hydrophobic-hydrophilic interactions between the polymer network and loaded drug molecules decide the release characteristics. The diffusion of DOX molecules and the relaxation of polymer chains determine the type of release mechanism of loaded drug molecules. After fitting the release data in different model equations, the release pattern was evaluated based on the regression coefficient 'R'. The regression coefficient for different model using different release data is listed in **Table 4.6**. The obtained R value at different temperatures for first-order release rate constant were found to be higher than those of zero-order release rate constants. It is therefore attributed to the fact that DOX release from the hydrogel at different temperatures followed first-order release profile. In Higuchi model, the value of R at different temperatures indicated that the drug release mechanism is diffusion controlled.

In Korsmeyer-Peppas model the general classification of diffusion from the polymeric matrix is as follows: if  $n$  is 0.5, then the drug released is because of Fickian diffusion (drug diffusion is dominant), if  $n$  is 1, then the drug released is because of other predominant factors like external stimuli and if  $0.5 < n < 1$ , non-Fickian or anomalous release (a synergistic effect of drug diffusion and external stimuli). The effect of surrounding temperature on the exponent value 'n' are listed in **Table 4.7**. From the **Table** it has been observed that most of the samples showed non-Fickian behaviour, and HG-4, HL-7 at 30 °C and HM-5 at 40 °C showed super case II transport, HL-7 at 40 °C & HM-5 at 37 °C did not fit into the Korsmeyer-Peppas model (Siepmann and Peppas. 2001; Ronald and Michael. 2012). Therefore, the release of DOX from these hydrogels may be considered as non-Fickian diffusion/super case II transport and swelling controlled. The hydrogel composition and its surrounding temperature have shown certain effect on the DOX release kinetics. Incorporation of GQDs in the PDEA hydrogel showed enhanced cumulative release at 40 °C with respect to time i.e., with

## RESULTS AND DISSCUSSION

increase in the surrounding environment temperature the cumulative release also increased. The GQDs may be used along with the thermosensitive hydrogels to obtain an excellent release effect.

**Table 4.6: DOX release kinetics of T36, HG-4, HL-7 and HM-5 hydrogel at different temperatures.**

Sample ID	DOX release Temperature (°C)	Zero-order kinetics		First-order kinetics		Higuchi model	
		$k_0$	$R^2$	$k_1$	$R^2$	$k_2$	$R^2$
T36	30	0.0740	0.94796	1.84445	0.94191	-5.1070	0.92417
	37	3.2361	0.96665	1.98828	0.97143	-5.4191	0.96739
	40	2.6263	0.96204	1.99182	0.96815	-7.1781	0.95854
HG-4	30	-10.2532	0.94021	1.8619	0.95934	-30.6474	0.92173
	37	19.8035	0.90803	1.9094	0.91396	8.1803	0.92376
	40	33.6931	0.91911	1.8167	0.92126	22.5301	0.93884
HL-7	30	-2.1555	0.95641	1.8391	0.90411	-16.2270	0.92257
	37	9.9104	0.84743	2.0201	0.91779	-15.0042	0.90798
	40	4.4692	0.91686	2.0523	0.89045	8.3852	0.92046
HM-5	30	-0.8970	0.94	1.8259	0.97091	-19.6419	0.965
	37	29.1142	0.84316	1.8426	0.9867	25.7979	0.9859
	40	-2.7497	0.95346	2.0411	0.98002	-31.6307	0.9849

## RESULTS AND DISCUSSION

**Table 4.7: Release exponent (n), correlation coefficient (R<sup>2</sup>) and mechanism of drug release (Korsmeyer-Peppas model) T36, HG-4, HL-7 and HM-5 hydrogels at 30 °C, 37 °C and 40 °C.**

Sample ID	DOX release Temperature (°C)	n	R <sup>2</sup>	Order of release
T36	30	0.9299	0.97525	non-Fickian mechanism
	37	0.7119	0.974	non-Fickian mechanism
	40	0.7146	0.98648	non-Fickian mechanism
HG-4	30	1.4592	0.95442	Super case II transport
	37	0.6552	0.91652	non-Fickian mechanism
	40	0.2215	0.9235	---
HL-7	30	1.178	0.95617	Super case II transport
	37	0.9989	0.90598	non-Fickian mechanism
	40	0.8833	0.95431	non-Fickian mechanism
HM-5	30	0.9455	0.9763	non-Fickian mechanism
	37	0.1148	0.96841	---
	40	1.4001	0.93892	Super case II transport

### 4.9 *In-vitro* biocompatibility of GQDs and hydrogels

The cytotoxicity of biomaterials is extremely important for their future applications. The capability of the cells to live in a toxic environment has been the basis of most of the cytotoxicity assays. In this study, the cytotoxicity of the GQDs, T36, HG-4, HL-7 and HM-5 and DOX loaded hydrogels are investigated by MTT assay in B16F10 cell lines. The cell viability was compared with the control group, as shown in **Figure 4.15**. From the figure it can be concluded that hydrogels and GQDs are non-cytotoxic. The exposure of cells at varying concentrations (62.5 to 1000 µg/mL) of GQDs (bare GQDs, leucine functionalized GQDs, methionine functionalized GQDs), T36, HG-4, HL-7, HM-5, and respective DOX loaded hydrogels had no apparent effect on cell viability.

## RESULTS AND DISCUSSION

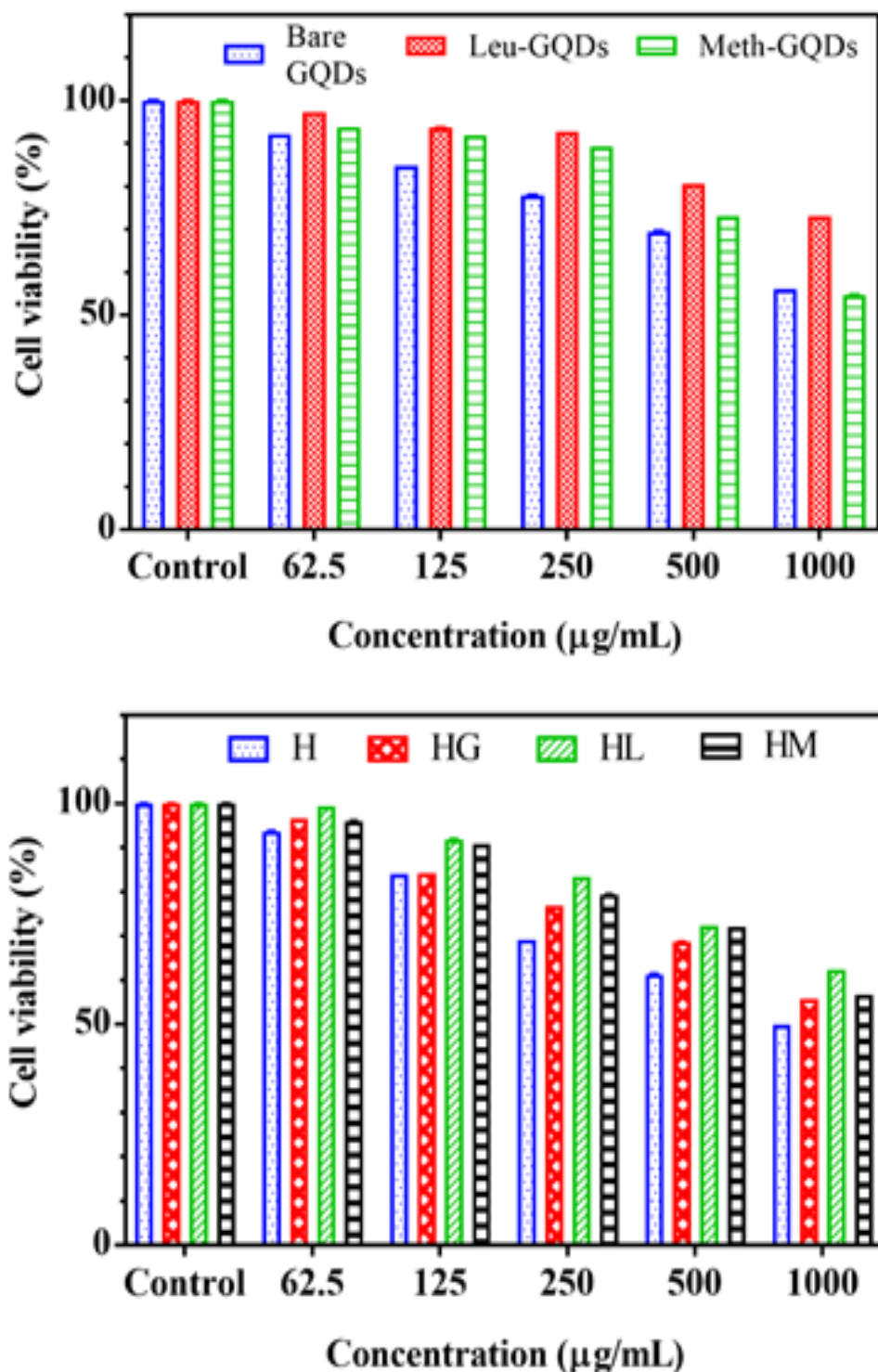
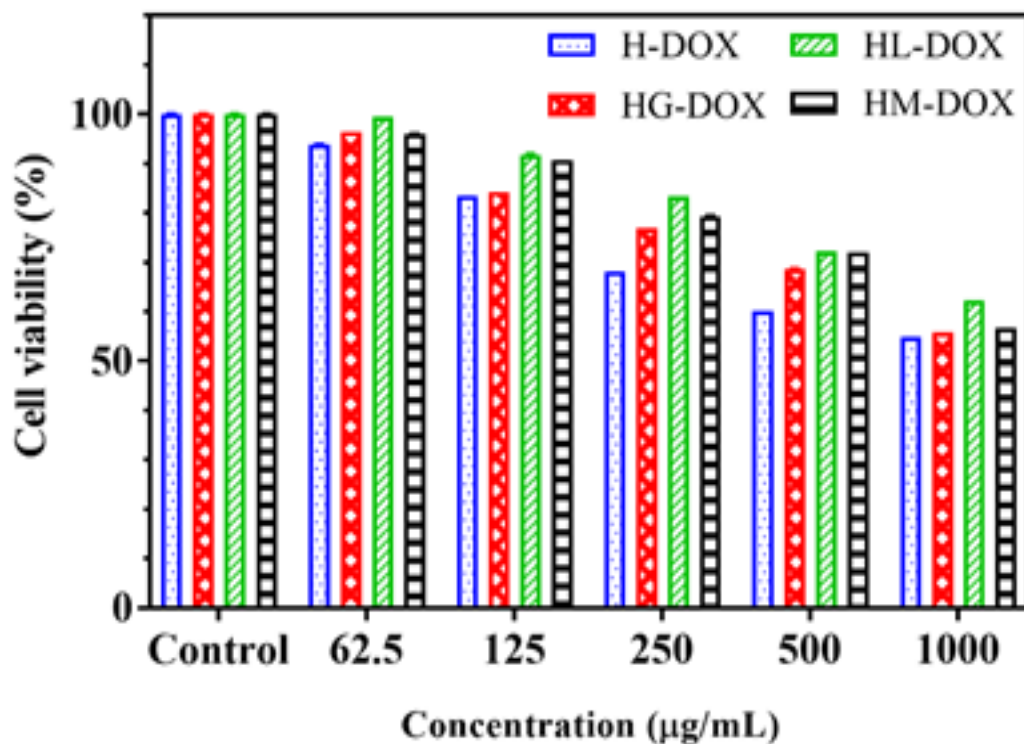


Figure 4.15: Percentage of Cell viability of B16F10 cells after treatment with (a) GQDs and (b) hydrogels extracts.



## RESULTS AND DISCUSSION

After 24 h, the samples were examined by the microscope as shown in **Figure 4.15** The microscopic images of control and other samples also showed that the cells are overwhelmingly viable, regardless of the concentration of hydrogels. These cytotoxicity data confirmed that the incorporation of GQDs into the PDEA were non-toxic.



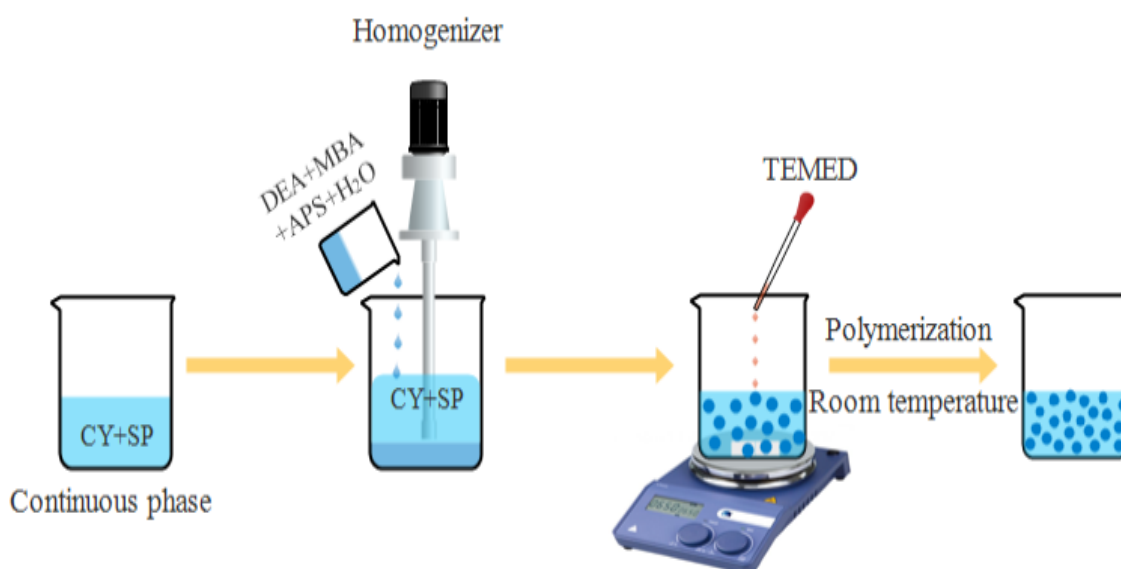
**Figure 4.15: Percentage of Cell viability of B16F10 cells after treatment with (c) GQDs and hydrogels extracts.**

# RESULTS AND DISCUSSION

## PART III

### 4.10 Synthesis and optimization of PDEA nanohydrogels

PDEA nanohydrogels were prepared by inverse emulsion polymerization method (**Scheme 4.4**). Stable w/o emulsion is formed by dispersing monomer droplets along with surfactant in a continuous oil phase (cyclohexane) at high shear force using homogenizer or a magnetic stirrer. Selection of surfactant is important which will ensure the stability of the emulsion as well as the resulting polymeric particles. The use of oil-soluble non-ionic surfactants with hydrophilic-lipophilic balance (HLB) value around 4.0 is generally used for conventional inverse emulsion polymerization (Landfester *et al.* 2000). Span 80 is a commercially available surfactant, which has HLB value of 4.3, is used in the study to form stable emulsions. In the w/o emulsion the monomer droplets which is a dispersed phase consists of DEA (monomer), MBA (cross-linker), APS/TEMED (initiator) and water. The continuous phase consists of non-ionic oil soluble surfactant (span 80) and oil (cyclohexane).



**Scheme 4.4: Schematic representation of PDEA nanohydrogel synthesis by inverse emulsion polymerization**

In this study, ammonium persulfate was used as a water soluble initiator with monomer. Generally, if polymerization was carried out at temperature more than 60 °C, APS tends to decompose to produce free radicals but LCST of PDEA is less than 60 °C (Mori and Kawaguchi, 2007, Kubota *et al.* 1990). If the reaction is conducted above 60 °C, the

## RESULTS AND DISCUSSION

newly formed PDEA chain would change its property from hydrophilic to hydrophobic and would precipitate from the water phase. The surfactants that are adsorbed on the surface of the water droplets would detach, and the emulsion would collapse. Therefore, the reaction temperature should be lower than the LCST of PDEA, and it has been reported that TEMED can form free radicals from persulfate at room temperature (Kubota *et al.* 1990). Therefore, TEMED was added after the formation of emulsion to initiate the polymerization at room temperature. Upon polymerization, the monomers inside the micelles reacted and formed polymeric nanohydrogels, surrounded by surfactant. Nanohydrogels thus formed were washed by repeated centrifugation and lyophilized. These nanohydrogels were used for further study.

### 4.11 Effect of parameters on synthesis of PDEA nanohydrogels

A series of thermos-responsive PDEA nanohydrogels were synthesized by inverse emulsion polymerization method. Stable w/o emulsion is formed by dispersing aqueous monomer droplets with the aid of surfactant in continuous oil phase. The dispersed phase consists of monomer (DEA), cross-linker (MBA), initiator (APS/TEMED) and water. Based on the previous optimization study on macro hydrogels, the concentration of the dispersed phase used for synthesis of nanohydrogel is as follows: DEA – 8.717 mmol, water – 5 mL, MBA – 129.7  $\mu\text{mol}$ , APS – 175.3  $\mu\text{mol}$  and TEMED 100  $\mu\text{L}$ . The other operating parameters which have influence on the particle size of the nanohydrogels are stirrer speed, water/oil ratio (weight ratio) and concentration of surfactant, which was optimized based on the particle size of the nanohydrogels.

#### 4.11.1 Effect of stirrer speed

The effect of stirring rate on mean diameter of the nanohydrogels synthesized, while keeping the other variables constant (water:oil ratio of 1:4 and the surfactant concentration of 2.25%) is as shown in **Table 4.8**. The mean size of the particle decreases with increase in the stirrer speed. High stirring rate provides the required shearing force to reduce the size of the emulsion droplet, resulting in decrease in size of the nanohydrogels.

## RESULTS AND DISSCUSSION

**Table 4.8: Effect of stirrer speed on the size of PDEA nanohydrogels**

Stirrer Speed (RPM)	Mean particle size (nm)	Standard deviation (nm)
300	1060±60.3	85.27708
400	706.4±81.1	114.6927
500	310.55±29.35	41.50717
<b>600</b>	<b>93.7±5.2</b>	<b>7.353911</b>
700	212.3±82.1	116.1069
800	406.25±66.5	94.11591

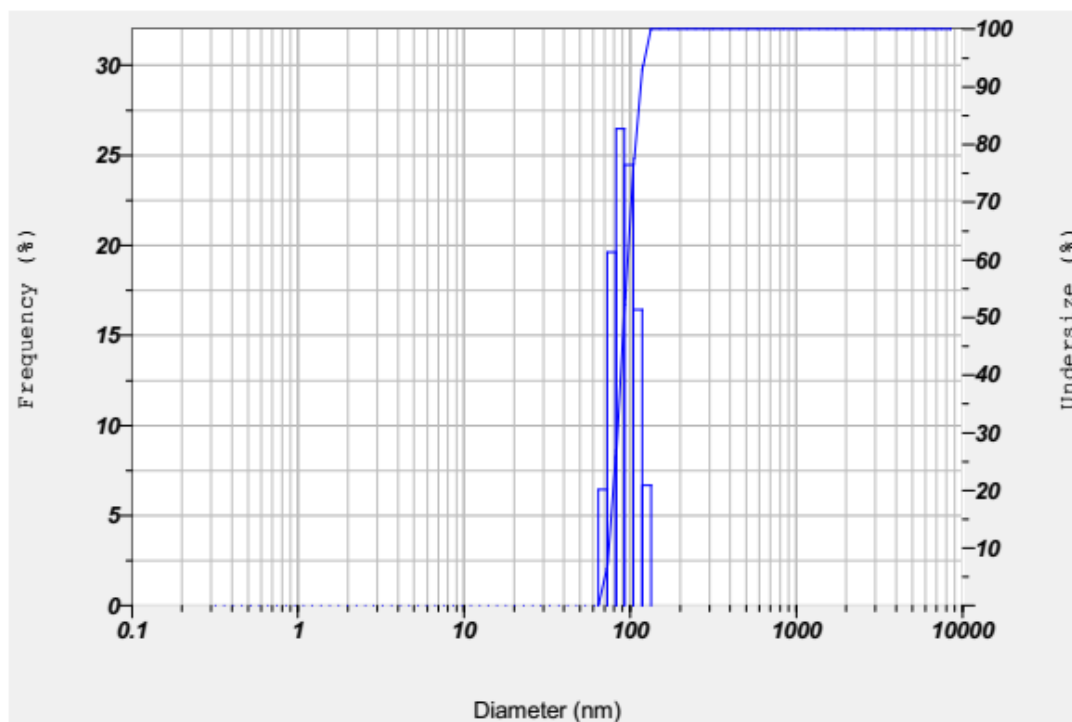


**Figure 4.16: Particle size distribution of PDEA nanohydrogels prepared at stirring speed 600 with 1:4 w/o ratio and 2.25% of surfactant**

Particle size reduced from 1060 nm to 93.7 nm on increasing the speed from 300 rpm to 600 rpm and then started to increase (Jose *et al.* 2010). However, when the stirring rate was higher than 600 rpm, the collision between the latex droplets and precursor particles increased, which led to the increase in particle size. From this analysis it could be concluded that maximum speed that should be maintained to achieve minimum size

## RESULTS AND DISCUSSION

is 600 rpm. **Figure 4.16** shows the particle size distribution of the nanohydrogels synthesized at 600 rpm.

### 4.11.2 Effect of W/O ratio

The ratio of aqueous phase (monomer phase or dispersed phase) to oil phase (continuous phase) has significant effect on the particle size of the nanohydrogels. The effect of w/o ratio on the size of the nanohydrogels was studied by varying the weight ratio of disperse and continuous phase from 1:2 to 1:7. The particle size distribution of PDEA nanohydrogel prepared with various w/o ratio were characterized by DLS. **Table 4.9** shows the influence of the water/oil ratio on the mean diameter of the nanohydrogels. From the table, it can be observed that the mean diameter of nanohydrogel reduces as the w/o ratio increased from 1:2 to 1:5. A minimum diameter of 77.75 nm was achieved at 1:5 w/o ratio. Beyond 1:5 w/o ratio, particle size increased. **Figure 4.17** shows the particle size distribution of the nanohydrogels synthesized at optimum stirrer speed of 600 rpm, optimum surfactant concentration of 2.5% and optimum water:oil ratio of 1:5.

**Table 4.9: Effect of water:oil ratio on the size of PDEA nanohydrogels**

<b>Water/oil ratio (wt:wt)</b>	<b>Mean particle size (nm)</b>	<b>Standard deviation (nm)</b>
1:2	683.15±64.8	91.71175
1:3	291.75±253.25	358.1496
1:4	191.1±46.9	66.32662
<b>1:5</b>	<b>77.75±2.35</b>	<b>3.323402</b>
1:6	131.15±1.55	2.192031
1:7	284.1±51.4	72.69058

The relative viscosity of the two phases has a strong influence on the particle size of the nanohydrogels. Singh *et al* (2017), has reported that optimum viscosity ratio should be  $0.05 \leq \eta_d/\eta_c \leq 5$  which produces finest emulsions. The optimum viscosity of water and cyclohexane was determined to be 0.9728 mPa. If the viscosity is too high, the

## RESULTS AND DISSCUSSION

emulsion droplets become resistant to break-up and start rotating in their own axis when subjected to shear (McClements. 2015; Singh *et al.* 2017).

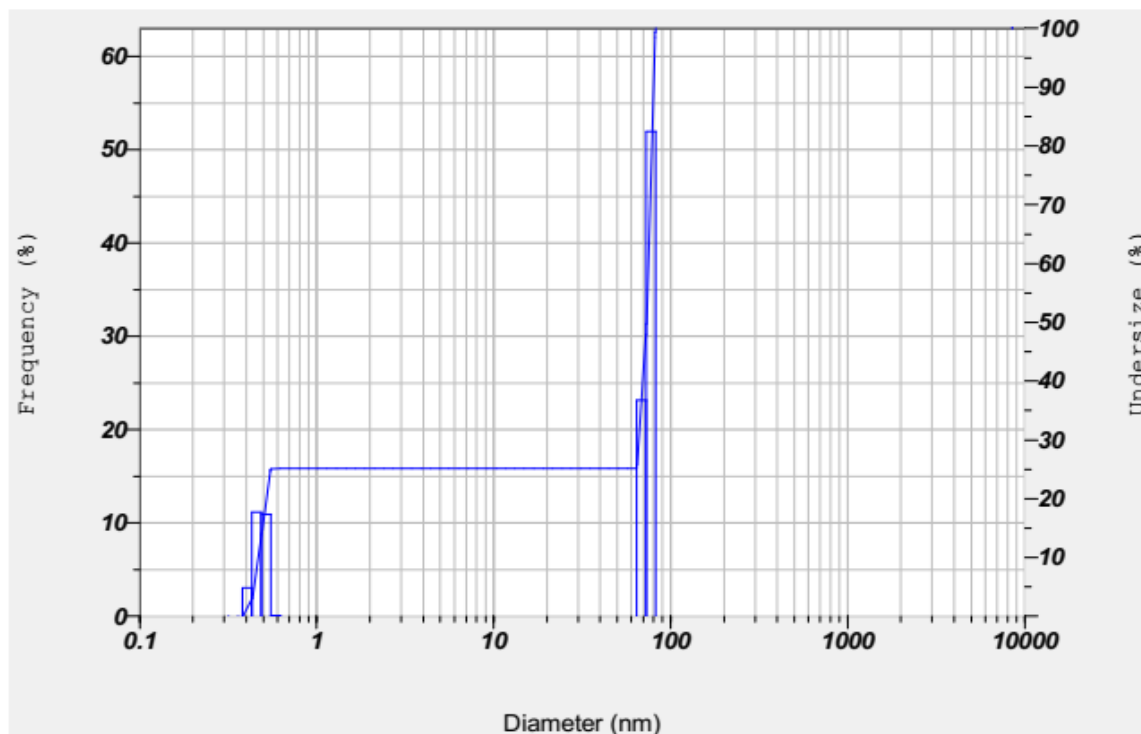


**Figure 4.17: Particle size distribution of PDEA nanohydrogels prepared at stirring speed 600 with 1:5 w/o ratio and 2.25% of surfactant**

### 4.11.3 Effect of surfactant concentration

In order to stabilize the emulsion surfactant is required. The influence of concentration of non-ionic surfactant (Span 80) on the synthesis of PDEA nanohydrogels was studied by preparing nanohydrogels with varying surfactant concentration (**Table 4.10**). It is known that the critical micellar concentration (CMC) of span in cyclohexane is 1.25-1.5 vol% of span 80 in cyclohexane (Chatterjee *et al.* 2001) and the surfactant concentration should be more than CMC to form micelles. Nanohydrogels were prepared using different concentration of surfactant (1.5 to 3 vol% of span 80 in cyclohexane), with water:oil ratio 1:5 and stirring speed at 600 rpm. As the concentration of span 80 increased from 1.5 to 3%, the average particle size was found to be decrease from 1.061  $\mu\text{m}$  to 64.2 nm.

## RESULTS AND DISCUSSION

**Table 4.10: Effect of surfactant concentration on the size of PDEA nanohydrogels**

Surfactant concentration (vol% of span 80 in cyclohexane)	Mean particle size (nm)	Standard deviation (nm)
1.5	1061.95±51.9	73.46839
1.75	842.2±58.6	82.87291
2	668±40.8	57.69991
2.25	517.45±17.6	24.81945
2.5	286.05±49.1	69.36718
2.75	160.9±22.8	32.24407
<b>3</b>	<b>64.2±4.4</b>	<b>6.22254</b>

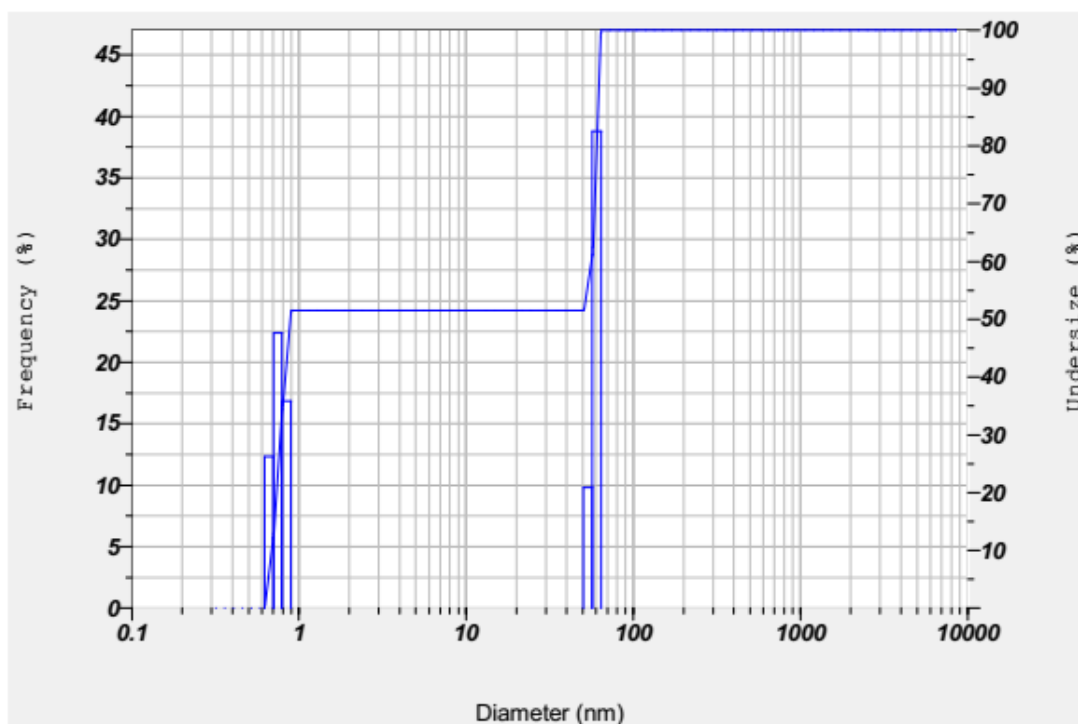


**Figure 4.18: Particle size distribution of PDEA nanohydrogels prepared at stirring speed 600 with 1:5 w/o ratio and 3% of surfactant**

The surfactant is a surface active agent and an increase in its concentration will stabilize greater surface area, and thus leading to smaller particle size. At the same time very high concentration of span 80 will lead to difficulty in getting rid of the surfactant from the final product. The results from table shows that nanohydrogels formed at 3% of

## RESULTS AND DISSCUSSION

span 80 in cyclohexane have lesser size which was used for further studies. **Figure 4.18** shows the particle size distribution of nanohydrogels synthesized using 3 vol% of span 80 and the average diameter of the particles is around 59.8 nm.

From the above discussion, we can conclude that the optimum composition required to produce nano sized PDEA hydrogel is DEA – 8.717 mmol; Water – 5 mL; MBA – 129.7  $\mu$ mol; APS – 175.3  $\mu$ mol and TEMED 100  $\mu$ L at the stirring speed 600 rpm with 1:5 w/o and 3% of surfactant concentration. This optimized composition was further used to prepare GQDs incorporated nanohydrogels.

### 4.12 Characterization of PDEA nanohydrogels

#### 4.12.1 Size and morphological analysis of PDEA nanohydrogels

The particle size distribution of prepared nanohydrogels are shown in **Table 4.10**. A broad range of sizes were observed in the prepared nanohydrogel samples which could be due to few premature termination of particle growth, which is caused by the presence of the oxygen in the reaction mixture (Panayiotou *et al.* 2007). The molecular weight ( $M_w$ ) of the synthesized nanohydrogels was determined by GPC using THF as eluent and polystyrene as standard. The  $M_w$  are as shown in **Table 4.11**. The polydispersity index of nanohydrogels was too small which was obtained by  $M_w/M_n$  was between 1.381 to 1.557. The  $M_w$  has increased due the incorporation of GQDs in PDEA nanohydrogels.

**Table 4.11: Particle size and molecular weight of nanohydrogels**

Sample ID	Particle size (nm)	Molecular weight (Mw)	Polydispersity index (Mw/Mn)
N	47 - 59.5	6634.36	1.557
NG	59.9 - 68.1	6653.33	1.409
NL	78.8 – 91.7	7642.67	1.381
NM	87.5 – 99	6856.96	1.450



## RESULTS AND DISCUSSION

Further, the TEM results are shown in **Figure 4.19**. The morphology of synthesized nanohydrogels by IEP shows nearly spherical shape with wide size range as shown in **Figure 4.19(a-d)**.

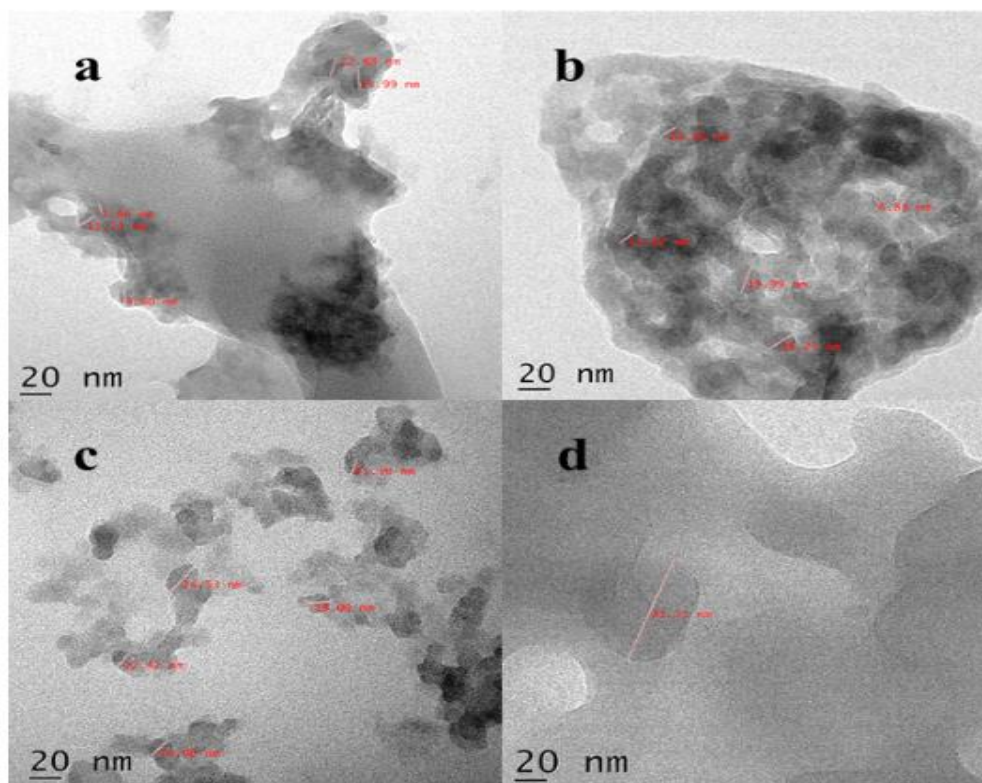


**Figure 4.19: TEM images of nanohydrogels with a scale bar of 20 nm: (a) N; (b) NG; (c) NL and (d) NM.**

The size of nanohydrogels was in the range of 3.56 nm – 12.88 nm for N, 6.89 nm – 19.99 nm for NG, 11.56 nm – 24.53 nm for NL and for NM it was 81.11 nm. The size range of particles observed by TEM was completely different from DLS measurement, and it could be due to the lyophilisation effect. Further, the irradiation of electron beam under reduced pressure might have affected the morphology of the particles (Panayiotou *et al.* 2007).

### 4.12.2 FT-IR and elemental analysis of nanohydrogels

The molecular structure of synthesized nanohydrogels like N, NG, NL, NM and GQDs (GQDs, GL and GM) was investigated using ATR – FTIR (Fourier transform infrared spectroscopy) which is shown in **Figure 4.20**. The absorption peaks in

## RESULTS AND DISCUSSION

**Figure 4.20 (a-c)** at  $2918\text{ cm}^{-1}$  to  $2957\text{ cm}^{-1}$  and peak in figure 5.5d at  $2924\text{ cm}^{-1}$  to  $2984\text{ cm}^{-1}$  are due to the C-H stretching vibrations of  $-\text{CH}_3$  and  $-\text{CH}_2-$  side groups in synthesized GQDs and PDEA nanohydrogels respectively (Chen *et al.* 2011; Wei *et al.* 2016). The significant peaks at  $1607\text{ cm}^{-1}$  to  $1617\text{ cm}^{-1}$  (**Figure 4.20d**) in the nanohydrogels can be attributed to the characteristic peak of the carbonyl group (amide I) C=O stretching vibration (Chen *et al.* 2010; Ngadaonye *et al.* 2012). The peak at  $1405\text{ cm}^{-1}$  to  $1444\text{ cm}^{-1}$  in nanohydrogels was due to symmetrical C-H bending. The bands ranging from  $1083\text{--}1262\text{ cm}^{-1}$  are attributed to the stretching of C-N (amide III) bond in the polymer (Chen *et al.* 2009). The characteristic band of -OH in both bare GQDs and functionalized GQDs incorporated PDEA are in the range of  $3206\text{--}3447\text{ cm}^{-1}$  (Naik *et al.* 2017). A characteristic stretching vibration band of aromatic C-C was observed at  $1607\text{--}1617\text{ cm}^{-1}$  for GQDs and  $1444\text{ cm}^{-1}$  for PDEA polymers (Li *et al.* 2013).

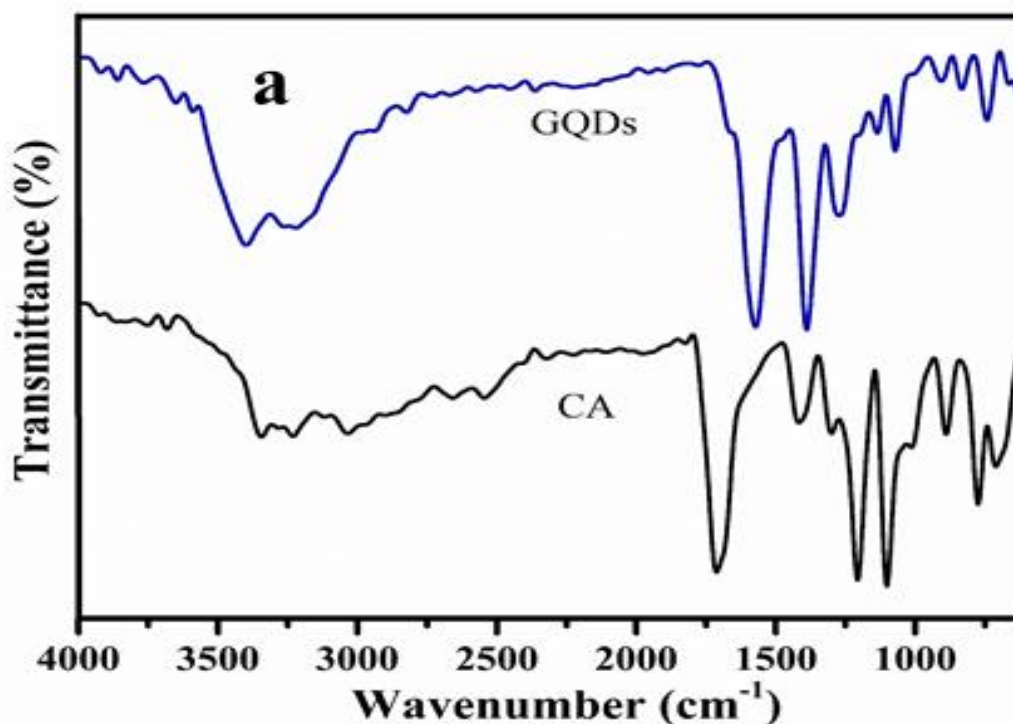


**Figure 4.20: FTIR spectra (a) GQDs**

## RESULTS AND DISCUSSION

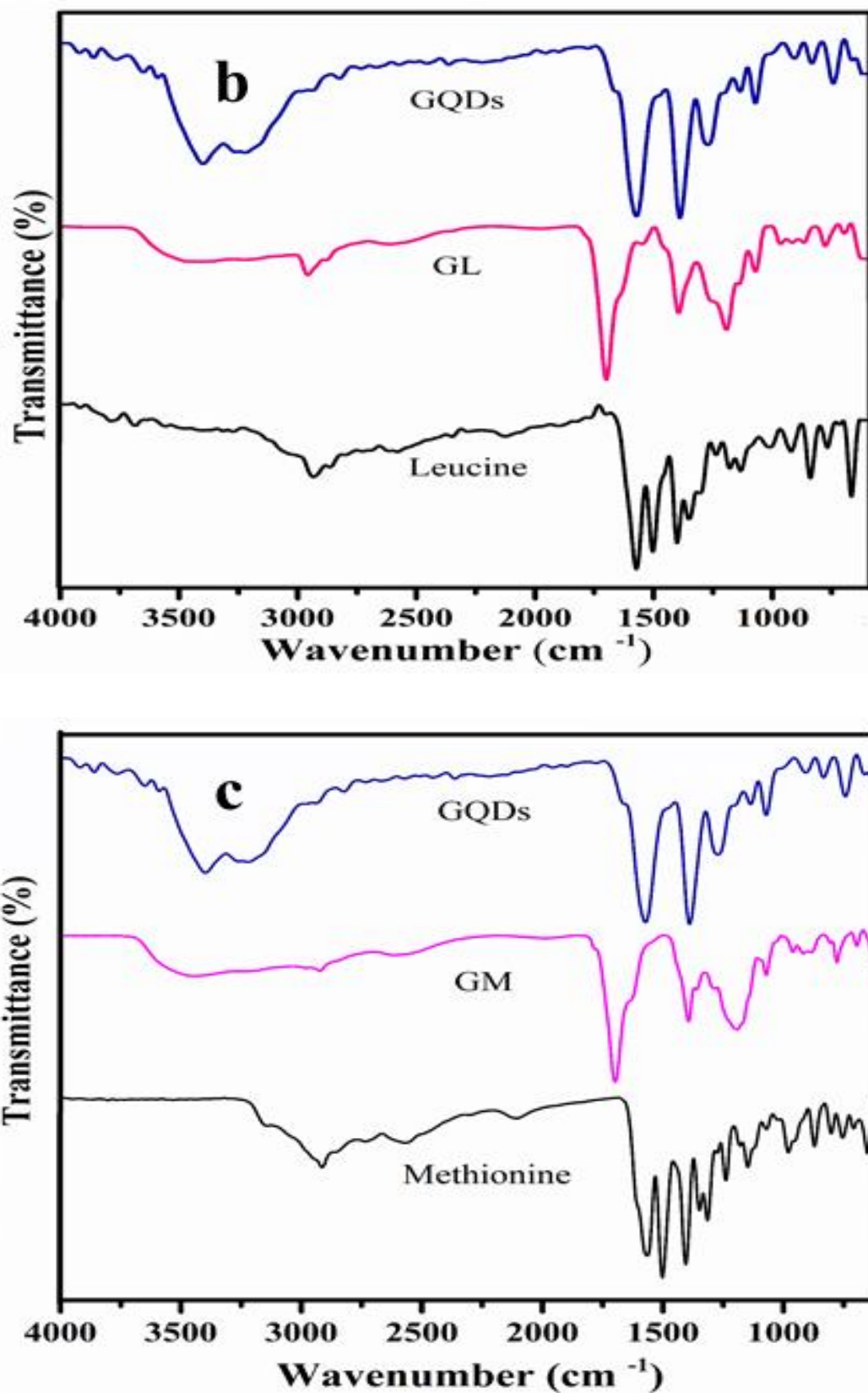
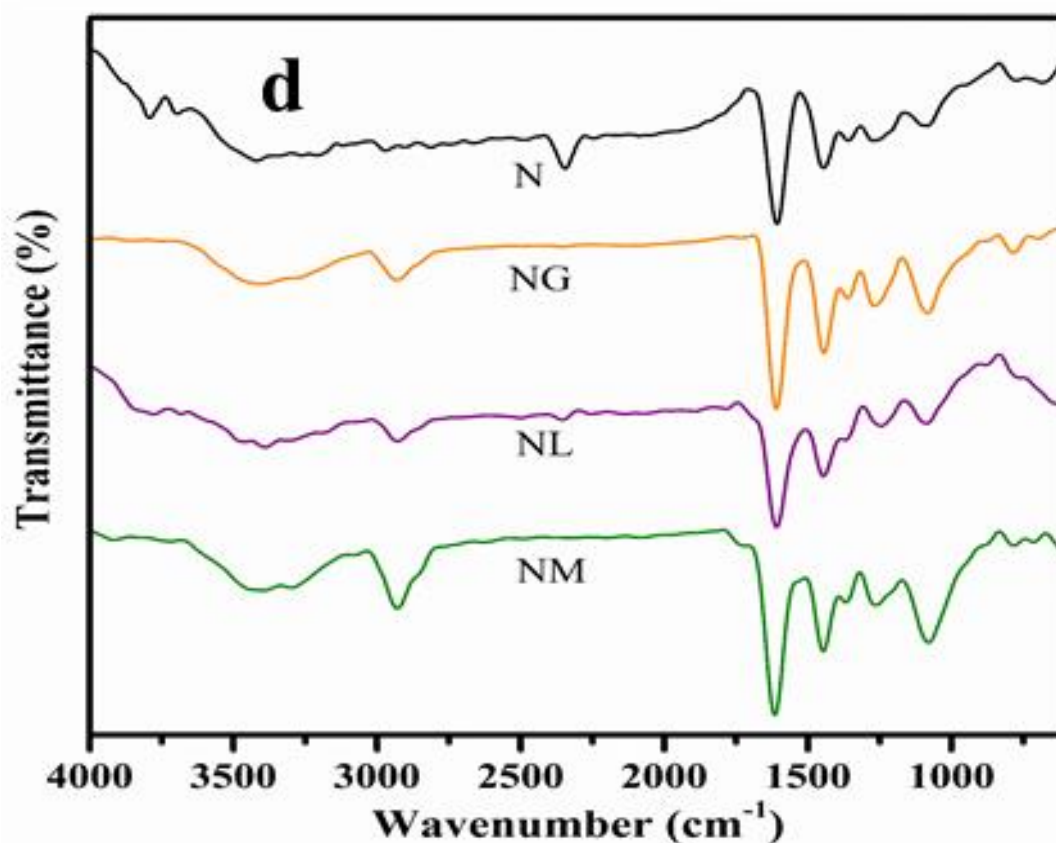


Figure 4.20: FTIR spectra (b) GM, (c) GL

## RESULTS AND DISCUSSION



**Figure 4.20: FTIR spectra (d) PDEA nanohydrogels**

A strong peak in GQDs at  $1388\text{--}1401\text{ cm}^{-1}$  is due to the C-H stretching vibration (Zeng *et al.* 2016) and C-O stretch represents the alcohol, carboxylic acid, and ester weak bands which were observed in the range of  $1101\text{--}1206\text{ cm}^{-1}$  (Qiu *et al.* 2015). The disappearance of the characteristic peaks of C=O stretch at  $1735\text{ cm}^{-1}$  and C-H bending at  $1441\text{ cm}^{-1}$  in GQDs incorporated PDEA shows the successful binding of GQDs with PDEA. The appearance of broad -OH peak at  $3466\text{ cm}^{-1}$  and small C-C peak at  $1452\text{ cm}^{-1}$  in GQDs incorporated PDEA confirms the presence of GQDs in PDEA. Further the presence of bare GQDs and functionalized GQDs was confirmed by elemental analysis.

The elemental analysis of the N, NG, NL and NM are shown in **Table 4.12**, where it represents the weight percentage of C, H, N and O. Increase in carbon and hydrogen percentage in nanohydrogels with bare GQDs and functionalized GQDs confirmed the presence of quantum dots. Also, the presence of N confirms the

## RESULTS AND DISCUSSION

functionalization of GQDs with leucine and methionine.

**Table 4.12: Elemental analysis of GQDs and PDEA nanohydrogels**

Sample ID	Carbon (%)	Hydrogen (%)	Oxygen (%)	Nitrogen (%)
GQDs	66.65	2.61	30.74	-
GL	46.04	6.03	42.67	5.26
GM	54.90	7.12	32	5.98
N	49.60	10.09	32.56	7.75
NG	60.51	12.32	17.95	9.22
NL	54.69	11.07	23.96	10.28
NM	62.44	12.79	15.61	9.16

### 4.12.3 Thermal gravimetric analysis of nanohydrogels

Thermal behaviour of the synthesized nanohydrogel was analysed using TGA and the results are illustrated in **Figure 4.21**. Thermogravimetric analysis of N, NG, NL and NM hydrogel was performed as a function of weight loss (%) versus temperature. TGA curve reveal the thermal stability of the dry nanohydrogels. As can be seen from **Figure 4.21**, three stages of weight loss are observed for all the nanohydrogels. The initial weight loss of 11.85%, 15.39%, 9.847% and 5.975% from N, NG, NL and NM respectively can be related to the evaporation of entrapped water molecules causing the dehydration from the polymer (Yu *et al.* 2015; Alper and Nuran. 2016).

The second weight loss of 60.27% for N, 53.612% for NG, 62.069% for NL and 64.925% for NM between 205.85 °C to 424.21 °C is due to the cleavage of the side-chain (-N(CH<sub>2</sub>CH<sub>3</sub>)) from PDEA, also the decomposition of oxygen-related functional groups and amides from the polymer matrix (Jin *et al.* 2014; Nuran and Hacer, 2018). The weight loss from NG, NL and NM nanohydrogels at temperatures of 205.85 °C to 424.21 °C region are due to the decomposition of functional groups containing O<sub>2</sub> such as amide, carbonyl, carboxyl, epoxy and hydroxyl groups from the polymer matrix and GQDs (Huang *et al.* 2016).

## RESULTS AND DISSCUSSION

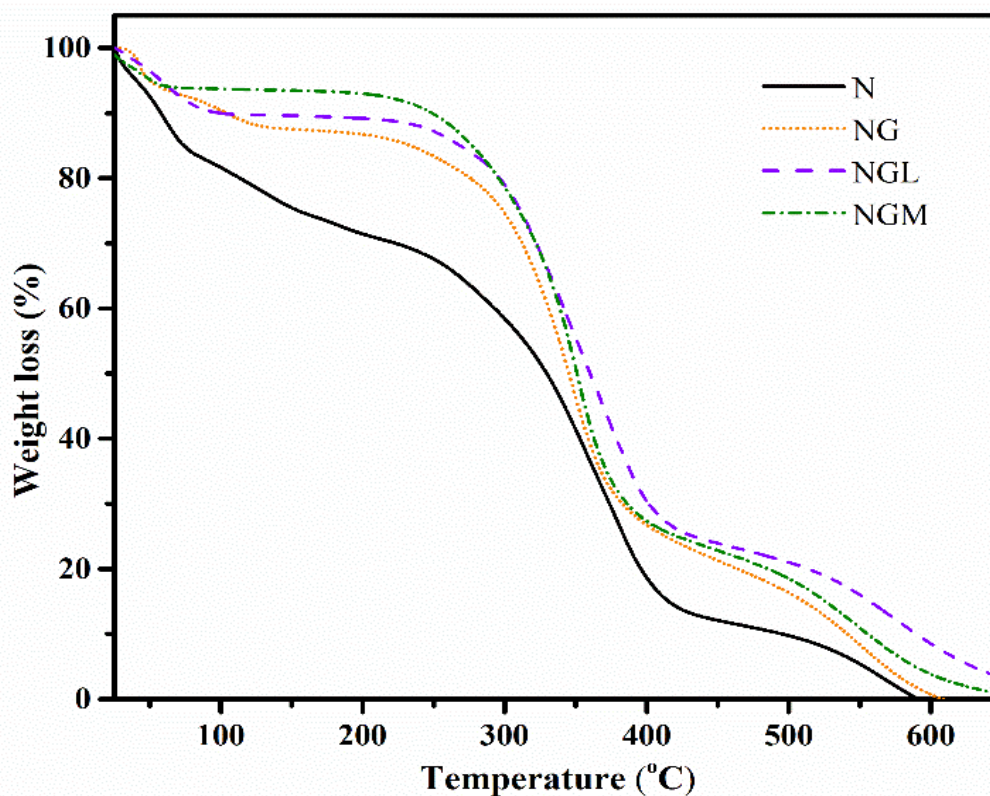


**Figure 4.21: TGA thermogram of PDEA nanohydrogels**

Final weight loss of 25.77% from N, 13.418% from NG, 23.776% from NL and 25.386% from NM weight loss are ascribed to the decomposition of carbon material and polymer backbones in PDEA and GQDs incorporated PDEA. 50% weight loss was observed at a temperature of 388.94 °C for N, 326.59 °C for NG, 357.38 °C for NL and 350.33 °C for NM which reveals that polymer is more thermally stable. The improved thermal resistance is due to combination of more covalent bonding through MBA as a cross-linker in PDEA (Alper and Nuran. 2016). The presence of GQDs in PDEA showed slower weight loss with stepwise degradation indicating that the GQDs affect the stability of the PDEA.

### 4.13 Studies on nanohydrogels degradation

Degradation studies were done over a period of 11 weeks, and immutability of degradation attained was used as a sole factor for termination of the experiment as shown in **Figure 4.22**. The sample N showed a maximum degradation of 84.95%. Constant degradation rate was observed from 8<sup>th</sup> week, and also showed a sudden



## RESULTS AND DISCUSSION

exponential degradation from 3<sup>rd</sup> week. Maximum degradation was observed between 3<sup>rd</sup> to 7<sup>th</sup> week after which stability was achieved. NG showed persistent degradation pattern in contrast to N. The NG showed a sudden spike in the degradation from 1<sup>st</sup> to 3<sup>rd</sup> week. Succeeding 3<sup>rd</sup> week, a steady increment was contemplated till 8<sup>th</sup> week followed by the regular pattern of degradation.

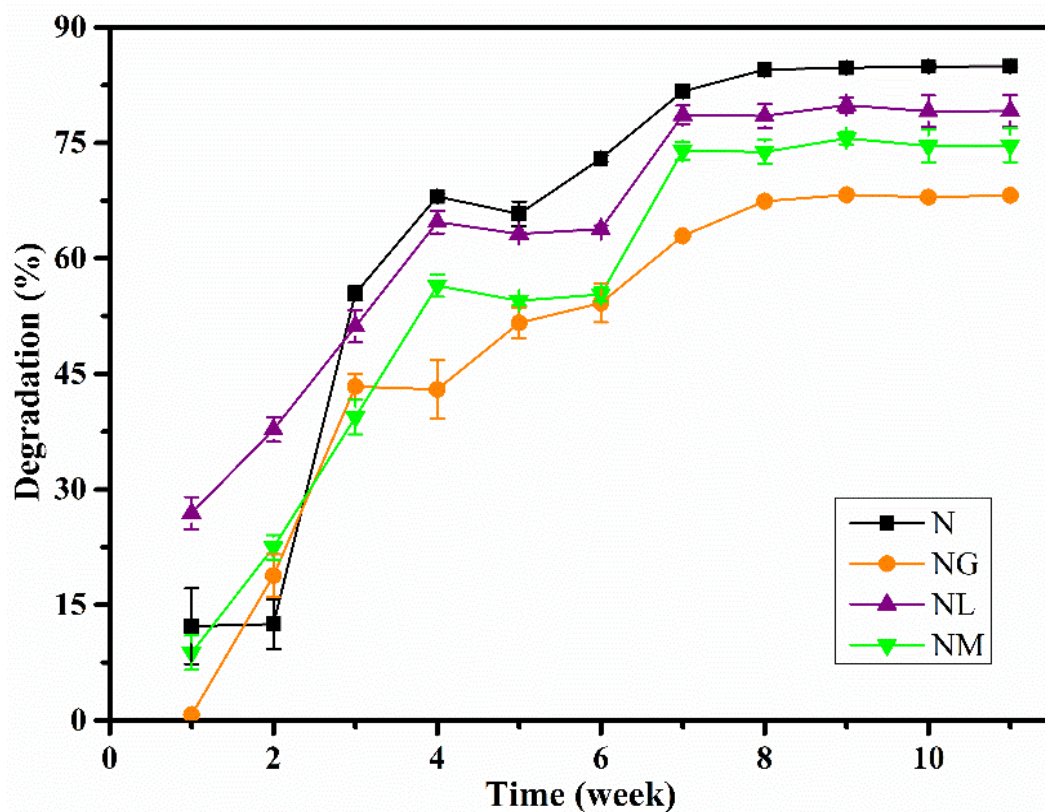


Figure 4.22: Degradation of nanohydrogels in PBS buffer

Maximal degradation venerated to N was also reduced and noted to be 68.17% for NG. Degradation could be ascribed to the presence of hydrolytic groups like ester, amine which break down easily by water (Jafari and Kaffashi. 2015). Supposedly, the difference in degradation could be accredited to the presence of hydrophilic moieties in NG, the formation of hydrogen bond between water and GQDs provides stability and thus, degradation becomes arduous. An assumable difference in degradation profiles of NG and NL/M could be due to propinquity of hydrophobic factions, i.e., leucine and methionine.

## RESULTS AND DISCUSSION

### 4.14 Doxorubicin loading and *in-vitro* release behaviour from nanohydrogels

The encapsulation efficiency (EE) and loading capacity (LC) of all the four polymers were recorded as shown in **Table 4.13**. It was observed that a distinct decrease in EE and LC as graphene quantum dots were grafted in nanohydrogels. There was two-fold declination in LC after functionalization, and this decline was associated with the increase in the molecular weight of polymers as moieties of graphene quantum dots were grafted in PDEA nanohydrogels. This could be explained by a non-analogous dispensation of the drug inside a nanohydrogel structure (Preethi *et al.* 2010).

**Table 4.13: Percentage of DOX encapsulation and loading into nanohydrogels**

Sample ID	Encapsulation efficiency (EE) (%)	Loading capacity (LC) (%)	LCST (°C)
N	85.873	0.2577	28-30
NG	41.220	0.1237	36-38
NL	41.692	0.1251	40-42
NM	47.350	0.1421	32-34

The response of nanohydrogels at different temperatures was studied to know the LCST of the nanohydrogels as shown in **Figure 4.23**. From the figure, it was observed that there is a significant change in release rate with respect to change in temperature. It was observed that below LCST, the response of hydrogel was weak compared to the response above LCST. The hydrophilic nature of hydrogel could be the reason for poor response rate below LCST (Maheshwari *et al.* 2014). Further increase in temperature has increased the release rate of the loaded drug.

The effect of drug release profile from the polymeric matrix with respect to time at three different temperatures, i.e., at 30 °C, 37 °C and 40 °C is shown in **Figure 4.24 (a-c)**. The cumulative release of DOX (30ppm) from samples N, NG, NL and NM was analyzed at physiological pH of 7.4 in PBS buffer by mimicking the body pH and elevated body temperatures attained during diseased conditions. Maximum release observed at 40 °C for all the nanohydrogels were N-85.98%, NG-86.35%,



## RESULTS AND DISCUSSION

NL-80.12% and NM-58.78% as shown in **Figure 4.24c**. Increase in the release of loaded drug at elevated temperature was due to change in LCST of the hydrogel that has caused the reversible phase transition. Below LCST, the polymer is hydrated but once LCST is exceeded, polymeric chains disintegrate and aggregate abruptly and thus, nanohydrogel shrinks drastically (Fundueanu *et al.* 2017).

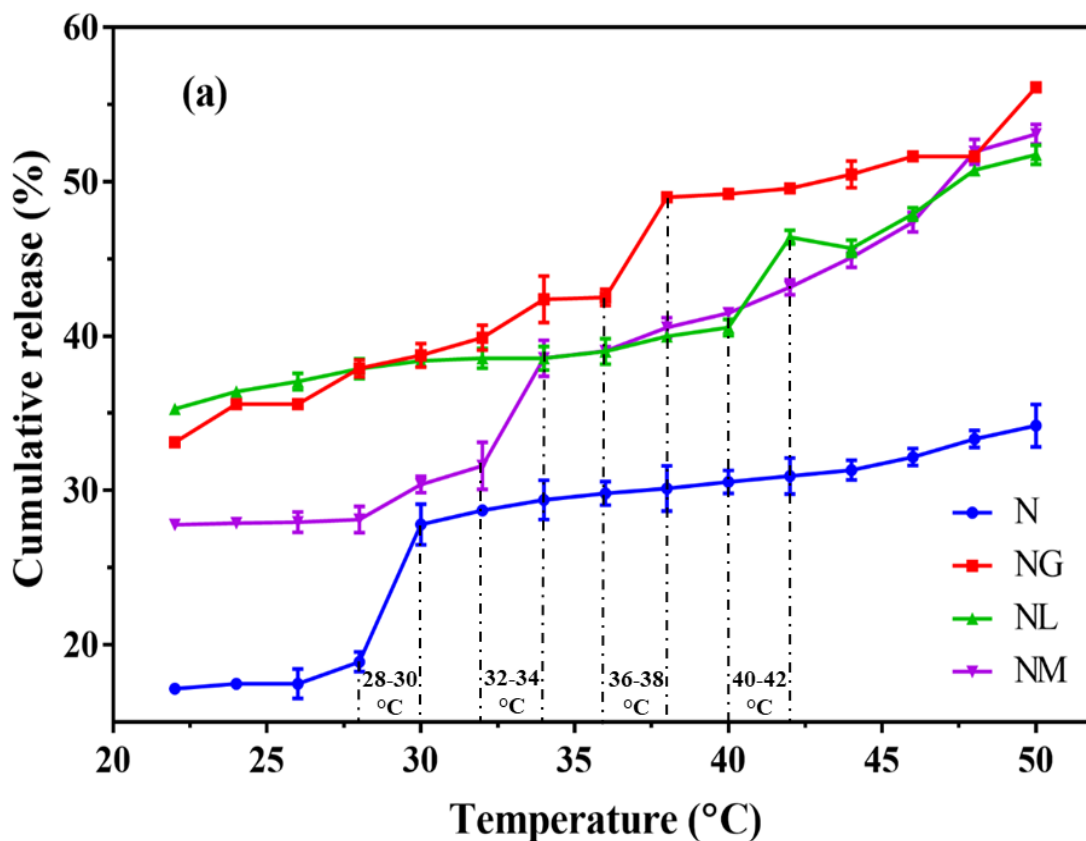


**Figure 4.23: Cumulative release (%) of PDEA nanohydrogels with varying temperature from 22 °C – 50 °C**

The sample N exhibited a controlled release up to 120 min at 40 °C, then attained a plateau presenting a steady release. Incorporation of GQDs showed a clear difference in the release profile of NG and it manifested a slower and controlled release expanding over a period of 480 min, also slightly higher than N. This phenomenon can be attributed to the incorporation of hydrophilic GQDs moieties in the hydrogel (Liu *et al.* 2015; Kuo *et al.* 2016). Further, GQDs could be able to prevent mesoporous leaking of DOX from nanohydrogel by lowering the rate of

## RESULTS AND DISSCUSSION

release. Higher temperature (40 °C) can weaken strength of the chemical bond between the polymer molecules and shrink the matrix resulting in its dissociation of DOX from the polymer and accelerating DOX release (Yao *et al.* 2017). Presence of GQDs in the polymer is beneficial as it possesses anticancer properties and it also able to enhance the activity of DOX (Sui *et al.* 2016; Wang *et al.* 2013). Leucine functionalized GQDs (NL) had a similar effect on the release profile as NG, although methionine functionalized GQDs (NM) did not show a satisfactory release profile. NM showed a burst DOX release in 30 min and remained relaxed throughout the rest of the experiment. The reason for this phenomena is the hydrophobic nature of methionine (Wolfenden. 2007) that has lowered the LCST of nanohydrogel favouring non-uniform burst release profile.

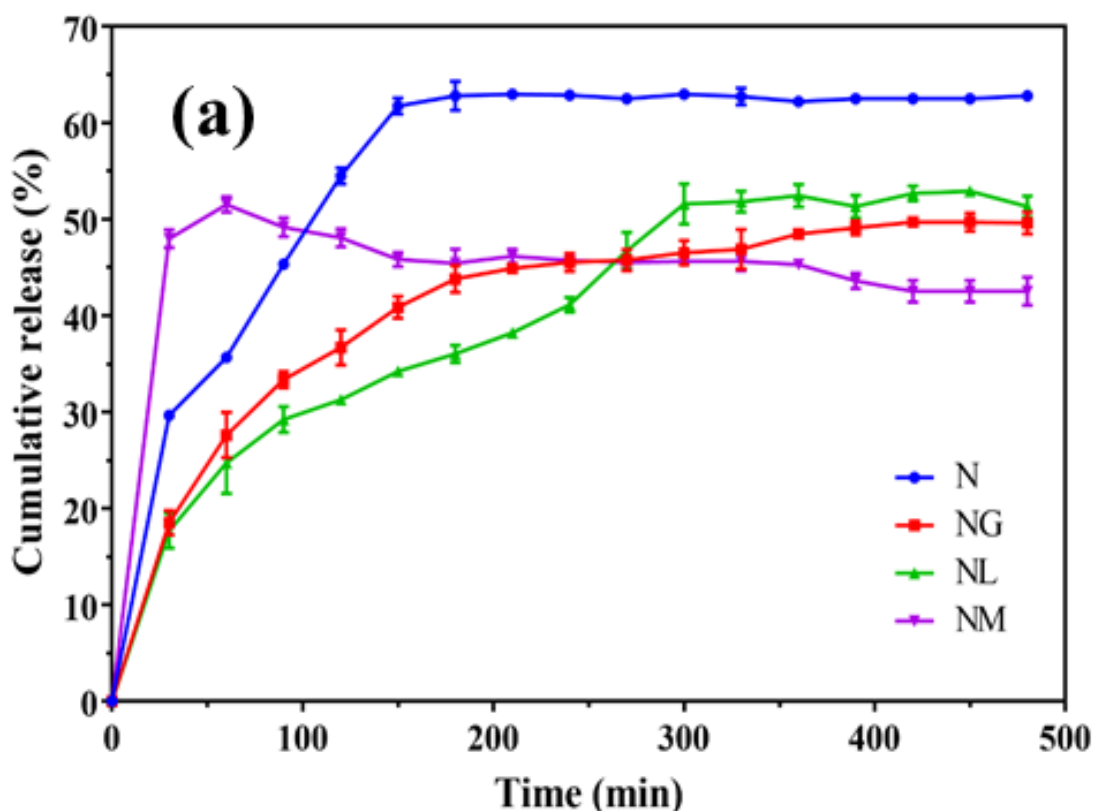
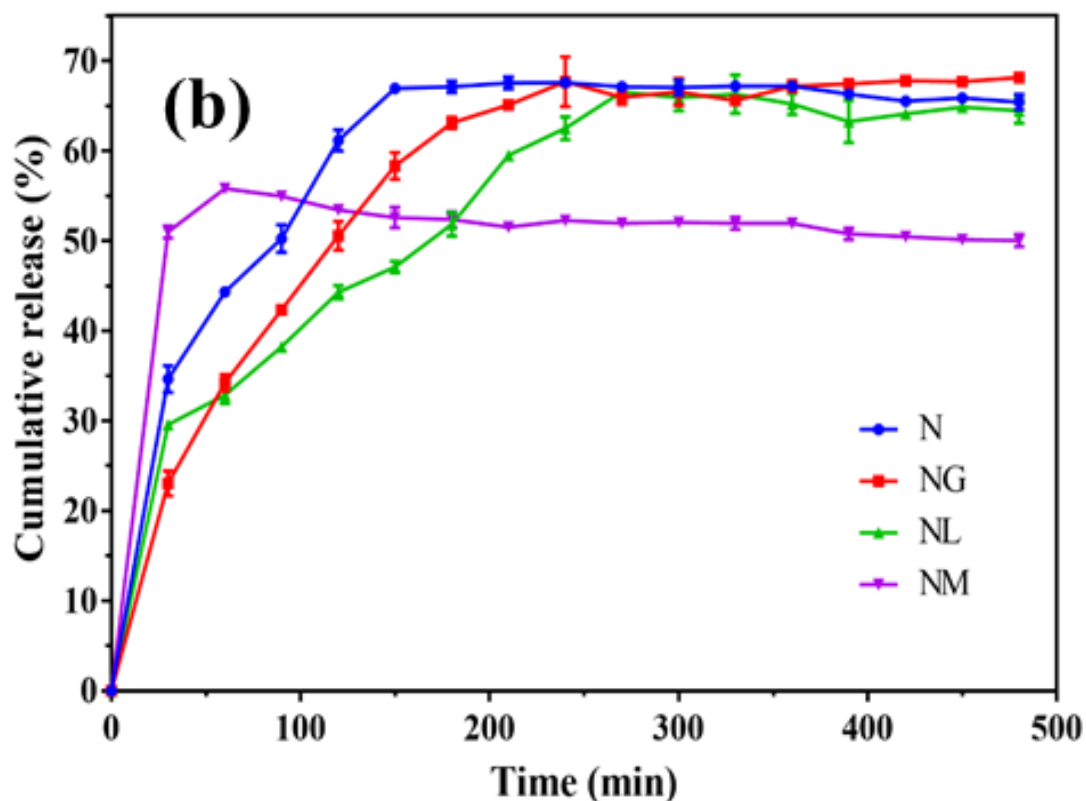


Figure 4.24: Cumulative release (%) of PDEA nanohydrogels with varying time interval (a) at 30 °C

## RESULTS AND DISCUSSION



**Figure 4.24: Cumulative release (%) of PDEA nanohydrogels with varying time interval (b) at 37 °C**

Further, at 37 °C the release of DOX from nanohydrogels was inferior as compared to 40 °C, i.e., 65.40% for N, 68.16% for NG, 64.47% for NL and 54.94% for NM as shown in **Figure 4.24b**. The N showed an upsurge release and became steady after 150 min, whereas NG and NL showed a more controlled elevated release up to 250 min and 300 min respectively. An abrupt and non-significant release of DOX was observed in NM, in contrast to 40 °C. Release studies at 30 °C exhibited a reduction of release as compared to 37 °C and 40 °C, as shown in **Figure 4.24a**. The release profile of nanohydrogels had a maximum release of 62.81% for N, 49.60% for NG, 51.34% for NL and 51.52% for NM. The NG, NL and NM showed a controlled and uniform release than N due to the change in their LCST (Liu *et al.* 2015). As the experiment progressed, the release profiles were accompanied by absorption and desorption of the drug which was due to re-absorption of DOX and induced precipitation in PBS buffer and degradation of free DOX via hydrolysis (Xu

## RESULTS AND DISSCUSSION

*et al.* 2017). These outcomes were further confirmed with mathematical modeling.

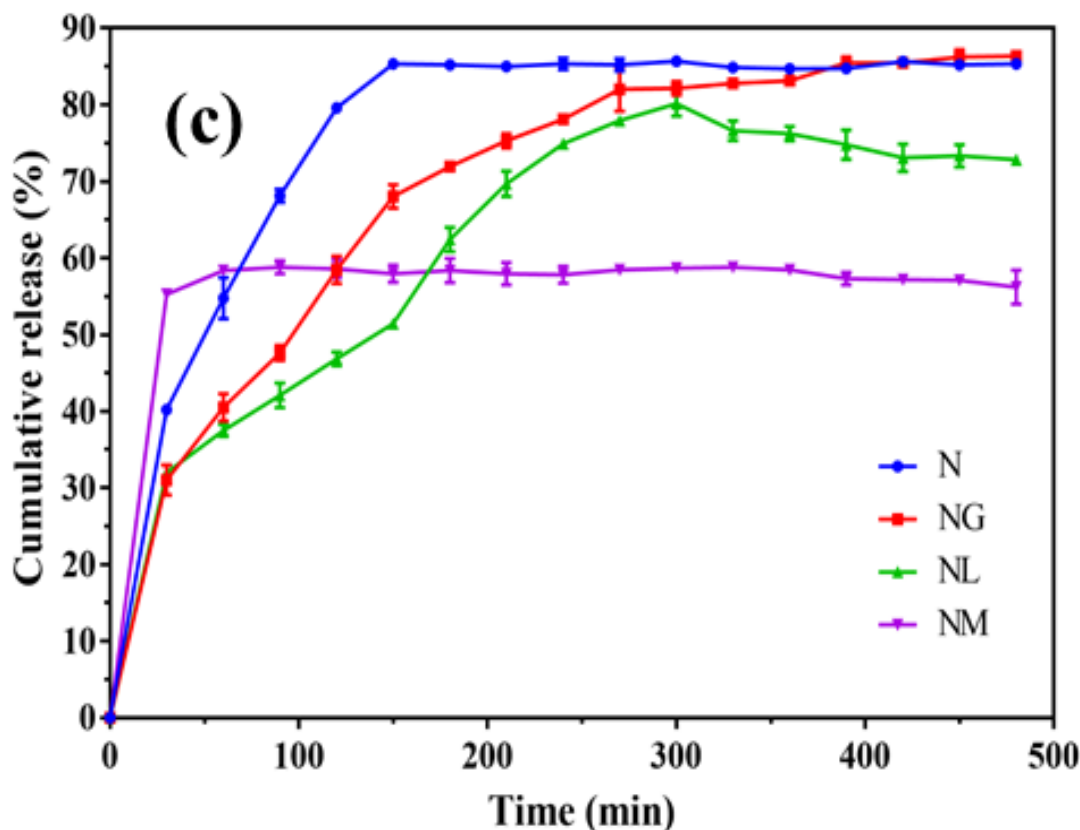


**Figure 4.24: Cumulative release (%) of PDEA nanohydrogels with varying time interval (c) at 40 °C**

### 4.15 Mathematical modelling of PDEA nanohydrogels

Mathematical modeling of drug release from a carrier is often attempted to describe the possible release mechanism (Yajing *et al.* 2015). The release data were fitted in zero-order, first-order, Higuchi, Korsmeyer-Peppas and Hixon-Crowell models to evaluate the DOX release mechanism which is tabulated in **Table 4.14**. The appropriate model was selected on the criterion of ideal fit by regression coefficient (R) values. The R values of zero-order, first-order, Higuchi, Korsmeyer-Peppas and Hixon-Crowell models at different release temperatures are given in **Table 4.14**. Value of R was found to be higher for zero-order release rate constant for sample N than those of first-order, Higuchi and Hixon-Crowell release rate constant. Thus, it imputed the fact that DOX release from the sample at different temperatures followed first-order release kinetics.

## RESULTS AND DISCUSSION

While in the Higuchi model, the R-value at different temperatures implies the diffusion-controlled drug release mechanism. Similarly, in Hixon-Crowell model, the R-value at a different temperature is due to change in surface area and diameter of nanohydrogels.

**Table 4.14: DOX release kinetics of PDEA nanohydrogel (zero order kinetic, first-order kinetic, Higuchi model, Korsmeyer-Peppas model and Hixon-Crowell model) at a different temperature.**

Sample ID	Temperature (°C)	Zero-order kinetic		First order kinetic		Higuchi model		Hixon Crowell model	
		k <sub>0</sub>	R <sup>2</sup>	k <sub>1</sub>	R <sup>2</sup>	k <sub>2</sub>	R <sup>2</sup>	k <sub>4</sub>	R <sup>2</sup>
N	30	0.277	0.993	-0.00226	0.98259	4.8745	0.96661	8.90E-04	0.98802
	37	0.271	0.988	-0.00249	0.98292	4.81045	0.97961	9.42E-04	0.98724
	40	0.384	0.971	-0.00522	0.99266	6.88795	0.99389	0.00171	0.99529
NG	30	0.13316	0.98178	-9.07E-04	0.99062	2.38313	0.99674	3.79E-04	0.98815
	37	0.24584	0.98876	-0.00214	0.99667	4.38272	0.99354	6.93E-04	0.99584
	40	0.27779	0.97573	-0.00289	0.98115	4.94255	0.97519	8.20E-04	0.98156
NL	30	0.13206	0.92413	-7.81E-04	0.94249	2.39861	0.97666	2.70E-04	0.9367
	37	0.15474	0.9819	-0.0011	0.98019	2.73083	0.96013	3.57E-04	0.98107
	40	0.16082	0.99855	-0.00121	0.9989	2.85317	0.9905	3.86E-04	0.99955
NM	30	- 0.02568	0.13181	2.16E-04	0.12186	- 0.39001	0.00542	-6.92E- 05	0.12515
	37	0.00285	-0.3266	-2.13E-05	- 0.32904	0.1256	- 0.29216	7.14E-06	-0.3283
	40	0.01855	0.15974	-1.86E-04	0.15377	0.37634	0.30768	5.63E-05	0.15575

In the Korsmeyer-Peppas model, the general classification of diffusion from the polymeric matrix is as follows: if  $n \leq 0.45$ , then the drug release was due to Fickian diffusion (drug diffusion is dominant); if  $n$  is 1, then the drug release was due to the other predominant factors like external stimuli; and if  $0.45 \leq n \leq 1$ , non-Fickian or anomalous release (a synergistic effect of drug diffusion and external stimuli) (Fariba and Ebrahim. 2009; Ronald *et al.* 2012; Yajing *et al.* 2015; Soha *et al.* 2017; Gouda *et*

## RESULTS AND DISSCUSSION

al. 2017). The effect of surrounding temperature on DOX release exponent (n) values are given in **Table 4.15** and the samples (N, NG and NL) showed the Fickian behavior. Due to erratic release in NM nanohydrogels, it could not be fitted in any model.

**Table 4.15: Release exponent (n), correlation coefficient (R<sup>2</sup>) and mechanism of drug release (Korsmeyer-Peppas model) of PDEA nanohydrogels at 30 °C, 37 °C and 40 °C**

Sample ID	Temperature (°C)	Korsmeyer-Peppas model			Order of release
		k <sub>3</sub>	R <sup>2</sup>	n	
N	30	-3.00221	0.95287	0.46447	Fickian mechanism
	37	-2.62329	0.97635	0.4084	Fickian mechanism
	40	-2.70332	0.99598	0.4805	Fickian mechanism
NG	30	-2.2624	0.99355	0.28468	Fickian mechanism
	37	-2.41219	0.98789	0.38766	Fickian mechanism
	40	-2.21476	0.9632	0.3752	Fickian mechanism
NL	30	-3.09247	0.98476	0.40689	Fickian mechanism
	37	-2.27839	0.93116	0.29973	Fickian mechanism
	40	-2.14823	0.97761	0.29062	Fickian mechanism
NM	30	-0.60475	-0.10931	-0.02732	-
	37	-0.69818	-0.21418	0.01679	-
	40	-0.68381	0.46849	0.03102	-

### 4.16 Biocompatibility studies of nanohydrogels

The cytotoxicity of biomaterials is extremely important for their future applications. The capability of the cells to live in a toxic environment has been the basis of most of the cytotoxicity assays. In this study, the cytotoxicity of the GQDs, T36, HG-4, HL-7 and HM-5 and DOX loaded hydrogels are investigated by MTT assay in B16F10 cell lines. The cell viability was compared with the control group, as shown in **Figure 4.25**.

## RESULTS AND DISCUSSION

It can be observed from **Figure 4.25a** that  $IC_{50}$  value of leucine functionalized GQDs and methionine functionalized GQDs are less than the  $IC_{50}$  value of bare GQDs. From **Figure 4.25b**, it can be observed that bare nanohydrogel (N) has  $IC_{50}$  value of 1000  $\mu\text{g/mL}$ , but the addition of bare GQDs has increased the  $IC_{50}$  value of bare nanohydrogels. Comparably, nanohydrogels grafted with functionalized GQDs has moderately better  $IC_{50}$  value which indicates that the leucine and methionine functionalization has increased the cytotoxicity of graphene quantum dots (**Figure 4.25b**).

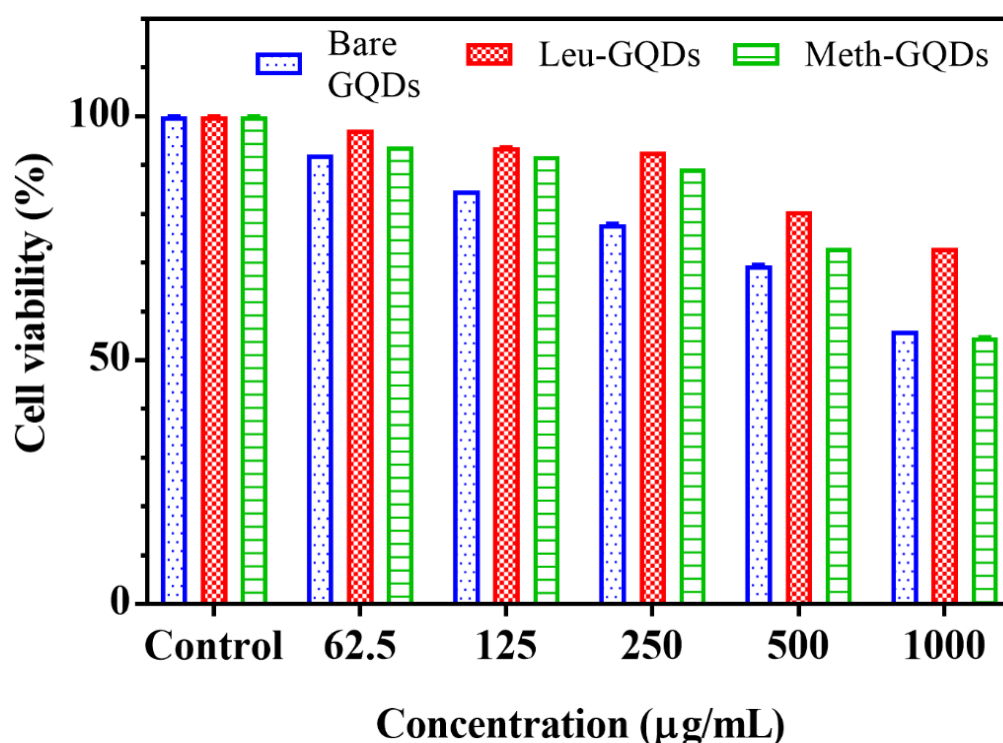


**Figure 4.25:** Percentage of cell viability of B16F10 cells after treatment: (a) with graphene quantum dots

Further, **Figure 4.25c** shows the cell viability of DOX-loaded different nanohydrogels.  $IC_{50}$  of bare GQDs grafted nanohydrogels is more compared to bare nanohydrogels; the addition of leucine functionalized GQDs and methionine functionalized GQDs has slightly reduced the  $IC_{50}$  value. The standard DOX has a very less  $IC_{50}$  value of 0.801  $\mu\text{g/mL}$  similar to literature (Yu *et al.* 2017) and comparably, DOX-loaded nanohydrogels has very high  $IC_{50}$  value. It shows that the nanohydrogels synthesized in present work can be used as a potential DOX carrier in the treatment of melanoma.

## RESULTS AND DISCUSSION

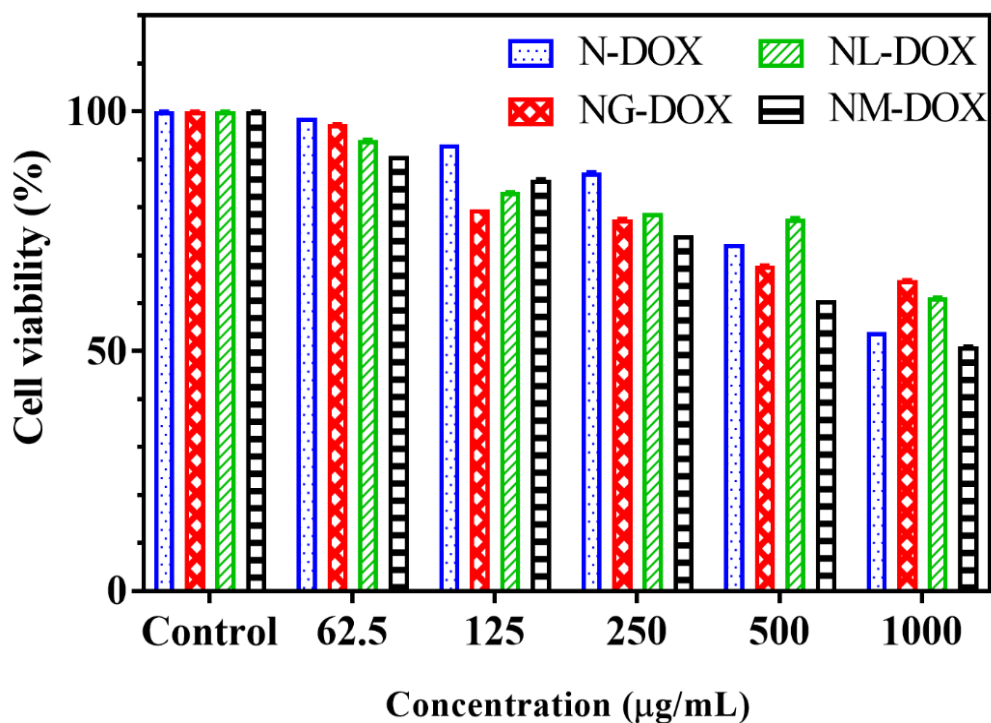
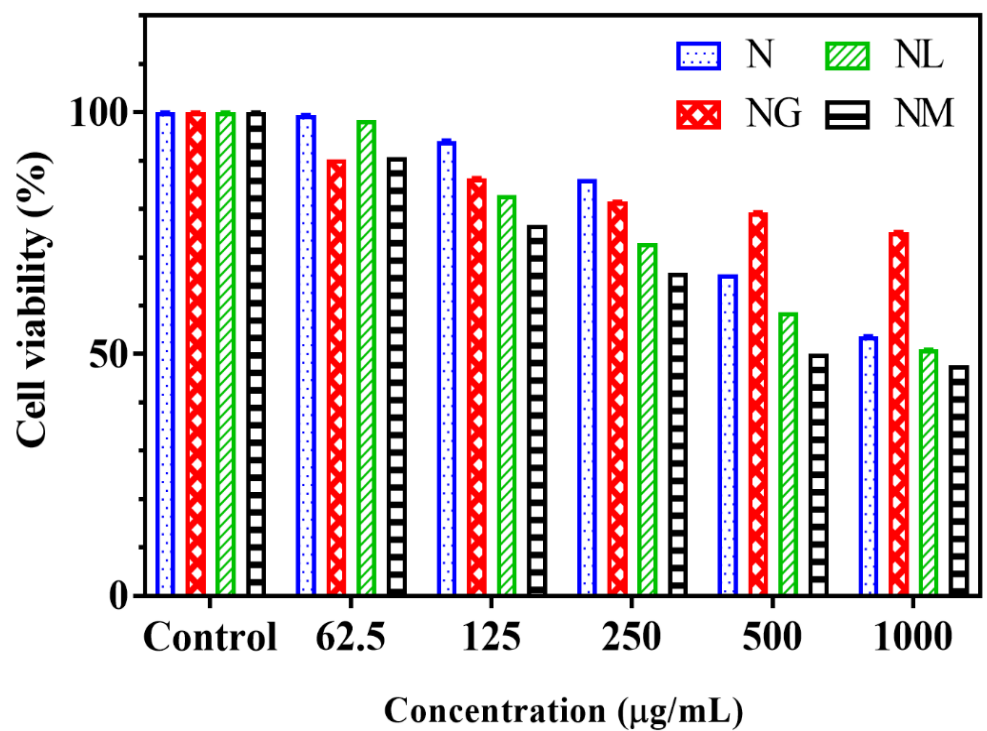


Figure 4.25: Percentage of cell viability of B16F10 cells after treatment: (b) with nanohydrogels (c) with DOX-loaded nanohydrogels



## RESULTS AND DISCUSSION

### PART IV

#### 4.17 *In-vivo* studies on melanoma tumor model and its treatment

The melanoma cells were inoculated in mice through intravenous injection, and the appearance of the tumor was observed after 7<sup>th</sup> day as illustrated in **Figure 4.26**. On the 7<sup>th</sup> day, black colored tumors were observed near the tail region which confirmed the presence of melanoma. The treatment for tumor was performed by administering DOX-loaded nanohydrogels via intraperitoneal route. The fixed therapeutic dosage was injected once a week for up to four weeks. The mice were observed for the effectiveness of the injected DOX-loaded nanohydrogels for cancer treatment.



**Figure 4.26: Fabrication of melanoma model via intravenous injection (tail vein) using B16F10 cell lines in C57BL6 mice. (a-c) demonstrating intravenous injection of B16F10 cell lines; (d-f) showing the appearance of tumor on the 7<sup>th</sup> day after injection.**

## RESULTS AND DISSCUSSION

### 4.18 Therapeutic effect on change in body weight, organ weight, and tumor count

The body weight of the mice was assessed regularly for evaluation of systemic toxicity before injecting the weekly booster dose (**Figure 4.27**). In the normal control group injected with PBS showed periodic weight gain, whereas, other groups experienced non-periodic weight gain and loss of weight. Mice injected with DOX experienced weight due to cachexia. Similarly, N loaded with DOX showed weight loss, but recovered at the end of the experiment. Other groups did not manifest any difference w.r.t to normal and disease groups. There were no eloquent changes recorded overall; thus body weight was considered as a non-significant factor in treatment groups. However, disease group showed the melanoma-related symptom.

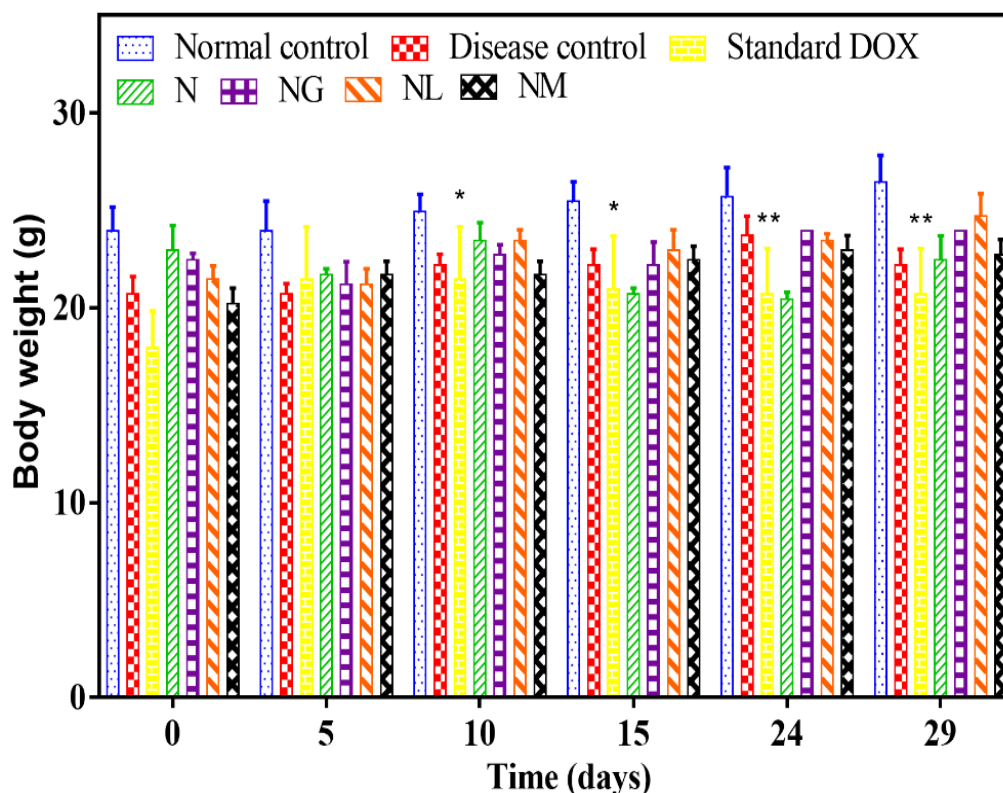


**Figure 4.27: Measured body weight of mice wrt time before inducing therapeutics**

After the mice were euthanized on the 29<sup>th</sup> day, all organs were removed and weighed (**Figure 4.28**) as it may indicate some toxic effect. DOX group showed

## RESULTS AND DISCUSSION

significant hepatomegaly, but effect of DOX was reduced by the DOX-loaded nanohydrogels (Agrawal *et al.* 2017). Disease group had shown significant hepatomegaly and splenomegaly. As per literature, splenomegaly is the hallmark of melanoma (Kamran *et al.* 2018). Spleen is the largest immune organ, which plays a cardinal role in the recirculation of lymphocytes. Enlarging of the spleen can be explicated to confinement of T lymphocytes in the spleen during lymphocyte recirculation (Fang *et al.* 2014). Therapeutic dose injected groups (group III-VII) displayed a considerable decrease in spleen weight w.r.t disease group, which showed the curing of splenomegaly. Although a decrease in kidney weight was observed, this dissentious result was not treated in any group.

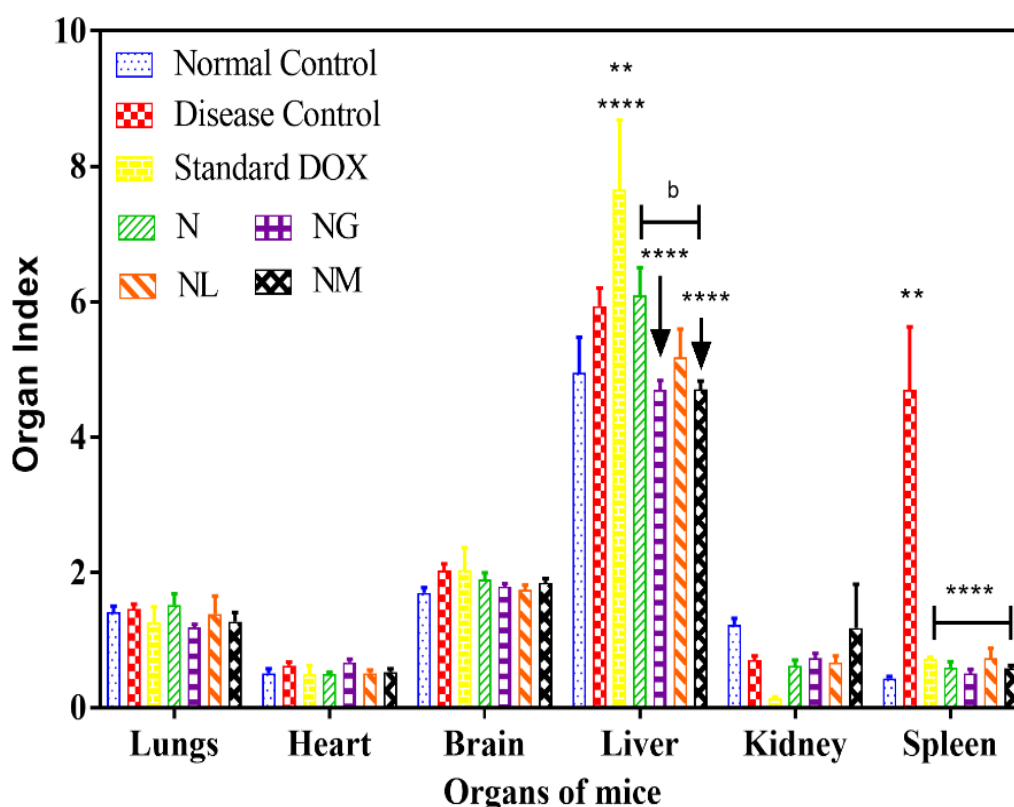


**Figure 4.28: Organ weight index of mice after euthanization.**

The maximum reduction in tumor count was observed in DOX injected mice, as shown in **Figure 4.29**. A pronounced reduction of tumor count was observed in DOX-loaded N and NG groups in comparison with the disease group (Jun *et al.* 2001). However, DOX-loaded NL and NM were unable to subdue the metastatic

## RESULTS AND DISSCUSSION

effect of cancer, probably because of increased LCST value and erratic release profile. There was no significant difference in tumor count of drug present in free or entrapped state. Thus, it deduced an interesting fact that neither of the nanohydrogels altered DOX chemically or physically, indeed allowed effortless release with induction of stimuli. It was comprehended that nanohydrogels were exemplary and faultless drug carriers.

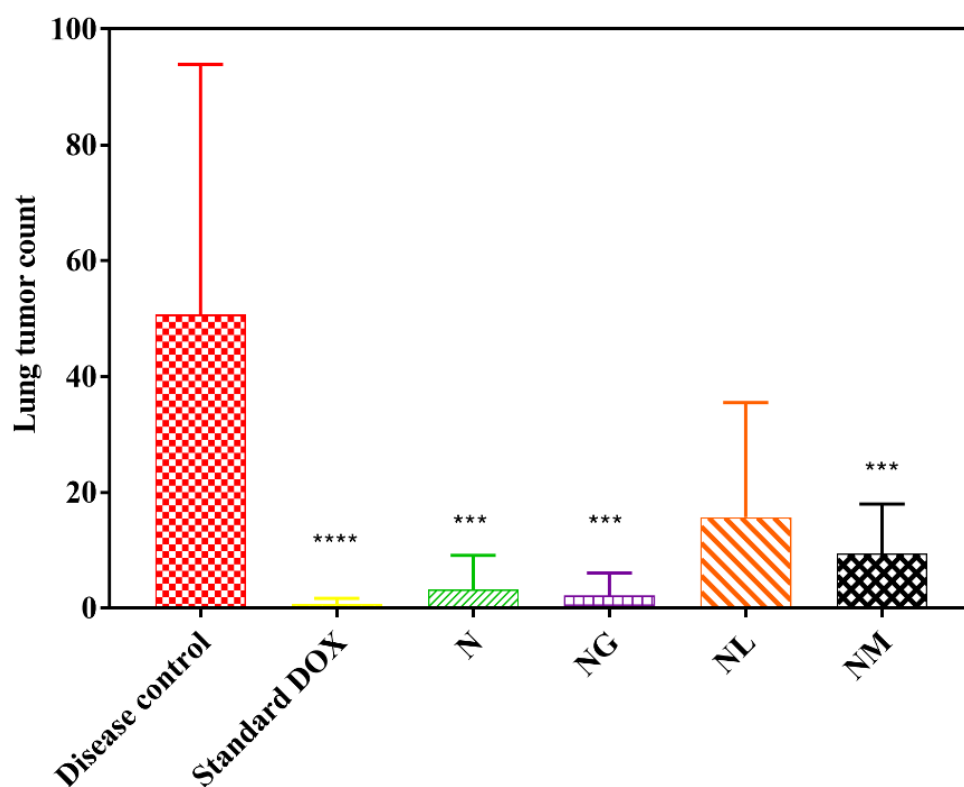


Figure 4.29: Metastatic count of lungs of mice after euthanization.

### 4.19 Evaluation of hematological parameters

The hematological framework is contemplated as a principle indicator of cancer development and prognostic factor for the positive or negative outcome (Rochet *et al.* 2012). **Figure 4.30** shows the effect of cancer on blood parameters. Diseased group showed notable lymphopenia (**Figure 4.30a**), thrombocytopenia (**Figure 4.30e**) and blood cell showed anemic conditions they are red blood cells (**Figure 4.30b**), haemoglobin (**Figure 4.30c**), hematocritic (**Figure 4.30d**). The above anomalies demonstrate poorer prognosis in diseased group which was administered

## RESULTS AND DISCUSSION

with PBS buffer alone (Rochet *et al.* 2012). Foundation of lymphopenia in melanoma is not well illuminated, but one of the reasons could be uninterrupted apoptosis of T lymphocyte caused by tumors (Kou *et al.* 2016). The anemic disorder can be attributed to many factors, like insufficiency of iron, hemolysis, damaged erythropoiesis, tumor cell annexation in erythropoietic environment and initiation of clotting torrent (Kim *et al.* 2014).

Imputation of thrombocytopenia (**Figure 4.30e**) can be associated with melanoma as tumor cells can trigger and agglomerate platelets that aggravate metastatic aptitude. Stimulation of platelets facilitates cell attachment, multiplication and chemotaxins, in turn promote tumorigenesis (Franco *et al.* 2015).

Effect of DOX on hematological parameters was identified in group III and it showed leukopenia. Leukopenia is a biological measurement of drug activity associated with the hematologic toxicity caused by drugs to predict the efficiency of the treatment (Liu *et al.* 2013). The above parameter was observed by a significant reduction in white blood cells (**Figure 4.30f**). Anemic conditions depicted by the disease model were recovered, but it is significantly different than normal (PBS injected) conditions, and similar results were observed in the literature (Desai *et al.* 2013). Nanohydrogel (N) loaded DOX-treated group IV exhibited significant monocytopenia (**Figure 4.30h**) and recovered from anemia, but recovery was less than the normal control group. The condition of monocytopenia and differentiation of myeloid progenitors was reduced which signifies an improvement in tumor conditions, and additionally it is a positive prognostic factor (Rochet *et al.* 2012). NG nanohydrogels loaded DOX (group V) revealed monocytopenia (**Figure 4.30h**). Rehabilitation of anemic conditions was similar to DOX and N loaded DOX nanohydrogels (group IV). NL nanohydrogels loaded DOX (group VI) showed only monocytopenia (**Figure 4.30h**), and anemic condition was not recovered. Hematological parameters were distinguishable as compared to disease group but dissimilar to the normal group. NM group dispensed granulocytopenia (**Figure 4.30g**), monocytopenia (**Figure 4.30g**) and rose in the number of hemoglobin (**Figure 4.30c**) w.r.t disease group, all the above conditions favoured better survival rate (Rochet *et al.* 2012).

## RESULTS AND DISSCUSSION

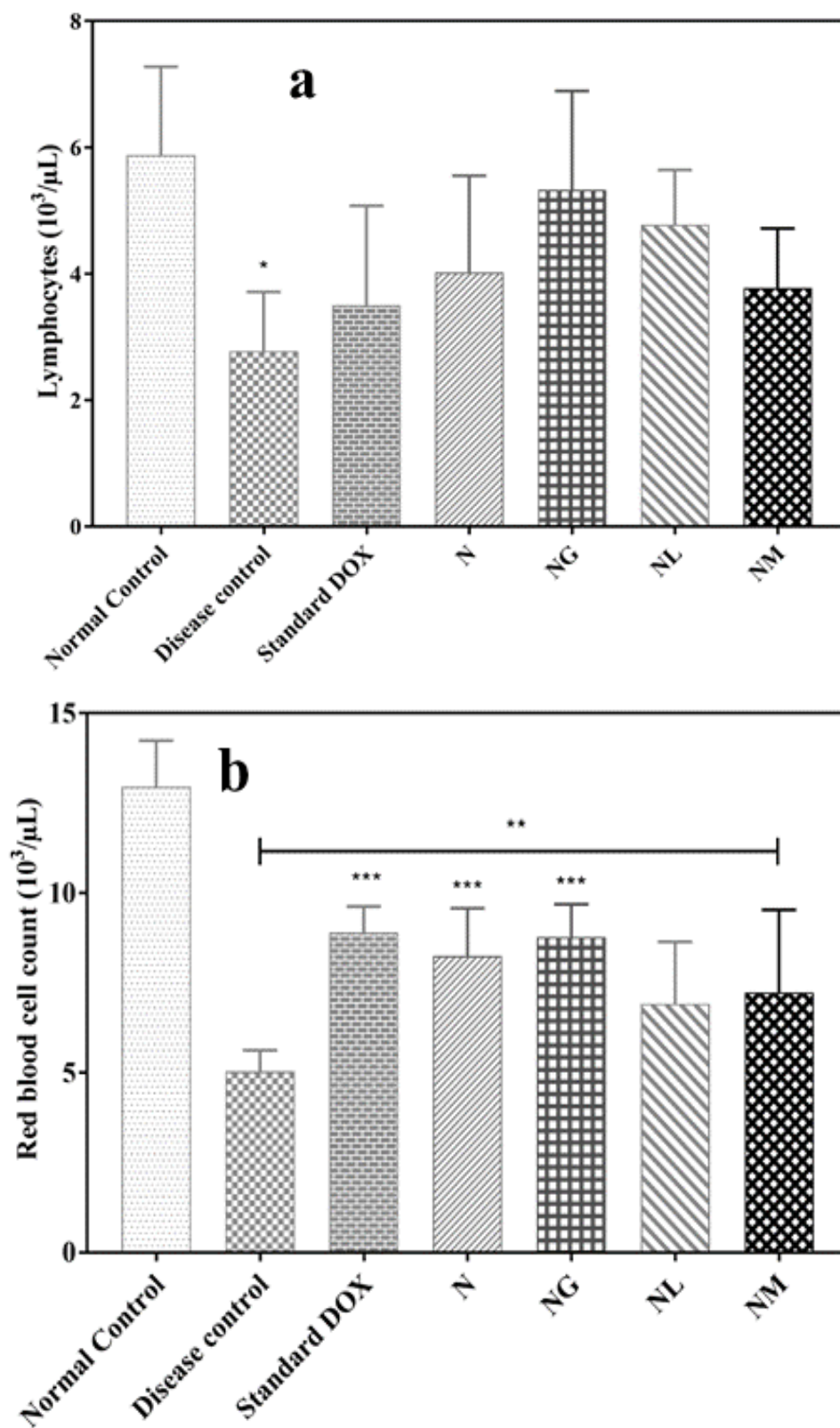


Figure 4.30: Estimation of hematological parameters after blood collection:  
(a) Lymphocyte count; (b) Red blood cell count



## RESULTS AND DISCUSSION

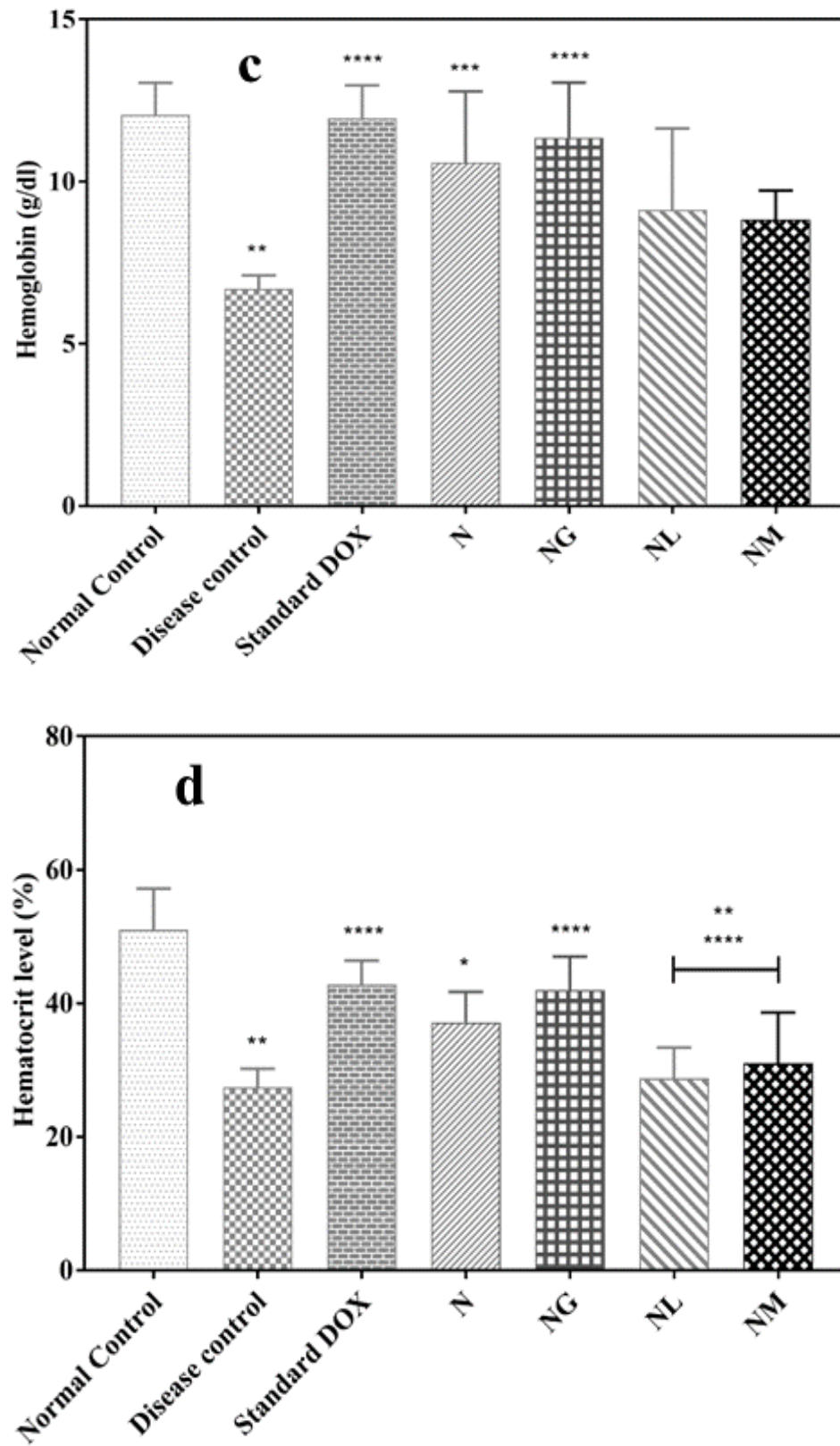


Figure 4.30: Estimation of hematological parameters after blood collection:  
(c) Hemoglobin count; (d) Hemocritic count

## RESULTS AND DISCUSSION

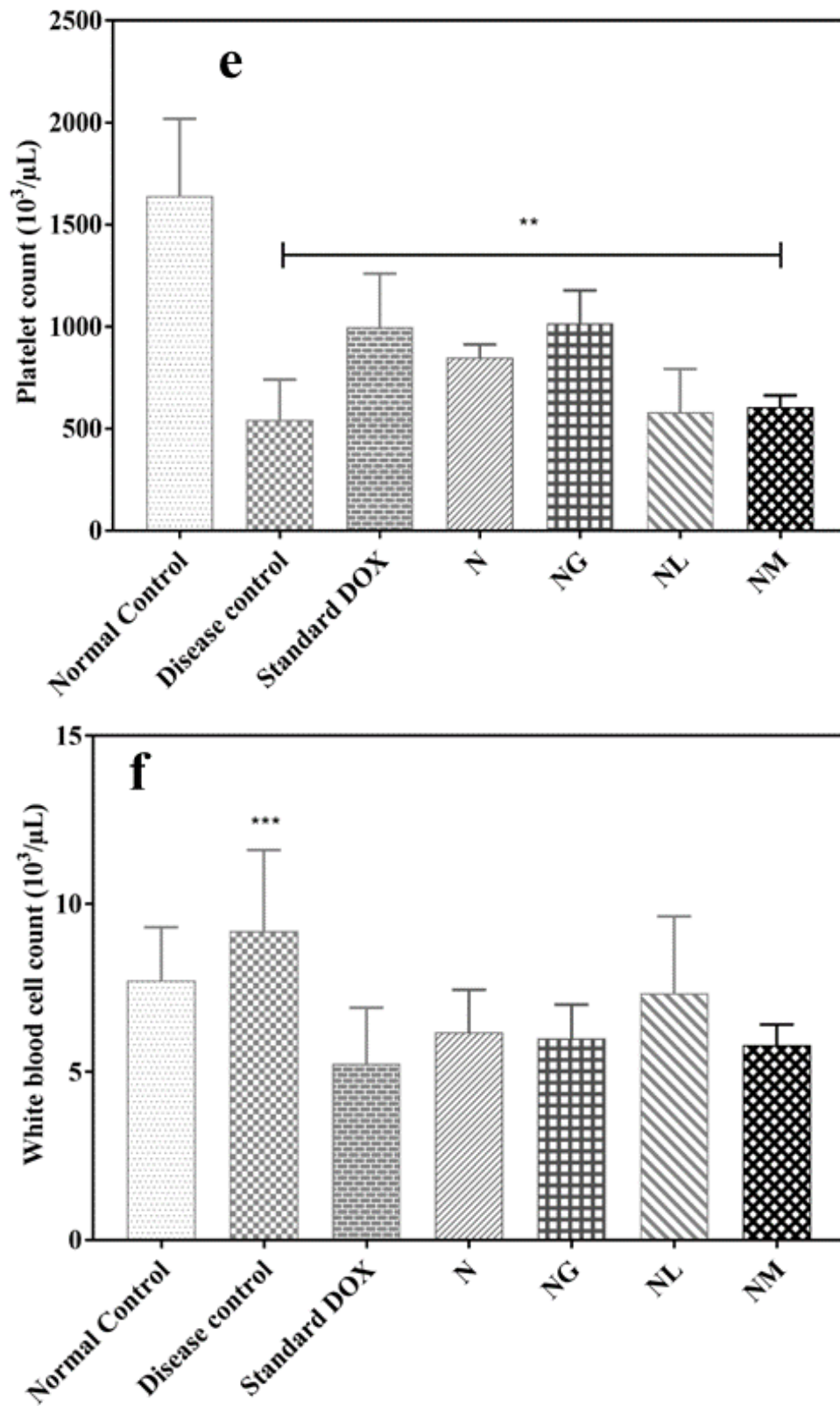


Figure 4.30: Estimation of hematological parameters after blood collection:  
(e) Platelet count; (f) White blood cell count



## RESULTS AND DISCUSSION

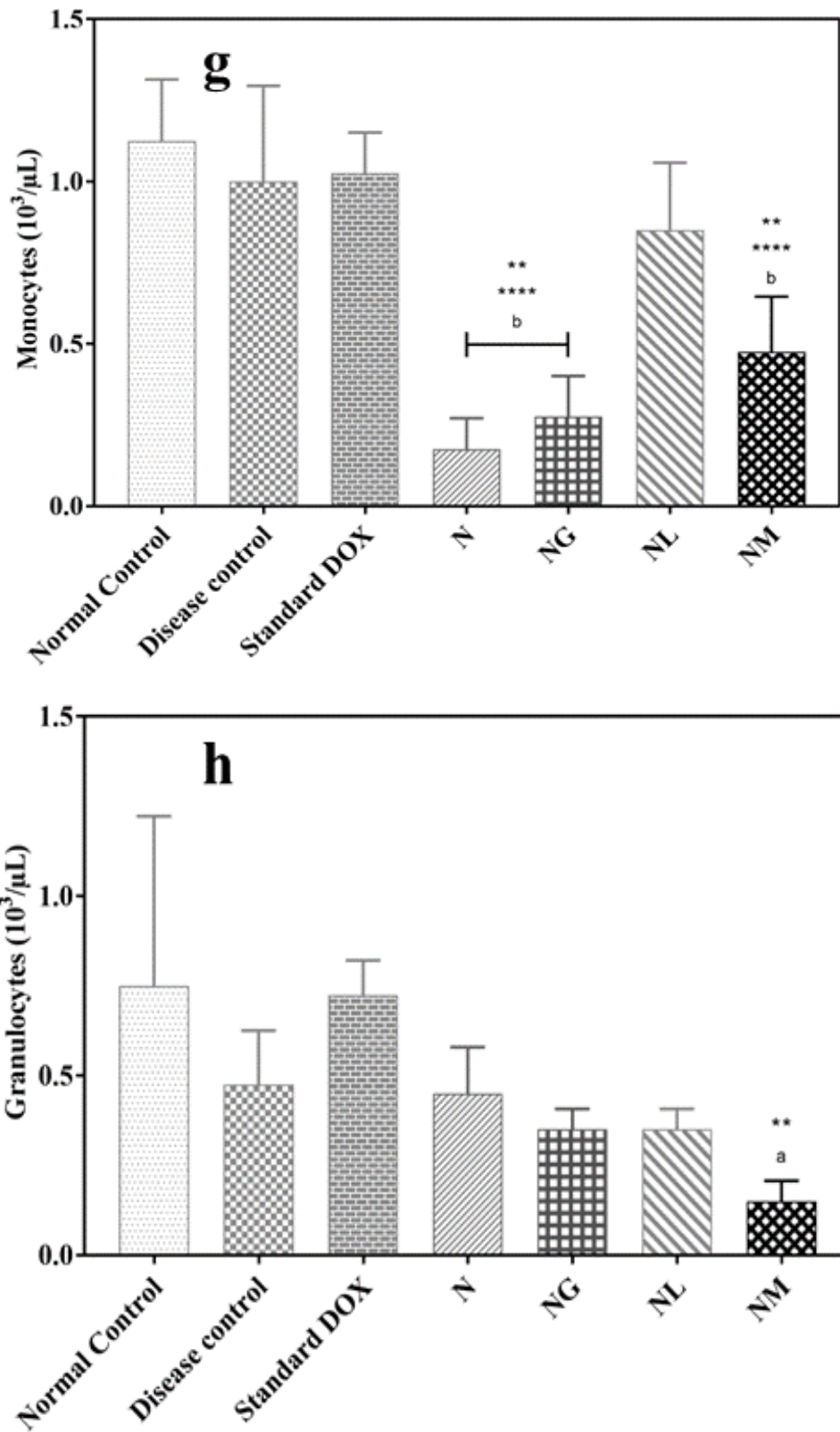


Figure 4.30: Estimation of hematological parameters after blood collection:  
(g) Granulocyte count (h) Monocyte count.

## RESULTS AND DISSCUSSION

All nanohydrogels showed a better prognosis factor, i.e. monocytopenia as compared to doxorubicin thus stating a refined anti-tumour activity. Also, showed a positive effect in one or the other aspect, but none of the treatments were able to recover from anemia.

### 4.20 Evaluation of cytokines level: TNF- $\alpha$ and IL-6

Cytokines have an integral role in tumor induction and progression. They can facilitate the generation and maintenance of robust anti-tumor immune responses, but they can also contribute to chronic inflammation and promote tumor formation, growth and metastasis (Brian *et al.* 2012). Among several inflammatory mediators, TNF- $\alpha$  and IL-6 were studied to know the antitumoral effect by nanohydrogels as shown in **Figure 4.31** and **Figure 4.32**. Levels of both TNF-  $\alpha$  and IL-6 cytokine can confirm the biocompatibility and immunogenicity of nanohydrogels.

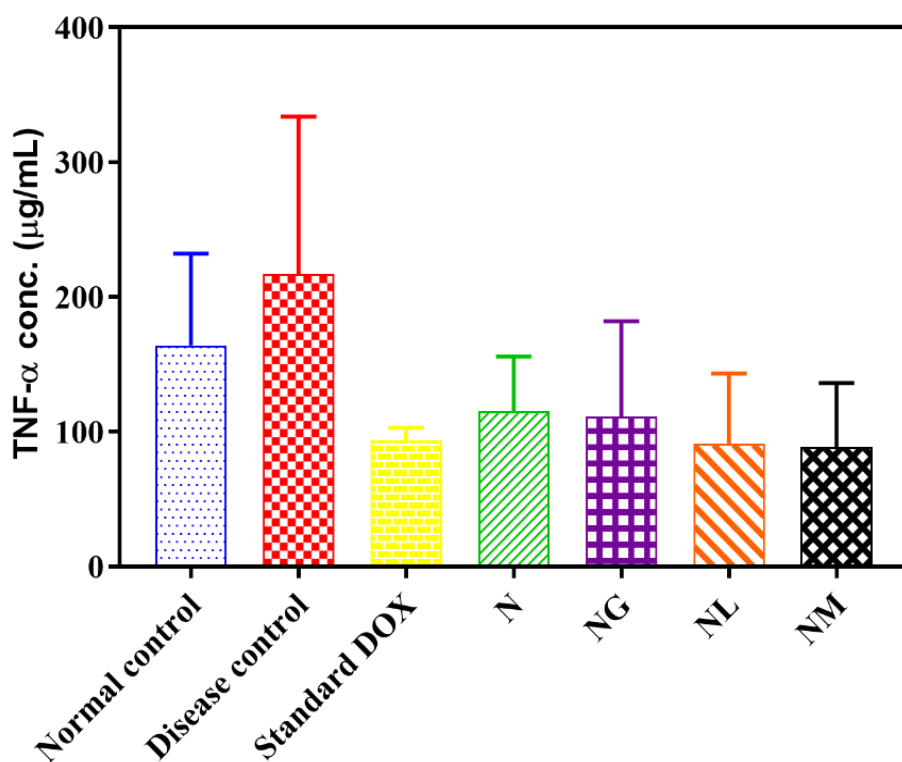


**Figure 4.31: Analysis of cytokine TNF-  $\alpha$  levels from the collected blood plasma of mice**

From the assay of TNF- $\alpha$  (**Figure 4.31**), no significant difference was observed in

## RESULTS AND DISCUSSION

disease and DOX-treated group with normal control. The difference in TNF- $\alpha$  levels in normal and disease control could be attributed to the better production of immunosuppressive environment inducing melanoma cells dedifferentiation. While DOX influence the levels of pro-inflammatory cytokines (TNF- $\alpha$  and IL-6) when functional damage is caused, suggesting its successful treatment (Pecoraro *et al.* 2016). Distinctly, nanohydrogels did not instigate the elevation of TNF- $\alpha$  levels which confirms non-immunogenic nature.

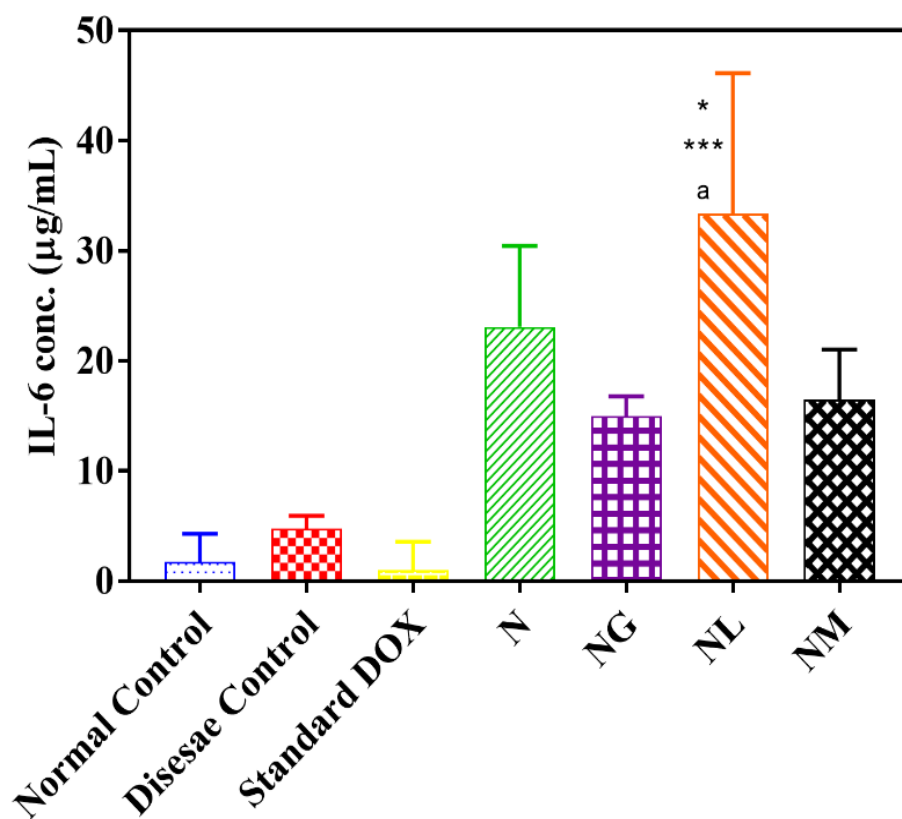


**Figure 4.32: Analysis of cytokine IL-6 levels from the collected blood plasma of mice**

The IL-6 levels (**Figure 4.32**) in disease and DOX as compared to normal were not crucially different. The outcome of disease control could have imputed to the attainment of an advanced stage of melanoma that has successfully evaded immune response through the resistance strategies as stated above. Indisputably, NL nanohydrogel was immunogenic as there was a significant increase in IL-6 levels in comparison with normal, disease and DOX controls. However, all other

## RESULTS AND DISSCUSSION

nanohydrogels were established to be non-immunogenic.

### 4.21 Histopathological analysis

Normal control group revealed a typical lung parenchyma morphology, and no abnormalities or tumor growth was observed (**Figure 4.33(a-b)**). Disease group showed the presence of melanin in the lung parenchyma (**Figure 4.33(c-d)**), thus distinctly showing tumor growth in the lungs. The DOX treated group showed standard lung parenchyma in compliance with a normal group that was entirely free of tumor and other abnormalities (**Figure 4.33(e-f)**). DOX-loaded N nanohydrogels revealed standard unaffected lung parenchyma; however, a few melanomas producing colonies were observed revealing tumor growth (**Figure 4.33(g-h)**). DOX-loaded NG nanohydrogels showed tumor affected bronchus without any lesions (**Figure 4.33i**), while lung parenchyma appeared to be normal (**Figure 4.33j**). DOX-loaded NL (**Figure 4.33(k-l)**) and DOX-loaded NM nanohydrogels (**Figure 4.33(m-n)**) showed normal lung parenchyma that was independent of aberrations but, a meagre number of tumor-forming colonies was distinguished. These results were by visual confirmation and metastatic lung count as shown in **Figure 4.33(b-c)**. In both histopathology and tumor count cases, complete rehabilitation of lungs from melanoma was not exhibited in any of the nanohydrogels, although it was found to be notably lower than the disease group affirming its potential application as a drug carrier.

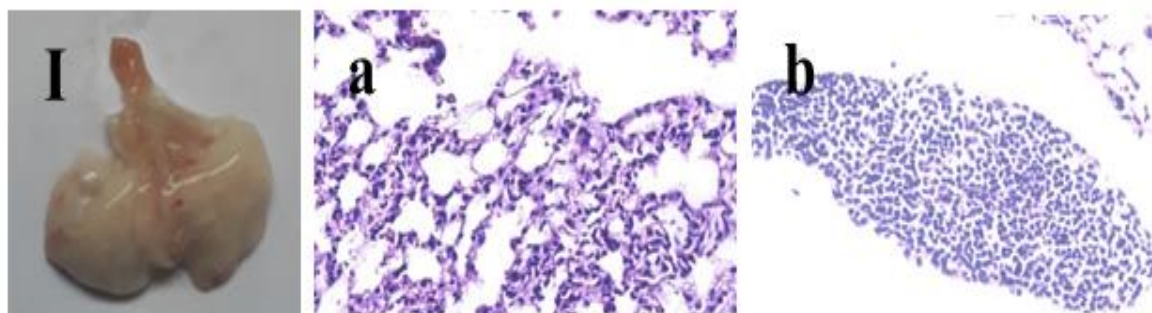


**Figure 4.33: Excised lung of mice from group I – VII. Histopathology of lung tissues (a-n) from groups I-VII at 100X resolution. (a-b) Normal control, absence of tumor cells can be distinctly seen.**

## RESULTS AND DISCUSSION

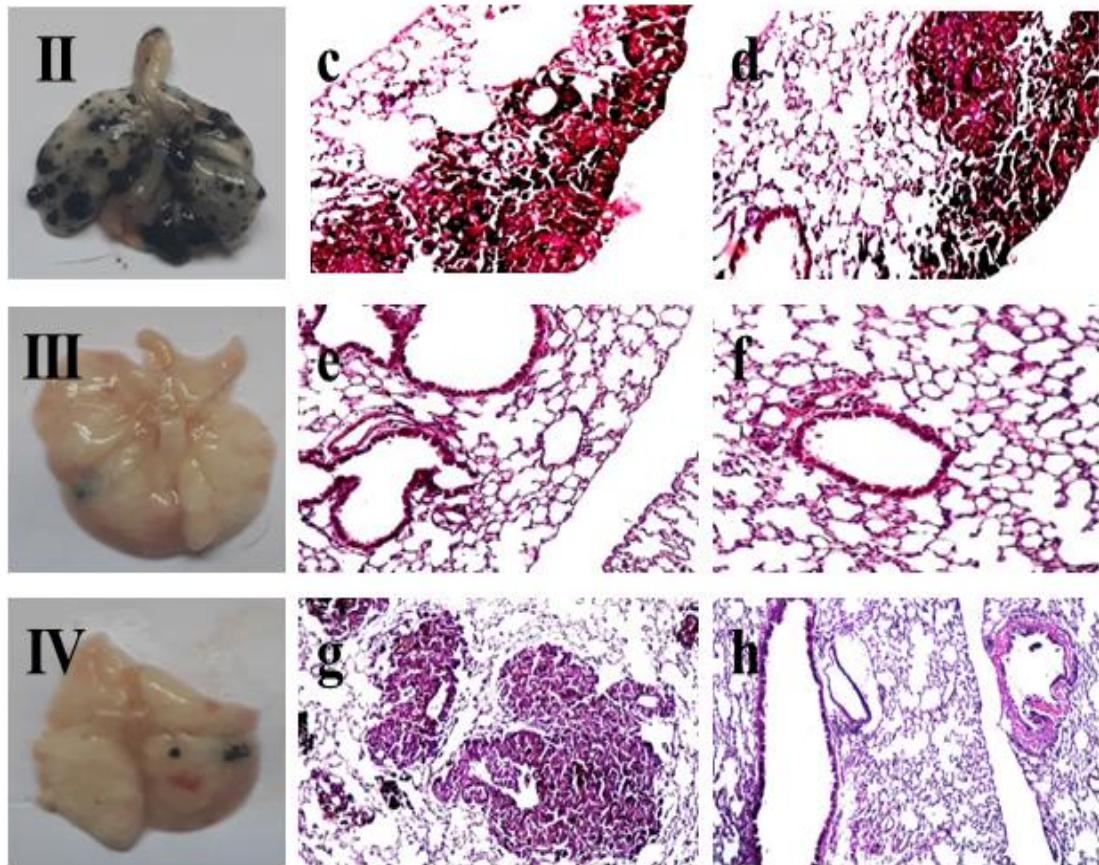


**Figure 4.33: Excised lung of mice from group I – VII. Histopathology of lung tissues (a-n) from groups I-VII at 100X resolution. (c-d) Disease control, presence of melanin-producing colonies is evident; (e-f) DOX-treated group, no tumor formation can be seen; (g-h) N-DOX treated group [(g) displays presence of melanoma, (h) displays normal lung parenchyma].**



## RESULTS AND DISCUSSION

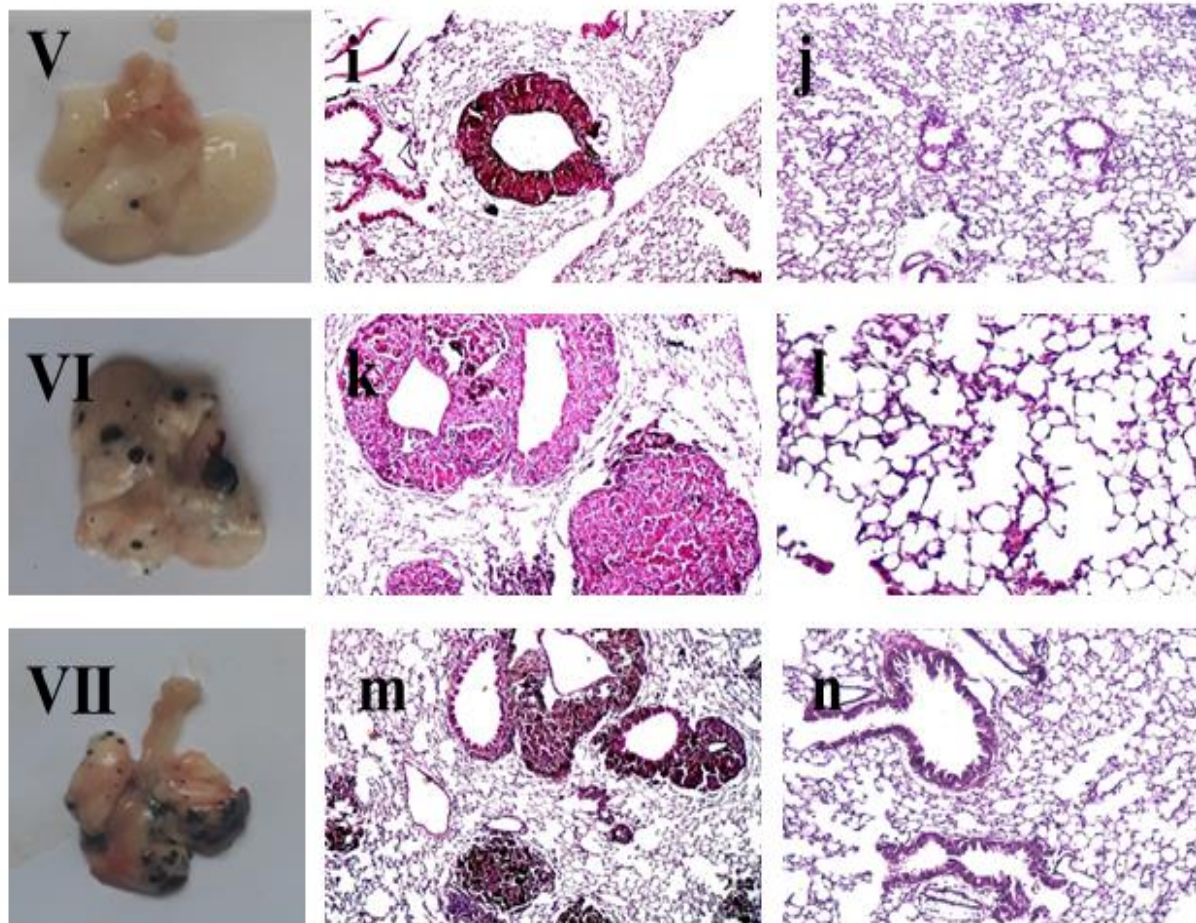


**Figure 4.33: Excised lung of mice from group I – VII. Histopathology of lung tissues (a-n) from groups I-VII at 100X resolution. (i-j) NG-DOX treated group [(i) reveals melanoma affected bronchus of lung, (j) reveals standard lung parenchyma]; (k-l) NGL-DOX-treated group [(k) exhibits appearance of melanoma tumor, (l) exhibits typical lung parenchyma]; (m-n) NGM-DOX-treated group [(m) demonstrate melanoma tumor cells, (n) demonstrate conventional lung parenchyma].**

**CHAPTER 5**  
**SUMMARY AND**  
**CONCLUSIONS**





# SUMMARY AND CONCLUSIONS

## CHAPTER 5

### 5 SUMMARY AND CONCLUSIONS

#### 5.1 Summary

The topic of this thesis encompassed the development and characterization of macro and nano forms of thermosensitive hydrogels intended for drug delivery applications. For drug delivery application, the LCST of the hydrogels should be near to the physiological temperature and also the hydrogel should be biocompatible with good stability. Therefore, DEA and GQDs were chosen as main monomer and nanomaterial for synthesis hydrogels (macro and nano) with desired properties. It was shown that synergistic properties of these hydrogels could be achieved by formation of hydrogels in macro and nano forms. However, in the field of drug delivery, nanohydrogels are beneficial than macrogels with fast response to temperature changes and better swelling properties. Taking their advantages into consideration, work presented in this thesis referred to physical forms of thermosensitive hydrogels (macrogels), with accent on thermosensitive nanohydrogels (nanogels) and their applicability in drug delivery. Biocompatible PDEA and GQDs incorporated macrogel and nanohydrogels were successfully synthesized by optimizing the process variables. The synthesized hydrogels were characterized and its drug release properties were studied. The release profiles were fitted in kinetic model and the results revealed that these hydrogels are thermosensitive and biocompatible and can be potentially used for biomedical applications. The major findings of the present study are listed below.

#### 5.2 Conclusions

- GQDs were synthesized by an easy and low-cost bottom-up method (microwave irradiation method). The synthesized GQDs were successfully functionalized using leucine and methionine.
- PDEA hydrogel with better swelling ratio and better stability was synthesized using free-radical-polymerization.
- PDEA hydrogel and GQDs grafted PDEA hydrogel showed LCST in the range of 29-40 °C.

## SUMMARY AND CONCLUSIONS

- The release studies of DOX at three different temperature showed a release of 39% at 30 °C, 33-54% at 37 °C and 38-66% at 40 °C. The percentage release was based on the total DOX absorbed in the hydrogel. The kinetic modeling release confirmed that the release mechanism is non-Fickian diffusion and it is relaxation-controlled diffusion.
- PDEA nanohydrogel were synthesized using inverse emulsion polymerization technique and the process parameters were optimized and particle size of 47 - 59.5 nm was achieved with better reproducibility.
- GQDs grafted PDEA nanohydrogel were synthesized under optimized conditions and the particle size of 68.1 to 87.5 nm was achieved with better reproducibility.
- The release profile analysed using DOX loaded nanohydrogels at different temperature showed a release percentage of 49.59-62.81% at 30 °C, 54.94-68.15% at 37 °C and 58.78-86.35% at 40 °C. Kinetic modeling reveals that the release mechanism of nanohydrogels is Fickian diffusion.
- *In-vitro* studies like cytotoxicity proved that the synthesized GQDs, hydrogel and nanohydrogel are non-toxic upto 1000 µg/mL and they are biocompatible and hence this can be used as a potential drug carrier.
- *In-vivo* studies were done to study the lung metastasis by melanoma cancer. The results showed rational and favorable prognosis which was confirmed by evaluating hematological parameters. The non-immunogenic nature of the nanohydrogel was evaluated using cytokine assay. Comprehensively, these results suggested that PDEA nanohydrogel have potential application as an intelligent drug carrier for melanoma cancer.

### 5.3 Future scope

Studies can be carried out on the polymer and GQDs structure:

- Functionalizing drug carrier with specific receptor molecules to bind specifically with cancer cells.
- Real time monitoring of the drug carrier to improve the drug release efficiency.

# **REFERENCES**



## REFERENCES

- Abdullah, N., Al, Lee, J. E., In, I., Lee, H., Lee, K. D., Jeong, J. H., Park, S. Y. (2013). "Target delivery and cell imaging using hyaluronic acid-functionalized graphene quantum dots". *Mol. Pharmaceutics*, 10, 3736–3744.
- Abebe, D. G. and Fujiwara, T. (2012). "Controlled thermoresponsive hydrogels by stereocomplexed PLA-PEG-PLA prepared via hybrid micelles of pre-mixed copolymers with different PEG lengths". *Biomacromolecules*, 13, 1828– 1836.
- Achiha, K., Ojima, R., Kasuya, Y. and Fujimoto, K. (1995). "Interactions between temperature-sensitive hydrogel microspheres and granulocytes." *Polym Advan Technol.*, 6(7), 534-540.
- Adnan, M., Hani, A. A., Asif, H. M., Musab, Al, Fozia, Al-N., Faten Al-H., *et al.* (2016). "Hydrogels 2.0: improved properties with nanomaterial composites for biomedical applications". *Biomed. Mater.*, 11, 014104.
- Agrawal, S. S., Gullaiya, S., Dubey, V., Nagar, A., Kumar, A., Nagar, P., Singh, V. (2012). "Effect of Demethoxycurcumin on biochemical markers, oxidative stress and histopathological alterations in Anthracyclin cardiotoxicity rat model". *J. Pharmacy Research*. 5, 3078-3083.
- Ahmed, E. M. (2015) "Hydrogel: Preparation, characterization, and applications: A review" *Journal of Advanced Research*, 6(2), 105-121.
- Ajji, Z., Othman, I. and Rosiak, J. M. (2005). "Production of hydrogel wound dressings using gamma radiation". *Nucl Instrum Meth B.*, 229(3-4), 375-380.
- Akbarzadeh, A., Rezaei-Sadabady, R., Davaran, S., Joo, S. W., Zarghami, N., Hanifehpour, Y., Nejati-Koshki, K. (2013). "Liposome: classification, preparation, and applications". *Nanoscale Res Lett.*, 8(1), 102.
- Akhtar, M. F., Hanif, M., Ranjha, N. M. (2016) "Methods of synthesis of hydrogels - A review". *Saudi Pharm. J.*, 24(5), 554-559.

## REFERENCES

Al-Badriyeh, D., Alameri, M., and Al-Okka, R. (2017). "Cost-effectiveness research in cancer therapy: a systematic review of literature trends, methods and the influence of funding". *BMJ Open*, 7, 1-11.

Alejandro, S. and Katia, P. S. (2017). "Polymeric Hydrogels as Technology Platform for Drug Delivery Applications". *Gels*, 3, 25-47.

Alfrey, T., Gurnee, E.F., Lloyd, W.G. (1966). "Diffusion in glassy polymers". *J. Polym. Sci. C*, 12, 249-261.

Alivisatos, A. P., Gu, W., Larabell, C., (2005). "Quantum dots as cellular probes". *Annu. Rev. Biomed. Eng.*, 7, 55–76.

Alper, A. and Nuran, I. (2016). "Microwave-assisted synthesis and characterization of sodium alginate-graft-poly (N, N-dimethylacrylamide)". *Int. J. Biological Macromol.*, 82, 530–540.

Alsirafy, S. A., Mesidy, S. M. El, Abou-Elela, E. N., Elfaramawy, Y. I. (2011). "Naproxen test for neoplastic fever may reduce suffering". *J. Palliat. Med.*, 14(5), 665–667.

Alvarez-Lorenzo, C., Bromberg, L., Concheiro, A. (2009). "Light-sensitive intelligent drug delivery systems". *Photochem. Photobiol.*, 85, 848–860.

Amélia, M.P.S., Gonçalves, da Silva, Sónia, I.C.L., Pedro, B., Telmo J.V.P., Mariana B., José M.G.M. (2008). "Thermo-responsiveness of poly(N,N-diethylacrylamide) polymers at the air–water interface: The effect of a hydrophobic block". *J. Colloid and Interface Science*, 327, 129–137.

Ana, C. F., Arménio, C. S., Jorge, F. J. C. (2015). "Bioabsorbable polymers in cancer therapy: latest developments" *The EPMA J.*, 6(22), 1-18.

Anastase-Ravion, S., Ding, Z., Pelle, A., Hoffman, A. S., Letourneur, D. (2001).

## REFERENCES

- “New antibody purification procedure using a thermally responsive poly (N-isopropylacrylamide)-dextran derivative conjugate”. *J Chromatogr B.*, 761(2), 247-254.
- Angelopoulos, S. A. and Tsitsilianis, C. (2006). “Thermo-reversible hydrogels based on poly(N,N-diethyl acrylamide)-block- poly(acrylic acid)-block-poly(N,N-diethyl acrylamide) double hydrophilic triblock copolymer”. *Macromolecular Chemistry and Physics*, 207(23), 2188-2194.
- Anghelache, A., Teodorescu, M., Sti’c, M., Kneževi’c-Jugovi’c, Z., Filipovi’c, J. (2014). “Novel crosslinked thermoresponsive hydrogels with controlled poly(ethylene glycol)—poly(propylene glycol) multiblock copolymer structure”. *Colloid Polym. Sci.*, 292, 829–838.
- Arijit, G., Abhijit, P., Oommen, S. S., Kumar, K. S. (2015). “Studies on thermoresponsive polymers: Phase behaviour, drug delivery and biomedical applications”. *Asian J. Pharma. Sci.*, 10(2), 99-107.
- Arrangoiz, R., Dorantes, J., Cordera, F., Juarez, M. M., Paquentin, E. M., and León, E. L. de. (2016). “Melanoma review: Epidemiology, risk factors, diagnosis and staging”. *J. Cancer Treat Res.*, 4, 1–15
- Arruebo, M., Vilaboa, N., Sáez-Gutierrez, B., Lambea, J., Tres, A., Valladares, M., González-Fernández, Á. (2011). “Assessment of the Evolution of Cancer Treatment Therapies”. *Cancers (Basel)*, 3(3), 3279-3330.
- Babu, V. R., Mallikarjun, V, Nikhal, S. R. and Srikanth, G. (2010). “Dendrimers: A new carrier system for drug delivery”. *IRJPAS.*, 1(1), 1-10.
- Bai, S., Thomas, C., Rawat, A. and Ahsan, F. (2006). “Recent progress in dendrimerbased nanocarriers”. *Crit. Rev. Ther. Drug Carrier Syst.*, 23(6), 437-495.
- Bajpai, A. K., Sandeep, K. S., Smitha, B., Sanjana, K. (2008). “Responsive polymers in controlled drug delivery”. *Prog. in Poly Sci.*, 33, 1088–1118.

## REFERENCES

Barron, V., Killion, J. A., Pilkington, L., Burke, G., Geever, L. M., Lyons, J. G., McCullagh, E., Higginbotham, C. L. (2016). "Development of chemically cross-linked hydrophilic– hydrophobic hydrogels for drug delivery applications". *European Poly. J.*, 75, 25–35.

Bawa, P., Pillay, V. Choonara, Y. E., du Toit, L. C. (2009). "Stimuli-responsive polymers and their applications in drug delivery". *Biomedical Materials*, 4, 001-015.

Bemmelen, J. M. V. (1894). "Der Hydrogel und das kristallinische Hydrat des kupferoxydes". *Z. Anorg. Chem.*, 5, 466.

Bennett, S. L., Melanson, D.A., Torchiana, D.F., Wiseman, D.M., Sawhney, A.S. (2003). "Next generation Hydrogel films as tissue sealants and adhesion barrier." *J. of Cardiac Surgery*, 18(6), 494-499.

Bhattacharya, R. and Mukherjee, P. (2008). "Biological properties of 'naked' metal nanoparticles". *Adv. Drug Deliv. Rev.*, 60, 1289–1306.

Bignotti, F., Penco, M., Sartore, L., Peroni, I., Mendichi, R., Casolaro, M. and D'amore, A. (2000). "Synthesis, characterisation and solution behaviour of thermo- and pH-responsive polymers bearing L-leucine residues in the side chains". *Polymer*, 41(23), 8247-8256.

Bindu, M., Ashok, V., Arkendu, C. (2012). "As A Review on Hydrogels as Drug Delivery in the Pharmaceutical Field". *Inter. J. Pharma. Chemi. Sci.*, 1(2), 642-661.

Biswas, A.K., Islam, M.R., *et al.*, (2014). "Nanotechnology based approaches in cancer therapeutics". *Adv. Nat. Sci.: Nanosci. Nanotechnol.*, 5, 043001.

Boisseau, P. and Loubaton, B. (2011). "Nanoscience and nanotechnologies: hopes and concerns Nanomedicine, nanotechnology in medicine" *C. R. Physique*, 12, 620–636.



## REFERENCES

- Bossard, F., Aubry, T., Gotzamanis, G., Tsitsilianis, C. (2006). "pH-Tunable rheological properties of a telechelic cationic polyelectrolyte reversible hydrogel". *Soft Matter.*, 2(6), 510-516.
- Bouwstra, J.A., Salomons-de Vries, M.A., van Miltenburg, J.C. (1995). "The thermal behaviour of water in hydrogels". *Thermochimica Acta*, 248, 319- 327.
- Bradley, M. and Vincent, B. (2005). "Interaction of Nonionic Surfactants with Copolymer Microgel Particles of NIPAM and Acrylic Acid". *Langmuir*, 21(19), 8630-8634.
- Brazel, C.S. and Peppas, N.A. (1999). "Mechanisms of solute and drug transport in relaxing , swellable , hydrophilic glassy polymers". *Polymer (Guildf)*. 40, 3383–3398.
- Brian, W. C. T., Kieran, F. S., Pamela, J. R. (2012). "Paradoxical Roles of Tumour Necrosis Factor-Alpha in Prostate Cancer Biology". *Prostate Cancer*, 2012, 1-8.
- Bromberg, L. and Levin, G. (1996). "Transesterification of poly(N,N-diethylacrylamide-co-glycol methacrylate) with diethyldithiophosphate: Facts and implications". *J. Polymer Science Part a-Polymer Chemistry*, 34, 2595-2602.
- Brownlee, M. and Cerami, A. (1979). "Glucose-controlled insulin delivery system: semi synthetic insulin bound to lectin". *Sci.*, 206, 1190–1191.
- Bruguerolle, B. (1998). "Chrono-pharmacokinetics current status". *Clin Pharmacokinet.*, 35, 83–94.
- Buwalda, S.J., Boere, K.W.M., Dijkstra, P.J., Feijen, J., Vermonden, T., Hennink, W.E., (2014). "Hydrogels in a historical perspective: from simple networks to smart materials". *J. Contr. Rel.* 190, 254-273.

## REFERENCES

- Cabane, E., Zhang, X., Langowska, K., Palivan, C. G., Meier, W. (2012). “Stimuli-Responsive Polymers and Their Applications in Nanomedicine”. *Biointerphases*, 7, 9-36.
- Cahalan, P. T., Coury, A. J., Jevne, A. H., Kallok M. J. (1988). “Hydrogel adhesive”. US Patent US4768523A.
- Cai, W. S., Gan, L. H., Tam, K. C. (2001). “Phase transition of aqueous solutions of poly( N , N -diethylacrylamide- co -acrylic acid) by differential scanning calorimetric and spectrophotometric methods”. *Colloid & Polymer Science*, 279(8), 793-799.
- Calejo, M. T., Kjoniksen, A. L., Pinazo, A., *et al.* (2012). “Thermoresponsive hydrogels with low toxicity from mixtures of ethyl (hydroxyethyl) cellulose and arginine-based surfactants”. *Int J Pharm.*, 436, 454–462.
- Candau F., (1997). “Inverse Emulsion and Microemulsion Polymerization -Emulsion Polymerization and Emulsion Polymers, Ed”. *Wiley*.
- Cao, P-f., Mangadlao, J., Dacula, A., Rigoberto, C. (2015). “Stimuli-Responsive Polymers and their Potential Applications in Oil-Gas Industry”. *Polymer Reviews*, 55(4), 706-733.
- Carvalho, C., Santos, R. X., Cardoso, S., Correia, S., Oliveira, P. J., Santos, M. S., Moreira, P. I. (2009). “Doxorubicin: the good, the bad and the ugly effect”. *Curr. Med. Chem.*, 16(25), 3267–3285.
- Chai, Q., Jiao, Y., Yu, X. (2017). “Hydrogels for Biomedical Applications: Their Characteristics and the Mechanisms behind them”. *Gels*, 3, 6-21.
- Chandra, A., Deshpande, S., Shinde, D.B., Pillai, V.K., Singh, N. (2014). “Mitigating the cytotoxicity of graphene quantum dots and enhancing their applications in bioimaging and drug delivery”. *ACS Macro Lett.*, 3, 1064-1068.

## REFERENCES

- Chang, C. S. (1988). "Measuring density and porosity of grain kernels using a gas pycnometer". *Cereal Chem*, 65, 13–15.
- Chaterji, S, Kwon, K. I., Park, K. (2007). "Smart polymeric gels: redefining the limits of biomedical devices". *Prog. Polym. Sci.*, 32, 1083–122.
- Chatterjee, M., Patra, A. and Brinker, J. (2001). "Cadmium Sulfide Aggregates through Reverse Micelles". *J. Am. Ceram. Soc.*, 84, 1439-1444.
- Chen, J. K. and Chang, C. J. (2014). "Fabrications and applications of stimulus-responsive polymer films and patterns on surfaces: A review". *Materials*, 7(2), 805–875.
- Chen, J., Liu, M., Chen, S. (2009). "Synthesis and characterization of thermo- and pH-sensitive kappa-carrageenan-g-poly (methacrylic acid)/poly (N, N –diethyl acrylamide) semi-IPN hydrogel". *Mater. Chem. Phys.* 115, 339–346.
- Chen, J., Liu, M., Chen, W., Zhang, N., Zhu, S., Zhang, S., Xiong, Y. (2011). "Synthesis, swelling and drug-release behaviour of a poly(N,N-diethylacrylamide-co-(2-dimethylamino) ethyl methacrylate) hydrogel". *J. Biomat. Sci. Poly.*, 22(8), 1049–1068.
- Chen, J., Liu, M., Liu, H., Ma, L. (2009). "Synthesis, swelling and drug release behavior of poly(N, N-diethylacrylamide-co-N-hydroxymethyl acrylamide) hydrogel". *Mat. Sci. Eng. C*, 29(7), 2116–2123.
- Chen, J., Liu, M., Liu, H., Ma, L., Gao, C., Zhu, S., Zhang, S. (2010). "Synthesis and properties of thermo- and pH-sensitive poly(diallyldimethylammonium chloride)/poly(N, N-diethylacrylamide) semi-IPN hydrogel". *Chem. Eng. J.*, 159(1–3), 247–256.
- Chintan, D. and Gayatri, P. (2015) "Application of Nanohydrogels in Drug Delivery Systems: Recent Patents Review". *Recent Patents on Nanotechnology*, 9, 17-25.

## REFERENCES

- Chung, H. J., Lee, Y., Park, T.G. (2008). “Thermo-sensitive and biodegradable hydrogels based on stereocomplexed Pluronic multi-block copolymers for controlled protein delivery”. *J. Control. Release: Off. J. Control. Release Soc.*, 127, 22–30.
- Chytry, V., Netopilik, M., Bohdanecky, M., Ulbrich, K. (1997). “Phase transition parameters of potential thermosensitive drug release systems based on polymers of N-alkylmethacrylamides”. *J Biomater Sci Polym Ed.*, 8, 817-824.
- Cohen, S., Lobel, E., Trevgoda, A. and Peled, Y. (1997). “A novel in situ-forming ophthalmic drug delivery system from alginates undergoing gelation in the eye”. *J Control Release*, 44(2-3), 201-208.
- Colonne, M., Chen, Y., Wu, K., Freiberg, S., Giasson, S., Zhu, X. X. (2007). “Binding of Streptavidin with Biotinylated Thermosensitive Nanospheres Based on Poly(*N,N*-diethylacrylamide-*co*-2-hydroxyethyl methacrylate)”. *Bioconjugate Chem.*, 18, 999-1003.
- Cuiyun, L., Shuangxia, R., Yu, D., Fengjie, T., Xin, W., Sufeng, Z., Shuhua, D., *et al.* (2014). “Efficacy, Pharmacokinetics, and Biodistribution of Thermosensitive Chitosan/ $\beta$ -Glycerophosphate Hydrogel Loaded with Docetaxel” *AAPS PharmSciTech.*, 15(2), 417-424.
- Danhier, F., Feron, O., Pr at, V. (2010). “To exploit the tumor microenvironment: Passive and active tumor targeting of nanocarriers for anti-cancer drug delivery”. *J. Control. Release*, 148(2), 135–146.
- Das, M., Zhang, H., Kumacheva, E. (2006). “Microgels: old materials with new applications”. *Annu Rev Mater Res.*, 36, 117-142.
- De Jong, H. W. and Borm, P. J. A. (2008) “Drug delivery and nanoparticles: Applications and hazards”. *Int. J of Nanomedicine*, 3(2), 133-149.

## REFERENCES

- Deo, S. V., Hazarika, S., Shukla, N. K., Kumar, S., Kar, M., Samaiya, A. (2005) "Surgical management of skin cancers: Experience from a regional cancer centre in North India." *Indian Journal of Cancer*, 42(3), 145-150.
- Desai, V. G., Herman, E. H., Moland, C. L., Branham, W. S., Lewis, S. M., Davis, K. J., George, N. I., Lee, T., Kerr, S., Fuscoe, J. C. (2013). "Development of doxorubicin-induced chronic cardiotoxicity in the B6C3F1 mouse model". *Toxicol. Appl. Pharmacol.*, 266, 109–121.
- Dhandapani, N. V., Thapa, A., Sandip, G., Shrestha, A., Shrestha, N., Bhattarai, R. S. (2013) "Liposomes as novel drug delivery system: A comprehensive review". *Int T Res Pharm Sci.*, 4(2), 187-193.
- Don, T. M., Huang, M. L., Chiu, A. C., Kuo, K. H., Chiu, W. Y., Chiu, L. H. (2008). "Preparation of thermo-responsive acrylic hydrogels useful for the application in transdermal drug delivery systems". *Mater Chem Phys.*, 107(2), 266-273.
- Dong, J., Wang, K., Sun, L., Sun, B., Yang, M., Chen, H., Wang, Y., Sun, J., and Dong, L. (2018). "Application of graphene quantum dots for simultaneous fluorescence imaging and tumor-targeted drug delivery". *Sensors Actuators B Chem.*, 256, 616–623.
- Dong, Y., Shao, J., Chen, C., Li, H., Wang, R., Chi, Y., Lin, X., Chen, G. (2012). "Blue luminescent graphene quantum dots and graphene oxide prepared by tuning the carbonization degree of citric acid". *Carbon*, 50(12), 4738–4743.
- Dunn, A. S. and Chong, L. C. H. (1970). "Application of theory of colloid stability and the problem of particle formation in aqueous solution of vinyl acetate". *Br Polym J.*, 2, 49-59.
- Ecgert, M. and Freltag, R. (1994). "Poly-N, N-diethylacrylamide Prepared by Group Transfer Polymerization: Synthesis, Characterization, and Solution Properties". *J. Polymer Science: Part A Polymer Chemistry*, 32, 803-813.

## REFERENCES

Eichenbaum, G., Kiser, P., Simon, S., Needham, D. (1998). “pH and ion-triggered volume response of anionic hydrogel microspheres”. *Macromolecules*, 31(15), 5084-5093.

Elford, W. J. (1930). “Structure in very permeable collodion gel films and its significance in filtration process”. *Proc R Soc Lond [Biol]*, 106(743), 216.

Elvati, P., Baumeister, E., and Violi, A. (2017). “Graphene quantum dots: effect of size, composition and curvature on their assembly.” *RSC Adv.*, 7(29), 17704–17710.

Enikő, K., Benjámín, G., András, S. (2017). “Preparation of pH-Responsive Poly(aspartic acid) Nanogels in Inverse Emulsion” *Periodica Polytechnica Chemical Engineering*, 61(1), 19-26.

Enrica, C. and Vitaliy, V. K. (2015). “Biomedical applications of hydrogels: A review of patents and commercial products”. *European Polymer J.*, 65, 252–267.

Fang, J. J., Zhu, Z. Y., Hui, D., Zheng, G. Q., Teng A. G., Liu, A. J. (2014). “Effect of spleen lymphocytes on the splenomegaly in hepatocellular carcinoma-bearing mice”. *Biomed. Environ. Sci.*, 27, 17–26.

Fariba, G. and Ebrahim, V. F. (2009). “Hydrogels in Controlled Drug Delivery Systems”. *Iranian Polymer J.* 18, 63-88.

Feil, H., Bae, Y. H., Feijen, J., Kim, S. W. (1993). “Effect of comonomer hydrophilicity and ionization on the lower critical solution temperature of N-isopropylacrylamide copolymers”. *Macromolecules*, 26(10), 2496-2500.

Feksa, L. R., Troian, E. A., Muller, C. D., Viegas, F., Machado, A. B., Rech, V. C. (2018) “Hydrogels for biomedical applications”. *Nanostructures for the Engineering of Cells, Tissues and Organs: From Design to Applications*. 403-438.

## REFERENCES

- Ferry, J. D. (1980). "Viscoelastic properties of polymers". John Wiley & sons, New York. 486-544.
- Figueiredo, S., Cabral, R., Luís, D., Fernandes, A. R., Baptista, P. V. (2014). "Integration of Gold nanoparticles and liposomes for combined anti-cancer drug delivery". In: Seifalian A. (ed.) Nanomedicine; University College London (UK); 2014.
- Fitzpatrick, S. D., Fitzpatrick, L. E., Thakur, A., Mazumder, M. A. J., Sheardown, H. (2012). "Temperature-sensitive polymers for drug delivery". *Expert Rev. Med. Devices*, 9, 339–351.
- Flory, P. J. (1953). "Principles of Polymer Chemistry". *Cornell University*, Ithaca, New York.
- Forrest, R. A., Swift, L. P., Rephaeli, A., Nudelman, A., Kimura, K.-I., Phillips, D. R., Cutts, S. M. (2012). "Activation of DNA damage response pathways as a consequence of anthracycline-DNA adduct formation". *Biochem. Pharmacol.*, 83(12), 1602–1612.
- Franco, A. T., Corken, A., Ware, J. (2015). "Platelets at the interface of thrombosis, inflammation, and cancer". *Blood*, 126, 582–588.
- Frédéric, B. and Margaret, F. (2013) "Global progress against cancer—challenges and opportunities". *Cancer Biol Med.*, 10, 183-186.
- Fujimoto, K., Mizuhara, Y., Tamura, N., Kawaguchi, H. (1993). "Interactions between thermosensitive hydrogel microspheres and proteins". *J Intel Mat Syst Str.*, 4(2), 184-189.
- Fundueanu, G., Constantin, M., Bucatariu, S., Ascenzi, P. (2017). "pH/thermo-responsive poly (N-isopropylacrylamide-co-maleic acid) hydrogel with a sensor and an actuator for biomedical applications". *Polymer*, 110, 177–186.

## REFERENCES

Gaharwar, A. K., Peppas, N. A., Khademhosseini, A. (2014) “Nanocomposite hydrogels for biomedical applications”. *Biotechnol Bioeng.* 111(3), 441–453.

Galaev, I. and Mattiasson, B. (2007). “Smart polymers: applications in biotechnology and biomedicine”. Second revised ed., Taylor & Francis, *CRC Press*, Boca Raton.

Galaev, I. Y. and Mattiasson, B. (2000). “‘Smart’ polymers and what they could do in biotechnology and medicine”. *Trends Biotechnol.*, 17(8), 335-340.

Gangrade, S. M. (2011). “Nanocrystals-a way for carrier free drug delivery”. *Pharma Buzz*, 6, 26-31.

Ganji, F., Vasheghani, F. S., Vasheghani F. E. (2010). “Theoretical Description of Hydrogel Swelling: A Review”. 19(5), 375-398.

Gao, X. and Dave, S. R. (2007). “Quantum dots for cancer molecular imaging”. *Adv Exp Med Boil.*, 620, 57-73.

Geisse, N. A. (2009). “AFM and Combined Optical Techniques”. *Mater Today*, 12, 40–5.

Gibas, I. and Janik, H. (2010). “Review: Synthetic Polymer Hydrogels For Biomedical Applications”. *Che. and Chem. Tech.*, 4, 297-304.

Goenka, S., Sant, V., Sant, S. (2014). “Graphene-based nanomaterials for drug delivery and tissue engineering”. *J Control Release.* 173(1), 75–88.

Goldman, E. R., Clapp, A. R., Anderson, G. P., Uyeda, H. T., Mauro, J. M., Medintz, I. L., Mattoussi, H. (2004). “Multiplexed toxin analysis using four colors of quantum dots fluororeagents”. *Anal. Chem.*, 76, 684–688.

Gong, J. and Osada, Y. (2004). “Low friction hydrogel having straight chain polymers and method for preparation”. US Patent US20040116305 A1.



## REFERENCES

- Gorgieva, S. and Kokol, V. (2012). "Preparation, characterization and in-vitro enzymatic degradation of chitosan-gelatine hydrogel scaffolds as potential biomaterials". *J. Biomed. Mater. Res. A*, 100, 1655–67.
- Gouda, R., Baishya, H., Qing, Z. (2017). "Application of Mathematical Models in Drug Release Kinetics of Carbidopa and Levodopa ER Tablets". *J. Develop. Drugs*, 6, 171-179.
- Graham, N. B. and Mc-Neil. (1984). "Hydrogels for controlled drug delivery". *Biomaterials*, 5(1), 27-36.
- Greaves, M. and Maley, C. C. (2012). "Clonal evolution in cancer". *Nature*, 481(7381), 306.
- Guenther, M.; Wallmersperger, T.; Keller, K.; Gerlach, G. (2013). "Swelling behaviour of functionalized hydrogels for application in chemical sensors". In *Intelligent Hydrogels*; Sadowski, G., Richtering, W., Eds., Springer: Cham, Switzerland, 265–273.
- Gulrez, H., Al-Assaf, S. K., Saphwan, O. G. (2011). "Hydrogels: Methods of Preparation, Characterisation and Applications". *Progress in Mol. and Envi. Bioeng. - From Analysis and Modeling to Tech. Appl.*, 117-150.
- Gupta, A. K., Maurya, S. D., Dhakkar, R. C., Singh, R. D. (2010). "pH sensitive interpenetrating hydrogel for eradication of *Helicobacter pylori*". *Int. J. Pharm. Sci.*, 3:924–32.
- Gupta, P., Vermani, K. and Garg, S. (2002). "Hydrogels: from controlled release to pH responsive drug delivery". *Drug Discov Today*, 7(10), 569-579.
- Guterres, S. S., Alves, M. P., Pohlmann, A. R. (2007). "Polymeric nanoparticles, nanospheres and nanocapsules, for cutaneous applications". *Drug Target Insights*, 2, 147.

## REFERENCES

Hamidi, M., Azadi, A., Rafiei, P. (2008). "Hydrogel nanoparticles in drug delivery". *Adv. Drug Delivery Rev.*, 60, 1638-1649.

Hao, Y. N., Guo, H. L., Tian, L., Kang, X. (2015). "Enhanced photoluminescence of pyrrolic-nitrogen enriched graphene quantum dots." *RSC Adv.*, 5, 43750.

Harasaki, A., Schmit, J., Wyant, J. C. (2001). "Offset of coherent envelope position due to phase change on reflection". *Appl. Optics*, 40, 2102–6.

Hayat, M. (1989). "Analytical Morphology: Theory, Applications & Protocols". Academic Press, San Diego.

He, C., Kim, S. W., Lee, D. S. (2008). "In situ gelling stimuli-sensitive block copolymer hydrogels for drug delivery". *J Control Release*, 127(3), 189-207.

Hejazi, R. and Amiji, M. (2003). "Chitosan-based gastrointestinal delivery systems". *J Control Release*, 89, 151–65.

Hench, L. L. and Jones, J. R. (2005). "Biomaterials, artificial organs and tissue engineering". 2nd ed. Cambridge, UK: Woodhead Publishing Limited, 227.

Herber, S., Olthuis, W., Bergveld, P., Berg, A. (2003). "Exploitation of a pH-sensitive hydrogel for CO<sub>2</sub> detection". In Proceedings of the Eurosensors XVII, European Conference on Solid-State Transducers, Guimaraes, Portugal.

Heymann, E. (1935). "Studies on sol-gel transformations. I. The inverse sol-gel transformation of methylcellulose in water". *Trans Faraday Soc.*, 31, 846-864.

Hinrichs, W. L. and Suhuermans, N. M. (1999). "Thermosensitive polymers as carrier for DNA delivery". *J Control Release*, 60, 249–59.

Hoare and T. R. and Kohane, D. S. (2008) "Hydrogels in drug delivery: Progress and challenges". *Polymer*, 49, 1993-2007.

## REFERENCES

- Hoffman, A. S. (2002). "Hydrogels for Biomedical Applications." *Adv Drug Deliv Rev.*, 54, 3-12.
- Hoffman, A. S. (2012). "Hydrogels for biomedical applications". *Adv Drug Deliv Rev.*, 64, 18–23.
- Hoffman, A. S., Afrassiabi, A., Dong, L. C. (1986). "Thermally reversible hydrogels: II. Delivery and selective removal of substances from aqueous solutions". *J Control Release*, 4(3), 213-222.
- Huang, J. J., Rong, M. Z., Zhang, M. Q. (2016). "Preparation of graphene oxide and polymer-like quantum dots and their one- and two-photon induced fluorescence properties". *Phys. Chem. Chem. Phys.*, 18, 4800–4806.
- Huang, X., Jain, P. K., El-Sayed, I. H., El-Sayed, M. A. (2007). "Gold nanoparticles: interesting optical properties and recent applications in cancer diagnostics and therapy". *Nanomedicine*, 2(5), 681-693.
- Huebsch, N., Kearney, C.J., Zhao, X., Kim, J., Cezar, C.A., Suo, Z., Mooney, D.J. (2014). "Ultrasound-triggered disruption and self-healing of reversibly cross-linked hydrogels for drug delivery and enhanced chemotherapy". *Proc. Natl. Acad. Sci. USA*, 111, 9762–9767.
- Huili, L., Ronglan, W., Jinlong, Z., Pingping, G., Wenchen, R., Shimei, X., Jide, W. (2015). "pH/Temperature Double Responsive Behaviors and Mechanical Strength of Laponite-Crosslinked Poly(DEA-co-DMAEMA) Nanocomposite Hydrogels". *J Polymer Science, Part B: Polymer Physics*, 53, 876–884.
- Iannazzo, D., Pistone, A., Salamò, M., Galvagno, S., Romeo, R., Giofrè, S. V, Branca, C., Visalli, G., and Pietro, A. Di. (2017). "Graphene quantum dots for cancer targeted drug delivery". *Int. J. Pharm.*, 518(1), 185–192.

## REFERENCES

- Iannazzo, D., Zicarelli, I., Pistone, A. (2017). "Graphene quantum dots: multifunctional nanoplatforms for anticancer therapy". *J. Mater. Chem. B*, 5(32), 6471–6489.
- Iijima, S. (1991). "Helical microtubules of graphitic carbon." *Nature*, 354, 56–58.
- Ijeoma, F. U. and Andreas, G. S. (2006). "Polymers in Drug Delivery". CRC Publications.
- Jafari, M. and Kaffashi, B. (2015). "Preparation and In vitro Evaluation of Isoniazid-Containing Dex-HEMA-Co-PNIPAAm Nanogels". *Ciência e Nat.*, 37, 55-62.
- Jagur-Grodzinski, J. (2010). "Polymeric gels and hydrogels for biomedical and pharmaceutical applications". *Polymers for Advanced Technologies*, 21, 27-47.
- Janel, K., Rahul, J., Praveena, V., Aniket, G., Shailee, P., Prakash, R. (2017). "Targeting Strategies for the Combination Treatment of Cancer Using Drug Delivery Systems". *Pharmaceutics*, 9, 46.
- Jen, A. C., Wake, M. C., Mikos, A. G. (1996). "Review: Hydrogels for cell immobilization". *Biotech.Bioengg.*, 50(4), 357-364.
- Jeong, B. and Gutowska, A. (2002). "Lessons from nature: stimuli-responsive polymers and their biomedical applications". *Trends Biotechnol.*, 20(7), 305-311.
- Jin, H. Z, Lee, Z.J., Song, K. W., Kim, M., Lee, G., Park, J.S. (2014). "Incorporation of graphene oxide into cyclodextrin-dye supramolecular hydrogel". *J. Inclusion Phenomena and Macrocyclic Chemistry*, 79, 357–363.
- Jing, Y., Zhu, Y., Yang, X., Shen, J., Li, C. (2011). "Ultrasound-Triggered Smart Drug Release from Multifunctional Core–Shell Capsules One-Step Fabricated by Coaxial Electrospray Method". *Langmuir*, 27, 1175–1180.

## REFERENCES

- Jinjun, S., Philip, W. K., Richard, W., Omid, C. F. (2017) "Cancer nanomedicine: progress, challenges and opportunities". *Nat Rev Cancer*, 17(1), 20–37.
- Joglekar, M. and Trewyn, B. G. (2013). "Polymer-based stimuli-responsive nanosystems for biomedical applications". *Biotechnology J.*, 8(8), 931-945.
- Jose, S., Dhanya, K., Cinu, T. A., Aleykutty, N. A. (2010). "Multiparticulate system for colon targeted delivery of ondansetron". *Indian J. Pharm. Sci.*, 72, 58-64.
- Ju, J., Zhang, R., He, S., Chen, W. (2014). "Nitrogen-doped graphene quantum dots-based fluorescent probe for the sensitive turn-on detection of glutathione and its cellular imaging". *RSC Adv.*, 4, 52583-52589.
- Jude, I. N., Luke, M. G., Kelsey, E. E., John, K., Damien, B. B., Clement, L. H. (2014). "Evaluation of Novel Antibiotic-Eluting Thermoresponsive Chitosan-PDEAAm Based Wound Dressings". *Int. J Polymeric Materials and Polymeric Biomaterials*, 63(17), 873-883.
- Jude, I. N., Luke, M., G., Martin, O. C., Clement, L. H. (2013). "Photopolymerised thermo-responsive poly(N, N-diethyl acrylamide)-based copolymer hydrogels for potential drug delivery applications". *J Polym Res.*, 19, 9822.
- Juillerat-Jeanneret, L. (2008). "The targeted deliver of cancer drugs across the blood-brain barrier: chemical modifications of drugs or drug-nanoparticles?" *Drug Discovery Today*, 13, 23-24.
- Jun, L., Bochu, W., Yazhou, W. (2006). "Thermo-sensitive polymers for controlled release drug delivery systems". *Int J Pharmacol.*, 2(5), 513-519.
- Jun, S., Jean, DeH., Donald, L., David, N. W., Carl, J. M., Yongyut, R., Joseph, K. H. M. (2001). "A Cell-Based Drug Delivery System for Lung Targeting: II. Therapeutic Activities on B16-F10 Melanoma in Mouse Lungs". *Drug Delivery*, 8, 71-76.

## REFERENCES

- Jung, K. O. (2017) "Polymers in Drug Delivery: Chemistry and Applications". *Mol. Pharmaceutics*, 14, 2459-2459.
- Kabanov, A. V., Batrakova, E. V., Alakhov, V. Y. (2002) "Pluronic block copolymers as novel polymer therapeutics for drug and gene delivery". *J Control Release*, 82, 189-212.
- Kaith, B. S., Jindal, R., Mittal, H. Kiran, K. (2010). "Temperature, pH and electric stimulus responsive hydrogels from Gum ghatti and polyacrylamide-synthesis, characterization and swelling studies". *Der Chemica Sinica*, 1(2), 44-54.
- Kamath, K. and Park, K. (1993). "Biodegradable Hydrogels in Drug delivery". *Adv Drug Deliv Rev*, 11, 59-84.
- Kamoun, E. A., Kenawy, E. S., Chen, X. (2017). "A review on polymeric hydrogel membranes for wound dressing applications: PVA-based hydrogel dressings". *J. Adv. Research*, 8, 217-233.
- Kamran, N., Li, Y., Sierra, M., Alghamri, M. S., Kadiyala, P., Appelman, H. D., Edwards, M., Lowenstein, P. R., Castro, M. G. (2018). "Melanoma induced immunosuppression is mediated by hematopoietic dysregulation". *Oncoimmunology*. 7(3), e1408750.
- Karimi, M., Sahandi, P. Z., Ghasemi, A, Amiri, M., Bahrami, M. (2016). "Temperature-Responsive Smart Nanocarriers for Delivery of Therapeutic Agents: Applications and Recent Advances". *ACS Appl. Mater. Interfaces*, 8(33), 21107–21133.
- Kashyap, N., Kumar, N., Kumar, M. N. V. R. (2004). "Smart gels for drug delivery applications". *Drug Deliver Technol.*, 4(7), 32-39.
- Katsnelson M. I. and Novoselov K. S. (2007). "Graphene: new bridge between condensed matter physics and quantum electrodynamics". *Solid State Commun.*, 143, 3–13.

## REFERENCES

- Kawaguchi, H., Fujimoto, K., Mizuhara, Y. (1992). "Hydrogel microspheres III. Temperature-dependent adsorption of proteins on poly-N-isopropylacrylamide hydrogel microspheres". *Colloid Polym Sci.*, 270(1), 53-57.
- Keheng, L., Wei, Liu., Yao, N., Dapeng, L., Dongmei, L., Zhiqiang, S. and Gang, W. (2017). "Technical synthesis and biomedical applications of graphene quantum dots". *J. Mater. Chem. B*, 5, 4811-4826.
- Khan, A., Othman, M. B. H., Razak, K. A., Akil, H. M. (2013). "Synthesis and physicochemical investigation of chitosan-pmaa-based dual-responsive hydrogels". *J. Polym. Res.*, 20, 1–8.
- Kikuchi, A. and Okano, T. (2002). "Intelligent thermoresponsive polymeric stationary phases for aqueous chromatography of biological compounds". *Prog Polym Sci.*, 27(6), 165-1193.
- Kikuchi, S., Chen, Y., Kitano, K., Sato, S. I., Satoh, T., Kakuchi, T. (2016). "B(C<sub>6</sub>F<sub>5</sub>)<sub>3</sub>-Catalyzed Group Transfer Polymerization of N,N-Disubstituted Acrylamide Using Hydrosilane: Effect of Hydrosilane and Monomer Structures, Polymerization Mechanism, and Synthesis of  $\alpha$ -End-Functionalized Polyacrylamides". *Macromolecules*, 49(8), 3049-3060.
- Kim, A., Rivera, S., Shprung, D., Limbrick, D., Gabayan, V., Nemeth, E., Ganz, T. (2014). "Mouse models of anemia of cancer". *PLoS One*, 9, 93283.
- Kim, I. S. and Oh, I. J. (2005). "Drug release from the enzyme-degradable and pH-sensitive hydrogel composed of glycidyl methacrylate dextran and poly(acrylic acid)". *Arch. Pharm. Res.*, 28, 983–987.
- Kim, J. J. and Park, K. (1999). "Smart hydrogels for bioseparation". *Bioseparation*, 7(4–5), 177–184.

## REFERENCES

- Kim, Y.-J., Matsunaga, Y.T. (2017). “Thermo-responsive polymers and their application as smart biomaterials”. *J. Mater. Chem. B.*, 5, 4307–4321.
- Kirakci K, Sicha, V., Holub, J., Kubat, P., Lang, K. (2014) “Luminescent hydrogel particles prepared by self-assembly of  $\alpha$ -cyclodextrin polymer and octahedral molybdenum cluster complexes”. *Inorg Chem Chem.*, 53, 13012-13018.
- Kirschner, C. M. and Anseth, K. S. (2013). “Hydrogels in healthcare: From static to dynamic material microenvironments”. *Acta Mater.*, 61, 931–944.
- Kishore, R., Scott, J. E., Francesca, A., Jeanne, A. H., Thayumanavan, S. (2017). “Utilizing Inverse Emulsion Polymerization to Generate Responsive Nanogels for Cytosolic Protein Delivery”. *Mol. Pharmaceutics*, 14(12), 4515–4524.
- Klier, J., Tucker, C. J., Kalantar, T. H., Green, D.P. (2000). “Properties and applications of microemulsions”. *Adv Mater.*, 12(23), 1751-1757.
- Kobayashi, J., Kikuchi, A., Sakai, K., Okano, T. (2002). “Aqueous chromatography utilizing hydrophobicity-modified anionic temperature-responsive hydrogel for stationary phases”. *J Chromatogr. A*, 958(1), 109-119.
- Koetting, M. C., Peters, J. T., Steichen, S. D., Peppas, N. A. (2015). “Stimulus-responsive hydrogels: Theory, modern advances, and applications”. *Materials Science and Engineering R.*, 93, 1–49.
- Kondiah, P. J., Choonara, Y. E., Kondiah, P. P.D., Marimuthu, T., Kumar, P., Du Toit, L. C., Pillay, V. (2016). “A review of injectable polymeric hydrogel systems for application in bone tissue engineering”. *Molecules*, 21, 1580-1613.
- Kopecek, J. (2003). Smart and genetically engineered biomaterials and drug delivery systems. *European Journal of Pharmaceutical Sciences*, 20(1), 1-16.



## REFERENCES

- Korsmeyer, R. W. and Peppas, N. A. (1983). "Solute and penetration diffusion in swellable polymers. III. Drug release from glassy P(HEMA-co-NVP) copolymers". *J. Control Rel.*, 1, 89-98.
- Kotera, A., Furusawa, K., Takeda, Y. (1970). "Colloid chemical studies of polystyrene latices polymerized without any surfaceactive agents. I. Method for preparing monodisperse latices and their characterization". *Kolloid-Z Z Polym.*, 239, 677-681.
- Kou, F., Lu, Z., Li, J., Zhang, X., Lu, M., Zhou, J., Wang, X., Gong, J., Gao, J., Li, J. (2016). "Pretreatment lymphopenia is an easily detectable predictive and prognostic marker in patients with metastatic esophagus squamous cell carcinoma receiving first-line chemotherapy". *Cancer Med.*, 5, 778–786.
- Kozlovskaya, V., Kharlampieva, E., Mansfield, M., Sukhishvili, S. (2006). "Poly(methacrylic acid) hydrogel films and capsules: Response to pH and ionic strength, and encapsulation of macromolecules". *Chem Mater.*, 18(2), 328-336.
- Kratz, K., Hellweg, T., Eimer, W. (2000). "A Influence of charge density on the swelling of colloidal poly(N-isopropylacrylamide-co-acrylic acid) microgels". *Colloid Surface A*, 170(2-3), 137-149.
- Kubota, K., Fujishige, S., Ando, I. (1990). "Solution properties of poly (N-isopropylacrylamide) in water". *Polym J.*, 22(1), 15-20.
- Kumar, G. S., Rajarshi, R., Dipayan, S., Uttam, K. G., Ranjit, T., Nilesh, M., Subhajit, S., Kalyan, K. C. (2014). "Amino-functionalized graphene quantum dots: origin of tunable heterogeneous photoluminescence". *Nanoscale*, 6, 3384.
- Kumar, M. (2000). "Nano and microparticles as controlled drug delivery devices". *J. Pharm. Pharm. Sci.*, 3(2), 234–258.
- Kumar, S. J. H. (2009). "Role of nanotechnology in drug delivery." <http://www.pharmainfo.net/santosh-kumar-jh/role-nanotechnology-drug-delivery>

## REFERENCES

(June 13, 2009).

Kuo, N. J., Chen, Y. S., Wu, C. W., Huang, C. Y., Chan, Y. H., Chen, I. W. P. (2016). "One-pot synthesis of hydrophilic and hydrophobic n-doped graphene quantum dots via exfoliating and disintegrating graphite flakes". *Sci. Rep.*, 6, 30426.

Kurisawa, M. and Yui, N. (1998). "Dual-stimuli-responsive drug release from interpenetrating polymer network-structured hydrogels of gelatin and dextran". *J Control Release*, 54, 191-200.

Kytai, T. N. (2011). "Targeted Nanoparticles for Cancer Therapy: Promises and Challenges" *J Nanomedic Nanotechnol*, 2, 5.

Landfester, K. (2003). "Miniemulsions for Nanoparticle Synthesis". *Top Curr Chem.*, 227, 75-123.

Landfester, K., Willert, M., Antonietti, M. (2000). "Preparation of polymer particles in non-aqueous direct and inverse miniemulsions". *Macromolecules*, 33(7), 2370-2376.

Langer, R. (1998). "Drug Delivery and Targeting". *Nature*, 392, 5.

Langer, R., and Peppas, N. (1983). "Chemical and Physical Structure of Polymers as Carriers for Controlled Release of Bioactive Agents: A Review". *J. Macromol. Sci.*, 23, 61.

Lee, S. C., Kwon, I. K., Park, K. (2013) "Hydrogels for delivery of bioactive agents: A historical perspective". *Adv. Drug Delivery Reviews*, 65, 17-20.

Lee, S. H. and Shin, H. (2007). "Matrices and scaffolds for delivery of bioactive molecules in bone and cartilage tissue engineering". *Adv Drug Deliver Rev.*, 59(4-5), 339-359.

## REFERENCES

- Lei, D., Yang, W., Gong, Y., Jing, J., Nie, H., Yu, B., Zhang, X. (2016). "Non-covalent decoration of carbon dots with folic acid via a polymer-assisted strategy for fast and targeted cancer cell fluorescence imaging". *Sensors Actuators B. Chem.*, 230, 714–720.
- Lenka, H., Jirí, S., Marek, R., Alexander, Z., Hana, K., Zdenka, S. (2016). "Phase transition in hydrogels of thermoresponsive semi-interpenetrating and interpenetrating networks of poly(N,N-diethylacrylamide) and polyacrylamide". *European Polymer J.*, 85, 1–13.
- Lessard, D. G., Ousalem, M., Zhu, X. X., Eisenberg, A., Carreau, P. J. (2003). "Study of the Phase Transition of Poly(N,N- diethylacrylamide) in Water by Rheology and Dynamic Light Scattering". *Polym Sci Part B: Polym Phys.*, 41, 1627-1637.
- Li, H., Wu, R., Zhu, J., Guo, P., Ren, W., Xu, S., Wang, J. (2015). "pH/Temperature Double Responsive Behaviors and Mechanical Strength of Laponite-Crosslinked Poly(DEA-co-DMAEMA) Nanocomposite Hydrogels". *J. polymer sci., part b: polymer phys.*, 53, 876–884.
- Li, H., Yu, B., Matsushima, H., Hoyle, C. E., Lowe, A. B. (2009). "The Thiol-Isocyanate Click Reaction: Facile and Quantitative Access to  $\omega$ -End-Functional Poly(N, N-diethyl acrylamide) Synthesized by RAFT Radical Polymerization." *Macromolecules*, 42, 6537–6542.
- Li, J., Wang, B., Wang, Y., Liu, P., Qiao, W. (2008). "Preparation and characterization of thermosensitive nanoparticles for targeted drug delivery". *J. Macromolecular Science A*, 45(10), 833–838.
- Li, K., Liu, W., Ni, Y., Li, D., Lin, D., Su, Z., We, G. (2017). "Technical synthesis and biomedical applications of graphene quantum dots". *J. Mater. Chem. B.*, 5 (10), 4811-4826.

## REFERENCES

- Li, L., Wu, G., Yang, G., Peng, J., Zhao, J., Zhu, J. J. (2013). "Focusing on luminescent graphene quantum dots: current status and future perspectives". *Nanoscale*, 5 (10), 4015-4039.
- Li, L.L., Ji, J., Fei, R., Wang, C.Z., Lu, Q., Zhang, J.R., Jiang, L. P., Zhu, J. J. (2012). "Synthesizing Graphene Quantum Dots for Gas Sensing Applications". *Adv. Funct. Mater.*, 22, 2971–2979.
- Li, W., Zhang, Z., Kong, B., Feng, S., Wang, J., Wang, L., Yang, J., Zhang, F., Wu, P., Zhao, D. (2013). "Simple and Green Synthesis of Nitrogen-Doped Photoluminescent Carbonaceous Nanospheres for Bioimaging." *Angew. Chem. Int. Ed.* 52, 1–6.
- Li, X., Zhao, D., Shi, X., Qiu, G., Lu, X. (2016). "Self-assembly and the hemolysis effect of monodisperse: N, N -diethylacrylamide/acrylic acid nanogels with high contents of acrylic acid". *Soft Matter*, 12(35), 7273-7280.
- Li, Y., Pan, S., Zhang, W., Du, Z. (2009). "Novel thermo-sensitive core-shell nanoparticles for targeted paclitaxel delivery". *Nanotechnology*, 20(6), 65104-65115.
- Liang, Q., Ma, W., Shi, Y., Li, Z., Yang, X. (2013). "Easy synthesis of highly fluorescent carbon quantum dots from gelatin and their luminescent properties and applications". *Carbon*, 60, 421–428.
- Lin, L., Rong, M., Lu, S., Song, X., Zhong, Y., Yan, J., Wang, Y., Chen, X. (2015). "A facile synthesis of highly luminescent nitrogen-doped graphene quantum dots for the detection of 2,4,6-trinitrophenol in aqueous solution". *Nanoscale*, 7, 1872–1878.
- Linbo, L., Lin, L., Chao, W., Kangyu, L., Ruohua, Z., Hong, Q., Yuqing, L. (2015). "Synthesis of nitrogen-doped and amino acid-functionalized graphene quantum dots from glycine, and their application to the fluorometric determination of ferric ion". *Microchim Acta.* 182, 763–770.

## REFERENCES

- Liu, F., Sun, Y., Zheng, Y., Tang, N., Li, M., Zhong, W., Du, Y. (2015). " Gram-scale synthesis of high-purity graphene quantum dots with multicolor photoluminescence". *RSC Adv.*, 5, 103428-103432.
- Liu, F., Tao, G. L, Zhuo, R. X. (1993). "Synthesis of thermal phase-separating reactive polymers and their applications in immobilized enzymes". *Polymer J.*, 25, 561–567.
- Liu, G., Qiu, Q., An, Z. (2012). "Development of thermosensitive copolymers of poly(2-methoxyethyl acrylate-co-poly(ethylene glycol) methyl ether acrylate) and their nanogels synthesized by RAFT dispersion polymerization in water". *Polym. Chem.*, 3(2), 504-513.
- Liu, H. Y. and Zhu, X. X. (1999). "Lower critical solution temperatures of N-substituted acrylamide copolymers in aqueous solutions". *Polymer*, 40(25), 6985-6990.
- Liu, H., Bian, F., Liu, M., Chen, S. (2008). "Synthesis of Poly (N , N - diethylacrylamide- co -acrylic acid ) Hydrogels with Fast Response Rate in NaCl Medium". *J. Applied Polymer Science*, 109, 3037–3043
- Liu, M., Leroux, J. C., Gauthier, M. A. (2015). "Conformation–function relationships for the comb-shaped polymer pOEGMA". *Prog. Polym. Sci.*, 48, 111–121.
- Liu, R. L., Wu, D. Q., Feng, X. L., Mullen, K. (2011). "Bottom-Up Fabrication of Photoluminescent Graphene Quantum Dots with Uniform Morphology". *J. Am. Chem. Soc.*, 133(39), 15221- 15223.
- Liu, S. and Liu, M. (2003) "Synthesis and Characterization of Temperature- and pH-Sensitive Poly (N , N -diethylacrylamide- co -methacrylic acid )" *J. Applied Polymer Science*, 90, 3563–3568.
- Liu, W., Zhang, C. C., Li, K. (2013). "Prognostic value of chemotherapy-induced leukopenia in small-cell lung cancer". *Cancer Biol. Med.* 10, 92-98.

## REFERENCES

- Liu, J. J., Zhang, X. L., Cong, Z. X., Chen, Z. T., Yang, H. H. and Chen, G. N., (2013) “Glutathione-functionalized graphene quantum dots as selective fluorescent probes for phosphate-containing metabolites”. *Nanoscale*, 5, 1810–1815.
- Lo, C. W., Zhu, D., Jiang, H. (2011). “An infrared-light responsive graphene-oxide incorporated poly(N-isopropylacrylamide) hydrogel nanocomposite”. *Soft Matter*, 7, 5604.
- Lopez, V. C., Raghavan, S. L., Snowden, M. J. (2004). “Colloidal microgels as transdermal delivery systems”. *React. Funct. Polym.*, 58(3), 175-185.
- Lu, X., Sun, M., Barron, A. E. (2011). “Non-ionic, thermo-responsive DEA/DMA nanogels: Synthesis, characterization, and use for DNA separations by microchip electrophoresis”. *J. Colloid and Interface Sci.*, 357, 345–353.
- Lu, Z. R., Kopečková, P., Kopeček, J. (2003). “Antigen responsive hydrogels based on polymerizable antibody Fab' fragment”. *Macromol Biosci.*, 3(6), 296-300.
- Luk, C. M., Tang, L. B., Zhang, W. F., Yu, S. F., Teng, K. S., Lau, S. P. (2012). “An efficient and stable fluorescent graphene quantum dot–agar composite as a converting material in white light emitting diodes”. *J. Mater. Chem.*, 22, 22378.
- Luke, M. G., John, G. L., Clement L. H. (2011). “Photopolymerisation and characterization of negative temperature sensitive hydrogels based on N, N-diethyl acrylamide”. *J Mater Sci* 46, 509–517.
- Luo, Z., Qi, G., Chen, K., Zou, M., Yuwen, L., Zhang, X., Huang, W., Wang, L. (2016). "Microwave-Assisted Preparation of White Fluorescent Graphene Quantum Dots as a Novel Phosphor for Enhanced White-Light-Emitting Diodes". *Adv. Funct. Mater.*, 26, 2739–2744.
- Ma, R., Xiong, D., Miao, F., Zhang, J. and Peng, Y. (2009). “Novel PVP/PVA hydrogels for articular cartilage replacement”. *Mater Sci Eng: C.*, 29(6), 1979-1983.

## REFERENCES

- Ma, X., Xi, J., Huang, X., Zhao, X. and Tang, X. (2004). "Novel hydrophobically modified temperature-sensitive microgels with tunable volume-phase transition temperature". *Mater Let.*, 58(27), 3400-3404.
- Maeda, H. (2012). "Macromolecular therapeutics in cancer treatment: The EPR effect and beyond". *J. Control. Release*, 164(2), 138–144.
- Mah, E. and Ghosh, R. (2013). "Thermo-responsive hydrogels for stimuli membranes". *Processes*, 1, 238-262.
- Mahammad, R. S., Madhuri, K., Dinakar, P. (2012). "Polymers in Controlled Drug Delivery Systems". *Int. J. Pharma Sci.*, 2(4), 112-116.
- Maheswari, B., JagadeeshBabu, P. E., Agarwal, M. (2014). "Role of N-vinyl-2-pyrrolidinone on the thermoresponsive behavior of PNIPAm hydrogel and its release kinetics using dye and vitamin-B<sub>12</sub> as model drug". *J. Biomat. Sci.*, 25(3), 269–86.
- Mahinroosta, M., Jomeh F. Z., Allahverdi, A., Shakoory, Z. (2018) "Hydrogels as intelligent materials: A brief review of synthesis, properties and applications". *Materials Today Chemistry*, 8, 42-55.
- Maitra, J. and Shukla, V. K. (2014). "Cross-linking in hydrogels—a review". *Amer J Polym Sci.*, 4, 25–31
- Marcelo, G., Prazeres, T. J. V., Charreyre, M. T., Martinho, J. M. G., Farinha, J. P. S. (2010). "Thermoresponsive micelles of phenanthrene-a-end-labeled poly(N-decylacrylamide-b-N,N-diethylacrylamide) in water." *Macromolecules*. 43, 501–510.
- Maria, H., Gabriela, C., Marta, M., Daniel, M., Conxita, S. (2018). "Influence of polymer concentration on the properties of nano-emulsions and nanoparticles obtained by a low-energy method". *Colloids and Surfaces A*, 536, 204–212.

## REFERENCES

Matthew, I. G. and Rachel, K. O'R. (2013). "To aggregate, or not to aggregate? Consideration in the design and application of polymeric thermally-responsive nanoparticles". *Chem. Soc. Rev.*, 42, 7204-7215.

Max, R. and Hannah, R. (2018). "Cancer". *Published online at OurWorldInData.org*. Retrieved from: '<https://ourworldindata.org/cancer>' [Online Resource].

McClements, D. J. (2015). "Food Emulsions: Principles, Practices, and Techniques". CRC press.

McDonald, T. O., Siccardi, M., Moss, D., Liptrott, N., Giardiello, M., *et al.* (2015) "The Application of Nanotechnology to Drug Delivery in Medicine". *Nanoengineering*, 173-223.

Meléndez-ortiz, H. I., Varca, G. H. C., Lugão, A. B., Bucio, E., Paulo, S. (2015). "Smart Polymers and Coatings Obtained by Ionizing Radiation: Synthesis and Biomedical Applications". *Open Journal of Polymer Chemistry*, 5, 17-33.

Miao, W.J., Shim, G.Y., Le, S.B., Lee, S.D., Choe, Y.S., Oh, Y.K. (2013). "Safety and tumor tissue accumulation of pegylated graphene oxide nanosheets for co-delivery of anticancer drug and photosensitizer". *Biomaterials*, 34, 3402-3410.

Mingqiang, L., Zhaohui, T., Dawei, Z., Hai, S., Huaiyu, L., Ying, Z., *et al.* (2015). "Doxorubicin-loaded polysaccharide nanoparticles suppress the growth of murine colorectal carcinoma and inhibit the metastasis of murine mammary carcinoma in rodent models". *Biomaterials*, 51, 161-172.

Miyata, T., Asami, N., Uragami, T. (1999). "A reversibly antigen-responsive hydrogel". *Nature*, 399(6738), 766-769.

Miyata, T., Uragami, T., Nakamae, K. (2002). "Biomolecule-sensitive hydrogels". *Adv Drug Deliver Rev.*, 54(1), 79-98.



## REFERENCES

- Mori, Y. and Kawaguchi, H. (2007). "Impact of initiators in preparing magnetic polymer particles by miniemulsion polymerization". *Colloid. Surface. B.*, 56(1), 246-254.
- Morteza, B., Naimeh, M., Mehadi, M. (2016). "An Introduction to Hydrogels and Some Recent Applications". *Emerg. Concepts Analysis Appl. Hydrogels*, 1–38.
- Mpho, N., Yahya, E. C., Charu, T., Lomas, K. T., *et al.* (2013). "Integration of Biosensors and Drug Delivery Technologies for Early Detection and Chronic Management of Illness." *Sensors*, 13, 7680-7713.
- Muhammad, R., Rosiyah, Y., Aziz, H., Muhammad, Y., Ahmad, D. A., Vidhya, S., Faridah, S., Cheyma, N. A. (2017). "pH Sensitive Hydrogels in Drug Delivery: Brief History, Properties, Swelling, and Release Mechanism, Material Selection and Applications". *Polymers*, 9, 137-174.
- Mukherjee, B., Niladri, S. D., Ruma, M., Priyanka, B., *et al.* (2014). "Current Status and Future Scope for Nanomaterials in Drug Delivery". 555-575.
- Mura, S., Nicolas, J., Couvreur, P. (2013). "Stimuli-responsive nanocarriers for drug delivery". *Nature materials*, 12, 991-1003.
- Murakami, Y. and Maeda, M. (2005) "DNA-responsive hydrogels that can shrink or swell". *Biomacromolecules*, 6, 2927–2929.
- Naik, J. P., Sutradhar, P., Saha, M. (2017). "Molecular scale rapid synthesis of graphene quantum dots ( GQDs )". *J. Nanostructure Chem.*, 7, 85–89.
- Namdeo, M., Bajpai, S. K., Kakkar, S. (2009). "Preparation of a magnetic-field-sensitive hydrogel and preliminary study of its drug release behavior". *J. Biomater. Sci. Polym. Ed.* 20, 1747–1761.
- Nebot, V. J., Armengol, J., Smets, J., Prieto, S. F., Escuder, B., Miravet, J. F. (2012).

## REFERENCES

- “Molecular Hydrogels from Bolaform Amino Acid Derivatives: A Structure–Properties Study Based on the Thermodynamics of Gel Solubilization”. *Chem. Eur. J.* 18, 4063 – 4072.
- Ngadaonye, J. I., Geever, L. M., Cloonan, M. O., Higginbotham, C. L., (2012). “Photopolymerised thermo-responsive poly(N,N-diethylacrylamide)-based copolymer hydrogels for potential drug delivery applications”. *J Polym Res.*, 19, 9822.
- Nicolas, S. and Jutta, R. (2010). “Synthesis of nanogels/microgels by conventional and controlled radical crosslinking copolymerization” *Polym. Chem.*, 1, 965–977.
- Nierzwicki, W. and Prins, W. (1975). “Sulfonated polysulfone” *J. Appl. Polym. Sci.*, 19, 1885.
- Nirala, N. R., Abraham, S., Kumar, V., Bansal, A., Srivastava, A. and Saxena, P. S. (2015). "Colorimetric detection of cholesterol based on highly efficient peroxidase mimetic activity of Graphene Quantum Dots". *Sens. Actuators, B.*, 218, 42–50.
- Nolan, C. M., Reyes, C. D., Debord, J. D., Garcia, A. J., Lyon, L. A. (2005). “Phase Transition Behavior, Protein Adsorption, and Cell Adhesion Resistance of Poly(Ethylene Glycol) Cross-Linked Microgel Particles”. *Biomacromolecules*, 6(4), 2032-2039.
- Nuran, I. and Hacer, K. (2018). “Thermoresponsive and biocompatible poly(vinyl alcohol)-graft poly(N, N-diethylacrylamide) copolymer: Microwave-assisted synthesis, characterization, and swelling behavior”. *J. Appl. Polym. Sci.*, 135, 45969.
- Nuran, I. and Şeyma, T. (2018) “Microwave based synthesis and spectral characterization of thermo-sensitive poly(N,N-diethylacrylamide) grafted pectin copolymer”. *Int. J. Biol. Macromol.*, 113, 669-680.
- Oh, J. K., Lee, D. I., Park, J. M. (2009). “Biopolymer-based microgels/nanogels for drug delivery applications”. *Prog Polym Sci.*, 34(12), 1261-1282.

## REFERENCES

- Otake, K., Inomata, H., Konno, M., Saito, S. (1990). "Thermal analysis of the volume phase transition with N-isopropylacrylamide gels". *Macromolecules*, 23(1), 283-289.
- Padilla, O. L., Ihre, H. R., Gagne, L., Fréchet, J. M. and Szoka, F. C. (2002). "Polyester dendritic systems for drug delivery applications: in vitro and in vivo evaluation". *Bioconjug Chem.*, 13(3), 453-461.
- Paek, K., Yang, H., Lee, J., Park, J. (2014). "Efficient Colorimetric pH Sensor Based on Responsive Polymer-Quantum Dot Integrated Graphene Oxide". *ACS Nano*. 8, 2848–2856
- Pan, L., Chortos, A., Yu, G., Wang, Y., Isaacson, S., Allen, R., Shi, Y., Dauskardt, R., Bao, Z. (2014). "An ultra-sensitive resistive pressure sensor based on hollow-sphere microstructure induced elasticity in conducting polymer film". *Nat. Commun.*, 5.
- Panayiotou, M. and Freitag, R. (2005). "Synthesis and characterisation of stimuli-responsive poly(N,N'- diethylacrylamide) hydrogels". *Polymer*, 46(3), 615-621.
- Panayiotou, M., Pöhner, C., Vandevyver, C., Wandrey, C., Hilbrig, F., Freitag, R. (2007). "Synthesis and characterisation of thermo responsive poly(N, N-diethyl acrylamide) microgels". *React Funct Polym.*, 67, 807–819.
- Pariksha, J. K., Yahya, E. C., Pierre, P. D. K., Thashree, M., Pradeep, K., Lisa, C. T., Viness, P. (2016). "A Review of Injectable Polymeric Hydrogel Systems for Application in Bone Tissue Engineering". *Molecules*, 21, 1580-1611.
- Park, K., Shalaby, W. S. W., Park, H. (1993). "Biodegradable Hydrogel for Drug Delivery". *Technomic Publi. Co., Inc., Lancaster, PA*, 252.
- Patil, J.S., Gurav, P. B., Mandave, S. V., *et al.* (2014). "Hydrogel system, a Smart and Intelligent Drug delivery Device: A systematic and Concise Review". *Ind. J. Novel Drug Deli.*, 6(2), 93-105.

## REFERENCES

- Pecoraro, M., Pizzo, M. D., Marzocco, S., Sorrentino, R., Ciccarelli, M., Iaccarino, G., Pinto, A., Popolo, A. (2016). “Inflammatory mediators in a short-time mouse model of doxorubicin-induced cardiotoxicity”. *Toxicol. Appl. Pharmacol.*, 293, 44–52.
- Pelton, R. (2000). “Temperature-sensitive aqueous microgels”. *Adv Colloid Interfac.*, 85(1), 1-33.
- Pelton, R. H. and Chibante, P. (1986). “Preparation of aqueous latices with N – isopropyl acrylamide”. *Colloid Surface.*, 20(3), 247-256.
- Peng, T. and Cheng, Y. L. (2001). “PNIPAAm and PMAA co-grafted porous PE membranes: living radical co-grafting mechanism and multi-stimuli responsive permeability”. *Polymer*, 42(5), 2091-2100.
- Peppas, N. A. (2012). “Hydrogels”. *An Introduction to Materials in Medicine*, 35-42.
- Peppas, N. A. and Mikos. A. G. (1986). “Preparation methods and structure of hydrogels”. *Hydrogels in Med. Pharm.*, CRC Press, Boca Raton, FL, 1, 1-27.
- Peppas, N. A., Bures, P., Leobandung, W., Ichikawa, H. (2000). “Hydrogels in pharmaceutical formulations”. *Eur J Pharm Biopharm.*, 50(1), 27-46.
- Peppas, N. A.; Hilt, J. Z.; Thomas, J. B. (2007). “Nanotechnology in therapeutics: Current technology and applications”. Norfolk, UK: Horizon Bioscience.
- Pilco-Ferreto, N. and Calaf, G. M. (2016). “Influence of doxorubicin on apoptosis and oxidative stress in breast cancer cell lines”. *Int. J. Oncol.*, 49(2), 753–762.
- Pinar, I. and Ozgur, O. (2017). “Novel stimuli-responsive hydrogels derived from morpholine: synthesis, characterization and absorption uptake of textile azo dye”. *Iraninan Poly. J.*, 26 (6), 391–404

## REFERENCES

- Pinkrah, V. T., Snowden, M. J., Mitchell, J. C., Seidel, J., Chowdhry, B. Z., Fern, G. R. (2003). "Physicochemical properties of poly (N-isopropylacrylamide-co-4-vinyl pyridine) cationic polyelectrolyte colloidal microgels". *Langmuir*, 19(3), 585-590.
- Popat, B. M and Sonali, S. A. (2017). "A hydrogels: Methods of preparation and applications". *Int. J. Adv. in Pharmaceutics*, 6, 79-85.
- Prager, G. W. and Poettler, M. (2012). "Angiogenesis in cancer". *Hamostaseologie*, 32(2), 105–114.
- Preethi, K. C., Siveen, K. S., Kuttan, R., Kuttan, G. (2010) "Inhibition of metastasis of B16F10 melanoma cells in C57BL/6 mice by an extract of *Calendula officinalis* L flowers". *Asian. Pac. J. Cancer. Prev.*, 11, 1773–1779.
- Qian, Z. Y., Fu, S. Z., Feng S. S. (2013) "Nanohydrogels as a prospective member of the nanomedicine family". *Nanomedicine*, 8(2), 161-164.
- Qinyuan, C., Yang, J., Xinjun, Y. (2017). "Hydrogels for Biomedical Applications: Their Characteristics and the Mechanisms behind Them". *Gels*, 3, 6-31.
- Qiu, J., Zhang, R., Li, J., Sang, Y., Tang, W., Gil, P.R., Liu, H. (2015). "Fluorescent graphene quantum dots as traceable , pH-sensitive drug delivery systems". *Int. J. Nanomedicine*, 10, 6709–6724.
- Qiu, Y. and Park, K. (2001). "Environment-sensitive hydrogels for drug delivery". *Adv. Drug Deliv. Rev.* 53, 321–339.
- Qu, D., Zheng, M., Zhang, L., Zhao, H., Xie, Z., Jing, X., Haddad, R. E., Fan, H., Sun, Z. (2014). "Formation mechanism and optimization of highly luminescent N-doped graphene quantum dots". *Sci. Rep.*, 4, 1–9.
- Quader, S. and Kataoka, K. (2017). "Nanomaterial-Enabled Cancer Therapy". *Molecular Therapy*, 25(7), 1-13.

## REFERENCES

Ramya, S. S. and Chidvila, V. (2013). "A Review on Skin Cancer". *Int. Research J. Pharmacy*, 4(8), 83-88.

Rasheed, T., Bilal, M. I., Hafiz, M. N. (2018). "The smart chemistry of stimuli-responsive polymeric carriers for target drug delivery applications". *Stimuli Responsive Polymeric Nanocarriers for Drug Delivery Applications*, 1, 61-99.

Rasool, N., Yasin, T., Heng, J. Y. Y., Akhter, Z. (2010). "Synthesis and characterization of novel ph, ionic strength and temperature- sensitive hydrogel for insulin delivery". *Polymer*, 51, 1687–1693.

Ritger, P. L. and Peppas, N. A. (1987a). "A simple equation for description of Solute Release I. Fickian and Non Fickian Release from Non Swellable Devices in the form of Slabs, Spheres, Cylinders or Discs". *J Control Release*, 5(1), 23-36.

Ritger, P. L. and Peppas, N. A. (1987b). "The simplest equation for description of solute release II. Fickian and anomalous release from swellable devices". *J Controlled Rel.*, 5(2), 37-42.

Roberta, B. R., Márcia, H. O., Andressa, T. F., Maíra, L. G., Alice, H. P., Maria, P. D. G. Marlus, C. (2015) "Nanotechnology-Based Drug Delivery Systems for Melanoma Antitumoral Therapy: A Review". *BioMed Research Int.*, 2015(841817), 1-22.

Rochet, N. M., Markovic, S. N., Porrata, L. F. (2012). "The role of complete blood cell count in prognosis-watch this space". *Oncol Hematol Rev.*, 8, 76–82.

Ronald, A. S. and Michael, J. R. (2012). "Fundamentals and Applications of Controlled Release Drug Delivery". *Adv. Delivery Sci. and Tech.*, 19-43.

Saranya, S. and Radha, K. V. (2014). "Review of Nanobiopolymers for Controlled Drug Delivery". *Poly-Plas. Tech. and Engi.*, 53(15), 1636-1646.

## REFERENCES

- Sasa, N. and Yamaoka, T. (1994). "Surface-activated photopolymer microgels". *Adv Mater.*, 6(5), 417-421.
- Sawai, T., Yamazaki, S., Ikariyama, Y., Aizawa, M. (1991). "pH-Responsive swelling of the ultrafine microsphere". *Macromolecules*, 24(8), 2117-2118.
- Schexnailder, P. and Schmidt, G. (2009) "Nanocomposite polymer hydrogels". *Colloid Polym Sci.*, 287, 1-11.
- Schild, H. G. (1992). "Poly (N-isopropylacrylamide): experiment, theory and application". *Prog Polym Sci.*, 17(2), 163-249.
- Schmaljohann, D., Oswald, J., Jørgensen, B., Nitschke, M., Beyerlein, D., Werner, C. (2003). "Thermo-responsive PNiPAAm-g-PEG films for controlled cell detachment". *Biomacromolecules*, 4(6), 1733-1739.
- Schroeder, K. L., Goreham, R. V., Nann, T. (2016). "Graphene Quantum Dots for Theranostics and Bioimaging". *Pharm Res.*, 33(10), 2337-57.
- Sen, M. and Sari, M. (2005). "Radiation synthesis and characterization of poly(N,N-dimethylaminoethylmethacrylate-co-N-vinyl 2-pyrrolidone) hydrogels." *Eur Polym J.*, 41(6), 1304-1314.
- Seon, J. K., Seoung gil Y., In Young, K., Sun, I. K. (2004). "Swelling Characterization of the Semiinterpenetrating Polymer Network Hydrogels Composed of Chitosan and Poly(diallyldimethylammonium chloride)" *J. Applied Poly. Sci.*, 91, 2876–2880.
- Shao, P., Wang, B., Wang, Y., Li, J., Zhang, Y. (2011). "The application of thermosensitive nanocarriers in controlled drug delivery". *J. of Nanomaterials*, 2011(389640), 1-12.
- Sharma, S., Kaur, P., Jain, A., Rajeswari, M. R., Gupta, M. N. (2003). "A smart bioconjugate of chymotrypsin". *Biomacromolecules*, 4(2), 330-336.

## REFERENCES

- Shin, Y., Park, J., Hyun, D., Yang, J., Lee, J. H., Kim, J. H., Lee, H. (2015). "Acid-free and oxone oxidant-assisted solvothermal synthesis of graphene quantum dots using various natural carbon materials as resources". *Nanoscale*, 7, 5633–5637.
- Shiroya, T., Tamura, N., Yasui, M., Fujimoto, K., Kawaguchi, H. (1995). "Enzyme immobilization on thermosensitive hydrogel microspheres". *Colloid Surface B*, 4(5), 267-274.
- Siamak, J. and Hassan, N. (2018). "Doxorubicin loaded carboxymethyl cellulose/graphene quantum dot nanocomposite hydrogel films as a potential anticancer drug delivery system". *Materials Science & Engineering C*, 87, 50–59.
- Siegel, R. A., Rathbone, M. J. (2012). "Overview of Controlled Release Mechanisms. In: Siepmann, J., *et al.*, Eds., Fundamentals and Applications of Controlled Release Drug Delivery". *Advances in Delivery Science and Technology*. 21-22.
- Siepmann, J. and Peppas, N.A. (2001). "Modeling of drug release from delivery systems based on hydroxypropyl methylcellulose (HPMC)". *Adv. Drug Delivery Reviews*, 48 139–157
- Silva, J., Alexandra, R. F., Pedro, V. B., (2014). "Application of Nanotechnology in Drug Delivery". 10.5772/58424.
- Singh, R., Lillard Jr, J.W., (2009). "Nanoparticle-based targeted drug delivery". *Exp. Mol. Pathol.* 86, 215–223.
- Singh, Y., Jaya, G. M., Kavit, R., Farooq, A. K., Mohini, C., Nitin, K. J., Manish, K. C. (2017). "Nanoemulsion: Concepts, development and applications in drug delivery". *J. Controlled Release*, 252, 28–49.
- Siqueira, N. M., Cirne, M. F. R., Immich, M. F., Poletto, F. (2018). "Stimuli-responsive polymeric hydrogels and nanogels for drug delivery applications" *Stimuli Responsive Polymeric Nanocarriers for Drug Delivery Applications*, 1, 343-374.



## REFERENCES

- Snowden, M. J., Thomas, D., Vincent, B. (1993). "Use of colloidal microgels for the absorption of heavy metal and other ions from aqueous solution". *Analyst*, 118(11), 1367-1369.
- Soga, O., van Nostrum, C. F., Fens, M., Rijcken, C. J., Schiffelers, R. M., Storm, G., Hennink, W. E. (2005). "Thermosensitive and biodegradable polymeric micelles for paclitaxel delivery". *J Control Release*, 103(2), 341-353.
- Soha, A., Hajar, A., Amir, A. (2017). "Mathematical modeling of drug release from swellable polymeric nanoparticles". *J. Applied Pharmaceutical Sci.*, 7, 125-133.
- Solans, C., Izquierdo, P., Nolla, J., Azemar, N., Garcia-Celma, M. J. (2005). "Nano-emulsions". *Current Opinion in Colloid & Interface Science*, 10, 102 – 110.
- Song, L., Shi, J., Lu, J., and Lu, C. (2015). "Structure observation of graphene quantum dots by single-layered formation in layered confinement space". *Chem. Sci.*, 6(8), 4846–4850.
- Sood, N., Bhardwaj, A., Mehta, S., Mehta, A. (2014). "Stimuli-responsive hydrogels in drug delivery and tissue engineering". *Drug Deliv.* 7544, 1–23.
- Soppimath, K. S., Aminabhavi, T. M., Dave, A. M., *et al.* (2002). "Stimulus-responsive "smart" hydrogels as novel drug delivery systems". *Drug Dev Ind Pharm.*, 28, 957–974.
- Sowmya, V., Ravinder, E., Esteban, F. D-L. (2017) "Recent Advances in Hydrogel-Based Drug Delivery for Melanoma Cancer Therapy: A Mini Review". *J. Drug Delivery* 2017(7275985), 1-9.
- Sponarova, D. and Horak, D. (2008). "Poly(N, N-diethyl acrylamide) Microspheres by Dispersion Polymerization". *J. Poly. Sci. Part A: Poly. Chem.*, 46, 6263-6271.

## REFERENCES

Staudinger, H. and Husemann, E. (1935). "Über hochpolymere verbindungen, 116. Mitteil.: Über das begrenzt quellbare poly-styrol". *Ber Deuts Chem Ges.*, 68, 1618-1634.

Strandmana, S., Lessard, D.G., Dusschotenb, D.V., Wilhelm, M.P.M., Wood-Adams, Spiessb, H.W., Zhu, X.X. (2012). "Two-dimensional Fourier transform rheological study on thermosensitivity of poly(N,N-diethylacrylamide) in aqueous solutions". *Polymer*, 53, 4800-4805.

Sudipta, S., Arun, K. M., Sunil, K., Pralay, M. (2018) "Controlled drug delivery vehicles for cancer treatment and their performance". *Signal Transduction and Targeted Therapy*, 3, 1-7.

Sui, X., Luo, C., Wang, C., Zhang, F., Zhang, J., Guo, S. (2016). "Graphene quantum dots enhance anticancer activity of cisplatin via increasing its cellular and nuclear uptake, Nanomedicine: Nanotechnology". *Biol. & Med.* 12, 1997–2006.

Susana, S., Ana, F., Francisco, V. (2012). "Modular Hydrogels for Drug delivery". *J. Biomateri. Nanobiotech.*, 3, 185-199.

Suvakanta, D., Narasimha, P. M., lilakanta, N., Prasanta, C. (2010). "Kinetic modeling on drug release from controlled drug delivery systems". *Acta poloniae pharmaceutica-drug research*, 67(3), 217-223.

Swapnil, S. B., Srikumar, M. R., Jong, O. K., Bhopal, M., Kruti. S. S., Haitao, L., *et al.* (2015). "Polypeptide-based nanogels co-encapsulating a synergistic combination of doxorubicin with 17-AAG show potent anti-tumor activity in ErbB2-driven breast cancer models". *J. Controlled Release*, 208, 59-66.

Tacar, O., Sriamornsak, P., Dass, C. R. (2013). "Doxorubicin: an update on anticancer molecular action, toxicity and novel drug delivery systems". *J. Pharm. Pharmacol.*, 65(2), 157–170.

## REFERENCES

- Tadros, T., Izquierdo, P., Esquena, J., Solans, C. (2004). "Formation and stability of nano-emulsions". *Adv Colloid Interfac Sci.*, 108, 303-318.
- Tang, L., Ji, R., Cao, X., Lin, J., Jiang, H., Li, X., Teng, K. S., Luk, C. M., Zeng, S., Hao, J., Lau, P. (2012). "Deep Ultraviolet Photoluminescence of Water-Soluble Self-Passivated Graphene Quantum Dots". *ACS Nano*. 6 (6), 5102–5110.
- Tauer, K., Hernandez, H., Kozempel, S., Lazareva, O., Nazaran, P. (2008). "Towards a consistent mechanism of emulsion polymerization—new experimental details". *Colloid Polym Sci.*, 286, 499–515.
- Tawona, N. C., Lissinda, H. du P., Minja, G., Josias, H. H., Jeanetta, du. P. (2014). "Review of Natural Compounds for Potential Skin Cancer Treatment". *Molecules*, 19, 11679-11721.
- Taylor, L. D. and Cerankowski, L. D. (1975). "Preparation of films exhibiting a balanced temperature dependence to permeation by aqueous solutions—a study of lower consolute behavior". *J Polym Sci Pol Chem.*, 13(11), 2551-2570.
- Thakur, S., Pramod, K. S., Malviya, R. (2017). "Utilization of Polymeric Nanoparticle in Cancer Treatment: A Review". *J Pharma Care Health Sys.*, 4(2), 1-12.
- Thickett, S. C. and Gilbert, R. G. (2007). "Emulsion polymerization: State of the art in kinetics and mechanisms". *Polymer*, 48, 6965-6991.
- Thorne, J. B., Vine, G. J., Snowden, M. J. (2011). "Microgel applications and commercial considerations". *Colloid Polym Sci.*, 289(5-6), 625-646.
- Tirumala, V. R. and Ilavsky, J. (2006). "Effect of chemical structure on the volume phase transition in neutral and weakly charged poly(N-alkyl(meth)acrylamide) hydrogels studied by ultrasmall-angle X-ray scattering". *J Chem Phys.*, 124, 234911–20.

## REFERENCES

- Torchilin, V. (2011). "Tumor delivery of macromolecular drugs based on the EPR effect". *Adv. Drug Deliv. Rev.*, 63(3), 131–135.
- Torre, L. A., Bray, F., Siegel, R. L., Ferlay, J., Lortet-Tieulent, J., Jemal, A. (2015). "Global cancer statistics, 2012". *CA. Cancer J. Clin.*, 65(2), 87–108.
- Ullah, F., Bisyrul, H., Othman, J., F., Ahmad, Z., Md. Akil, H. (2015). "Classification, processing and application of hydrogels: A review". *Mat. Sci. and Engi. C*, 57, 414–433.
- Valappil, M. O., Pillai, V. K., Alwarappan, S. (2017). "Spot lighting graphene quantum dots and beyond: Synthesis, properties and sensing applications". *Applied Materials Today*, 9, 350–371.
- Vamvakaki, M., Palioura, D., Spyros, A., Armes, S. and Anastasiadis, S. (2006). "Dynamic light scattering vs H-1 NMR investigation of pH-responsive diblock copolymers in water". *Macromolecules*, 39(15), 5106-5112.
- Varaprasad, K., Raghavendra, G. M., Jayaramudu, T., Yallapu, M. M., Sadiku, R. (2017) "A mini review on hydrogels classification and recent developments in miscellaneous applications". *Mat. Sci. and Engi. C*, 79, 958-971.
- Vilar, G., Tulla-Puche, J., and Albericio, F. (2012). "Polymers and drug delivery systems". *Curr. Drug Deliv.*, 9(4), 367–394.
- Vincent, B. R. I. A. N. (2006). "Microgels and core-shell particles". In *Surface Chemistry in Biomedical and Environmental Science*, Springer, Netherlands, 11-22.
- Wang, C., Wu, C., Zhou, X., Han, T., Xin, X., Wu, J., Zhang, J., Guo, S. (2013). "Enhancing Cell Nucleus Accumulation and DNA Cleavage Activity of Anti-Cancer Drug via Graphene Quantum Dots". *Sci. Rep.*, 3, 2852-2860.

## REFERENCES

- Wang, J. and Qiu, J. (2015). "Luminescent Graphene Quantum Dots: As Emerging Fluorescent Materials for Biological Application". *Science of Advanced Materials*, 7, 1-11.
- Wang, W. and Qin, W. A. (2010). "Preparation, Swelling and Water-Retention Properties of cross-linked Superabsorbent Hydrogels Based on Guar Gum". *Adv Material research*, 96, 177-182.
- Wang, X., Sun, X., Lao, J., He, H., Cheng, T., Wang, M., Wang, S., Huang, F. (2014). "Multifunctional graphene quantum dots for simultaneous targeted cellular imaging and drug delivery". *Colloids Surf B:Biointerfaces*, 122, 638-644.
- Wang, Y., Song, C., Yu, X., Liu, L., Han, Y., Chen, J., Fu, J. (2017). "Thermo-responsive hydrogels with tunable transition temperature crosslinked by multifunctional graphene oxide nanosheets". *Compos. Sci. Technol.*, 151, 139–146.
- Wang, Z. C., Xu, X. D., Chen, C. S., Wang, G. R., Wang, B., Zhang, X. Z., Zhuo, R. X. (2008). "Study of Novel Hydrogels Based on. Thermosensitive PNIPAAm with pH Sensitive PDMAEMA Grafts". *Colloid Surf. B.*, 67, 245.
- Wang, Z., Dabrosin, C., Yin, X., Fuster, M. M., Arreola, A., Rathmell, W. K., Generali, D., Nagaraju, G. P., El-Rayes, B., Ribatti, D. (2015). "Broad targeting of angiogenesis for cancer prevention and therapy". *Semin. Cancer Biol.*, S224–S243.
- Ward, M. A. and Georgiou, T. K. (2011). "Thermoresponsive Polymers for Biomedical Applications." *Polymers*, 3, 1215-1242.
- Webb, B. A., Chimenti, M., Jacobson, M. P., Barber, D. L. (2011). "Dysregulated pH: a perfect storm for cancer progression". *Nat. Rev. Cancer*, 11(9), 671.
- Wei, W., Qi, X., Li, J., Zuo, G., Sheng, W., Zhang, J., Dong, W. (2016). "Smart macroporous salectan/poly (N, N-diethylacrylamide) semi-IPN hydrogel for anti-inflammatory drug delivery". *ACS Biomater. Sci. Eng.*, 2(8), 1386–1394.

## REFERENCES

- Weissman, J. M., Sunkara, H. B., Albert, S. T., Asher, S. A. (1996). "Thermally switchable periodicities and diffraction from mesoscopically ordered materials". *Science*, 274(5289), 959-963.
- Wichterle, O. (1971). "Hydrogels". in: H.F. Mark, N.G. Gaylord (Eds.), *Encyclopedia of Polymer Science and Technology*, Interscience, New York, USA, 273.
- Wichterle, O. and Lim, D. (1960). "Hydrophilic gels for biological use". *Nature*, 185, 117-118.
- William, B. L., David, R. K., Brandon, V. S., Peppas, N. A. (2010) "Polymers for Drug Delivery Systems". *Annu Rev Chem Biomol Eng.*, 1, 149–173.
- Wolfenden, R. (2017). "Experimental Measures of Amino Acid Hydrophobicity and the Topology of Transmembrane and Globular Proteins". *J. Gen. Physiol.*, 129, 357-362.
- Wu, X., Tian, F., Wang, W., Chen, J., Wu, M., Zha, J. X. (2013). "Fabrication of highly fluorescent graphene quantum dots using L-glutamic acid for in vitro/in vivo imaging and sensing". *J. Mat. Chem. C.*, 1, 4676– 4684.
- Wu, Z. L., Gao, M. X., Wang, T. T., Wan, X. Y., Zhenga, L. L., Huang, C. Z. (2014). "A general quantitative pH sensor developed with dicyandiamide N-doped high quantum yield graphene quantum dots". *Nanoscale*, 6, 3868.
- Xiao, X. C. (2007). "Effect of the initiator on thermosensitive rate of poly(N-isopropylacrylamide) hydrogels". *Express Polymer Letters*, 1(4), 232–235.
- Xiayun, Z., Zhongduo, Y., Dengmin, X., Donglei, L., Zhenbin, C., *et al.* (2018). "Design and synthesis study of the thermo-sensitive poly (N-vinylpyrrolidone-b- N, N-diethylacrylamide)". *Des Monomers Polym.*, 21(1), 43–54.

## REFERENCES

- Xu, F., Kang, E., Neoh, K. (2006). "pH- and temperature-responsive hydrogels from cross linked triblock copolymers prepared via consecutive atom transfer radical polymerizations". *Biomaterials*, 27, 2787–2797.
- Xu, X., Wang, X., Luo, W., Qian, Q., Li, Q., Han, B., Li, Y. (2017). "Triple cell-responsive nanogels for delivery of drug into cancer cells". *Colloids Surf. B. Biointerfaces*, 163, 362–368.
- Xu, Y., Guo, J., Chen, D., Cao, L., Dong, M. (2018). "Synthesis and Thermo-thickening Behavior of Graft Copolymers Based on poly(N,N-Diethylacrylamide-co-N,N-Dimethylacrylamide) Side Chains". *Polymer - Plastics Technology and Engineering*, 57(12), 1265-1276.
- Xuan, W., Ruiyi, L., Saiying, F., Zaijun, L., Guangli, W., Zhiguo, G. (2017). "D-penicillamine-functionalized graphene quantum dots for fluorescent detection of Fe<sup>3+</sup> in iron supplement oral liquids". *Sensors Actuators B. Chem.*, 243, 211–220.
- Yajing, W., Jiu, W., Hongjiang, X., Liang, G., Jiabi, Z. (2015). "Investigation of dual-sensitive nanogels based on chitosan and N-isopropylacrylamide and its intelligent drug delivery of 10-hydroxycamptothecin". *Drug Deliv.*, 22, 803–813.
- Yan, F., Jiajun, T., Sierin, L., Siowling, S. (2018). "Rupturing cancer cells by the expansion of functionalized stimuli-responsive hydrogels". *NPG Asia Materials*, 10, e465.
- Yan, X., Cui, X., Li, B., Li, L. S. (2010). "Large, Solution-Processable Graphene Quantum Dots as Light Absorbers for Photovoltaics". *Nano Lett.*, 10, 1869–1873.
- Yan, X., Cui, X., Li, L. (2010). "Synthesis of Large, Stable Colloidal Graphene Quantum Dots with Tunable Size". *J. Am. Chem. Soc.*, 132, 5944–5945.
- Yang, F., Teves, S. S., Kemp, C. J., Henikoff, S. (2014). "Doxorubicin, DNA torsion, and chromatin dynamics". *Biochim. Biophys. Acta*, 1845(1), 84–89.

## REFERENCES

Yao, X., Niu, X., Ma, K., Huang, P., Grothe, J., Kaskel, S., Zhu, Y. (2017). "Graphene Quantum Dots-Capped Magnetic Mesoporous Silica Nanoparticles as a Multifunctional Platform for Controlled Drug Delivery, Magnetic Hyperthermia, and Photothermal Therapy". *Small*, 13, 2225-2236.

Yasuhiro, K. and Yoshiaki, T. (2016). "Synthesis of Thermo-Responsive Polymer via Radical (Co)polymerization of N,N-Dimethyl- $\alpha$ -(hydroxymethyl)acrylamide with N,N-Diethyl acrylamide". *Polymers*, 8, 374-381

Yasui, M., Shiroya, T., Fujimoto, K., Kawaguchi, H. (1997). "Activity of enzymes immobilized on microspheres with thermosensitive hairs". *Colloid Surface B.*, 8(6), 311-319.

Yin, L., Fei, L., Cui, F., Tang, C., Yin, C. (2007). "Superporous hydrogels containing poly (acrylic acid- co -acrylamide )/ O -carboxymethyl chitosan interpenetrating polymer networks". *Biomaterials*, 28, 1258–1266.

Yom-Tov, O., Neufeld, L., Seliktar, D., Bianco-Peled, H. (2014) "A novel design of injectable porous hydrogels with in situ pore formation". *Acta Biomater.*, 10, 4236–4246.

Yoshida, R. and Okano, T. (2010). "Biomedical Applications of Hydrogels Handbook" 19–44.

Yoshida, R., Uchida, K., Kaneko, Y., Sakai, K., Kikuchi, A., Sakurai, Y., Okano, T. (1995). "Comb-type grafted hydrogels with rapid deswelling response to temperature changes". *Nature*, 374, 240–242.

Young, R. J., Kinloch, I. A., Gong, L., Novoselov, K. S. (2012). "The mechanics of graphene nanocomposites: a review". *Compos. Sci. Technol.*, 72, 1459–1476.

Yu, D. S., Yan, H. Y., Wu, C. L., Hung, S. H. (2017). "Comparison of therapeutic efficacy of lipo-doxorubicin and doxorubicin in treating bladder cancer". *Urol. Sci.*, 28,



## REFERENCES

200–205.

Yu, J., Fan, H., Huang, J., Chen, J. (2011). “Fabrication and evaluation of reduction-sensitive supramolecular hydrogel based on cyclodextrin/polymer inclusion for injectable drug-carrier application”. *Soft Matter*, **7**, 7386–7394.

Yu, M., Zhiying, S., Johnny, V., Orit, K. P., Andrew, Z. W. (2016) “Application of nanotechnology to cancer radiotherapy”. *Cancer Nano*, **7**, 11.

Yu, X., Zhang, W., Zhang, P., Su, Z. (2017). "Fabrication technologies and sensing applications of graphene-based composite films: Advances and challenges". *Biosens. Bioelectron.*, **89**, 72–84.

Yu, Y., De Andrade, L.C.X., Fang, L., Ma, J., Zhang, W., Tang, Y. (2015). “Graphene oxide and hyperbranched polymer-toughened hydrogels with improved absorption properties and durability”. *J. Mater. Sci.*, **50**, 3457–3466.

Yuekui, Z., Shanshan, T., Jiamin, G., Murad, A., Shunxiu, C., Zhaocong, Y., Fangfang, Z., Yumeng, S., Minjie, S., Ran, M., Li, Z., Liang, J. (2017) “Targeted delivery of doxorubicin by nano-loaded mesenchymal stem cells for lung melanoma metastases therapy.” *Scientific reports*, **7**, 44758.

Zardad, A. Z., Choonara, Y., du Toit, L., Kumar, P., Mabrouk, M., Kondiah, P., Pillay, V. (2016). “A review of thermoand ultrasound-responsive polymeric systems for delivery of chemotherapeutic agents”. *Polymers*, **8**, 359.

Zeng, M., Wang, X., Yu, Y., Zhang, L., Shafi, W., Huang, X., Cheng, Z. (2016). “The Synthesis of Amphiphilic Luminescent Graphene Quantum Dot and Its Application in Miniemulsion Polymerization”. *J. Nanomater.*, **2016**(6490383), 1-8.

Zhang, J. T. and Jandt, K. D. (2008). “A novel approach to prepare porous poly(N-isopropylacrylamide) hydrogel with superfast shrinking kinetics”. *Macromol Rapid Comm.*, **29**(7), 593-597.

## REFERENCES

Zhang, N., Liu, M., Shen, Y., Chen, J., Dai, L., Gao, C. (2011). "Preparation, properties, and drug release of thermo- and pH-sensitive poly((2-dimethylamino)ethyl methacrylate)/poly(N,N-diethylacrylamide) semi-IPN hydrogels". *J. Mater. Sci.* 46, 1523–1534.

Zhang, P., Huang, Y., Lu, X., Zhang, S., Li, J., Wei, G., Su, Z. (2014). "One-Step Synthesis of Large-Scale Graphene Film Doped with Gold Nanoparticles at Liquid–Air Interface for Electrochemistry and Raman Detection Applications". *Langmuir*, 30, 8980–8989.

Zhang, W., Ding, Y., Feng, Q., Wei, N., Li, S., Liu, Z., Li, X., Li, L. (2016). "Synthesis and characterization of poly (N-isopropylacrylamide)/graphene oxide nanocomposite hydrogels by using glow discharge electrolysis plasma". *Soft Mater.* 4468, 1539–4468.

Zhang, W., Zhang, P., Su, Z., Wei, G. (2015). "Recent advances in the fabrication and structure-specific applications of graphene-based inorganic hybrid membranes". *Nanoscale*, 7, 18364–18378.

Zhang, Y., Liu, T., Wang, Q., Zhao, J., Fang, J., Shen, W. (2012) "Synthesis of novel poly(N,N-diethylacrylamide-co-acrylic acid) (P(DEA-co-AA)) microgels as carrier of horseradish peroxidase immobilization for pollution treatment". *Macromolecular Research*, 20(5), 484-489.

Zhao, X., Yang, L., Li, X., Jia, X., Liu, L., Zeng, J., Guo, J., Liu, P. (2015.). "Functionalized graphene oxide nanoparticles for cancer cell-specific delivery of antitumor drug". *Bioconjug. Chem.* 26, 128–136.

Zhao, X., Zhang, P., Chen, Y., Su, Z., Wei, G. (2015). "Recent advances in the fabrication and structure-specific applications of graphene-based inorganic hybrid membranes". *Nanoscale*, 7, 5080–5093.

## REFERENCES

Zheng, X. T., Ananthanarayanan A., Luo K. Q., Chen P. (2014). "Glowing Graphene Quantum Dots and Carbon Dots: Properties, Syntheses, and Biological Applications." *Small*, 11, 1620–1636.

Zhou, L., Geng, J., Liu, B. (2013). "Graphene Quantum Dots from Polycyclic Aromatic Hydrocarbon for Bioimaging and Sensing of Fe<sup>3+</sup> and Hydrogen Peroxide". *Part. Part. Syst. Charact.*, 30, 1086–1092.

## REFERENCES

# **APPENDICES**



APPENDIX I

AI.1 Calibration curve for Doxorubicin (DOX)

Standard solutions of the DOX in the range of 5 to 40 PPM in increment of 5 PPM were prepared in milli-Q water. The absorbance was read against milli-Q water blank at 480 nm.

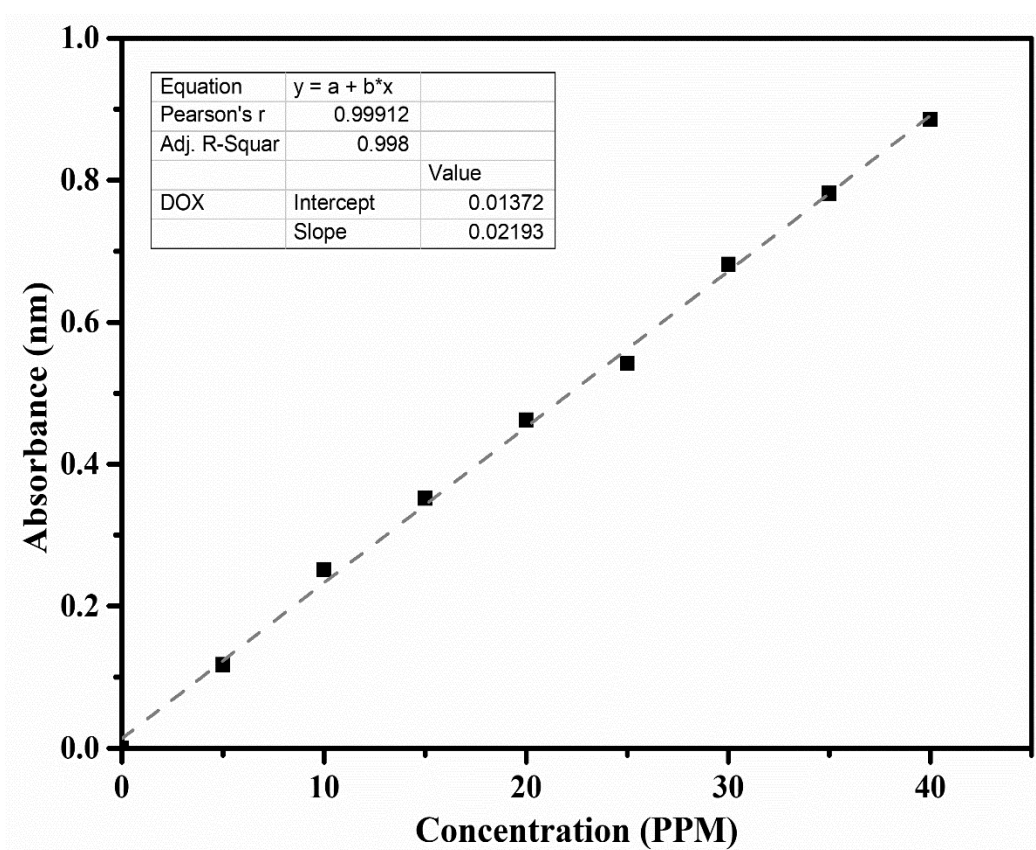
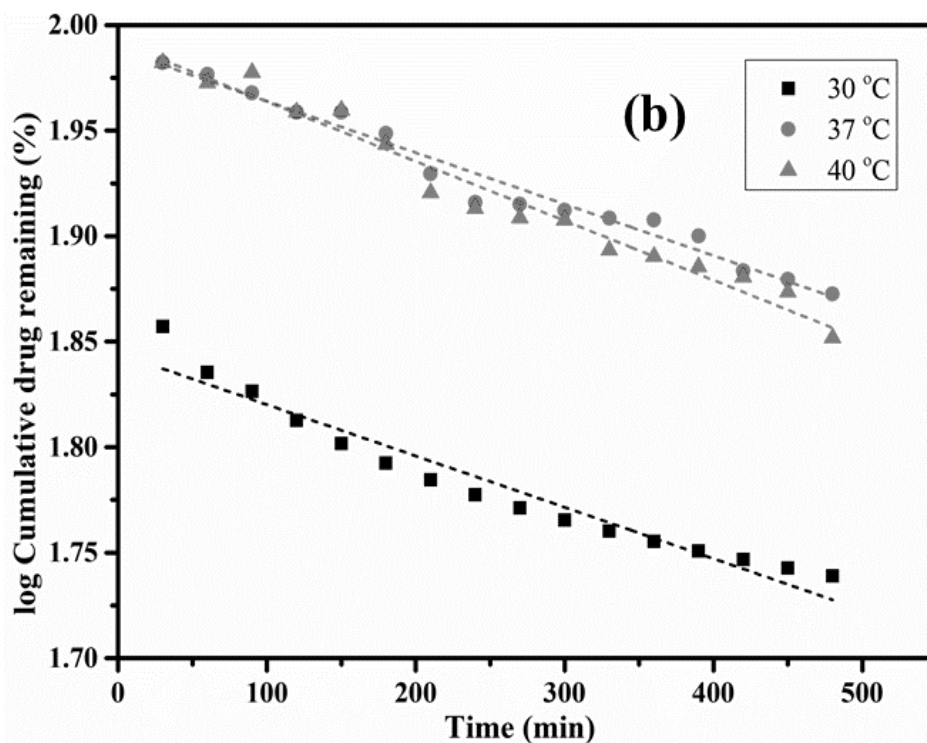
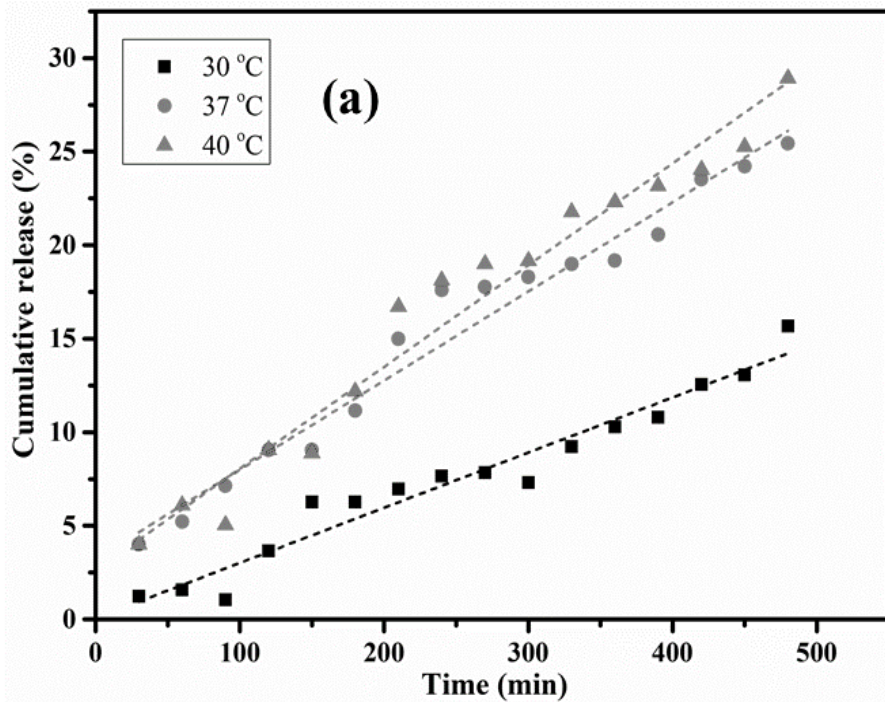


Figure AI.1: Calibration curve for Doxorubicin

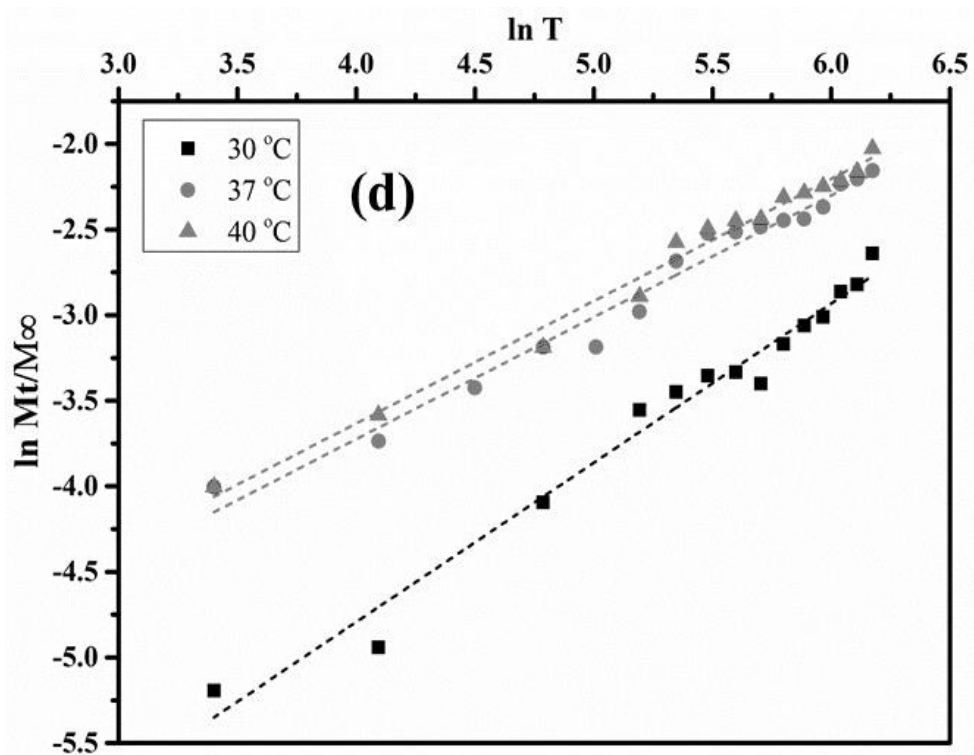
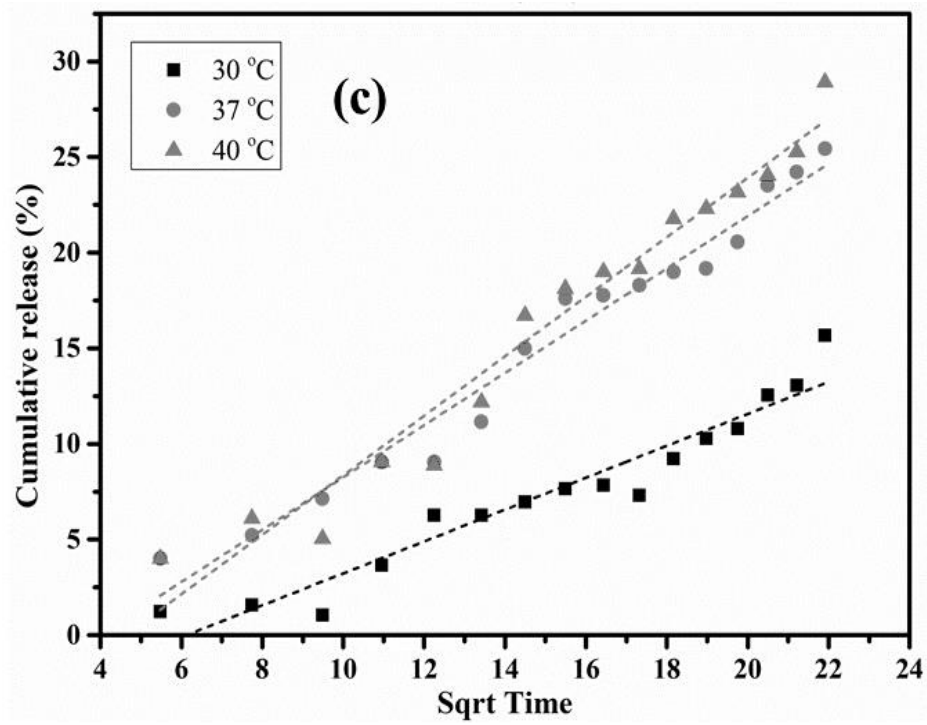
# APPENDICES

## AI.2 Dox release kinetics studied for T36 hydrogel at different temperature



AI.2: Dox release kinetics studied for T36 hydrogel at different temperature:  
(a) % Cumulative release vs time (Zero-order kinetics); (b) % log cumulative drug remaining vs time (First-order kinetics)

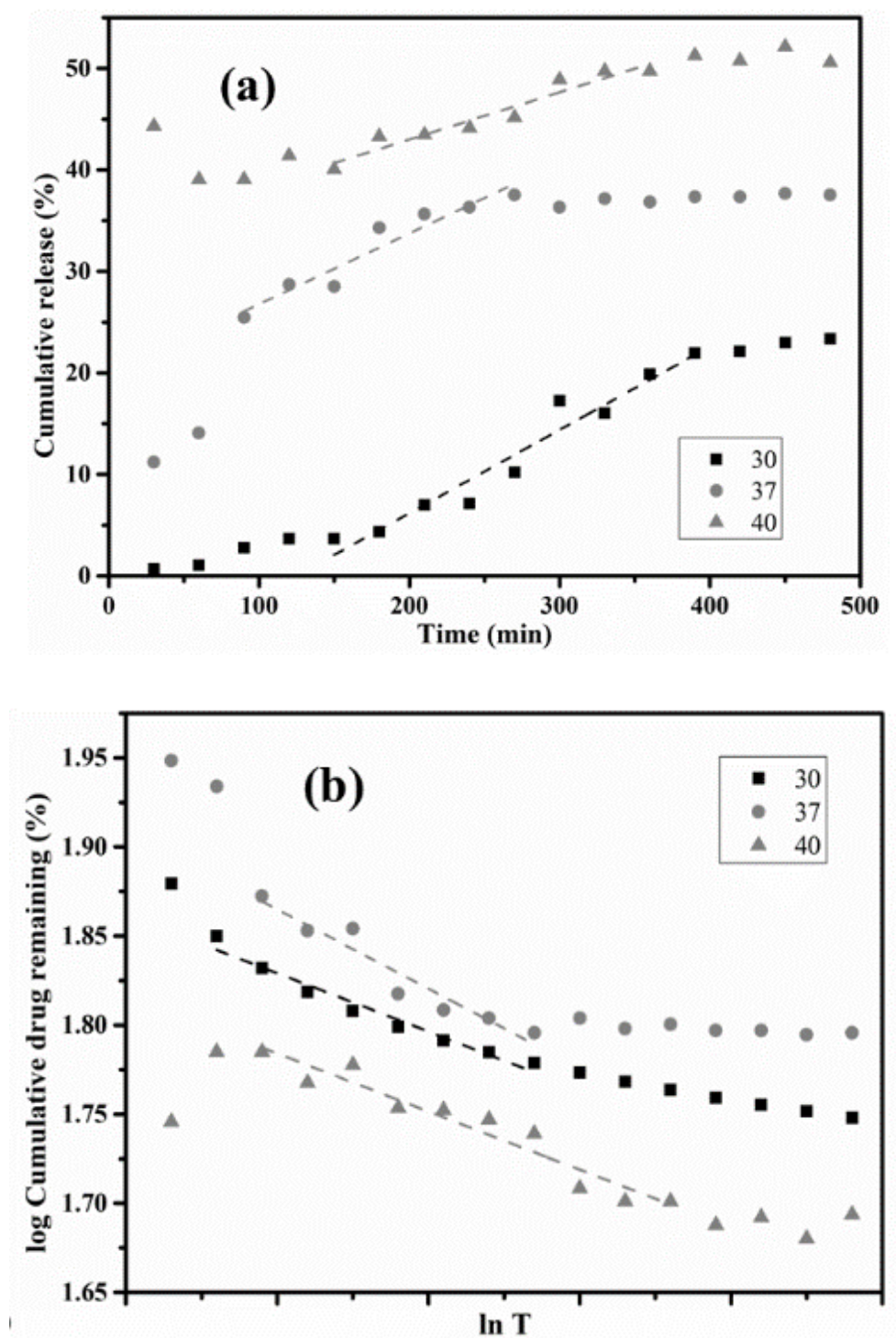




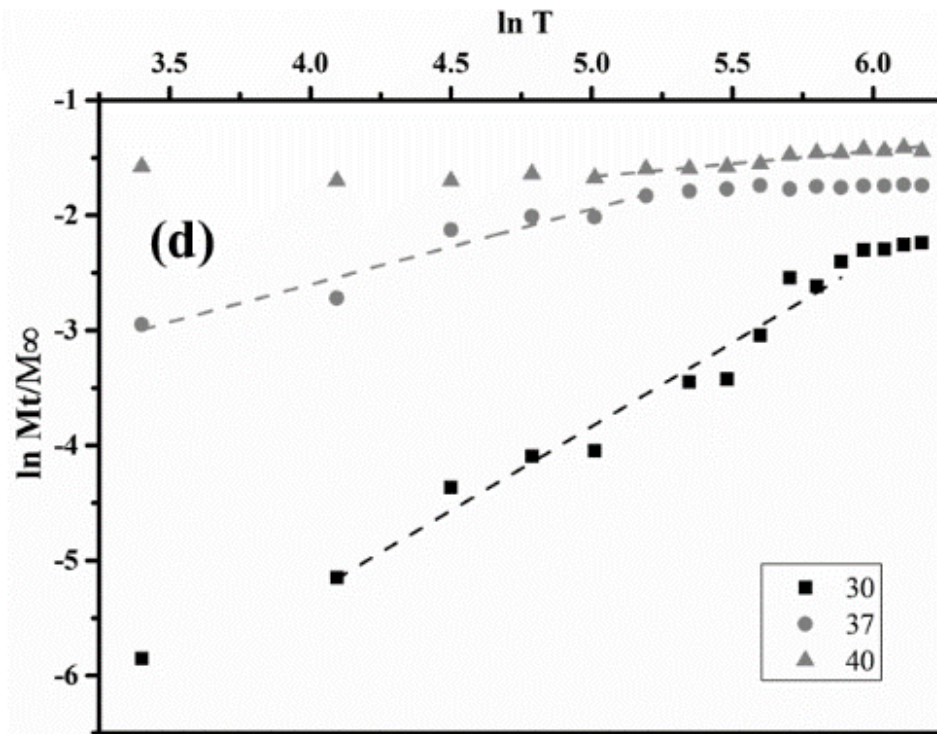
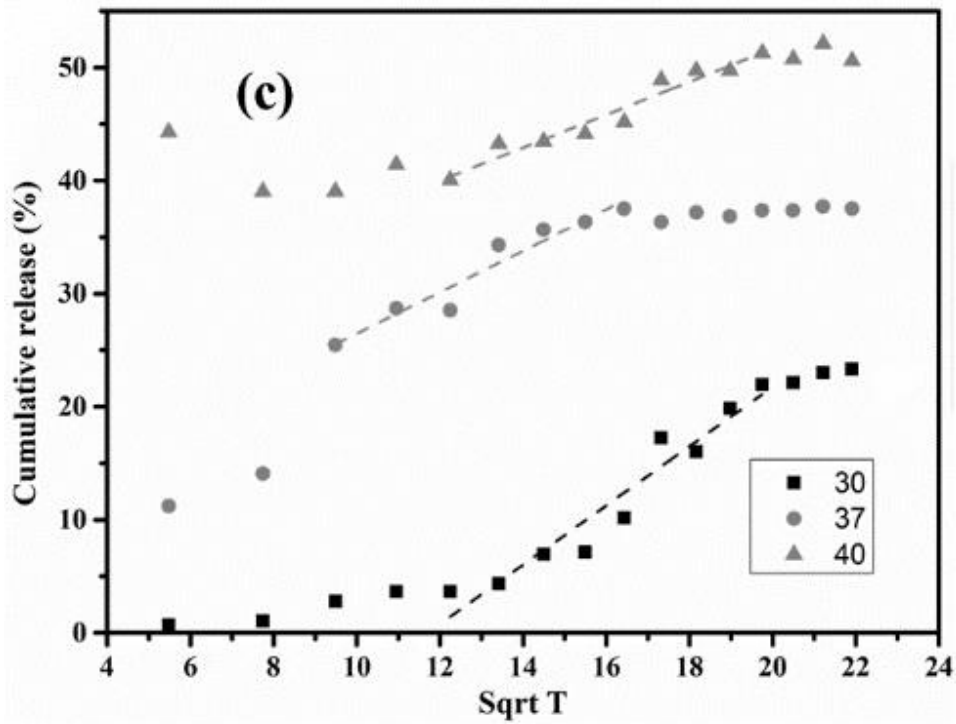
AI.2: Dox release kinetics studied for T36 hydrogel at different temperature: (c) % Cumulative release vs sqrt of time (Higuchi model) and (d)  $\ln M_t/M_\infty$  vs  $\ln T$  (Korsmeyer-Peppas model)

## APPENDICES

### AI.3 Dox release kinetics studied for HG-4 hydrogel at different temperature



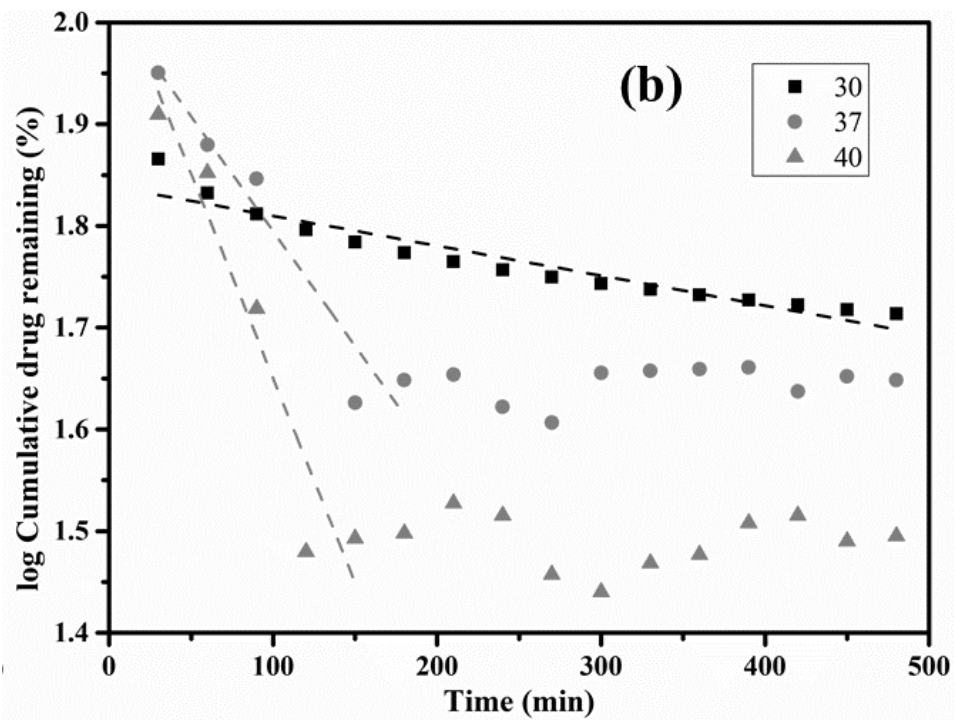
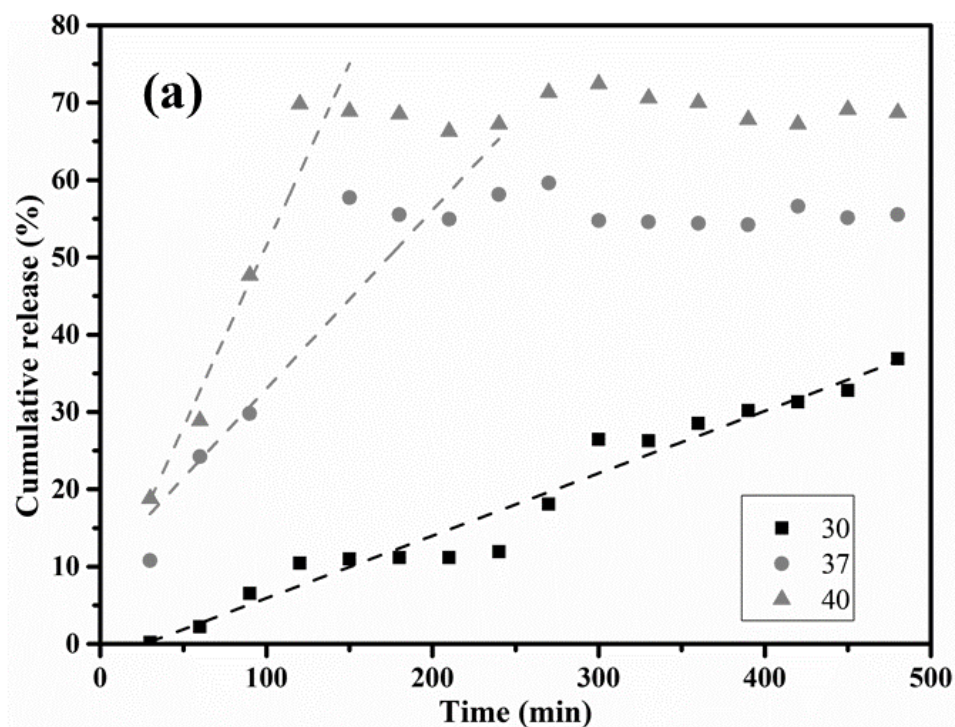
AI.3: Dox release kinetics studied for HG-4 hydrogel at different temperature: (a) % Cumulative release vs time (Zero-order kinetics); (b) % log cumulative drug remaining vs time (First-order kinetics)



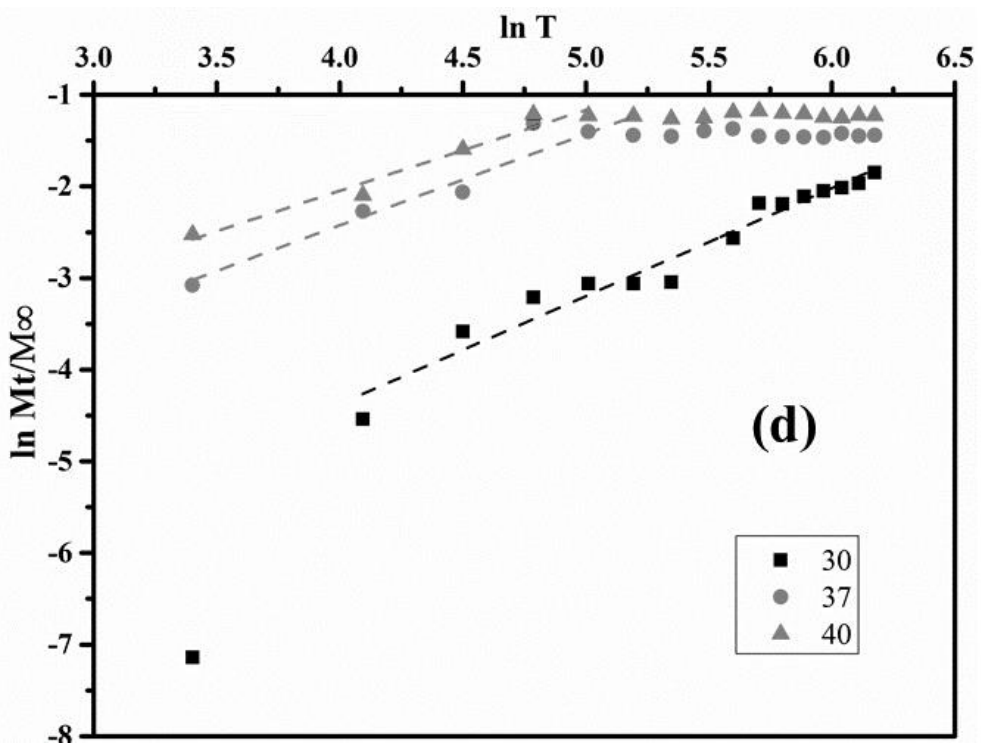
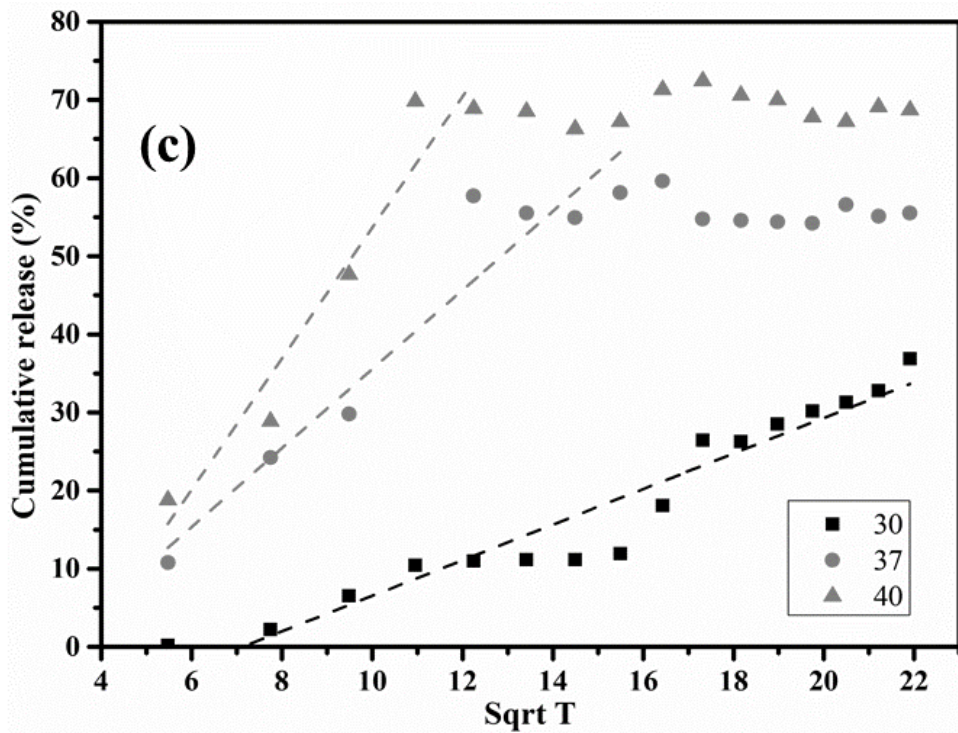
AI.3: Dox release kinetics studied for HG-4 hydrogel at different temperature: (c) % Cumulative release vs sqrt of time (Higuchi model) and (d)  $\ln M_t/M_\infty$  vs  $\ln T$  (Korsmeyer-Peppas model)

# APPENDICES

## AI.4 Dox release kinetics studied for HL-7 hydrogel at different temperature



AI.4: Dox release kinetics studied for HL-7 hydrogel at different temperature:  
(a) % Cumulative release vs time (Zero-order kinetics); (b) % log cumulative drug remaining vs time (First-order kinetics)

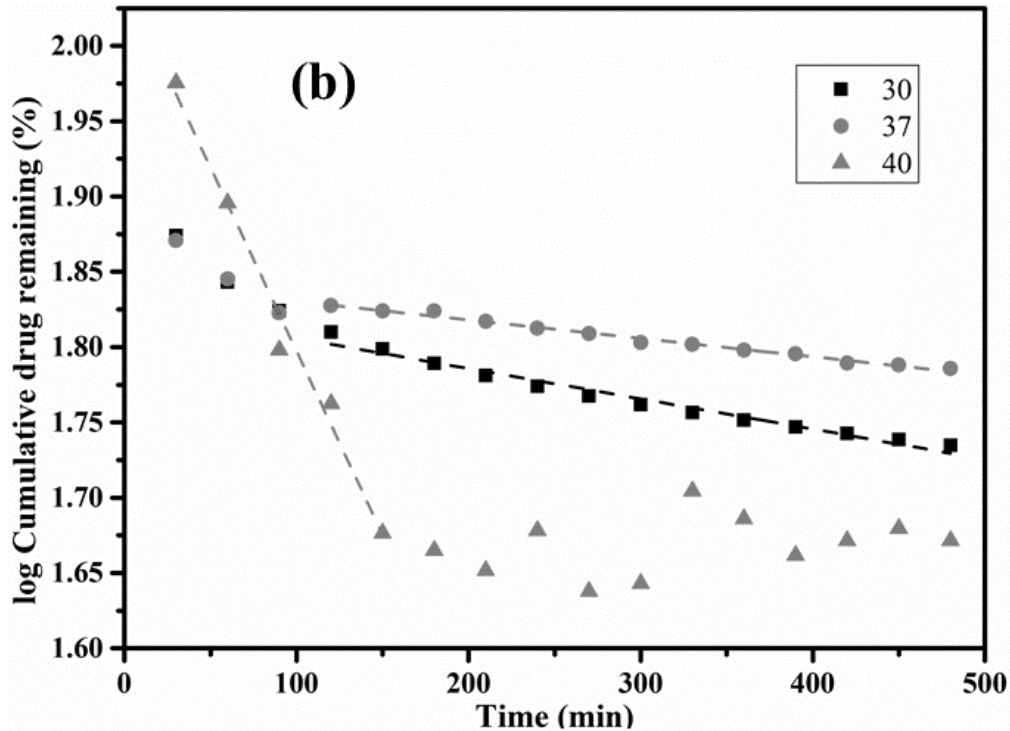
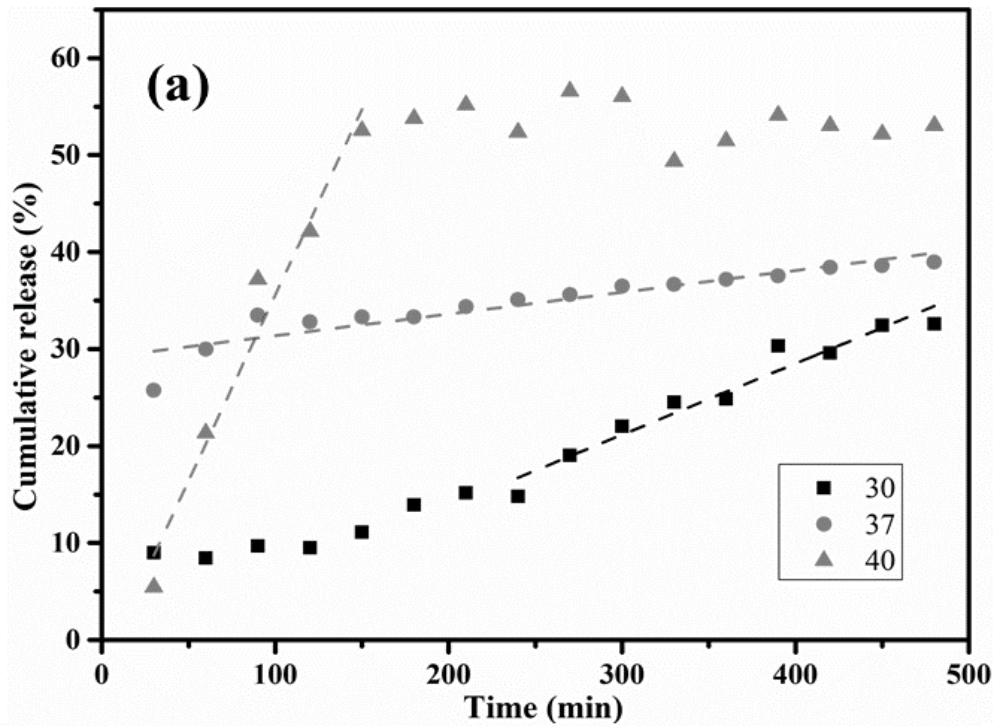


AI.4: Dox release kinetics studied for HL-7 hydrogel at different temperature: (c) % Cumulative release vs sqrt of time (Higuchi model) and (d)  $\ln M_t/M_\infty$  vs  $\ln T$  (Korsmeyer-Peppas model)

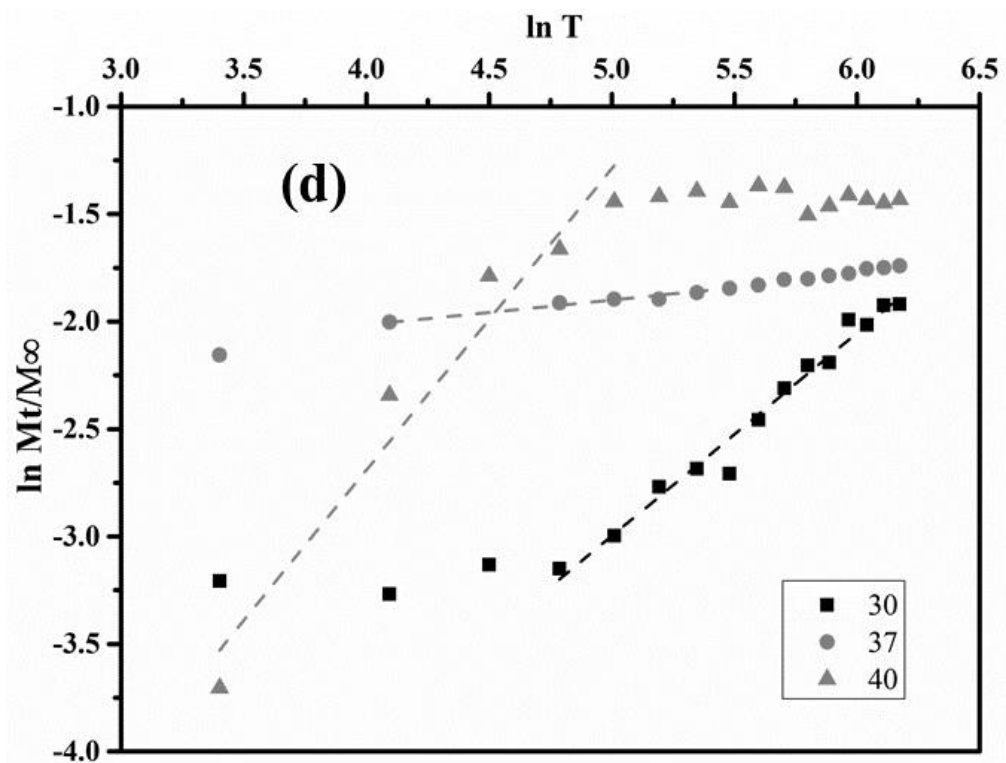
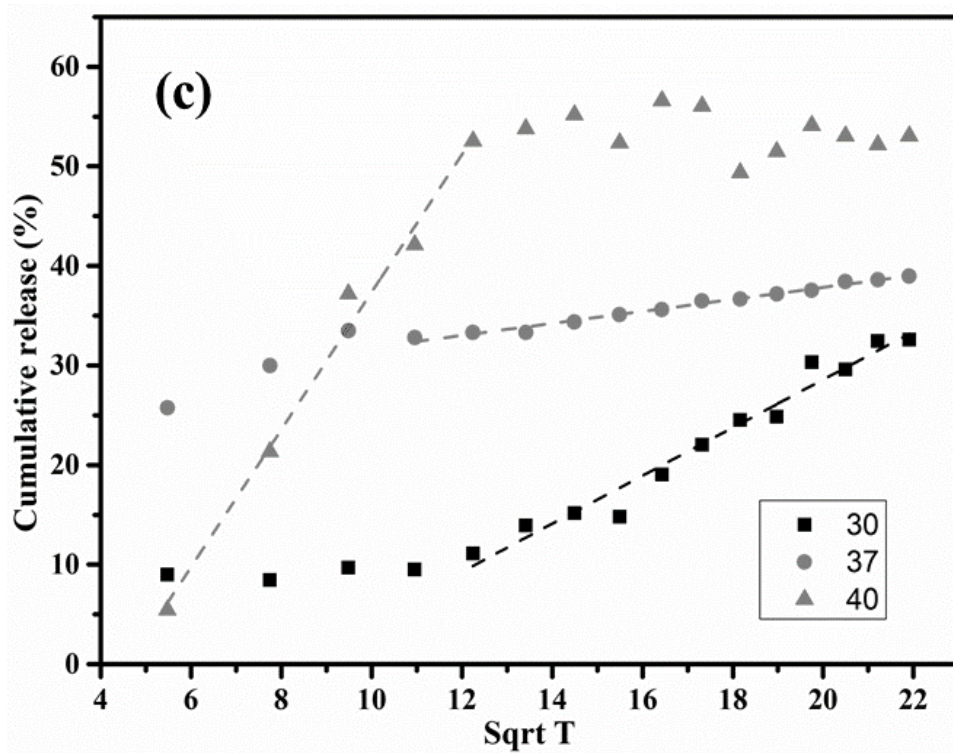


# APPENDICES

## AI.5 Dox release kinetics studied for HM-5 hydrogel at different temperature



AI.5: Dox release kinetics studied for HM-5 hydrogel at different temperature: (a) % Cumulative release vs time (Zero-order kinetics); (b) % log cumulative drug remaining vs time (First-order kinetics)



AI.5: Dox release kinetics studied for HM-5 hydrogel at different temperature: (c) % Cumulative release vs sqrt of time (Higuchi model) and (d)  $\ln M_t/M_\infty$  vs  $\ln T$  (Korsmeyer-Peppas model)

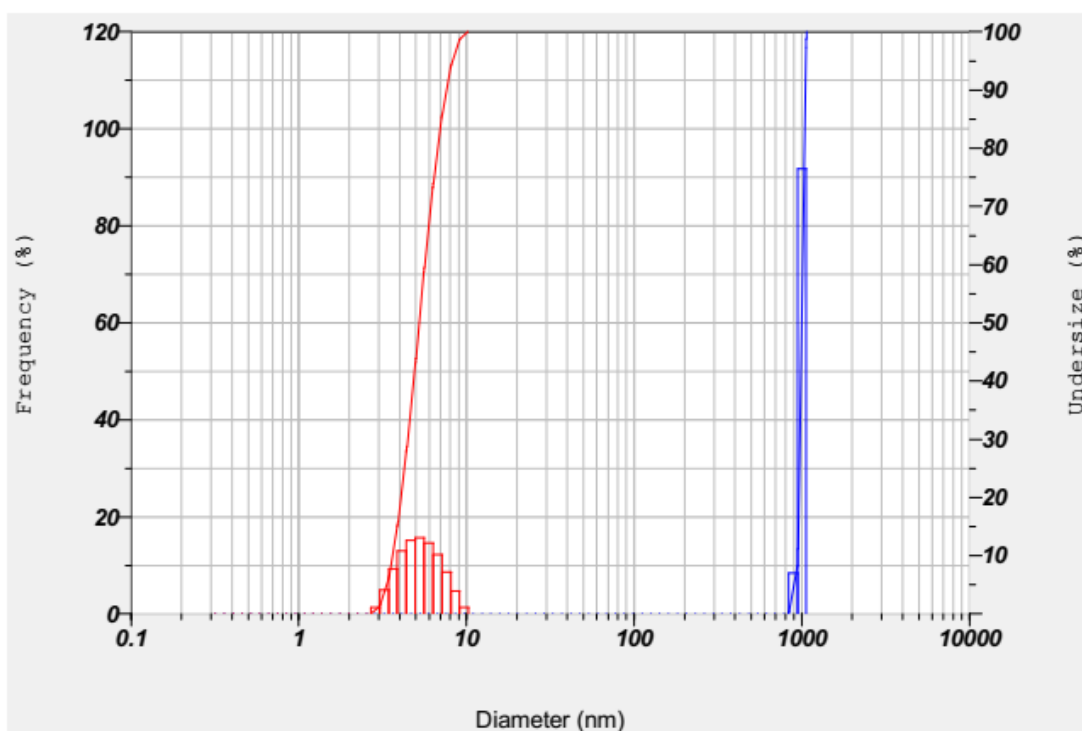
# APPENDICES

## APPENDIX II

### AII Particle size analysis of PDEA nanohydrogels synthesized by inverse emulsion polymerization method

#### AII.1 Effect of stirrer speed

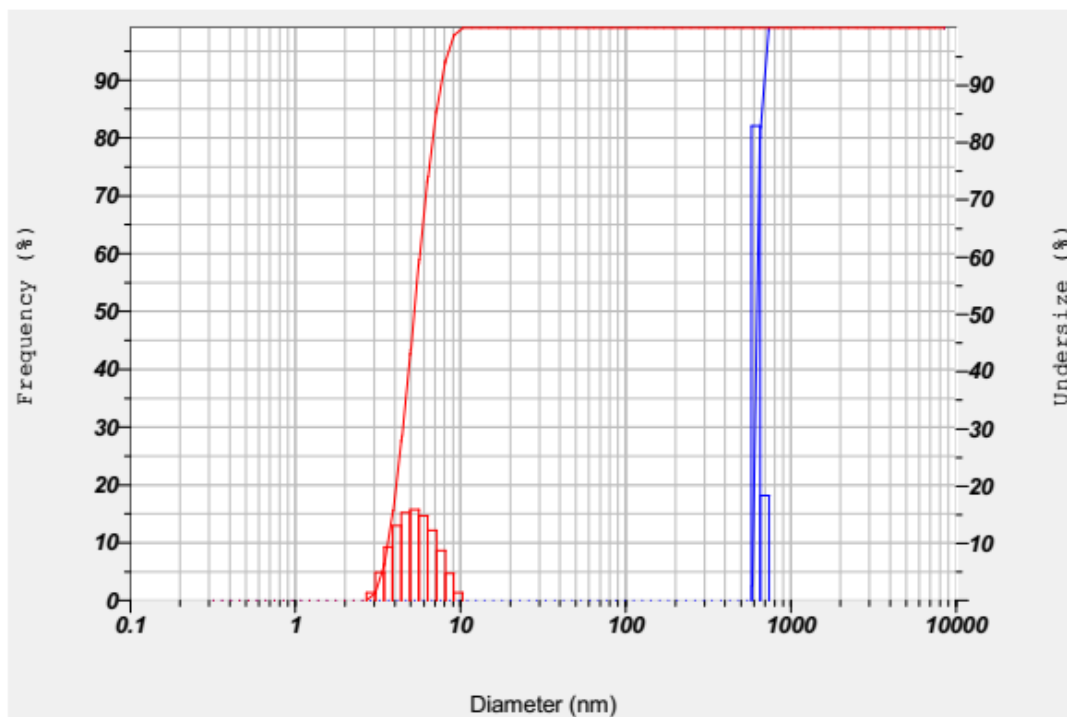
PDEA nanohydrogels were prepared using different stirrer speed while keeping the other variables constant (Water:oil ratio of 1:4 and surfactant concentration of 2.25%).



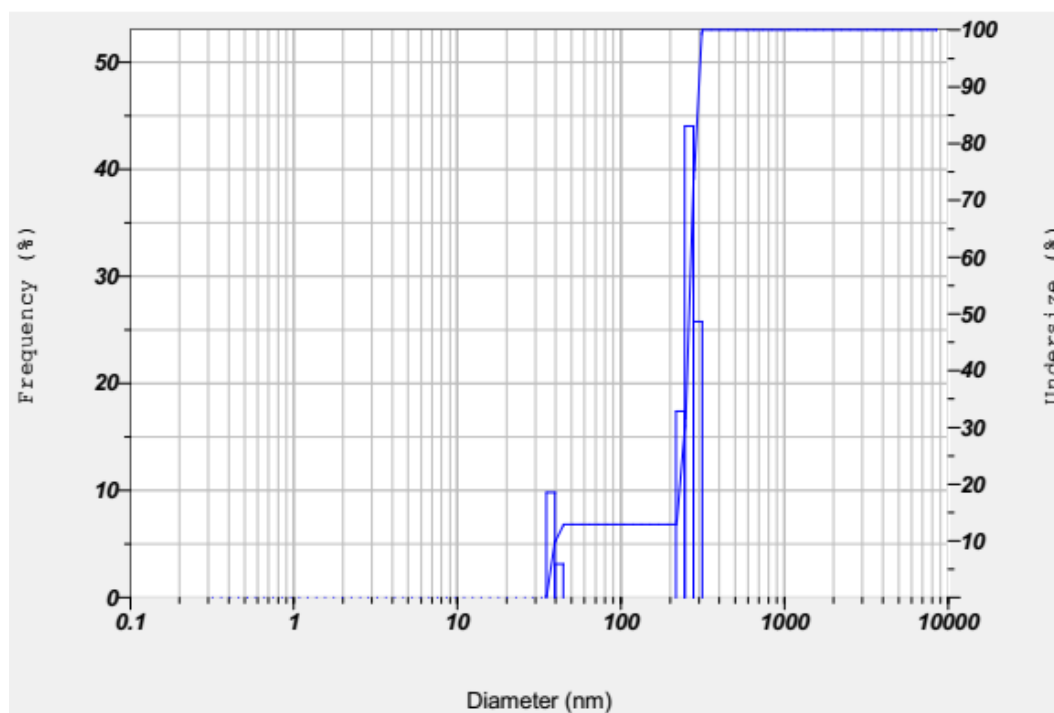
**AII.1.1: Particle size measured at stirrer speed 300 rpm**



# APPENDICES

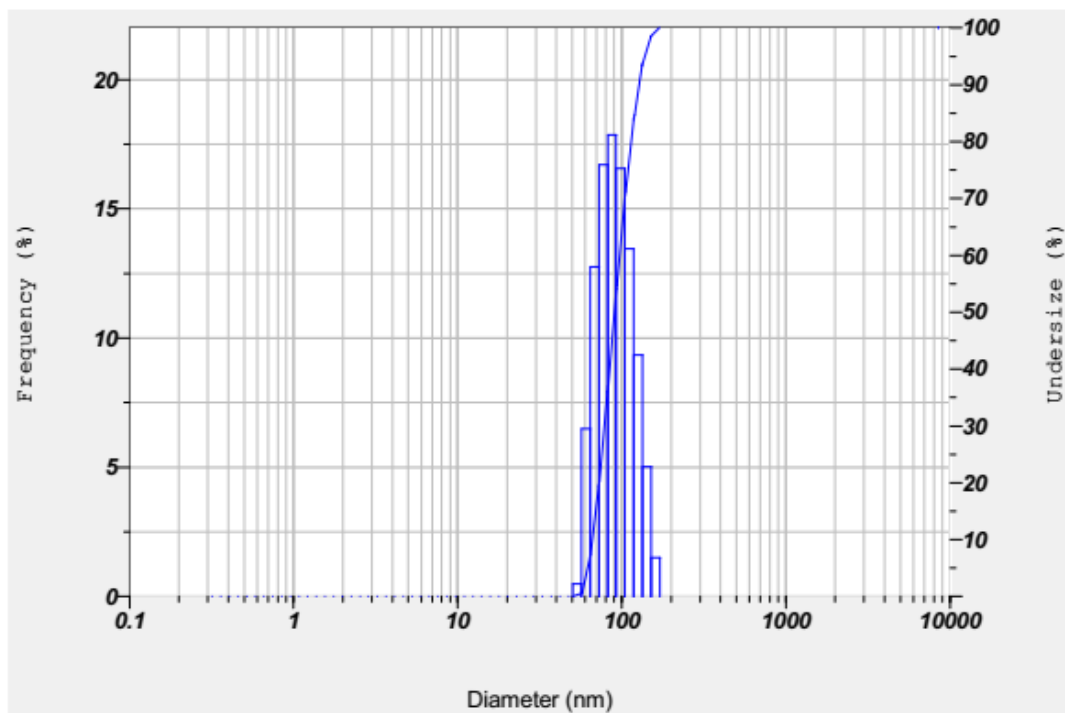


**AII.1.2: Particle size measured at stirrer speed 400 rpm**

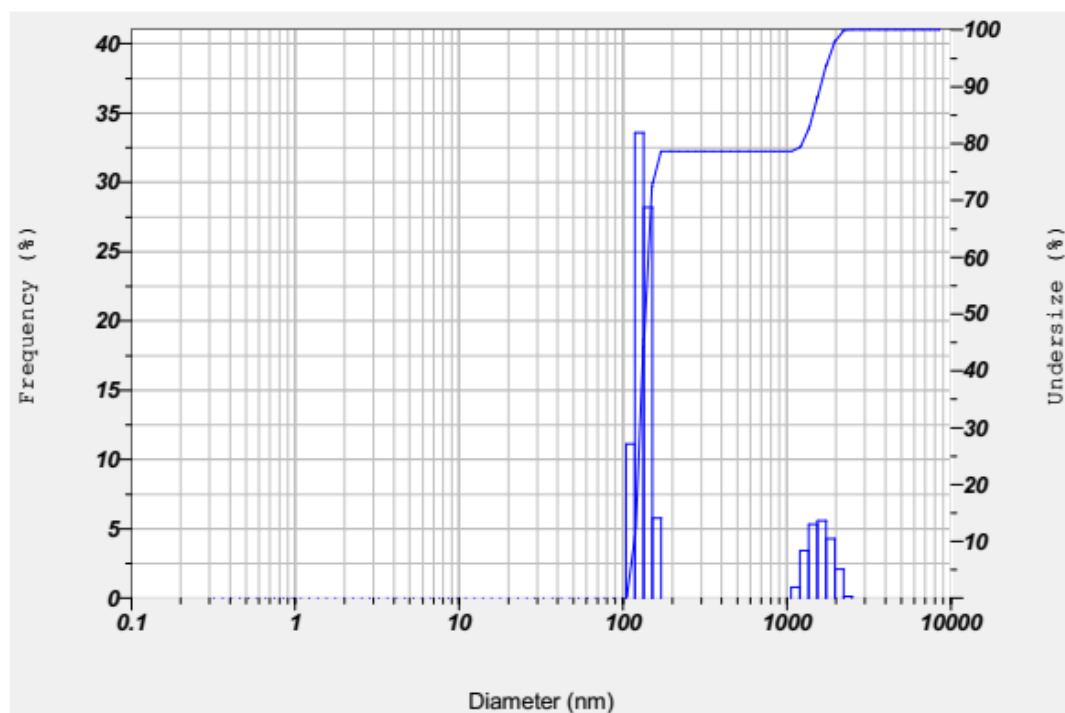


**AII.1.3: Particle size measured at stirrer speed 500 rpm**

# APPENDICES

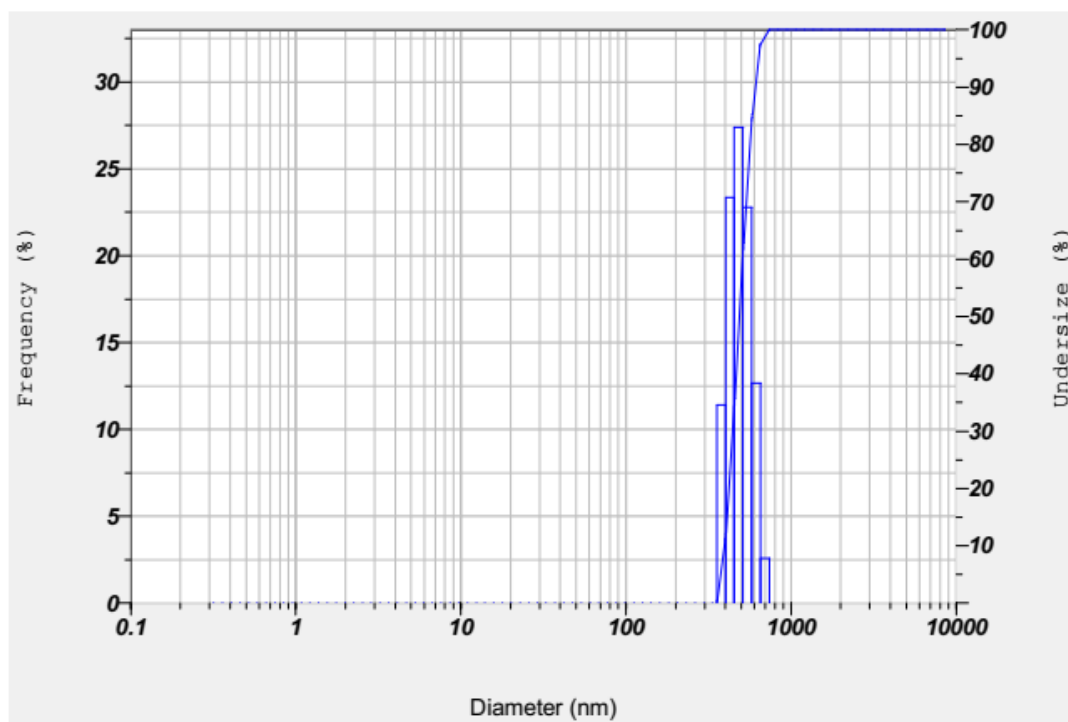


**AII.1.4: Particle size measured at stirrer speed 600 rpm**



**AII.1.5: Particle size measured at stirrer speed 700 rpm**

## APPENDICES

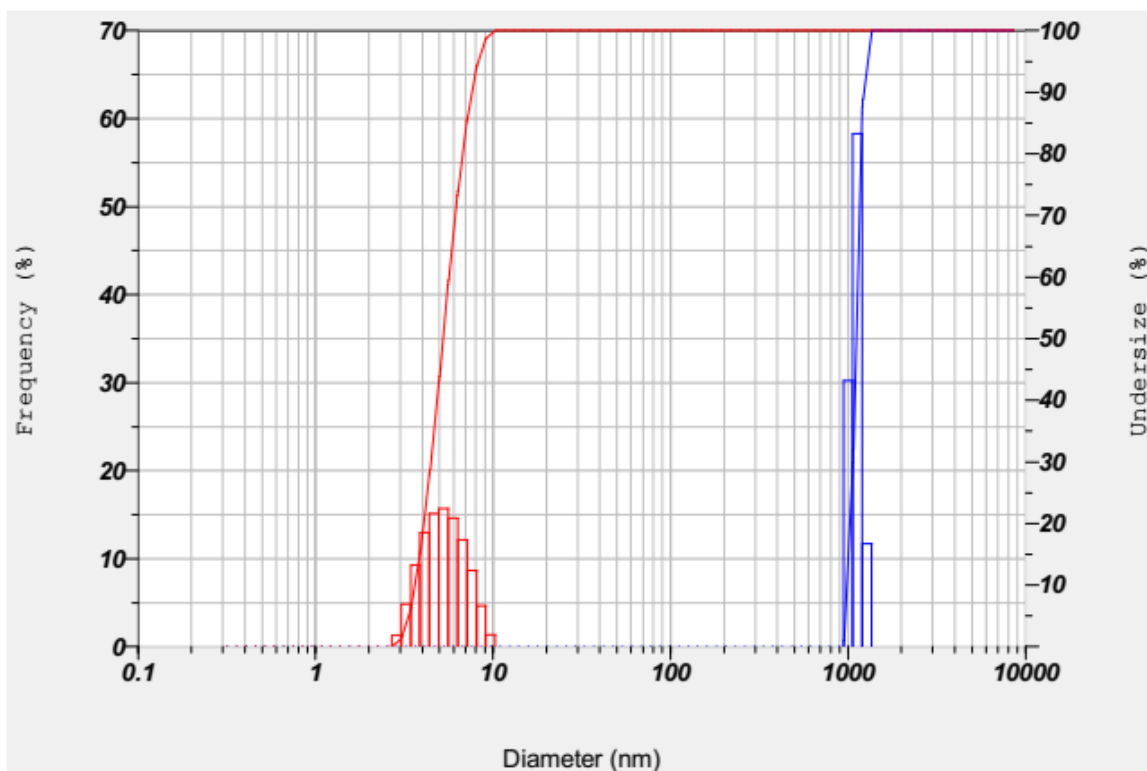


**AII.1.6: Particle size measured at stirrer speed 800 rpm**

# APPENDICES

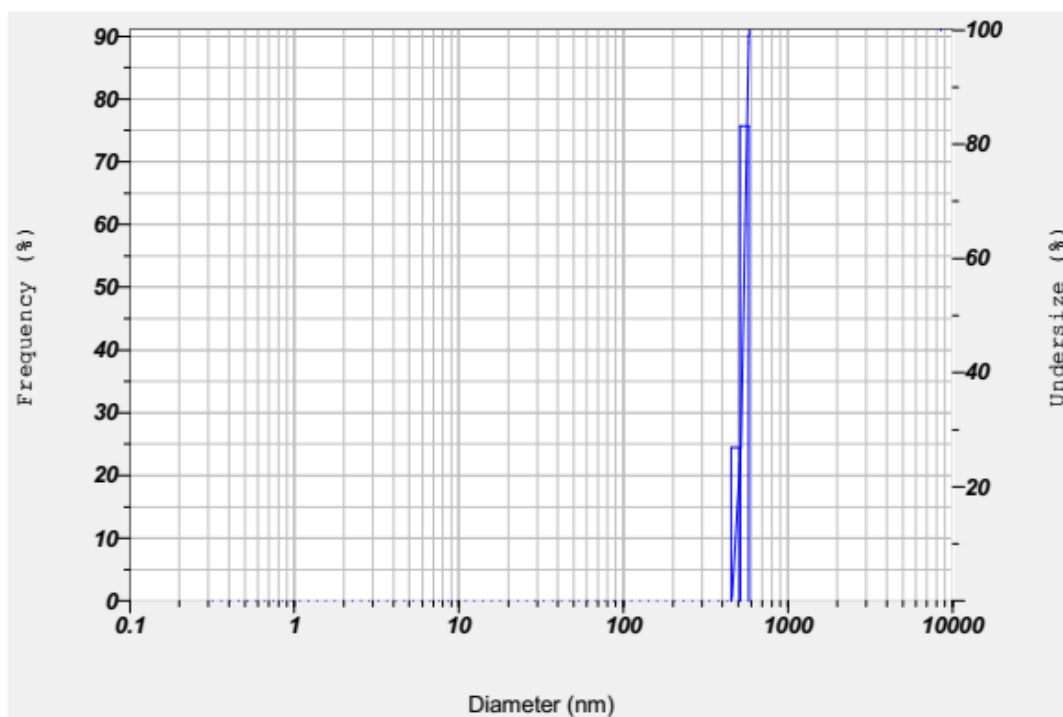
## AII.2 Effect of water-oil ratio

PDEA nanohydrogels were prepared using different water-oil (w/o) ratio while keeping the other variables constant (stirrer speed of 600 rpm and surfactant concentration 2.5%).

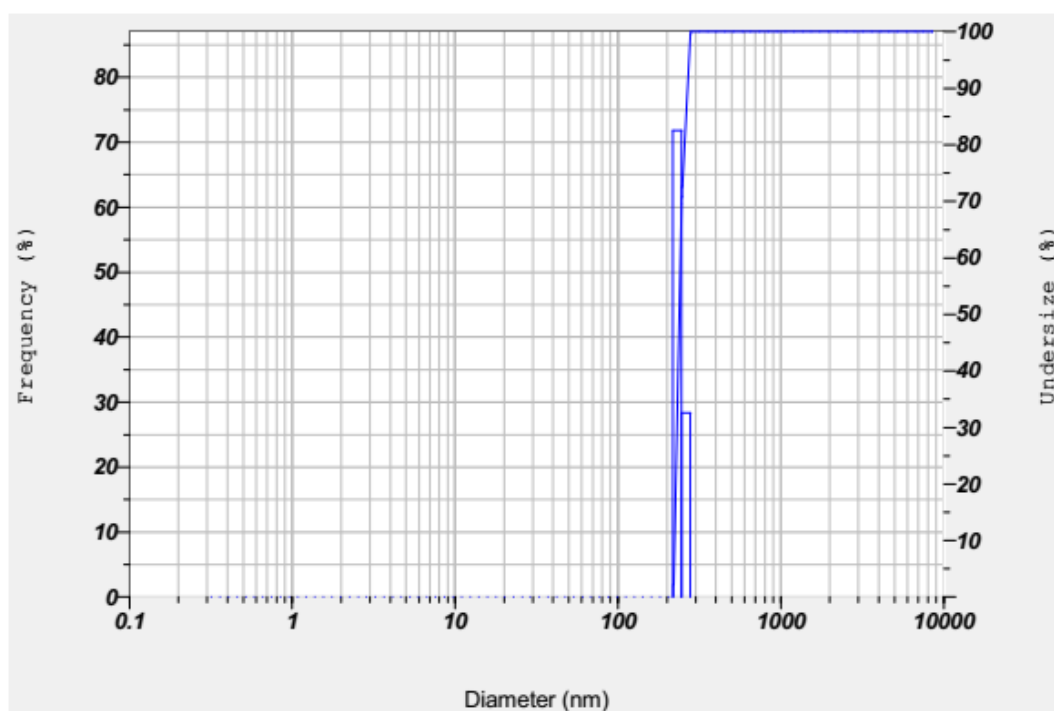


**AII.2.1: Particle size measured at w/o ratio 1:2**

## APPENDICES

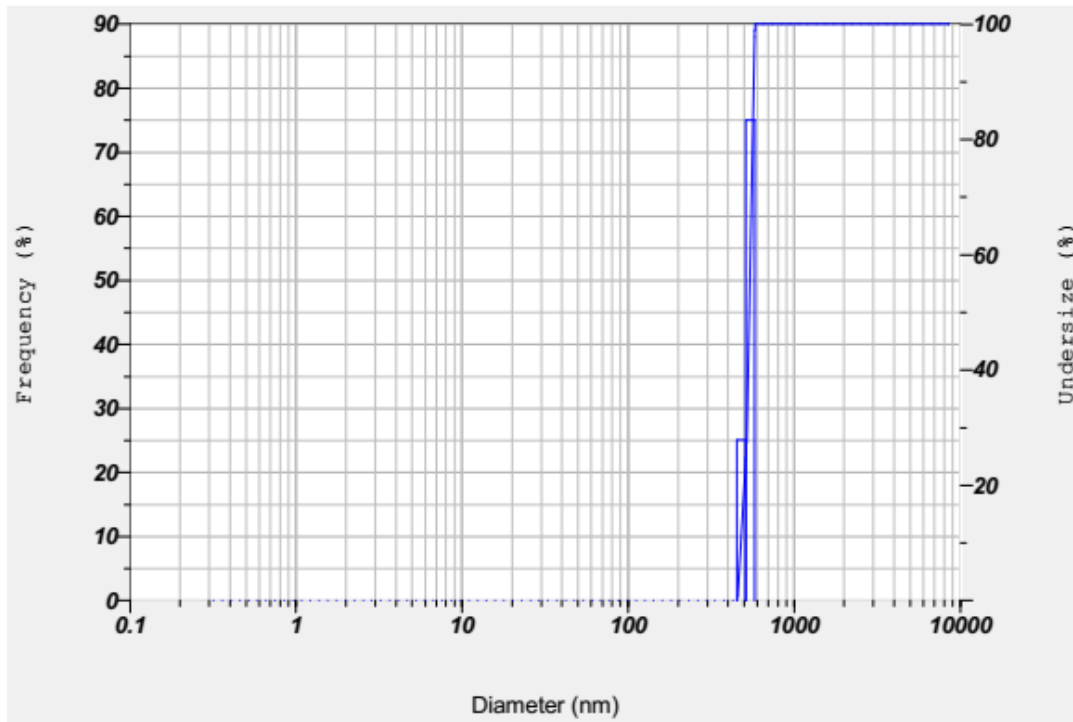


**AII.2.2: Particle size measured at w/o ratio 1:3**

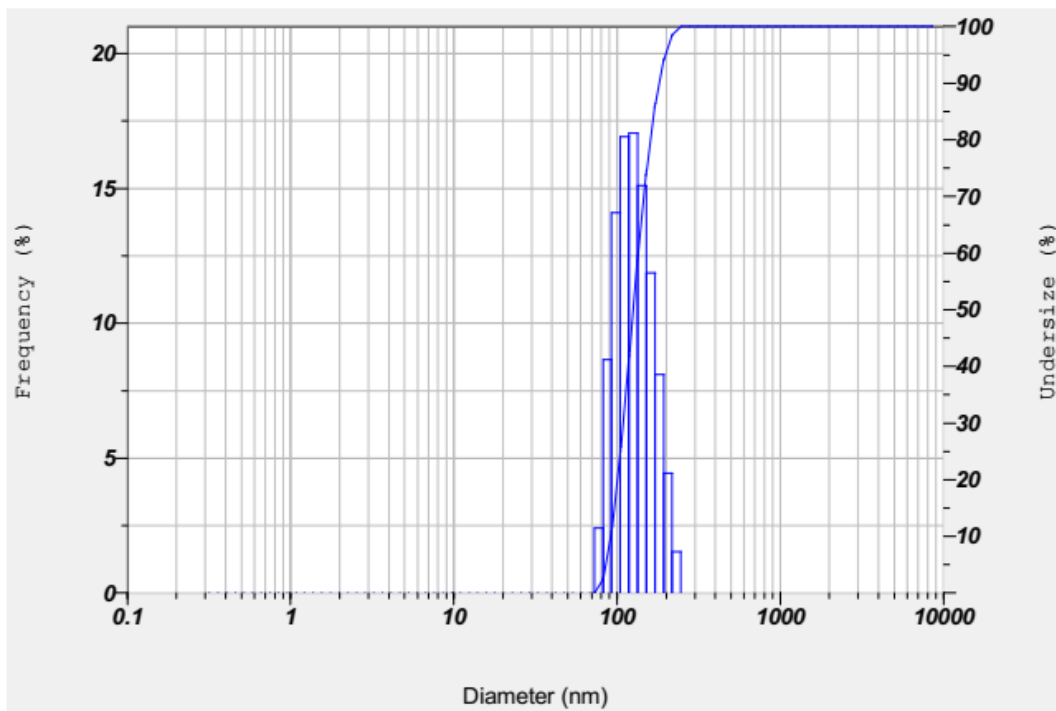


**AII.2.3: Particle size measured at w/o ratio 1:4**

# APPENDICES

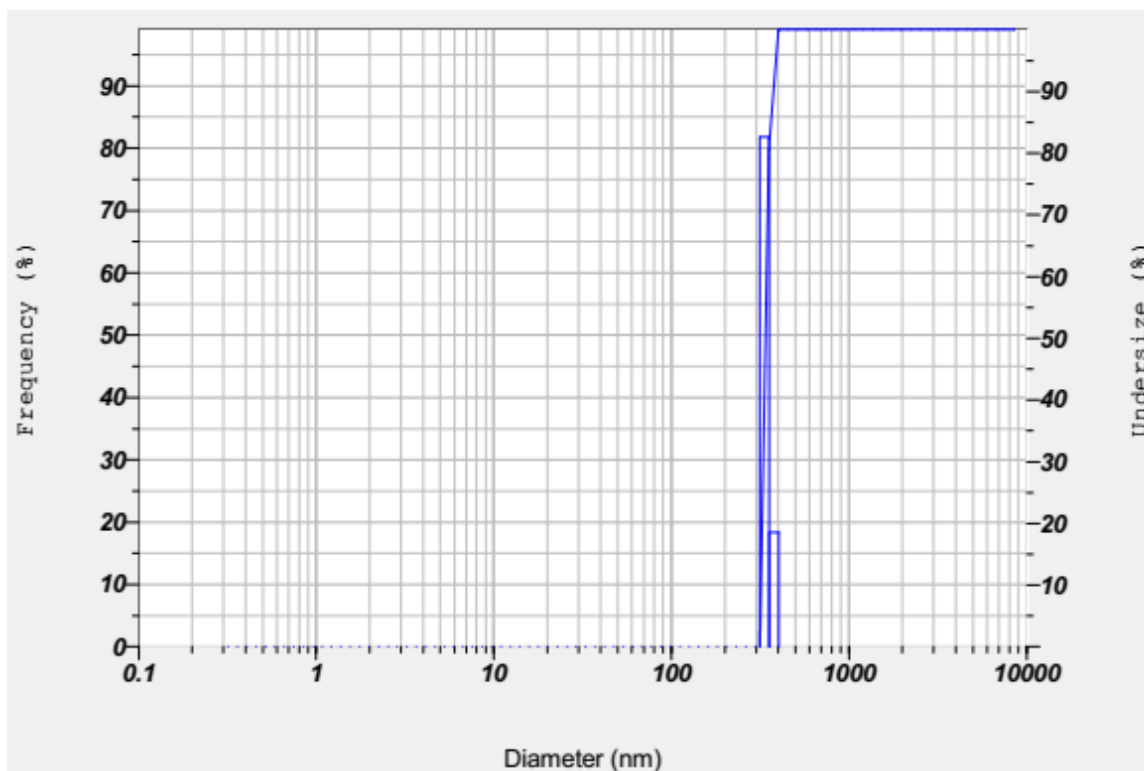


**AIL.2.4: Particle size measured at w/o ratio 1:5**



**AIL.2.5: Particle size measured at w/o ratio 1:6**

## APPENDICES

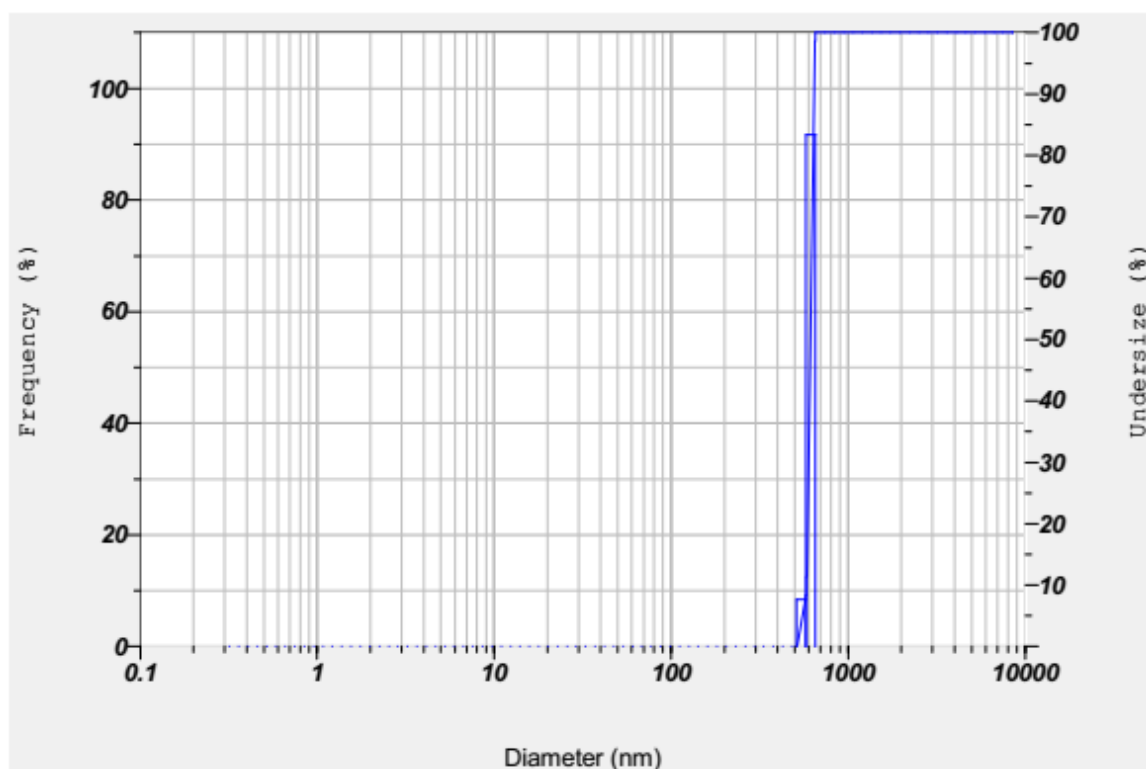


**AII.2.6: Particle size measured at w/o ratio 1:7**

## APPENDICES

### AII.3 Effect of surfactant concentration

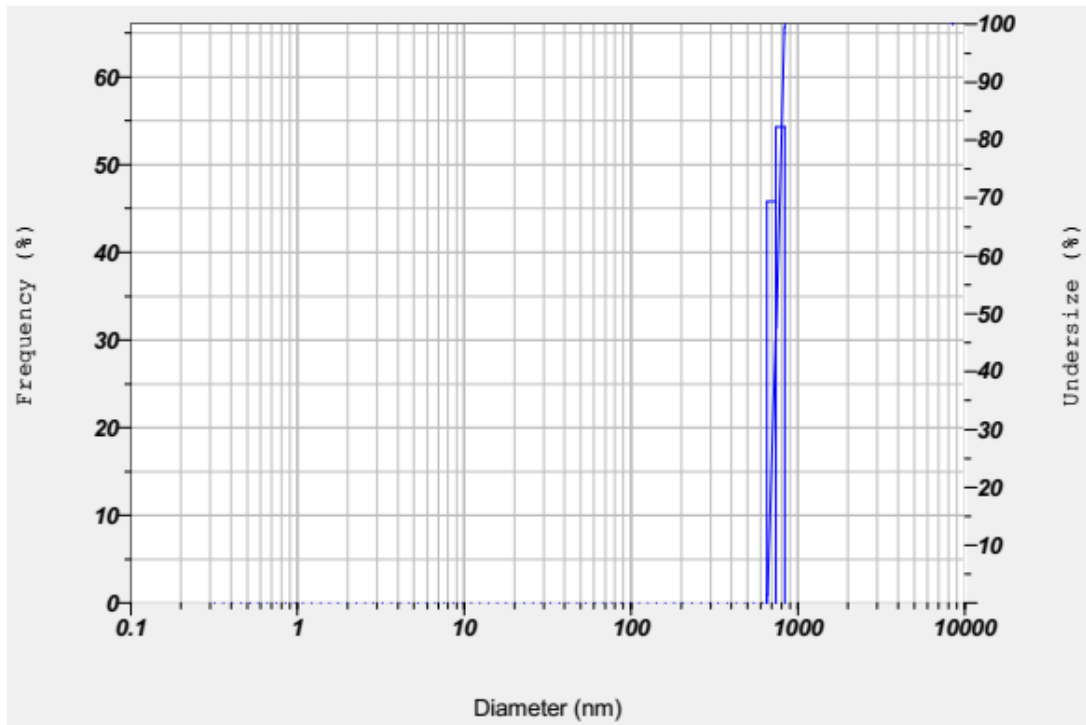
PDEA nanohydrogels were prepared using different concentration of surfactant (vol% of span 80 in cyclohexane) while keeping the other variables constant (stirrer speed of 600 rpm and water:oil ratio of 1:5).



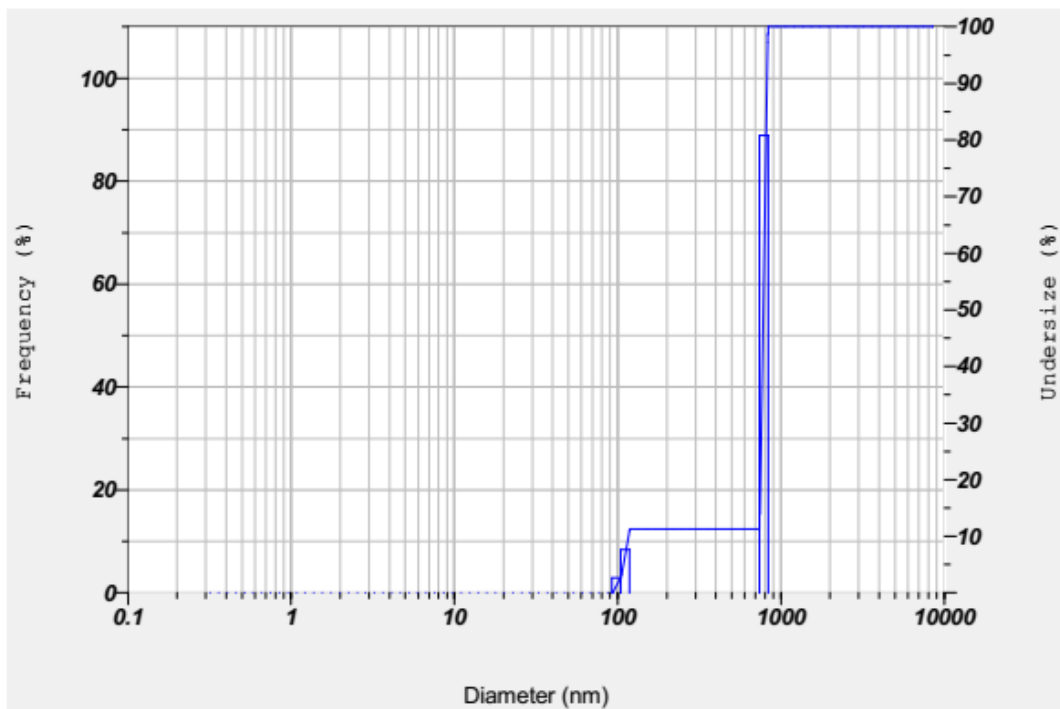
**AII.3.1: Particle size measured at surfactant concentration of 1.5%**



# APPENDICES

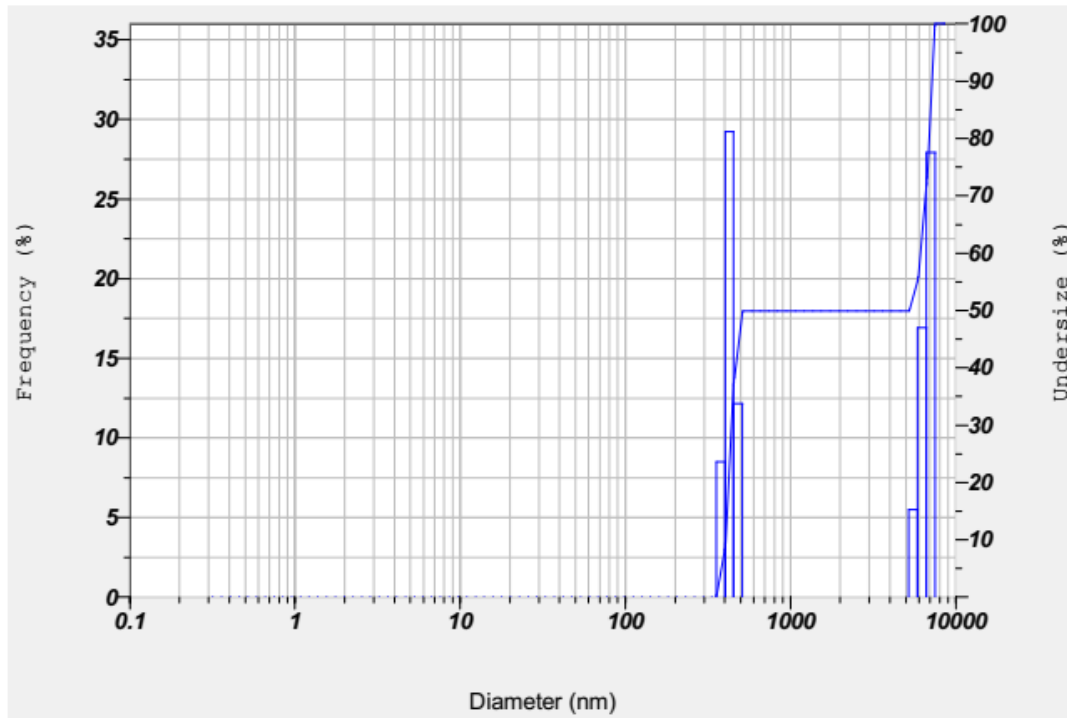


**AII.3.2: Particle size measured at surfactant concentration of 1.75%**

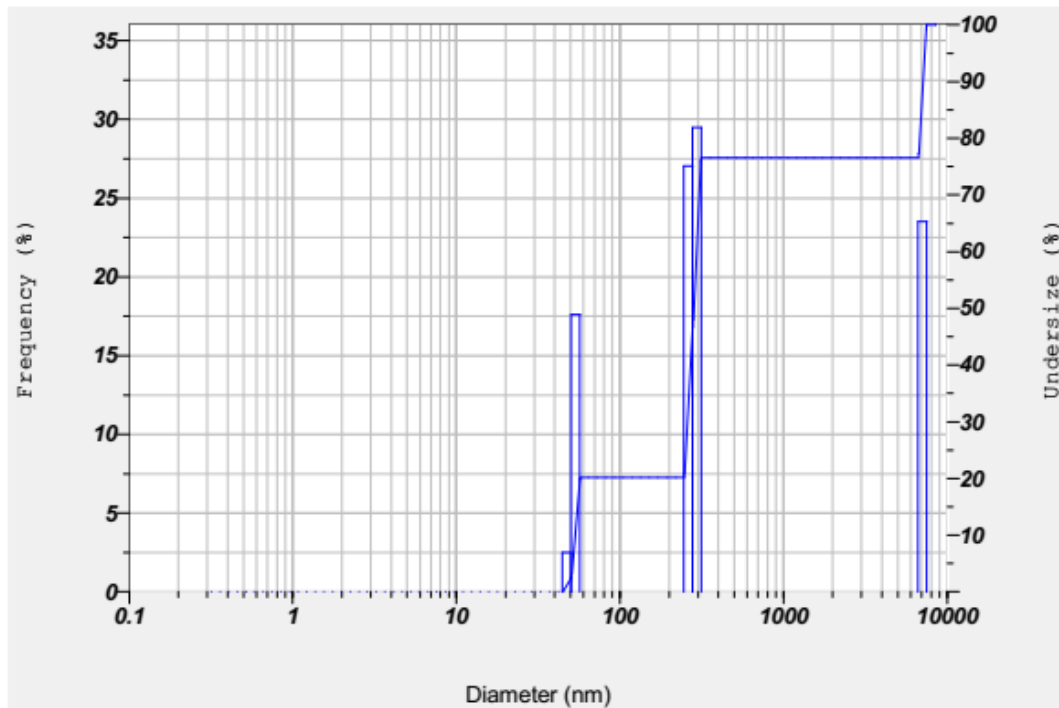


**AII.3.3: Particle size measured at surfactant concentration of 2%**

# APPENDICES

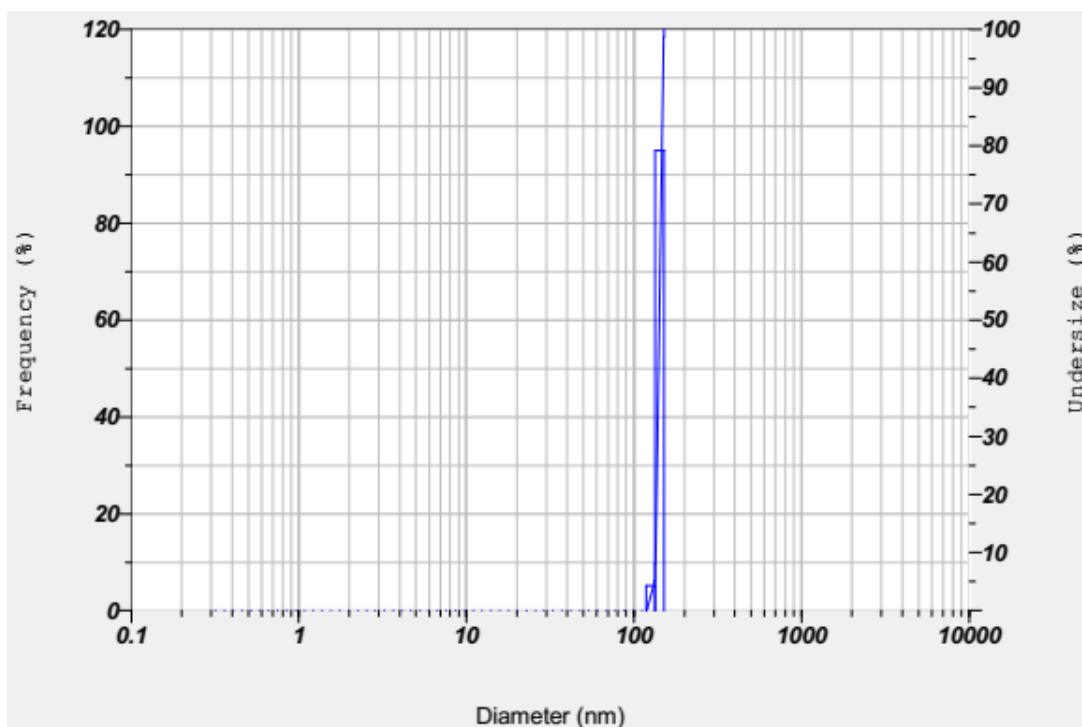


**AII.3.4: Particle size measured at surfactant concentration of 2.25%**

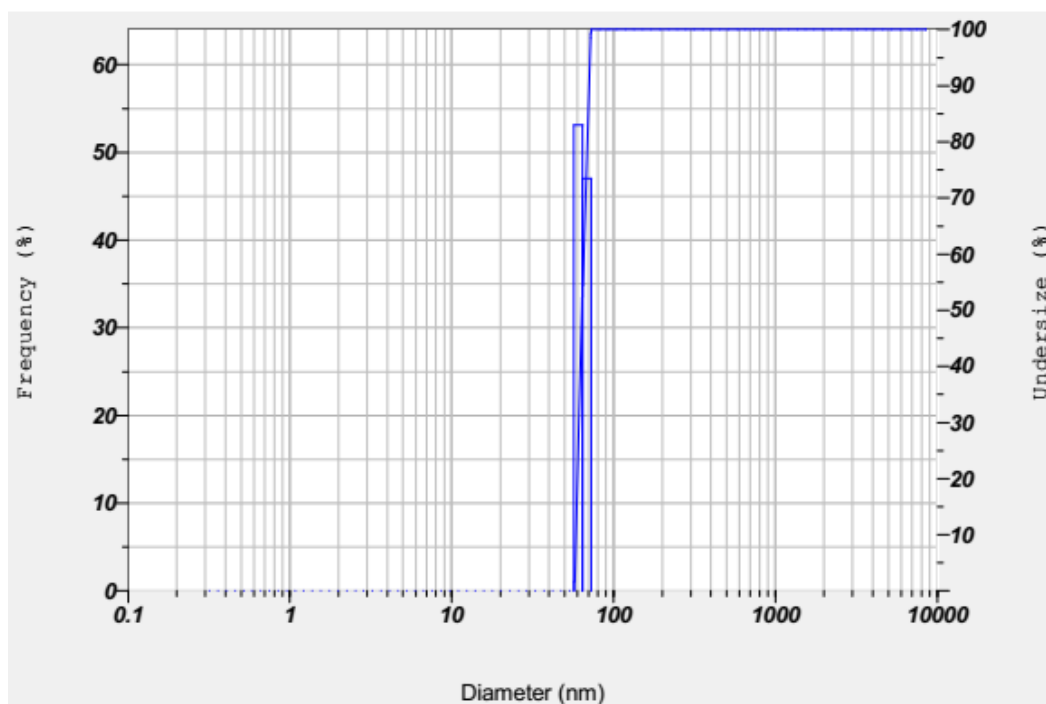


**AII.3.5: Particle size measured at surfactant concentration of 2.5%**

## APPENDICES



**AII.3.6: Particle size measured at surfactant concentration of 2.75%**

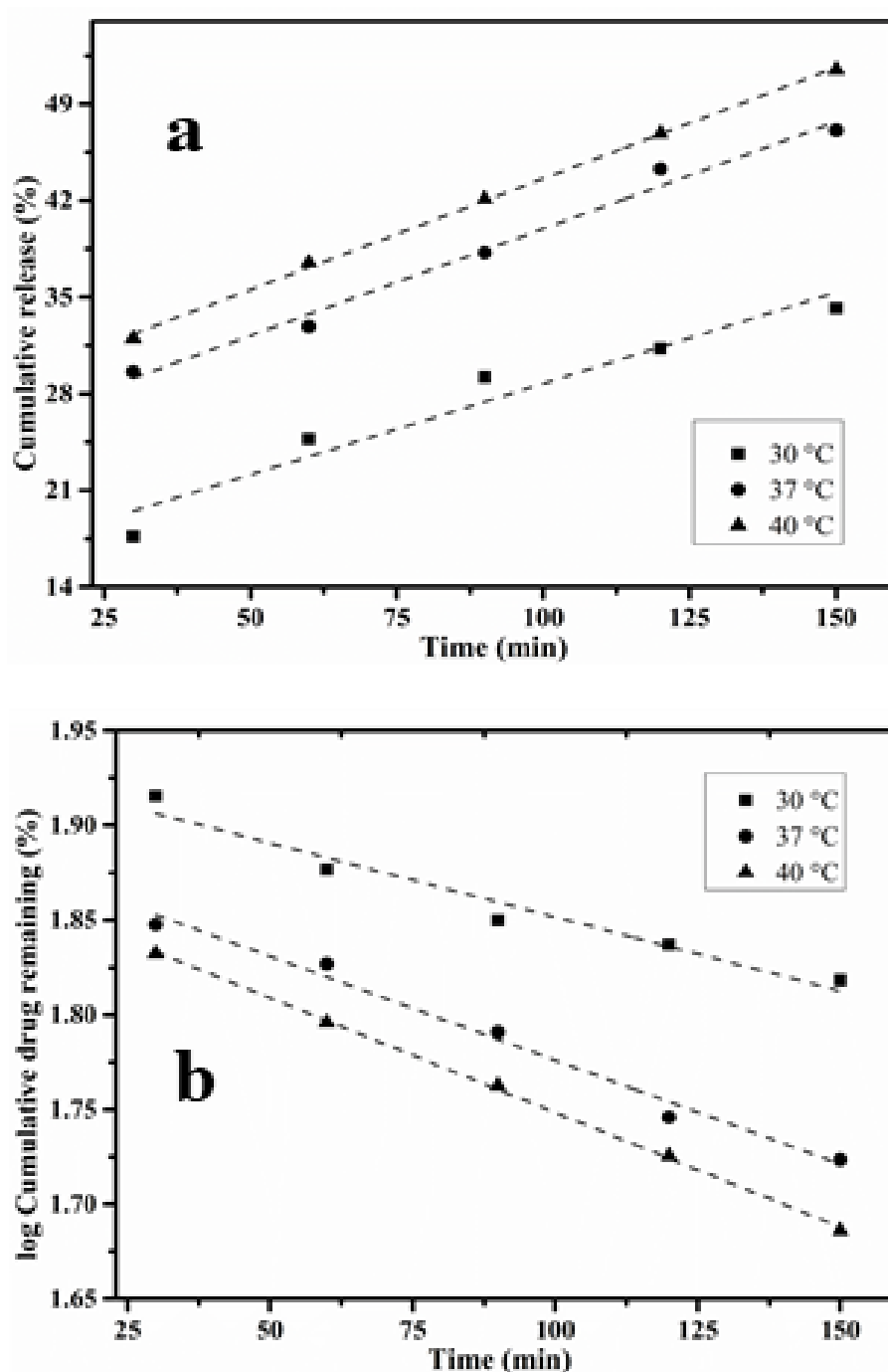


**AII.3.7: Particle size measured at surfactant concentration of 3%**

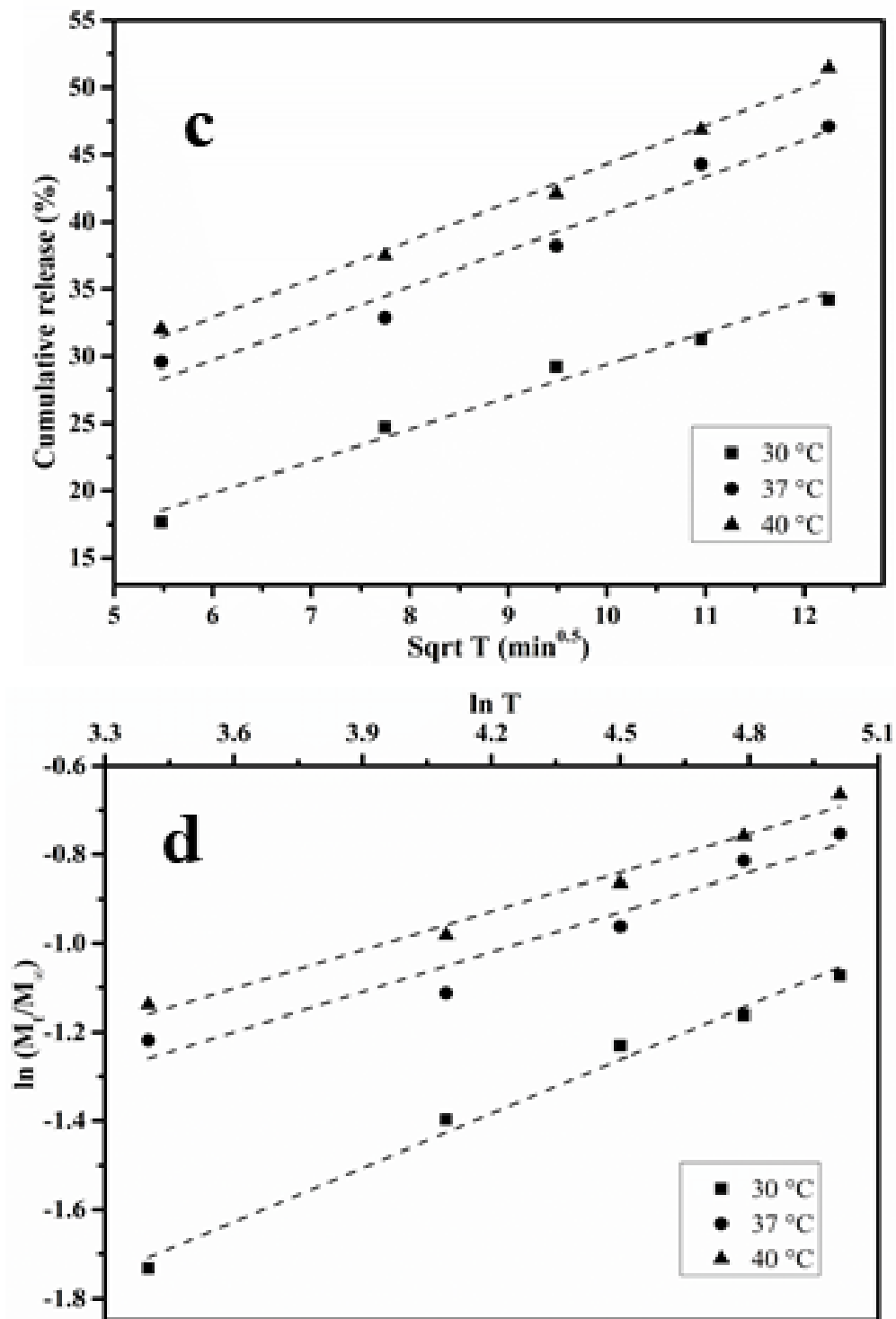
# APPENDICES

## APPENDIX III

### AIII.1 Dox release kinetics studied for N nanohydrogel at different temperature

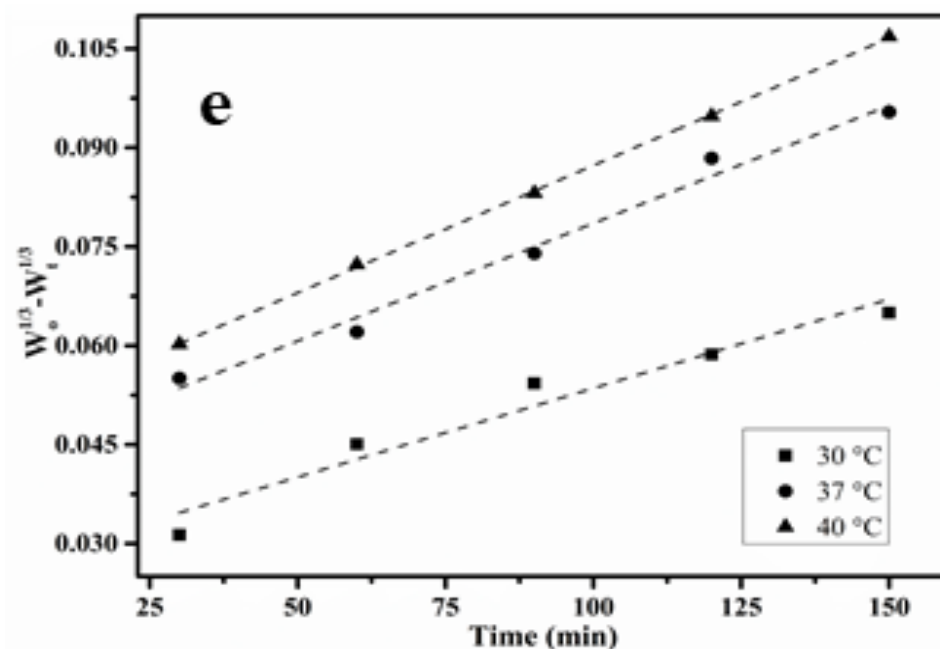


AIII.1: Dox release kinetics studied for N nanohydrogel at different temperature: (a) % Cumulative release vs time (Zero-order kinetics); (b) % log cumulative drug remaining vs time (First-order kinetics)



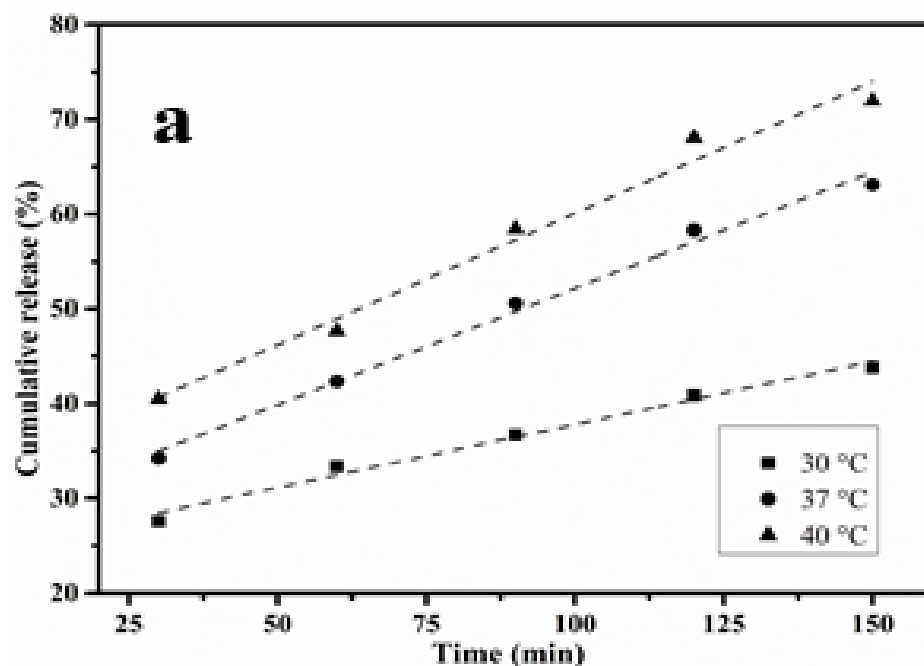
**AIII.1: Dox release kinetics studied for N nanohydrogel at different temperature: (c) % Cumulative release vs sqrt of time (Higuchi model) and (d) ln  $M_t/M_\infty$  vs ln T (Korsmeyer-Peppas model)**

## APPENDICES

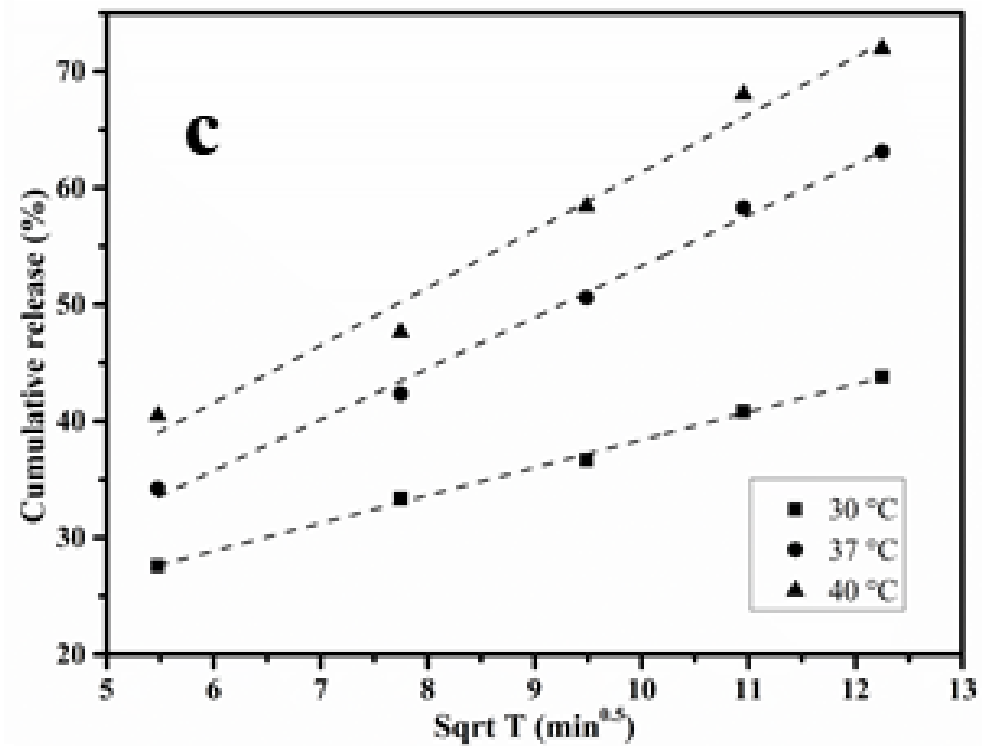
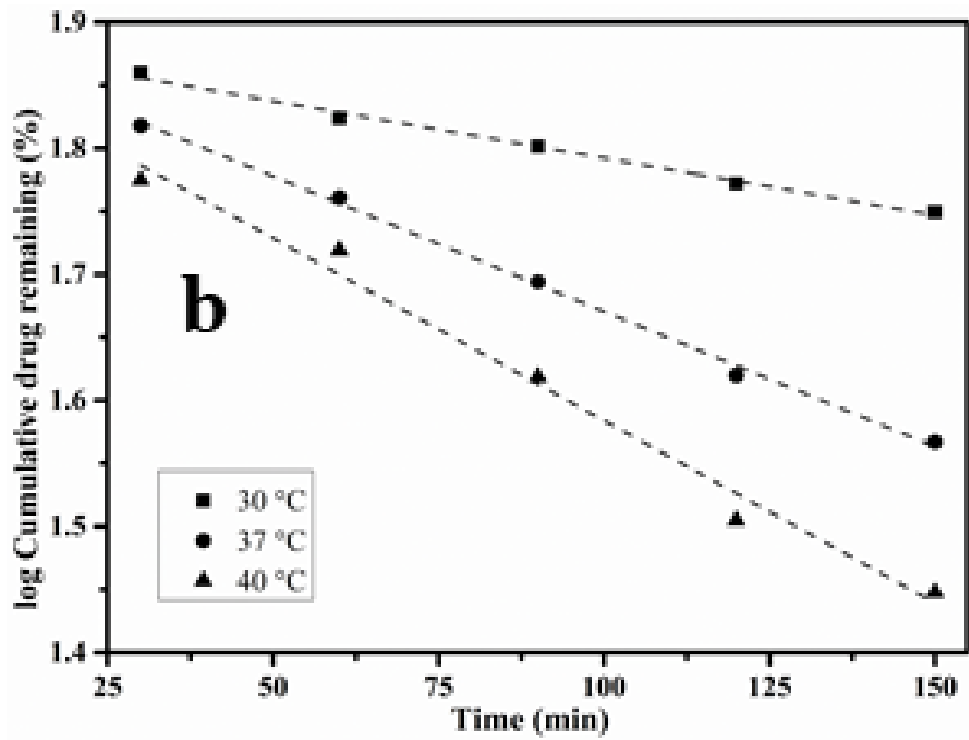


AIII.1: Dox release kinetics studied for N nanohydrogel at different temperature: (e)  $W_o^{1/3} - W_t^{1/3}$  vs time (Hixon-Crowel model)

AIII.2 Dox release kinetics studied for NG nanohydrogel at different temperature

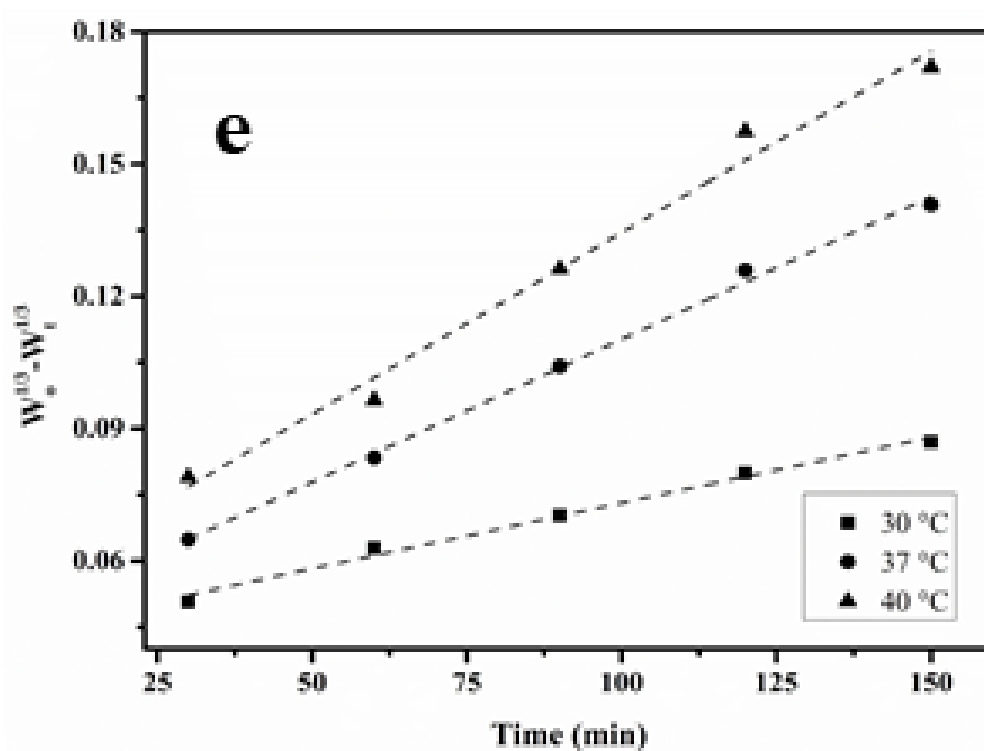
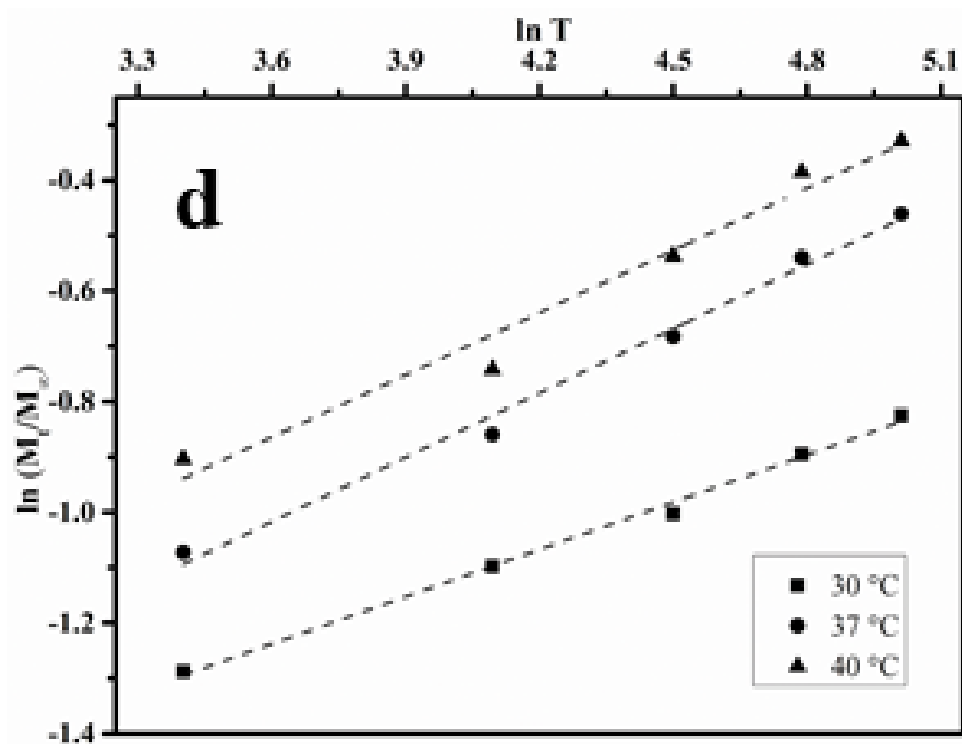


AIII.2: Dox release kinetics studied for NG nanohydrogel at different temperature: (a) % Cumulative release vs time (Zero-order kinetics)



AIII.2: Dox release kinetics studied for NG nanohydrogel at different temperature: (b) % log cumulative drug remaining vs time (First-order kinetics); (c) % Cumulative release vs sqrt of time (Higuchi model)

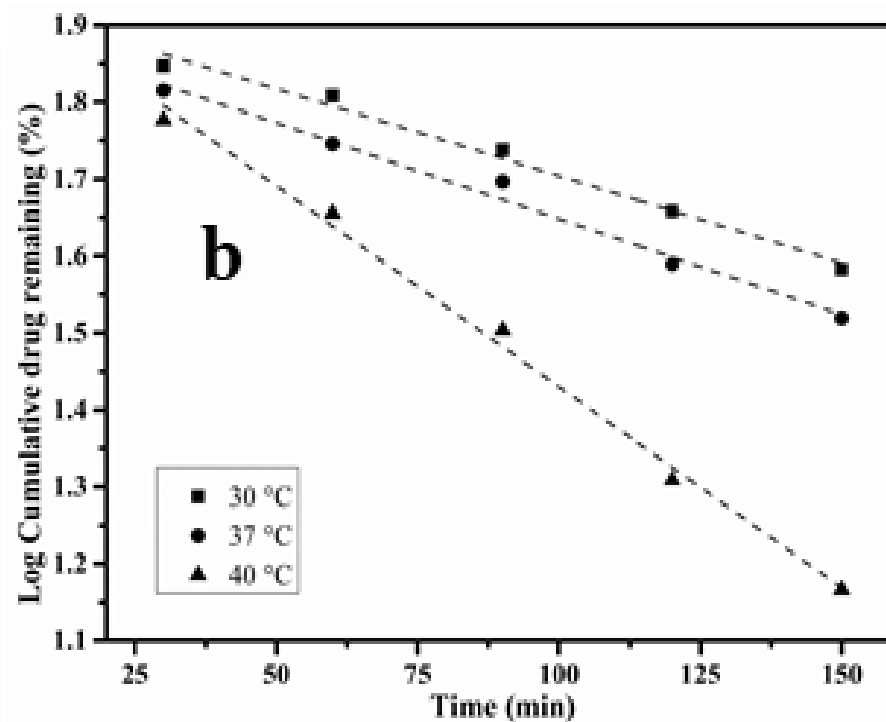
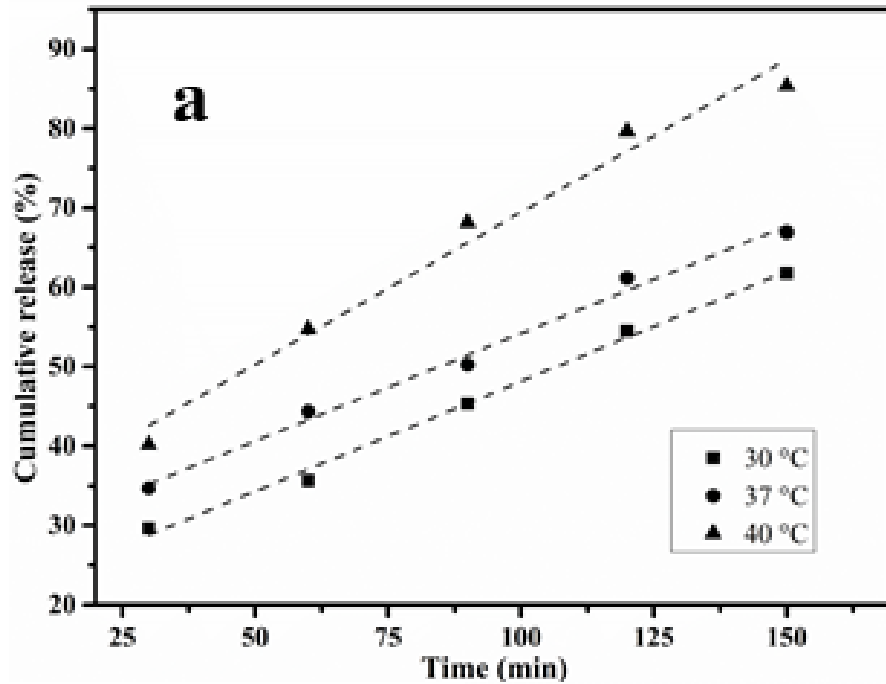
## APPENDICES



**AIII.2: Dox release kinetics studied for NG nanohydrogel at different temperature: (d)  $\ln M_t/M_\infty$  vs  $\ln T$  (Korsmeyer-Peppas model) and (e)  $W_\infty^{1/3} - W_t^{1/3}$  vs time (Hixon-Crowel model)**

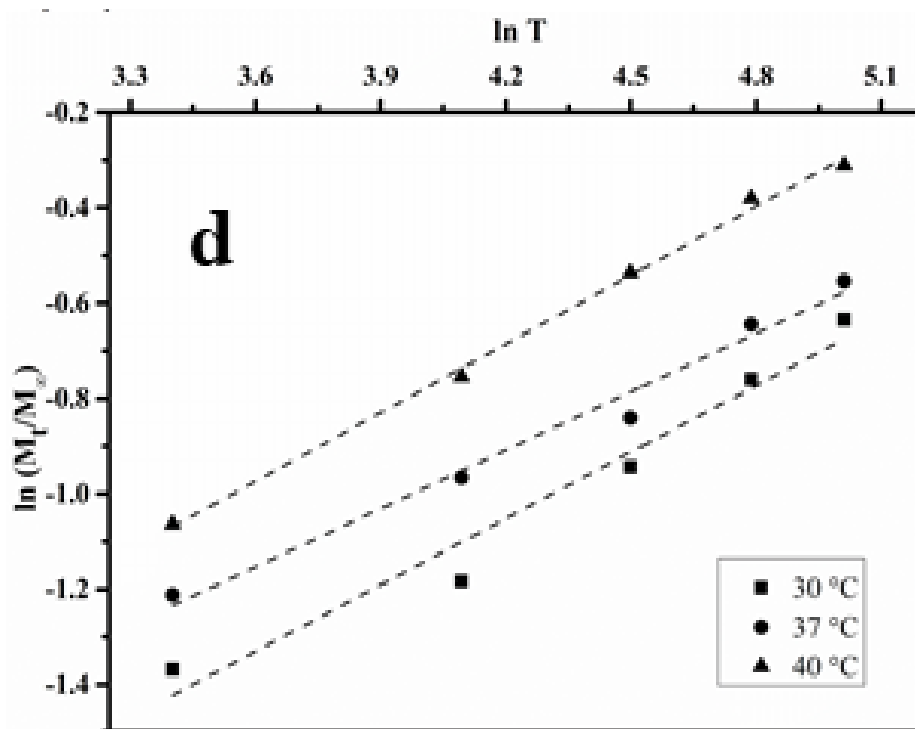
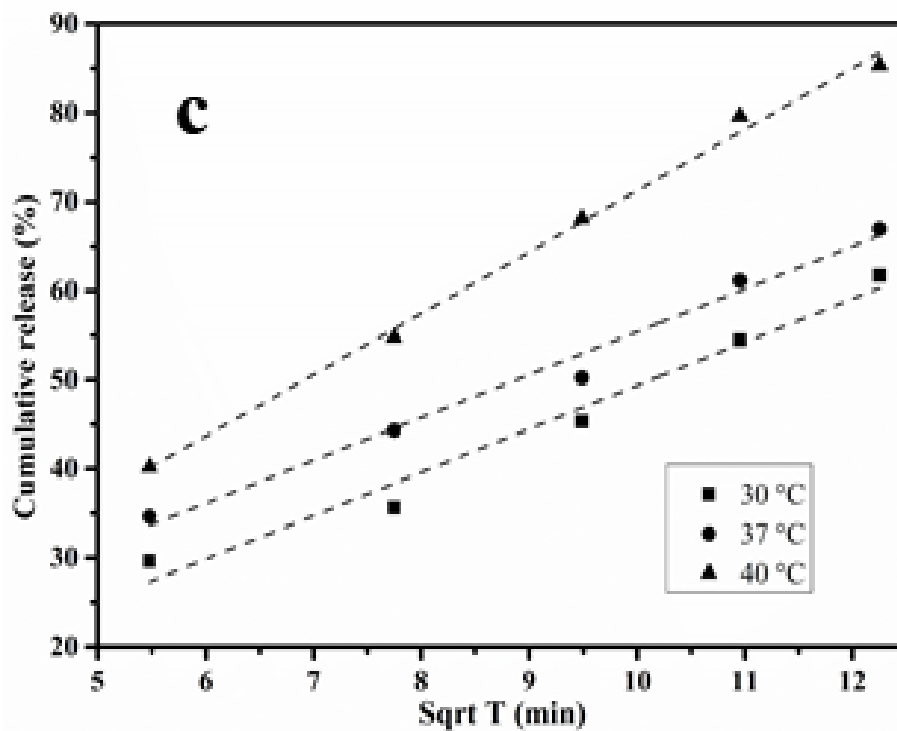


## AIII.3 Dox release kinetics studied for NL nanohydrogel at different temperature

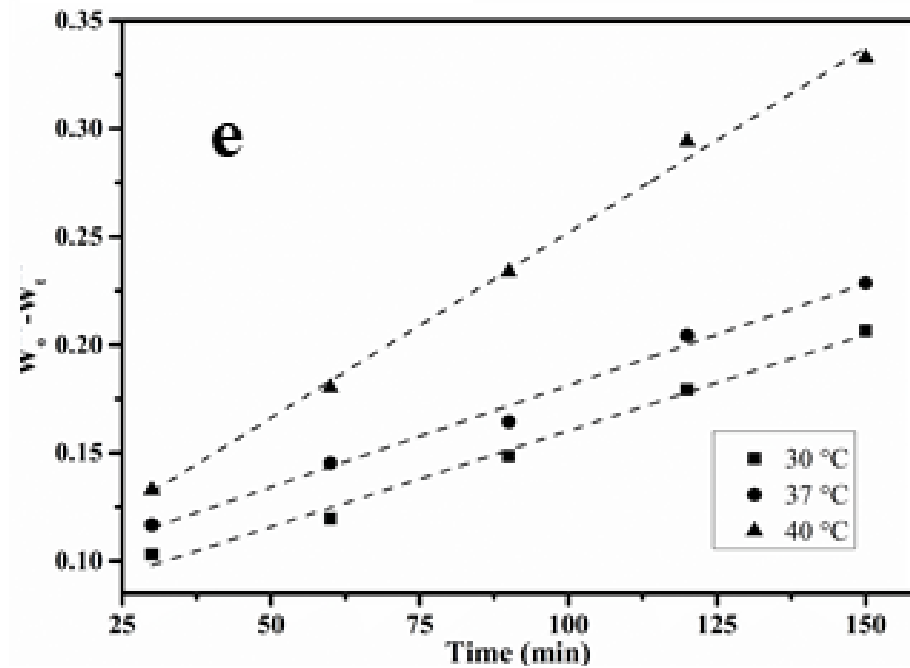


AIII.3: Dox release kinetics studied for NL nanohydrogel at different temperature: (a) % Cumulative release vs time (Zero-order kinetics); (b) % log cumulative drug remaining vs time (First-order kinetics)

## APPENDICES

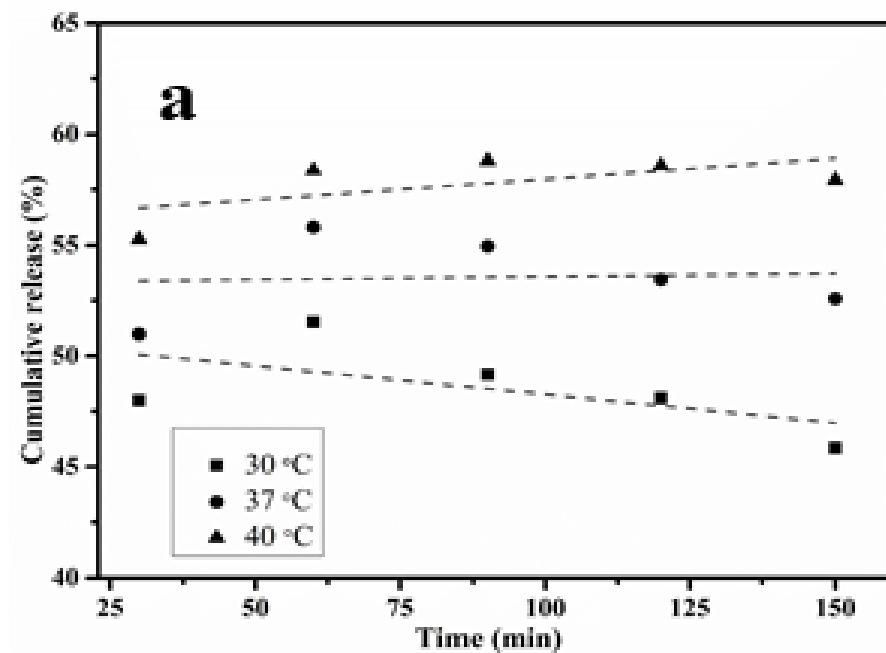


**AIII.3: Dox release kinetics studied for NL nanohydrogel at different temperature: (c) % Cumulative release vs sqrt of time (Higuchi model); (d)  $\ln M_t/M_\infty$  vs  $\ln T$  (Korsmeyer-Peppas model)**



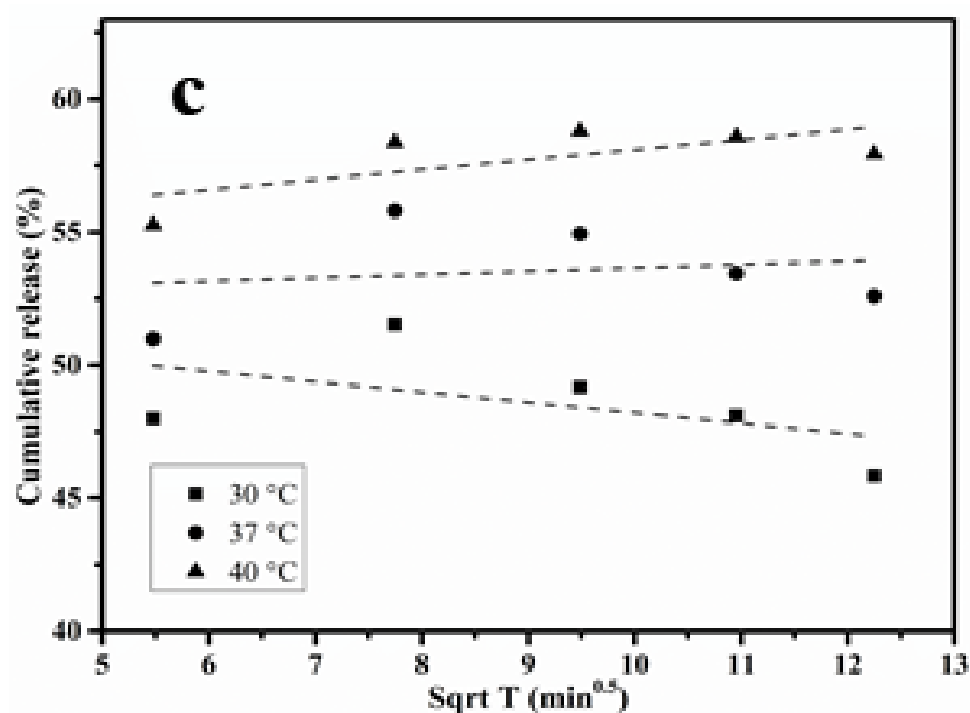
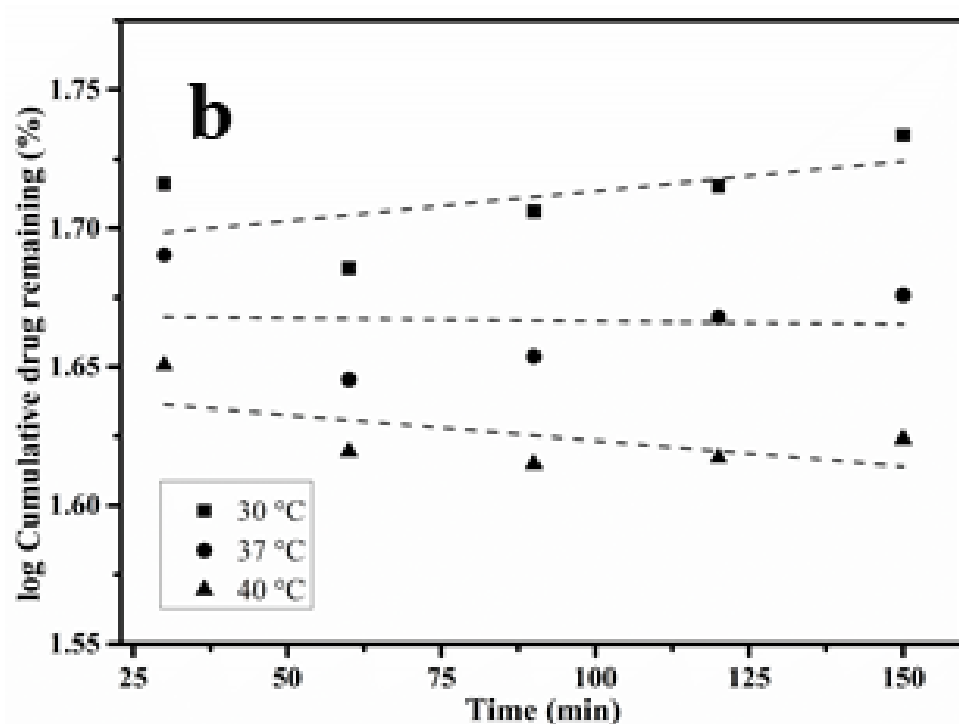
AIII.3: Dox release kinetics studied for NL nanohydrogel at different temperature: (e)  $W_0^{1/3} - W_t^{1/3}$  vs time (Hixon-Crowel model)

AIII.4 Dox release kinetics studied for NM nanohydrogel at different temperature

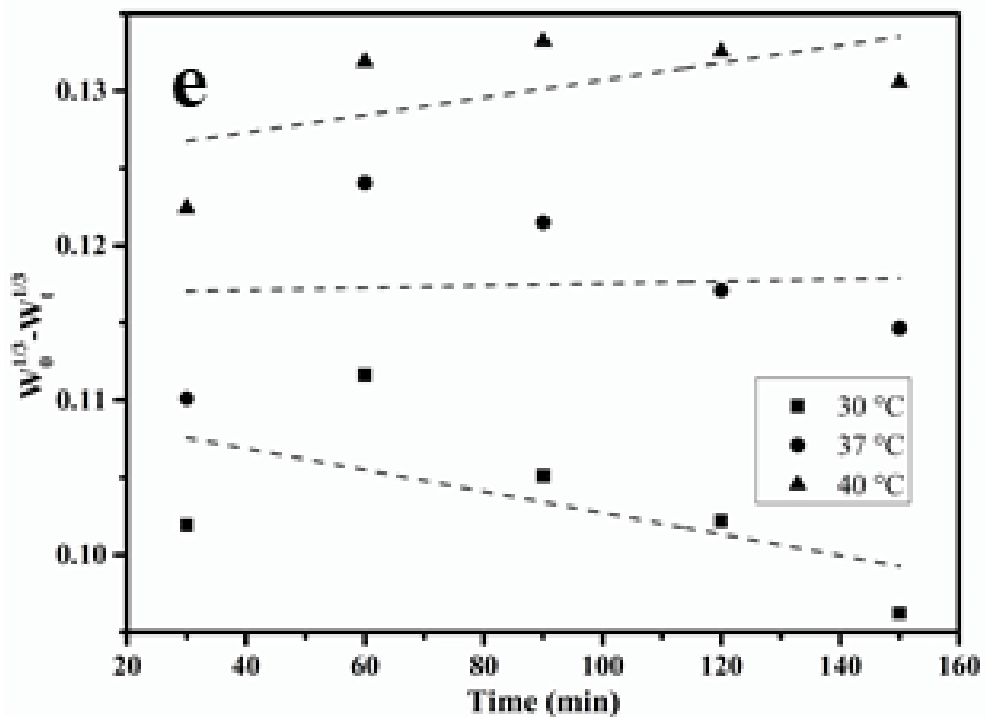
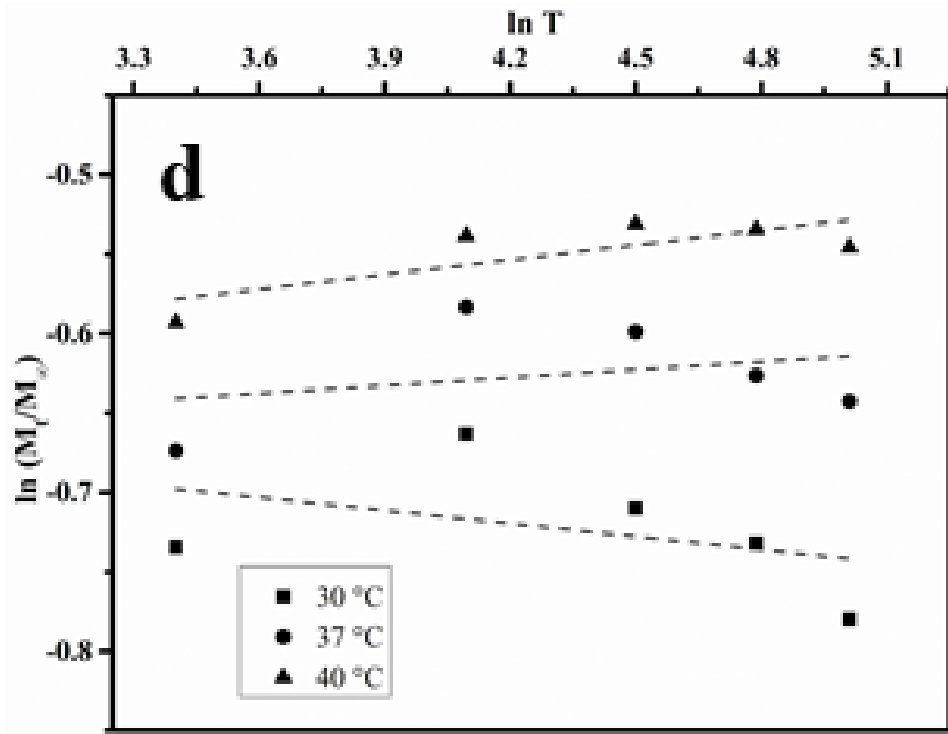


AIII.4: Dox release kinetics studied for NM nanohydrogel at different temperature: (a) % Cumulative release vs time (Zero-order kinetics)

## APPENDICES



**AIII.4: Dox release kinetics studied for NM nanohydrogel at different temperature: (b) % log cumulative drug remaining vs time (First-order kinetics); (c) % Cumulative release vs sqrt of time (Higuchi model)**



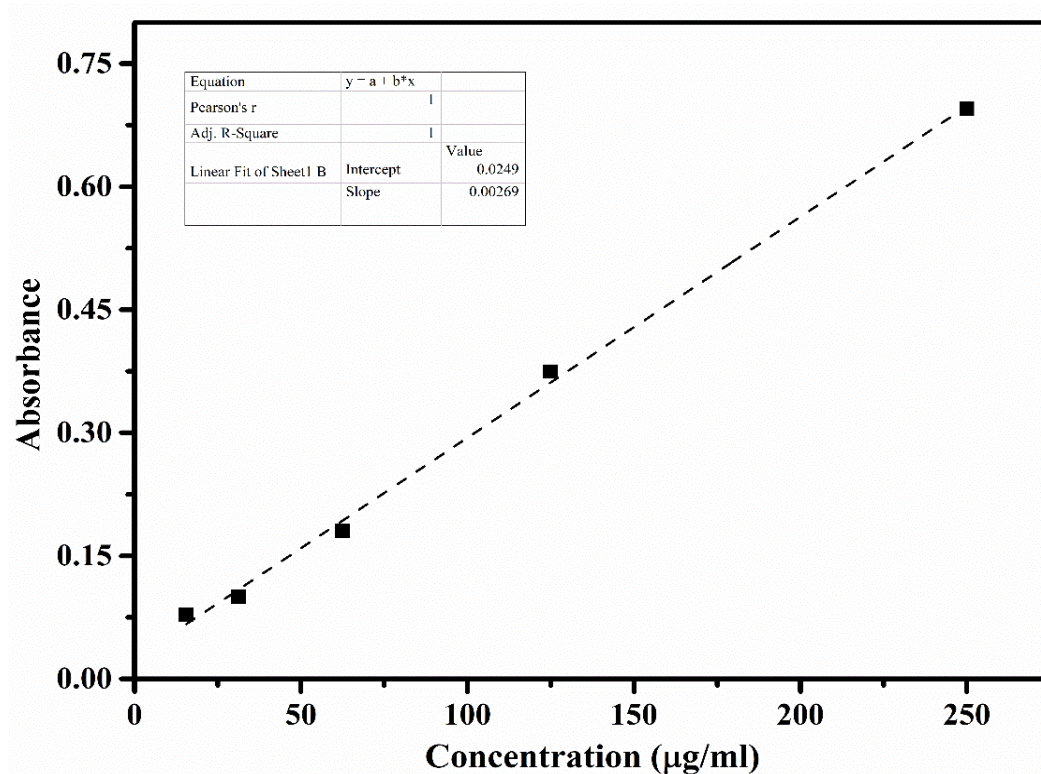
**AIII.4: Dox release kinetics studied for NM nanohydrogel at different temperature: (d)  $\ln M_t/M_\infty$  vs  $\ln T$  (Korsmeyer-Peppas model) and (e)  $W_o^{1/3} - W_t^{1/3}$  vs time (Hixon-Crowel model)**

# APPENDICES

## APPENDIX IV

### AIV.1 Calibration curve for tumor necrosis factor (TNF- $\alpha$ )

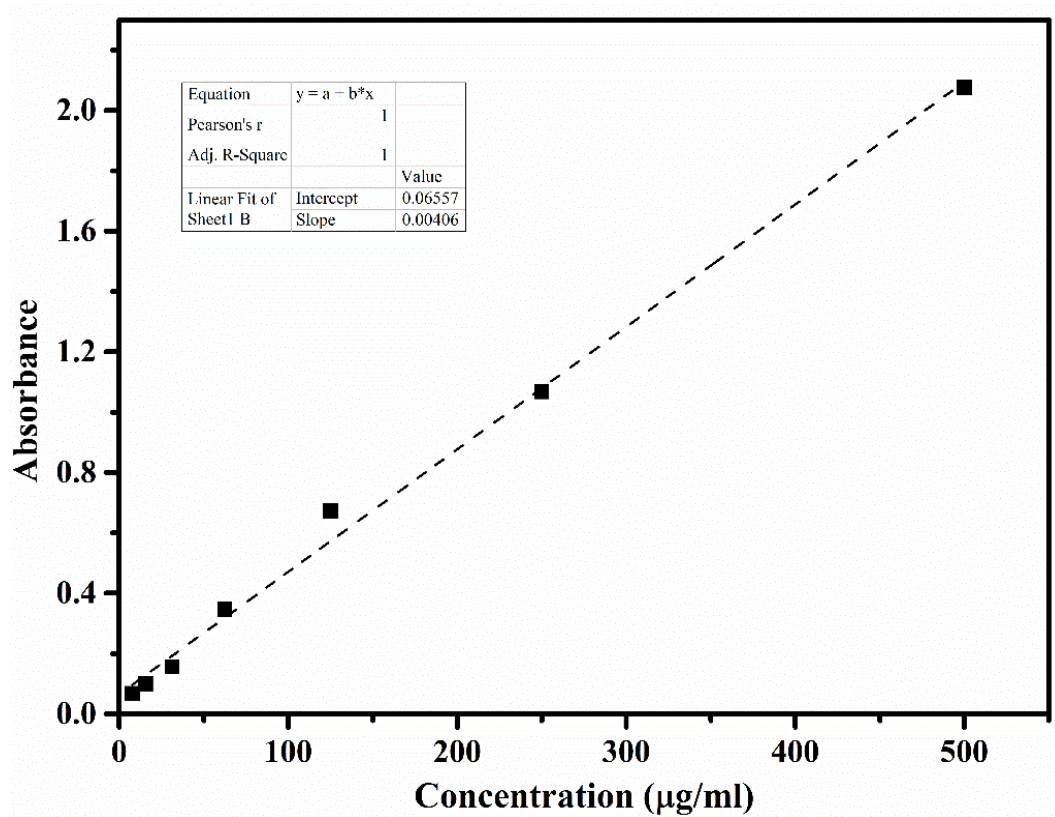
Standard curve for known concentrations of the TNF- $\alpha$  in accordance with manufactures instruction. The absorbance was read at 450 nm.



AIV.1: Standard curve of TNF- $\alpha$  at 450 nm

**AIV.2 Calibration curve for interlukin-6 inhibitor (IL-6)**

Standard curve for known concentrations of the IL-6 in accordance with manufactures instruction. The absorbance was read at 450 nm.



**AIV.2: Standard curve of IL-6 at 450 nm**

## **APPENDICES**



**RESEARCH  
PUBLICATIONS**



# RESEARCH PUBLICATIONS

## RESEARCH PUBLICATIONS

### (A) Research Papers in International Journals

1. **Sushma Havanur** and JagadeeshBabu P. E (2018). “Role of Graphene quantum dots synthesized through pyrolysis in the release behaviour of temperature responsive poly(N, N – diethyl acrylamide) hydrogels loaded with doxorubicin.” *International Journal of Polymer Analysis and characterization*, 23(7), 606-620.  
DOI: 10.1080/1023666X.2018.1484207
2. **Sushma Havanur**, Varisha Farheen and P E JagadeeshBabu (2018). “Synthesis and optimization of poly (N, N – diethyl acrylamide) hydrogel and evaluation of its anticancer drug doxorubicin’s release behavior”. *Iranian Polymer. Journal*, DOI: 10.1007/s13726-018-0680-z.
3. **Sushma Havanur**, Inayat Batish, Karthik Gourishetti, Sri Pragnya, JagadeeshBabu P E, Nithesh Kumar. (2018) “Poly(N,N-diethyl acrylamide)/functionalized graphene quantum dots hydrogels loaded with doxorubicin as a nano-drug carrier for metastatic lung cancer in mice ”. *Material Science & Engineering C* (Under review).

### (B) Paper/Poster Presented in International Conference

1. **Sushma Havanur** and JagadeeshBabu P. E (2016). “Synthesis and characterization of poly (N, N – diethyl acrylamide) macro-hydrogels for drug delivery application.” *International conference on Advanced materials and Technology (ICMAT-16)*, 26-28 May 2016, SJCE, Mysore, 146.
2. **Sushma Havanur** and JagadeeshBabu P. E (2017). “Synthesis and characterization of Graphene quantum dots and its application in stimuli responsive hydrogel as drug carrier.” *International conference on Nanoscience and Nanotechnology (ICONN-2017)*, SRM University, Kattankulathur, 769.

## **BIO-DATA**

**SUSHMA ISHWAR HAVANUR**

**Email ID:** sushmaih.1987@gmail.com

**Contact no:** +91-8105611163

### **Personal Details:**

<b>Name</b>	: Sushma Ishwar Havanur
<b>Father's name</b>	: Ishwar Havanur
<b>Date of birth</b>	: 19 July, 1987
<b>Gender</b>	: Female
<b>Nationality</b>	: Indian
<b>Permanent address</b>	: Sushma I Havanur, D/O, I G Havanur, Near P & T Quarters, P B Road, Ranebennur-581115, Haveri, Karnataka, India.

### **Educational qualification:**

- Ph.D. in Chemical Engineering (CGPA – 6), 2014-2019  
Department of Chemical Engineering,  
National Institute of Technology Karnataka,  
Surathkal, Mangalore, Karnataka.
- M.Tech in Nanoscience and Technology (68.88%), 2010-2012  
Kuvempu University,  
Shankargatta, Shimoga, Karnataka.
- B.Tech in Biotechnology (69.10%), 2006-2010  
Department of Biotechnology,  
Bapuji Institute of Engineering & Technology,  
Davangere, Karnataka.

### **Declaration:**

I hereby declare that the above written particulars are true to the best of my knowledge.

**Place:** Surathkal, India

**SUSHMA ISHWAR HAVANUR**

**Date:** 27/04/2019